THE GOLDEN FUTURE IN MEDICINAL CHEMISTRY: PERSPECTIVES AND RESOURCES FROM OLD AND NEW GOLD-BASED DRUG CANDIDATES

EDITED BY: Alessandro Pratesi, Sanja Grguric-Sipka, Lara Massai, Wukun Liu and Benoît Bertrand

PUBLISHED IN: Frontiers in Chemistry

frontiers Research Topics

ISSN 1664-8714
ISBN 978-2-88966-751-2
DOI 10.3389/978-2-88966-751-2

About Frontiers

Frontiers is more than just an open-access publisher of scholarly articles: it is a pioneering approach to the world of academia, radically improving the way scholarly research is managed. The grand vision of Frontiers is a world where all people have an equal opportunity to seek, share and generate knowledge. Frontiers provides immediate and permanent online open access to all its publications, but this alone is not enough to realize our grand goals.

Frontiers Journal Series

The Frontiers Journal Series is a multi-tier and interdisciplinary set of open-access, online journals, promising a paradigm shift from the current review, selection and dissemination processes in academic publishing. All Frontiers journals are driven by researchers for researchers; therefore, they constitute a service to the scholarly community. At the same time, the Frontiers Journal Series operates on a revolutionary invention, the tiered publishing system, initially addressing specific communities of scholars, and gradually climbing up to broader public understanding, thus serving the interests of the lay society, too.

Dedication to Quality

Each Frontiers article is a landmark of the highest quality, thanks to genuinely collaborative interactions between authors and review editors, who include some of the world's best academicians. Research must be certified by peers before entering a stream of knowledge that may eventually reach the public - and shape society; therefore, Frontiers only applies the most rigorous and unbiased reviews.
Frontiers revolutionizes research publishing by freely delivering the most outstanding research, evaluated with no bias from both the academic and social point of view. By applying the most advanced information technologies, Frontiers is catapulting scholarly publishing into a new generation.

What are Frontiers Research Topics?

Frontiers Research Topics are very popular trademarks of the Frontiers Journals Series: they are collections of at least ten articles, all centered on a particular subject. With their unique mix of varied contributions from Original Research to Review Articles, Frontiers Research Topics unify the most influential researchers, the latest key findings and historical advances in a hot research area! Find out more on how to host your own Frontiers Research Topic or contribute to one as an author by contacting the Frontiers Editorial Office: frontiersin.org/about/contact

THE GOLDEN FUTURE IN MEDICINAL CHEMISTRY: PERSPECTIVES AND RESOURCES FROM OLD AND NEW GOLD-BASED DRUG CANDIDATES

Topic Editors:
Alessandro Pratesi, University of Pisa, Italy
Sanja Grguric-Sipka, University of Belgrade, Serbia
Lara Massai, University of Florence, Italy
Wukun Liu, Nanjing University of Chinese Medicine, China
Benoît Bertrand, UMR8232 Institut Parisien de Chimie Moléculaire (IPCM), France

Citation: Pratesi, A., Grguric-Sipka, S., Massai, L., Liu, W., Bertrand, B., eds. (2021). The Golden Future in Medicinal Chemistry: Perspectives and Resources from Old and New Gold-Based Drug Candidates. Lausanne: Frontiers Media SA.
doi: 10.3389/978-2-88966-751-2

Table of Contents

frontiers in Chemistry

EDITORIAL
published: 18 March 2021
doi: 10.3389/fchem.2021.665244

Editorial: The Golden Future in Medicinal Chemistry: Perspectives and Resources From Old and New Gold-Based Drug Candidates

Lara Massai[1], *Sanja Grguric-Sipka*[2], *Wukun Liu*[3], *Benoît Bertrand*[4] *and Alessandro Pratesi*[5]*

[1]Laboratory of Metals in Medicine (MetMed), Department of Chemistry "U. Schiff", University of Florence, Florence, Italy, [2]Faculty of Chemistry, University of Belgrade, Belgrade, Serbia, [3]School of Pharmacy, Nanjing University of Chinese Medicine, Nanjing, China, [4]Sorbonne Université, CNRS, Institut Parisien de Chimie Moléculaire (IPCM), Paris, France, [5]Department of Chemistry and Industrial Chemistry (DCCI), University of Pisa, Pisa, Italy

Keywords: gold complexes, anticancer compounds, mode-of-action, protein metalation, anticancer immunity, mass spectrometry, dihydrofolate reductase, enzyme inhibition

Editorial on the Research Topic

The Golden Future in Medicinal Chemistry: Perspectives and Resources From Old and New Gold-Based Drug Candidates

Gold compounds started to play an important role in modern medicine after the discovery of the efficacy of some gold salts against tuberculosis strains by Robert Koch (Sigel et al., 2018). In the 20's of the last century, Jacques Forestier introduced the idea of using some gold(I) polymeric thiolates for the cure of rheumatoid arthritis (RA), which lead to the birth of gold-based treatments for RA (Kean et al., 1985). However, the turning point had been represented by the development of the orally-administrable Au(I)-based drug auranofin (AF) by Sutton (Sutton, 1986).

Between the end of 1970s and the mid-1980s, the first scientific studies highlighted the *in vitro* antiproliferative properties of auranofin against cancer cells (Mirabelli et al., 1985). This cornerstone finding, also in the light of the heavy side effects of the platinum-based chemotherapy, triggered the interest of the scientific community towards a possible "repurposing" of auranofin as prospective anticancer drug.

In the following years, gold compounds have received large attention, and an impressive number of structurally diverse gold(I) and gold(III) complexes were prepared, such as those stabilized by phosphines or by nitrogen donors, that were found to induce important anticancer effects both *in vitro* and *in vivo* (Marzo et al., 2019). Thanks to several mechanistic studies, preferential gold binding to proteins, instead of DNA, was demonstrated with the occurrence of different pathways to cytotoxicity. Mitochondria and oxidative phosphorylation's pathways emerged as the primary intracellular targets for cytotoxic gold complexes (Scalcon et al., 2018). Moreover, inhibition of the seleno-enzyme thioredoxin reductase (TrxR) seems to be a common mechanistic trait to explain the antiproliferative actions of several gold complexes, as strong TrxR inhibition may eventually lead to apoptosis (Magherini et al., 2018).

Although the ferment that animates the scientific community on the investigation of gold-based drug candidates, the real and entire picture of the involved mechanisms and modes of action for these compounds remains largely undepicted.

To deepen the knowledge on the gold-based complexes, this Research Topic encloses some fundamental contributions from worldwide outstanding researchers working in this field. In particular, the areas covered range across the synthesis and characterization of new gold

OPEN ACCESS

Edited and reviewed by:
Michael Kassiou,
The University of Sydney, Darlington, NSW, Australia

Correspondence:
Alessandro Pratesi
alessandro.pratesi@unipi.it

Specialty section:
This article was submitted to Medicinal and Pharmaceutical Chemistry, a section of the journal Frontiers in Chemistry

Received: *07 February 2021*
Accepted: *09 February 2021*
Published: *18 March 2021*

Citation:
Massai L, Grguric-Sipka S, Liu W, Bertrand B and Pratesi A (2021) Editorial: The Golden Future in Medicinal Chemistry: Perspectives and Resources From Old and New Gold-Based Drug Candidates. Front. Chem. 9:665244. doi: 10.3389/fchem.2021.665244

N-heterocyclic carbenes (Au-NHCs), to the study of protein metalation processes, to the discovery of new mode-of-action, and up to the search of unexplored molecular targets.

In the furrow of the research on the forefather of gold-based compounds, namely auranofin, Tolbatov et al. described an integrated experimental and theoretical study on the reactivity of AF and its iodide derivative (AF-I) toward relevant amino acid residues or their molecular models, such as the histidine, cysteine, methionine, and selenocysteine, that may represent the possible binding sites. Interestingly, the energetic barriers for the bond formation between the gold compounds and the targets have been calculated through computational methods. The obtained results pointed out that the replacement of the thiosugar moiety with iodide significantly affects the overall reactivity toward the selected targets, contributing to enhance the antitumoral activity of AF-I compared with AF.

A very informative analytical technique such as the high-resolution ESI mass spectrometry, has been successfully applied by Massai et al. to the study of protein metalation by a selected panel of Au(III) complexes. These compounds were reacted with two representative proteins, i.e. human serum albumin and human carbonic anhydrase I, and with the C-terminal dodecapeptide of TrxR. ESI-MS analysis permits to elucidate the nature of the resulting metal–protein adducts from which the main features of the occurring metallodrug–protein reactions can be inferred. In some cases, MS data have been integrated with other independent biophysical measurements for a comprehensive description of the occurring processes.

Because of their oxidizing character, Au(III) complexes are considered an interesting and promising class of potential anticancer compounds involving, beyond the protein metalation, probably also the oxidative cell stress. Radisavljević and co-workers summarized in their review the chemistry of some mononuclear and polynuclear gold(III) complexes. In particular, a special description has been deserved for gold(III) complexes with nitrogen-donor inert ligands and their kinetic behavior toward different biologically relevant nucleophiles. Mechanisms of interaction with DNA, serum albumin, and cytotoxic activity have been thoroughly discussed also in the light of computational calculations.

To date, a great number of different structures of gold compounds have been investigated for their anticancer properties and, among these, Au-NHCs hold great potential. It has been demonstrated that the antiproliferative effects of several gold NHCs were related to their antimitochondrial effects associated with potent inhibition of TrxR. Tong et al. in their review have masterfully summarized the efforts spent in the last years not only on the study of Au(III)-NHC, but also on porphyrin and pincer-type cyclometalated gold complexes. From this description, emerge the anticancer properties of gold(III) compounds and the identification of molecular targets involved in the mechanisms of action. Moreover, particular attention has been devoted to the chemical formulation strategies that have been adopted for the delivery of cytotoxic gold compounds, and for ameliorating the *in vivo* toxicity.

Another class of drug candidates, i.e., imidazolate phosphane gold(I) compounds, has been studied by Galassi and coworkers. They performed enzymatic assays on the inhibition potential of the studied compounds toward the dihydrofolate reductase (DHFR), an enzyme involved in metabolic pathways crucial for cancer cell's growth and survival and overexpressed in tumor cells. The results have been compared to those obtained for TrxR, the most recognized molecular target for gold compounds.

As completion of this Research Topic's overview, the role of gold compounds in anticancer immunity has been elucidated in a review by Yue et al., that summarizes the complex relationship between various gold derivatives and the immune system. Gold complexes seem to reverse tumor immune escape and directly facilitate the functions of immune cells, leading to enhanced anticancer effects. In particular, the paper described the antitumor effects of gold drugs and their relationships with various aspects of antitumor immunity, including innate immunity, adaptive immunity, immunogenic cell death, and immune checkpoints, as well as their roles in adverse effects.

This Research Topic aims to give to the readership a new point of view on the current research on gold-based drug candidates, covering different aspects, from the synthesis of new molecules to the study of their relationship with biomolecular targets and the immune system. As Guest Editors, we believe that this collection could be useful to disseminate the last advancements in the research of gold anticancer drugs.

AUTHOR CONTRIBUTIONS

All authors listed have made a substantial, direct, and intellectual contribution to the work and approved it for publication.

FUNDING

This work was supported by the Beneficentia Stiftung, Vaduz (BEN2020/34) and the University of Pisa (Rating Ateneo 2019-2020). The Fondazione Italiana per la Ricerca sul Cancro (AIRC, Milan) and Fondazione Cassa Risparmio di Firenze (Multiuser Equipment Program 2016, ref. code 19650) are also acknowledged.

REFERENCES

Kean, W. F., Forestier, F., Kassam, Y., Buchanan, W. W., and Rooney, P. J. (1985). The history of gold therapy in rheumatoid disease. *Semin. Arthritis Rheum.*, 14, 180 doi:10.1016/0049-0172(85)90037-X

Magherini, F., Fiaschi, T., Valocchia, E., Becatti, M., Pratesi, A., Marzo, T., et al. (2018). Antiproliferative effects of two gold(I)-N-heterocyclic carbene complexes in A2780 human ovarian cancer cells: a comparative proteomic study. *Oncotarget* 9, 28042–28068. doi:10.18632/oncotarget.25556

Marzo, T., Massai, L., Pratesi, A., Stefanini, M., Cirri, D., Magherini, F., et al. (2019). Replacement of the thiosugar of Auranofin with iodide enhances the anticancer potency in a mouse model of ovarian cancer. *ACS Med. Chem. Lett.* 10, 656–660. doi:10.1021/acsmedchemlett.9b00007

Mirabelli, C. K., Johnson, R. K., Sung, C. M., Faucette, L., Muirhead, K., and Crooke, S. T. (1985). Evaluation of the *in vivo* antitumor activity and *in vitro*

cytotoxic properties of auranofin, a coordinated gold compound, in murine tumor models. *Cancer Res.* 45, 32–39.

Scalcon, V., Bindoli, A., and Rigobello, M. P. (2018). Significance of the mitochondrial thioredoxin reductase in cancer cells: an update on role, targets and inhibitors. *Free Radic. Biol. Med.* 127, 62–79. doi:10.1016/j.freeradbiomed.2018.03.043

Sigel, A., Sigel, H., Freisinger, E., and Sigel, R. K. O. (2018). *Metallo-drugs: development and action of anticancer agents*. Berlin: Walter de Gruyter GmbH. doi:10.1515/9783110470734

Sutton, B. M. (1986). Gold compounds for rheumatoid arthritis. *Gold Bull.* 19, 15–16. doi:10.1007/BF03214639

Conflict of Interest: The authors declare that the research was conducted in the absence of any commercial or financial relationships that could be construed as a potential conflict of interest.

frontiers in Chemistry

MINI REVIEW
published: 20 May 2020
doi: 10.3389/fchem.2020.00379

Gold(III) Complexes: An Overview on Their Kinetics, Interactions With DNA/BSA, Cytotoxic Activity, and Computational Calculations

*Snežana Radisavljević and Biljana Petrović**

Department of Chemistry, Faculty of Science, University of Kragujevac, Kragujevac, Serbia

In the last few years, metallodrugs play a key role in the development of medicinal chemistry. The choice of metal ion, its oxidation state and stability, and the choice of inert and labile ligands are just some of the very important facts which must be considered before starting the synthesis of complexes with utilization in medicinal purpose. As a result, a lot of compounds of different transition metal ions found application for diagnostic and therapeutic purpose. Beside all, gold compounds have attracted particular attention. It is well-known that gold compounds could be used for the treatment of cancer, HIV, rheumatoid arthritis (chrysotherapy), and other diseases. This metal ion has unoccupied d-sublevels and possibility to form compounds with different oxidation states, from −1 to +5. However, gold(I) and gold(III) complexes are dominant in chemistry and medicine. Especially, gold(III) complexes are of great interest due to their structural similarity with cisplatin. Accordingly, this review summarizes the chemistry of some mononuclear and polynuclear gold(III) complexes. Special attention is given to gold(III) complexes with nitrogen-donor inert ligands (aliphatic or aromatic that have a possibility to stabilize complex) and their kinetic behavior toward different biologically relevant nucleophiles, mechanism of interaction with DNA/bovine serum albumin (BSA), cytotoxic activity, as well as computational calculations.

Keywords: gold(III) complexes, DNA, bovine serum albumin (BSA), kinetics, cytotoxicity, computational calculations, density functional theory (DFT) calculations

OPEN ACCESS

Edited by:
Sanja Grguric-Sipka, University of Belgrade, Serbia

Reviewed by:
Tiziano Marzo, University of Pisa, Italy
George Psomas, Aristotle University of Thessaloniki, Greece

****Correspondence:***
Biljana Petrović
biljana.petrovic@pmf.kg.ac.rs

Specialty section:
This article was submitted to Medicinal and Pharmaceutical Chemistry, a section of the journal Frontiers in Chemistry

Received: *10 March 2020*
Accepted: *09 April 2020*
Published: *20 May 2020*

Citation:
Radisavljević S and Petrović B (2020) Gold(III) Complexes: An Overview on Their Kinetics, Interactions With DNA/BSA, Cytotoxic Activity, and Computational Calculations. Front. Chem. 8:379. doi: 10.3389/fchem.2020.00379

INTRODUCTION

It is already known that cancer is a huge global problem (Abdnoor and Albdali, 2019). Due to that fact, discovery and utilization of different anticancer agents are the most investigated field. The first metal-based anticancer agent was cisplatin, discovered in 1969 (Rosenberg et al., 1969). After application of cisplatin, other platinum(II) complexes (carboplatin, oxaliplatin) were employed with the same aim (Sankarganesh et al., 2019). The promising results of usage of platinum complexes in medicinal purpose have led to the synthesis of different transition metal ion compounds and study of their potential antitumor activity (Jung and Lippard, 2007; Kim et al., 2008; Garcia et al., 2009; Wu et al., 2009). The most common are complexes of copper, vanadium, ruthenium (Lazarević et al., 2017; Leon et al., 2017), rhodium (Chen et al., 2017), nickel, palladium (Jahromi et al., 2016), iron, cobalt, gold (Ott and Gust, 2007; Romero-Canelón and Sadler, 2013), and others. But, only a few of them, such as complexes of palladium(II), nickel(II), and copper(II),

represent promising candidates for the treatment of cancer (Al-Masoudi et al., 2010; Andrew and Ajibade, 2018; Malik et al., 2018; Abdnoor and Albdali, 2019), while some of them, such as metalloid compound arsenic trioxide, are approved (Park et al., 2000; Miller et al., 2002). Namely, published results confirm the fact that metal complexes represent an arsenal with a wide and fundamental potential against cancer than small organic molecules (Luo et al., 2014; Rescifina et al., 2014; Alafeefy et al., 2015) due to possibility to change their properties with the right choice of oxidation state. Moreover, the choice of ligand has great impact on solubility, reactivity, and biological activity as well (Savić et al., 2016).

Chrysotherapy is closely connected with usage of gold(I) compounds in medicine, and it is known from ancient time (Sadler and Sue, 1994; Pricker, 1996; Shaw, 1999). The beginning of the twentieth century was very important for "gold chemistry" due to the discovery of Koch connected with utilization of potassium gold(I)-cyanide like anti-tuberculosis agent (Sadler, 1976). Almost at the same time, Forestier discovered usage of gold(I) complexes in the treatment of rheumatoid arthritis (Pope et al., 2002). At the end of the twentieth century, Food and Drug Administration allowed utilization of auranofin, a gold(I) complex, as oral anti-arthritic drug (Chaffman et al., 1984). Besides auranofin, other gold(I) compounds, such as aurothiomalate or aurothioglucose, were used like anti-arthritic agents. Further investigation in this field included the study of some gold(III) compounds with promising anti-inflammatory, antiparasitic, and anticancer activities (Navarro, 2009; Ott, 2009; Travnicek et al., 2012; Bertrand and Casini, 2014; Giorgio and Merlino, 2020). The results show that the primary modes of action for gold complexes are interactions with cysteine or selenocysteine containing various enzymes (tioredoxin reductase, phosphatases, cathepsin) (Roder and Thomson, 2015), while some of them undergo autophagy or interaction with topoisomerase I or ubiquitin–proteasome system (Milacic and Dou, 2009; Soave et al., 2017).

Considering that gold(III) ion forms complexes with square-planar geometry, similar to the structure of cisplatin, a number of different gold(III) complexes were studied as potential antitumor drugs. The published results confirm that these complexes can act against tumors which are resistant to cisplatin treatment as well as some of them give significant values for *in vitro* and *in vivo* cytotoxicity (μM) against solid cancer tumors without systemic toxicity (Sun and Che, 2009; Ronconi et al., 2010; Nordon et al., 2014; Huang et al., 2018; Wang et al., 2019).

Also, many scientists revealed that gold(III) complexes have great potential in the prevention of cancer (Bertrand and Casini, 2014), HIV, bronchial asthma, and like antimicrobial agents (Ott, 2009; Glišić and Duran, 2014). But, very fast hydrolysis and reduction to Au(I) or Au(0) indicate the lability of gold(III) complexes. On the other hand, their promising stability can be reached by the careful choice of appropriate inert ligands (such as polydentate ligands with sulfur, oxygen, or nitrogen as donor atoms) (Ott and Gust, 2007). Literature evidences the DNA-independent activation of some gold(III) complexes, while for some of them were proved binding to DNA, leading to the potential cytotoxic activities (Patel et al., 2013). Based on the previously mentioned, we have decided to write this review that cover interactions of novel gold(III) complexes with small biomolecules, DNA, model proteins, such as bovine serum albumin (BSA), their kinetic properties, and biological activity supported by computational calculations.

BIOLOGICAL TARGETS FOR GOLD(III) COMPLEXES

The interactions between newly synthesized gold(III) complexes that contain structurally distinct nitrogen-donor ligands (**Figure 1**), such as 2,6-*bis*(5-*tert*-butyl-1H-pyrazol-3-yl)pyridine (complex **1**), 2,6-*bis*(5-*tert*-butyl-1-methyl-1H-pyrazol-3-yl)pyridine (complex **2**), 2,6-*bis*((4S, 7R)−1,7,8,8-tetramethyl-4,5,6,7-tetrahydro-1H-4,7-methanoindazol-3-yl)pyridine (complex **3**), 1,4-diaminobutane (complexes **4** and **7**), 1,6-diaminohexane (complexes **5** and **8**), 1,8-diaminooctane (complexes **6** and **9**), combination of 2,2′-bipyridine and N-(3-((4-nitrophenyl) thio)phenyl)methanediimine (complex **10**), and (Z)-1-(4-morpholinophenyl)-N-((4-(trifluoromethyl) pyrimidin-2-yl)methyl)methanimine (complex **11**) (Radisavljević et al., 2018, 2019; Sankarganesh et al., 2019; Tabrizi et al., 2020), and primary biomolecules were examined by different experimental methods. These complexes were selected having in mind that the presence of different nitrogen-donor inert ligands in the structure of some gold(III) complexes have great potential to stabilize metal ion and improve its binding affinity toward biomolecules under physiological conditions (Radisavljević et al., 2019).

The study of potential anticancer activity of different transition metal ion complexes primarily considers their interactions with small biomolecules, such as amino acids, peptides, nucleosides, nucleotides, and further the interactions with DNA and proteins. In this respect, interactions with L-methionine (L-Met), L-histidine (L-His), guanine (Guo), guanosine-5′-monophosphate (5′-GMP), inosine (Ino), and inosine-5′-monophosphate (5′-IMP) are very important and must be emphasized. These interactions are dependent on redox properties, electrophilicity, and kinetic lability of complexes. Sometimes, reactivity of the nucleophiles indicates deactivation of complexes (Gukathasan et al., 2019). For example, the reduction possibility of L-glutathione is well-known. Its concentration in the cells is 10 mM (Williams et al., 2017), so the chosen complexes must avoid reduction before reaching to the target. In general, square-planar complexes undergo two pathways for substitution (Skibsted, 1986; Tobe and Burgess, 1999). The first is solvolytic, which includes formation of solvent-complex before substitution with nucleophile. The second is direct attack by the nucleophile. In order to clarify interactions, substitution reactions of gold(III) complexes **1**–**3** with Guo and 5′-GMP, and further with DNA, were followed by stopped-flow technique. For these experiments, concentration of ligand was always at least a 10-fold excess, so the reactions are followed under *pseudo*-first order. The substitution was studied in the presence of 150 mM NaCl to avoid solvolysis and provoke direct nucleophile attack. The obtained values for the

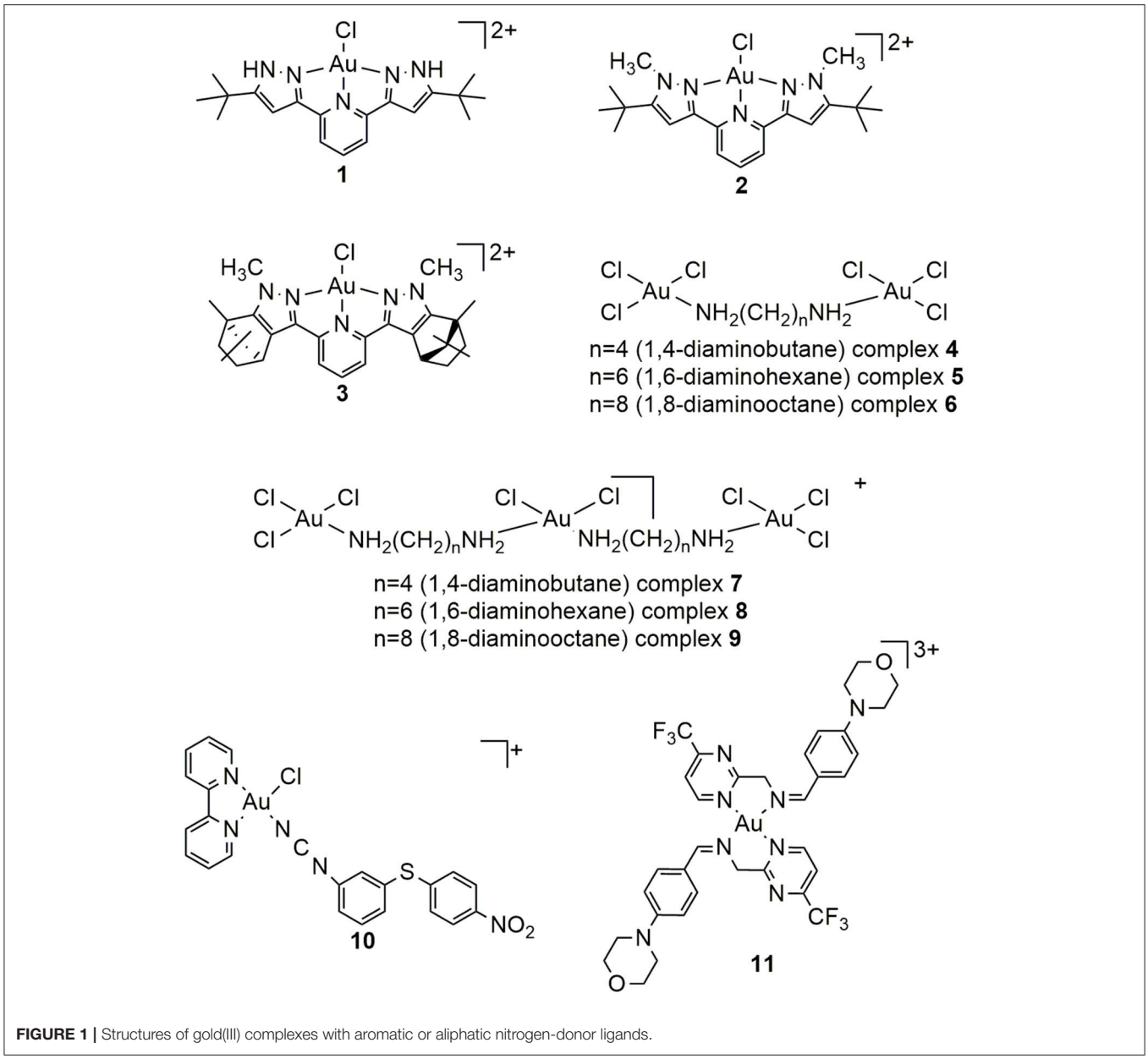

FIGURE 1 | Structures of gold(III) complexes with aromatic or aliphatic nitrogen-donor ligands.

rate constants are given in **Table S1**. Also, negative values of entropy of activation $\Delta S^{\neq}$ confirmed the associative mode of substitution for all studied systems. In comparison, complex **1** has shown the best activity. This could be explained by the presence of methyl groups in the structure of complexes **2** and **3** which decrease the reactivity of complexes due to their positive inductive effect as well as steric hindrance during the formation of five-coordinated transition state (Hofmann et al., 2003; Jaganyi et al., 2004). Monofunctional gold(III) complexes with terpyridine or diethylenetriamine as inert ligands show similar mechanisms of substitution (Deković et al., 2012).

It is well-known that DNA is the main target for platinum(II) complexes, while some gold(III) complexes can cause direct DNA damage (Patel et al., 2013). Interactions between CT-DNA molecule and studied complexes were examined by different experimental methods (UV-Vis, fluorescence measurements, or viscosity). The UV-Vis method was used just to reveal the interaction between complexes and CT-DNA, but exact mode of binding could not have been predicted on this way. In the case of complexes **1**–**9** and **11**, different spectra were obtained after addition of CT-DNA (**Figure S1**). The values of intrinsic binding constants K_b (M^{-1}) for complexes **1**–**9** were calculated and given in **Table 1**. This observation was the evidence for very good affinity for binding of complexes toward CT-DNA.

The same conclusion was derived for structurally similar complexes with terpyridine ligands (Liu et al., 1995; Messori et al., 2005; Shi et al., 2006). The other method, fluorescence spectroscopy, was employed in the aim to clarify the mode

TABLE 1 | The DNA-binding constants (K_b) and Stern–Volmer constants (K_{sv}) from EB–DNA fluorescence for complexes **1–9** and bovine serum albumin (BSA) constants and parameters (K_{sv}, k_q, K, and n) derived for complexes **4–9** (Radisavljević et al., 2018, 2019).

Complex	K_b [M^{-1}]	K_{sv} [M^{-1}]	K_{sv} [M^{-1}]	k_q[M^{-1} s^{-1}]	K [M^{-1}]	n
1	$(5.7 \pm 0.1) \times 10^3$	$(1.6 \pm 0.1) \times 10^4$	$(6.71 \pm 0.07) \times 10^4$	$(6.71 \pm 0.07) \times 10^{12}$	$(2.05 \pm 0.04) \times 10^4$	0.6
2	$(4.6 \pm 0.1) \times 10^3$	$(4.0 \pm 0.1) \times 10^3$				
3	$(1.6 \pm 0.1) \times 10^3$	$(3.0 \pm 0.1) \times 10^4$				
4	$(3.72 \pm 0.04) \times 10^3$	$(3.54 \pm 0.04) \times 10^4$				
5	$(1.91 \pm 0.06) \times 10^4$	$(4.01 \pm 0.05) \times 10^4$	$(8.04 \pm 0.08) \times 10^4$	$(8.04 \pm 0.08) \times 10^{12}$	$(5.82 \pm 0.06) \times 10^4$	0.45
6	$(1.69 \pm 0.05) \times 10^4$	$(1.65 \pm 0.02) \times 10^4$	$(4.41 \pm 0.05) \times 10^4$	$(4.41 \pm 0.05) \times 10^{12}$	$(1.84 \pm 0.06) \times 10^4$	0.64
7	$(7.50 \pm 0.02) \times 10^3$	$(6.339 \pm 0.004) \times 10^4$	$(1.320 \pm 0.004) \times 10^5$	$(1.320 \pm 0.004) \times 10^{13}$	$(3.87 \pm 0.04) \times 10^4$	0.65
8	$(9.85 \pm 0.03) \times 10^3$	$(1.956 \pm 0.002) \times 10^4$	$(7.131 \pm 0.005) \times 10^4$	$(7.131 \pm 0.005) \times 10^{12}$	$(1.98 \pm 0.02) \times 10^4$	0.59
9	$(1.56 \pm 0.05) \times 10^4$	$(4.783 \pm 0.002) \times 10^4$	$(1.289 \pm 0.008) \times 10^5$	$(1.289 \pm 0.008) \times 10^{13}$	$(6.02 \pm 0.05) \times 10^4$	0.82

of interaction between complexes and DNA. For fluorescence measurements, besides DNA, classical intercalator ethidium-bromide (EB) was involved. The changes in the spectra of complexes **1–9** and **11** indicated good possibility of complexes to replace EB from EB-DNA adduct and bound to DNA *via* intercalation (**Figure S2**).

To confirm this mode of binding, viscosity measurements were done as well. The viscosity of DNA is dependent on the length changes and can clarify the intercalative binding (Li et al., 2010). After addition of complexes **1–9** or **11** to CT-DNA solution, the increasing of viscosity was explained by elongation of DNA helix due to the insertion of complex between base pairs (**Figure S3**).

The transportation of metal ions in the bloodstream may be affected by the high affinity of them for aminoacidic residues of plasma proteins, in particular serum albumin. Besides, serum albumins have impact on various physiological functions. They affect colloid osmotic blood pressure, and they are in charge for constant blood pH (He and Carter, 1992). Some previous research evidence worth antioxidant activity of albumins as well as the protection of oxidative stress (Bourdon et al., 1999). Serum albumins are general ligands for hematin, fatty acids, and bilirubin. Therefore, they can bind metal ions or complexes (Bal et al., 1998; Marcon et al., 2003) as well. The domains of serum albumin are I, II, and III, and each of these has subdomains A and B. Subdomains IIA and IIIA are free for binding of ligands or complexes and their other names are Sudlow site I and site II (Carter et al., 1989; Carter and Ho, 1994). The differences between human serum albumin (HSA) and BSA are number of amino acid residues (585 for HSA; 582 for BSA), molecular weight (66.5 kDa for HSA; 66 kDa for BSA) and number of tryptophan (Trp) residues (Trp at position 214 for HSA; Trp at positions 213 and 134 for BSA) (Paul et al., 2019). Beside these differences, the high structural homology makes BSA a suitable model in these investigations. Interactions between gold(III) complexes and BSA were followed by fluorescence spectroscopy and for complexes **4–9** formation of BSA–gold(III) compound was confirmed (**Figure S4**). BSA-binding constants (K) and other parameters, such as K_{sv}, Stern-Volmer quenching constant; k_q, quenching constant; K, BSA-binding constant; and n, number of binding sites per albumin, derived for complexes **4–9** are given in **Table 1**. Accordingly, during the experiments were not mentioned the reduction of gold(III) complexes upon interaction with protein, respectively.

CYTOTOXIC ACTIVITY OF GOLD(III) COMPLEXES

The cytotoxicity and selectivity of different transition metal ion complexes on various cancer cells play the key role in the design and development of new potential anticancer agents. At the beginning of the twenty-first century, gold(III) porphyrin complex, with satisfying physiological stability, was reported like promising anticancer agent with IC_{50} values in the range of 0.73–0.11 μM. The studies against normal and cisplatin-resistant ovarian cancer have shown the ability of gold(III) porphyrin complex, *in vitro* and *in vivo*, to exceed cisplatin resistance without affecting health tissue (Lum et al., 2014; Bauer et al., 2019). Furthermore, carbamate-based Au(III) complexes were used for animal experiments and based on the observed data of clinical studies gave promising results of good anticancer effects (Marzano et al., 2011; Gu et al., 2019). All these facts have contributed to the assumption that gold(III) complexes have different modes of action compared with platinum antitumor active compounds (Nobili et al., 2009).

The potential activity of **1–11** was estimated by 3-(4,5-dimethythiazol-. 2-yl)-2,5-diphenyl tetrazolium bromide (MTT) test on different cell lines (A549, A375, and LS-174 for complex **1**, 4T1 and CT26 for complexes **1–3**, MDA-MB-231, HCT-116 for complexes **1–9**, MRC-5 for complexes **4–9**, MCF-7 for complexes **10–11**, HT-29 for complex **10**, HepG2 and NHDF for complex **11**, HeLa for complexes **1–3** and **10–11**). The results are summarized in **Table S2**.

Complexes **1–3** have shown better antitumor effects than cisplatin in the case of both breast cancer cell lines (MDA-MB-231 or 4T1). Cytotoxicity against CT26 was weaker than against HCT116 and much lower for than for cisplatin. Consequently, results have shown the reduction of the amount of antiapoptotic protein Bcl-2 in the presence of complexes **1–3**, but there was not emphasized significant reduction in the activation of Bax protein. Complexes **1–3** had a possibility to increase the

amount of capsase-3 compared to untreated cells (Zarić et al., 2020). These results confirm a different influence of bulky inert tridentate nitrogen-donor ligand on activity toward different cell lines. The promising IC_{50} values for complex **1** led to the further examination of this complex. Investigation of cell cycle phase distribution in A375 cells after addition of complex **1** indicated the interaction with DNA. Results of apoptotic potential of complex **1** showed increasing of the percentage of cells in early as well as in late apoptosis. The treatment of A375 cells, first with N-acetyl-L-cysteine and after with complex **1,** suggested impact on reactive oxygen species (ROS) level and antiproliferative effects. After 3 h of cell treatment, decrease in ROS level was noticed, which pointed out the possibility of complex to interfere level of ROS in A375 cells. Complex **10** indicated generation of ROS in a stronger way than cisplatin. ROS and mitochondria are very important to explain apoptosis induction by gold(III) complexes in the case of cancer (Živanović et al., 2017).

For complex **10,** notable cytotoxicity was noticed against HT-29 and MCF-7 cancer cell lines in comparison with cisplatin, while for HeLa cancer cells, activity was the same like for cisplatin (Tabrizi et al., 2020). The results of cytotoxicity against MRC-5 (non-tumorigenic cells) for complex **10** were much higher than for cisplatin. All examined complexes showed significant cytotoxicity compared with cisplatin (Petrović et al., 2015) or with some other platinum(IV) complexes (Stojković et al., 2014) and palladium(II) complexes (Altaf et al., 2017).

For complexes **4–9** cytotoxic effects were noticed ($IC_{50} < 100\,\mu M$) as well. After 1 day of treatments, these results were significant, in comparison with $K[AuCl_4]$ (**Table S2**). Generally, complexes **7–9** have shown better cytotoxicity. Namely, the longer diamine chain as well as the number of diamines led to the increasing of hydrophobic properties and makes gold(III) complexes more appropriate and flexible for entrance in the cells. The highest activity of complexes **4–9** was remarked for colorectal cancer cells (HCT-116).

COMPUTATIONAL CALCULATIONS

The highest occupied molecular orbital (HOMO) and lowest unoccupied molecular orbital (LUMO) present the useful tool which can be used to clarify chemical reactivity as well as stability of compounds (Solomon et al., 2012, 2014). DFT calculations for complexes **4–9** show that they possess distorted square-planar coordination geometry. HOMOs for dinuclear complexes were concentrated on one gold center, while for trinuclear complexes, LUMOs were concentrated on the central gold(III) ion.

Computational calculations are very powerful methods for prediction or explanation of DNA/BSA interactions with complexes, binding places, and binding affinity (Warren et al., 2006). Based on the results obtained by molecular docking, differences in ligand structures (aromatic or aliphatic) were emphasized (**Figure S5**). For these experiments, 1BNA (DNA structure dodecamer) was used due to the fact that interactions with 1BNA can reflect interactions with DNA. Docking analysis for complexes **1–3** and **11** showed interaction *via* intercalation, while complexes **4–9** fitted in the minor groove on DNA. Results for complexes **1–3** have shown that only complex **1** can form H-bonds because of hydrogen atoms (**Figure 1**). The presence of these H-bonds had great impact on stabilization of complex **1**–DNA product. The weakest interaction between complex **3** and DNA was confirmed due to the intercalation between base pairs which is not complete. Explanation for this is steric hindrance for complex **3** which led to negative value of binding energy. In the case of complexes **4–9,** the presence of diamine length allowed better interaction with DNA. Also, docking results indicated that complexes **4–9** can be bound to BSA to subdomain IIA (site I) forming hydrogen bonds, while electrostatic and hydrophobic interactions had the major impact on binding (Radisavljević et al., 2019). For complex **11** was proved the presence of hydrogen bonds with Arg185, Leu189, Thr190, Ser192, Pro240, Glu424, Ser428, Ile552, and Arg458 on the active site of BSA (Sankarganesh et al., 2019).

CONCLUSION

We described here the characteristics of some newly synthesized gold(III) complexes as well as their interactions with important biomolecules and DNA/BSA by different experimental methods and by theoretical calculations. The results of the substitution reactions show a good affinity of complexes **1–3** toward different biomolecules, such as Guo, 5′-GMP, and DNA. Presented results have indicated the good possibility for interaction between gold(III) complexes and DNA/BSA, with high values of binding constants. Interactions with DNA are confirmed with constants in the range between 10^3 and 10^4 (M^{-1}) determined by UV-Vis and fluorescence measurements, respectively, while the calculated constants for BSA interactions are in the range between 10^4 and 10^5 (M^{-1}). All results were supported with computational calculations, and clear explanations of the reactions with DNA/BSA were obtained by molecular docking studies. Biological investigations of studied gold(III) complexes toward different cell lines emphasized their potential compared with cisplatin or $K[AuCl_4]$. All observed results could be very useful for further investigation of potential anticancer drugs, having in mind that a lot of scientists every day make efforts to find new transition metal complexes with better activity and selectivity than cisplatin.

AUTHOR CONTRIBUTIONS

SR wrote the manuscript. BP supervised the manuscript.

FUNDING

This work was supported by the Serbian Ministry of Education, Science and Technological Development (Agreement No. 451-03-68/2020-14/200122).

ACKNOWLEDGMENTS

The authors gratefully acknowledge financial support of the Ministry of Education, Science and Technological Development, Republic of Serbia.

SUPPLEMENTARY MATERIAL

The Supplementary Material for this article can be found online at: https://www.frontiersin.org/articles/10.3389/fchem.2020.00379/full#supplementary-material

REFERENCES

Abdnoor, Z. M., and Albdali, A. J. (2019). Synthesis, characterization, and anticancer activity of some azole-heterocyclic complexes with gold(III), palladium(II), nickel(II), and copper(II) metal ions. *J. Chin. Chem. Soc.* 66, 1474–1483. doi: 10.1002/jccs.201900010

Alafeefy, A. M., Ashour, A. E., Prasad, O., Sinha, L., Pathak, S., Alasmari, F. A., et al. (2015). Development of certain novel N-(2-(2-(2-oxindolin-3-ylidene)hydrazinecarbonyl)phenyl)-benzamides and 3-(2-oxoindolin-3-ylideneamino)-2-substituted quinazoli-4(3H)-ones as CFM-1 analogs: design, synthesis, QSAR analysis and anticancer activity. *Eur. J. Med. Chem.* 92, 191–201. doi: 10.1016/j.ejmech.2014.12.048

Al-Masoudi, N., Abdullah, B., Ess, A., Loddo, R., and LaColla, P. (2010). Platinum and palladium-triazole complexes as highly potential antitumor agents. *Arch. Pharm.* 343, 222–227. doi: 10.1002/ardp.200900140

Altaf, M., Monim-Ul-Mehboob, M., Kawde, A. N., Corona, G., Larcher, R., Ogasawara, M., et al. (2017). New bipyridine gold(III) dithiocarbamate-containing complexes exerted a potent anticancer activity against cisplatin-resistant cancer cells independent of p53 status. *Oncotarget* 8, 490–505. doi: 10.18632/oncotarget.13448

Andrew, F., and Ajibade, P. (2018). Synthesis, characterization and anticancer studies of bis-(N-methyl-1-phenyldithiocarbamato) Cu(II), Zn(II), and Pt(II) complexes: single crystal X-ray structure of the copper complex. *J. Coord. Chem.* 71, 2776–2786. doi: 10.1080/00958972.2018.1489537

Bal, W., Christodoulou, J., Sadler, P. J., and Tucker, A. (1998). Multi-metal binding site of serum albumin. *J. Inorg. Biochem.* 70, 33–39. doi: 10.1016/s0162-0134(98)00010-5

Bauer, E. B., Bernd, M. A., Schütz, M., Oberkofler, J., Pöthig, A., Reich, R. M., et al. (2019). Synthesis, characterization, and biological studies of multidentate gold(I) and gold(III) NHC complexes. *Dalton Trans.* 48, 16651–16625. doi: 10.1039/c9dt03183a

Bertrand, B., and Casini, A. (2014). A golden future in medicinal inorganic chemistry: the promise of anticancer gold organometallic compounds. *Dalton Trans.* 43, 4209–4219. doi: 10.1039/C3DT52524D

Bourdon, E., Loreau, N., and Blache, D. (1999). Glucose and free radicals impair the antioxidant properties of serum albumin. *FASEB J.* 13, 233–244. doi: 10.1096/fasebj.13.2.233

Carter, D. C., He, X. M., Munson, S. H., Twigg, P. D., Gernert, K. M., Broom, M. B., et al. (1989). Three-dimensional structure of human serum albumin. *Science* 244, 1195–1198.doi: 10.1126/science.2727704

Carter, D. C., and Ho, J. X. (1994). Structure of serum albumin. *Adv. Protein Chem.* 45, 153–203.doi: 10.1016/s0065-3233(08)60640-3

Chaffman, M., Brodgen, R. N., Heel, R. C., Speight, T. M., and Avery, G. S. (1984). Auranofin. A preliminary review of its pharmacological properties and therapeutic use in rheumatoid arthritis. *Drugs* 27, 378–424. doi: 10.2165/00003495-198427050-00002

Chen, Z., Orvig, C., and Liang, H. (2017). Multi-target metal-based anticancer agents. *Curr. Top. Med. Chem.* 17, 3131–3145. doi: 10.2174/1568026617666171004155437

Deković, A., Petrović, B., Bugarčić, Ž. D., Puchta R, and van Eldik, R. (2012). Kinetics and mechanism of the reactions of Au(III) complexes with some biologically relevant molecules. *Dalton Trans.* 41, 3633–3641. doi: 10.1039/C2DT11843B

Garcia, M. H., Morais, T. S., Florindo, P., Piedade, M. F. M., Moreno, V., Ciudad, C., et al. (2009). Inhibition of cancer cell growth by ruthenium(II) cyclopentadienyl derivative complexes with heteroaromatic ligands. *J. Inorg. Biochem.* 103, 354–361. doi: 10.1016/j.jinorgbio.2008.11.016

Giorgio, A., and Merlino, A. (2020). Gold metalation of proteins: structural studies. Coord. *Chem. Rev.* 407, 213175. doi: 10.1016/j.ccr.2019.213175

Glišić, B. D., and Duran, M. I. (2014). Gold complexes as antimicrobial agents: an overview of different biological activities in relation to the oxidation state of the gold ion and the ligand structure. *Dalton Trans.* 43, 5950–5969. doi: 10.1039/C4DT00022F

Gu, G., Chen, C., Wang, Q., Gao, Z., and Xu, M. (2019). Cytotoxicity and dna binding ability of two novel gold(III) complexes. *J. Appl. Spectros.* 86, 618–622. doi: 10.1007/s10812-019-00868-4

Gukathasan, S., Parkin, S., and Awuah, S. G. (2019). Cyclometalated Gold(III) complexes bearing DACH ligands. *Inorg. Chem.* 58, 9326–9340. doi: 10.1021/acs.inorgchem.9b01031

He, X. M., and Carter, D. C. (1992). Atomic structure and chemisty of human serum albumin. *Nature* 358, 209–215. doi: 10.1038/358209a0

Hofmann, A., Jaganyi, D., Munro, O. Q., Liehr, G., and van Eldik, R. (2003). Electronic tuning of the liability of Pt(II) complexes through π-acceptor effects. Correlations between thermodynamic, kinetic, and theoretical parameters. *Inorg Chem.* 42, 1688–1700. doi: 10.1021/ic020605r

Huang, K. B., Wang, F. Y., Tang, X. M., Feng, H. W., Chen, Z. F., Liu, Y. C., et al. (2018). Organometallic Gold(III) complexes similar to tetrahydroisoquinoline induce ER-stress-mediated apoptosis and pro-death autophagy in A549 cancer cells. *J. Med. Chem.* 61, 3478–3490. doi: 10.1021/acs.jmedchem.7b01694

Jaganyi, D., Reddy, D., Gertenbach, J. A., Hofmann, A., and van Eldik, R. (2004). Role of chelate substituents and cis σ-effect on the rate of ligand substitution at Pt(N-N-N) and Pt(N-N-C) centres. *Dalton Trans*. 27, 299–304. doi: 10.1039/B311595J

Jahromi, E., Divsalar, A., Soboury, A., Khaleghizadeh, S., Mansouri-Torshizi, H., and Kostova, I. (2016). Palladium complexes: new candidates for anti-cancer drugs. *J. Iran. Chem. Soc.*13, 967–989. doi: 10.1007/s13738-015-0804-8

Jung, Y., and Lippard, S. J. (2007). Direct cellular responses to platinum-induced DNA damage. *Chem. Rev.* 107, 1387–1407. doi: 10.1021/cr068207j

Kim, E., Rye, P. T., Essigmann, J. M., and Croy, R. G. (2008). A bifunctional platinum(II) antitumor agent that forms DNA adducts with affinity for the estrogen receptor. *J. Inorg. Biochem.* 103, 256–261. doi: 10.1016/j.jinorgbio.2008.10.013

Lazarević, T., Rilak, A., and Bugarčić, Ž. D. (2017). Platinum, palladium, gold and ruthenium complexes as anticancer agents: current clinical uses, cytotoxicity studies and future perspectives. *Eur. J. Med. Chem.* 142, 8–31. doi: 10.1016/j.ejmech.2017.04.007

Leon, I. E., Cadavid-Vargas, J. F., Di Virgilio, A. L., and Etcheverry, S. B. (2017). Vanadium, ruthenium and copper compounds: a new class of nonplatinum metallodrugs with anticancer activity. *Curr. Med. Chem.* 24, 112-148. doi: 10.2174/0929867323666160824162546

Li, D. D., Tian, J. L., Gu, W., Liu, X., and Yan, S. P. (2010). A novel 1,2,4-triazole-based copper(II) complex: synthesis, characterization, magnetic property and nuclease activity. *J. Inorg. Biochem.* 104, 171–179. doi: 10.1016/j.jinorgbio.2009.10.020

Liu, H. Q., Cheung, T. C., Peng, S. M., and Che, C. M. (1995). Novel luminescent cyclometalated and teroyridine Gold(III) complexes and DNA binding studies. *J. Chem. Soc. Chem. Commun.* 1995, 1787–1788. doi: 10.1039/C39950001787

Lum, C. T., Sun, R. W.-Y., Zou, T., and Che, C.-M. (2014). Gold(III) complexes inhibit growth of cisplatin-resistant ovarian cancer in association with upregulation of proapoptotic PMS2 gene. *Chem. Sci.* 5, 1579–1584. doi: 10.1039/C3SC53203H

Luo, H., Yang, S., Cai, Y., Peng, Z., and Liu, T. (2014). Synthesis and biological evaluation of novel 6-chloro-quinazolin derivatives as potential antitumor agents. *Eur. J. Med. Chem.* 84, 746–752. doi: 10.1016/j.ejmech.2014.07.053

Malik, M., Dar, O., Gull, P., Wani, M., and Hashmi, A. (2018). Heterocyclic Schiff base transition metal complexes in antimicrobial and anticancer chemotherapy. *MedChemComm.* 9, 409–436.doi: 10.1039/C7MD00526A

Marcon, G., Messori, L., Orioli, P., Cinellu, M. A., and Minghetti, G. (2003). Reactions of gold(III) complexes with serum albumin. *Eur. J. Biochem.* 270, 4655–4661. doi: 10.1046/j.1432-1033.2003.03862.x

Marzano, C., Ronconi, L., Chiara, F., Giron, M. C., Faustinelli, I., Cristofori, P., et al. (2011). Gold(III)-dithiocarbamato anticancer agents: activity, toxicology and histopathological studies in rodents. *Int. J. Cancer* 129, 487–496. doi: 10.1002/ijc.25684

Messori, L., Marcon, G., Innocenti, A., Gallori, E., Franchi, M., and Orioli, P. (2005). Molecular recognition of metal complexes by DNSA: a comparative study of the interactions of the parent complexes [PtCl(TERPY)]Cl and [AuCl(TERPY)]Cl_2 with double stranded DNA. *Bioinorg. Chem. Appl.* 3, 239–253. doi: 10.1155/BCA.2005.239

Milacic, V., and Dou, Q. P. (2009). The tumor proteasome as a novel target for gold(III) complexes: implications for breast cancer therapy. *Coord. Chem. Rev.* 253, 1649–1660. doi: 10.1016/j.ccr.2009.01.032

Miller, W. H. Jr., Schipper, H. M., Lee, J. S., Singer, J., and Waxman, S. (2002). Mechanisms of action of arsenic trioxide. *Cancer Res.* 62, 3893–3908. Available online at: https://cancerres.aacrjournals.org/content/62/14/3893

Navarro, M. (2009). Gold complexes as potential anti-parasitic agents. *Coord. Chem. Rev.* 253, 1619–1626. doi: 10.1016/j.ccr.2008.12.003

Nobili, S., Mini, E., Landini, I., Gabbiani, C., Casini, A, and Messori, L. (2009). Gold compounds as anticancer agents: chemistry, cellular pharmacology, and preclinical studies. *Med. Res. Rev.* 30, 550–580. doi: 10.1002/med.20168

Nordon, C., Boscutti, G., and Fregona, D. (2014). Beyond platinums: gold complexes as anticancer agents. *Anticancer Res.* 34, 487–492. doi: 10.0250-7005/2014

Ott, I. (2009). On the medicinal chemistry of gold complexes as anticancer drugs. *Coord. Chem. Rev.* 253, 1670–1681. doi: 10.1016/j.ccr.2009.02.019

Ott, I., and Gust, R. (2007). Non platinum metal complexes as anti-cancer drugs. *Arch Pharm.* 340, 117–126. doi: 10.1002/ardp.200600151

Park, W. H., Seol, J. G., Kim, S., Hyun, J. M., Jung, C. W., Lee, C. C., et al. (2000). Arsenic trioxide-mediated growth inhibition in MC/CAR myeloma cells via cell cycle arrest in association with induction of cyclin-dependent kinase inhibitor, p21, and apoptosis. *Cancer Res.* 60, 3065–3071. Available online at: https://cancerres.aacrjournals.org/content/60/11/3065

Patel, M. N., Bhatt, B. S., and Dosi, P. A. (2013). Synthesis and evaluation of gold(III) complexes as efficient DNA binders and cytotoxic agents. *Spectrochim. Acta A* 110, 20–27. doi: 10.1016/j.saa.2013.03.037

Paul, S., Ghanti, R., Sardar, P. S., and Majhi, A. (2019). Synthesis of a novel coumarin derivative and its binding interaction with serum albumins. *Chem.Heterocycl. Com.* 55, 607–611. doi: 10.1007/s10593-019-02505-6

Petrović, V. P., Živanović, M. N., Simijonović, D., Dorović, J., Petrović, Z. D., and Marković, S. D. (2015). Chelate *N,O*-palladium(II) complexes: synthesis, characterization and biological activity. *RSC Adv.* 5, 86274–86281. doi: 10.1039/C5RA10204A

Pope, J. E., Hong, P., and Koehler, B. E. (2002). Prescribing trends in disease modifying antirheumatic drugs for rheumatoid arthritis: a survey of practicing Canadian rheumatologists. *J. Rheumatol.* 29, 255–260. Available online at: http://www.jrheum.org/content/jrheum/29/2/255.full.pdf

Pricker, S. P. (1996). Medicinal usage of gold compounds: past, present and future. *Gold Bull.* 29, 53–60. doi: 10.1007/BF03215464

Radisavljević, S., Bratsos, I., Scheurer, A., Korzekwa, J., Masnikosa, R., Tot, A., et al. (2018). New gold pincer-type complexes: synthesis, characterization, DNA binding studies and cytotoxicity. *Dalton Trans.* 47, 13696–13712. doi: 10.1039/c8dt02903b

Radisavljević, S., Ćoćić, D., Jovanović, S., Šmit, B., Petković, M., Milojević, N., et al. (2019). Synthesis, characterization, DFT study, DNA/BSA-binding affinity, and cytotoxicity of some dinuclear and trinuclear gold(III) complexes. *J Biol. Inorg. Chem.* 24, 1057–1076. doi: 10.1007/s00775-019-01716-8

Rescifina, A., Yagni, C., Varrica, M. G., Pistara, V., and Corsaro, A. (2014). Recent advances in small oganic molecules as DNA intercalating agents: synthesis, activity, and modeling. *Eur. J. Med. Chem.* 74, 95–115. doi: 10.1016/j.ejmech.2013.11.029

Roder, C., and Thomson, M. J. (2015). Auranofin: repurposing an old drug for a golden new age. *Drugs R. D.* 15, 13–20. doi: 10.1007/s40268-015-0083-y

Romero-Canelón, I., and Sadler, P. J. (2013). Next-generation metal anticancer complexes: multitargeting via redox modulation. *Inorg. Chem.* 52, 12276–12291. doi: 10.1021/ic400835n

Ronconi, L., Aldinucci, D., Dou, P. Q., and Fregona, D. (2010). Latest insights into the anticancer activity of Gold(III)-dithiocarbamato complexes. *Anticancer Agents Med. Chem.* 10, 283–292. doi: 10.2174/187152010791162298

Rosenberg, B., Vancamp, L., Trosko, J. E., and Mansour, V. H. (1969). Platinum compounds: a new class of potent antitumour agents. *Nature* 222, 385–386.doi: 10.1038/222385a0

Sadler, P. J. (1976). The biological chemistry of gold. *Gold Bull.* 9, 110–118. doi: 10.1007/BF03215415

Sadler, P. J., and Sue, R. E. (1994). The chemistry of gold drugs. *Metal Based Drugs* 1, 107–144. doi: 10.1155/MBD.1994.107

Sankarganesh, M., Raja, J. D., Revathi, N., Solomon, R. V., and Kumar, R. S. (2019). Gold(III) complex from pyrimidine and morpholine analogue Schiff base ligand: synthesis, characterization, DFT, TDDFT, catalytic, anticancer, molecular modeling with DNA and BSA and DNA binding studies. *J Mol. Liq.* 294:111655. doi: 10.1016/j.molliq.2019.111655

Savić, N. D., Milivojević, D. R., Glišić, B. D., Ilić-Tomić, T., Veselinović, J., Pavić, A., et al. (2016). A comparative antimicrobial and toxicological study of gold(III) and silver(I) complexes with aromatic nitrogen-containing heterocycles: synergistic activity and improved selectivity index of Au(III)/Ag(I) complexes mixture. *RSC Adv.* 6, 13193–13206. doi: 10.1039/c5ra26002g

Shaw, C. F. (1999). Gold-based therapeutic agents. *Chem. Rev.* 99, 2589–2600. doi: 10.1021/cr980431o

Shi, P., Jiang, Q., Zhao, Y., Zhang, Y., Lin, J., Lin, L., et al. (2006). DNA binding properties of novel cytotoxic gold(III) complexes of terpyridine ligands: the impact of steric and electrostatic effects. *J. Biol. Inorg. Chem.* 11, 745–752. doi: 10.1007/s00775-006-0120-y

Skibsted, L. H. (1986). *Advances in Inorganic and Bioinorganic Mechanisms*. (London, UK: Academic Press), 137–183.

Soave, C. L., Guerin, T., Liu, J., and Dou, Q. P. (2017). Targeting the ubiquitin-proteasome system for cancer treatment: discovering novel inhibitors from nature and drug repurposing. *Canc. Metastasis Rev.* 36, 717–736. doi: 10.1007/s10555-017-9705-x

Solomon, R. V., Jagadeesan, R., Vedha, S. A., and Venuvanalingam, P. (2014). A DFT/TDDFT modeling of bithiophene azo chromophores for optoelectronic applications. *Dyes Pigments* 100, 261–268. doi: 10.1016/j.dyepig.2013.09.016

Solomon, R. V., Veerapandian, P., Vedha, S. A., and Venuvanalingam, P. (2012). Tuning nonlinear optical and optoelectronic properties of vinyl coupled triazene chromophores: a density functional theory and time-dependent density functional theory investigation. *J. Phys. Chem. A* 116, 4667–4677. doi: 10.1021/jp302276w

Stojković, D., L., Jevtić, V. V., Radić, G. P., Dačić, D. S., Curčić, M. G., et al. (2014). Stereospecific ligands and their complexes. Part XII. Synthesis, characterization and *in vitro* antiproliferative activity of platinum(IV) complexes with some O,O′-dialkyl esters of (S,S)-ethylenediamine-N,N′-di-2-propanoic acid against colon cancer (HCT-116) and breast cancer (MDA-MB-231) cell lines. *J. Mol. Struct.* 1062, 21–28. doi: 10.1016/j.molstruc.2014.01.020

Sun, R. W. Y., and Che, C. M. (2009). The anti-cancer properties of gold(III) compounds with dianionic porphyrin and tetradentate ligands. *Coord. Chem. Rev.* 253, 1682–1691. doi: 10.1016/j.ccr.2009.02.017

Tabrizi, L., Zouchoune, B., and Zaiter, A. (2020). Theoretical and experimental study of gold(III), palladium(II), and platinum (II) complexes with 3-((4-nitrophenyl)thio) phenylcyanamide and 2,2′-bipyridine ligands: cytotoxic activity and interaction with 9-methylguanine. *Inorg.Chim. Acta* 499:119211. doi: 10.1016/j.ica.2019.119211

Tobe, M. L., and Burgess, J. (1999). *Inorganic Reaction Mechanisms*. Essex: Addison Wesley Longman Inc., 70–112.

Travnicek, Z., Starha, P., Vanco, J., Silha, T., Hosek, J., Suchy, P. Jr., et al. (2012). Anti-inflammatory Active Gold(I) complexes involving 6-substituted-purine derivatives. *J. Med. Chem.* 55, 4568–4579. doi: 10.1021/jm201416p

Wang, F. Y., Feng, H. W., Liu, R., Huang, K. B., Liu, Y. N., and Liang, H. (2019). Synthesis, characterization and antitumor activity of novel gold (III) compounds with cisplatin-like structure. *Inorg. Chem. Com.* 105, 55–58.doi: 10.1016/j.inoche.2019.04.031

Warren, G. L., Andrews, C. W., Capelli, A. M., Clarke, B., LaLonde, J., Lambert, M. H., et al. (2006). A critical assessment of docking programs and scoring functions. *J. Med. Chem.* 49, 5912–5931. doi: 10.1021/jm050362n

Williams, M., Green, A. I., Fernandez-Cestau, J., Hughes, D. L., O', Connell, M. A., Searcey, M., et al. (2017). (C^N^{pz}^C)Au^{III} complexes of acyclic carbine ligands: synthesis and anticancer properties. *Dalton Trans.* 46, 13397–13408. doi: 10.1039/C7DT02804K

Wu, C. H., Wu, D. H., Liu, X., Guoyiqibayi, G., Guo, D. D., Lv, G., et al. (2009). Ligand-based neutral ruthenium(II) arene complex: selective anticancer action. *Inorg. Chem.* 48, 2352–2354. doi: 10.1021/ic900009j

Zarić, M. M., Canović, P. P., Pirković, M. S., Knežević, S. M., živkovićZarić, R. S., Popovska Jovičić, B., et al. (2020). New gold pincer-type complexes induce caspase-dependent apoptosis in human cancer cells *in vitro*. *Vojnosanitetski Pregled*. doi: 10.2298/VSP190507002Z

Živanović, M. N., Košarić, J. V., Šmit, B., Šeklić, D. S., Pavlović, R. Z., and Marković, S. D. (2017). Novel seleno-hydantoin palladium(II) complex–antimigratory, cytotoxic and prooxidative potential on human colon HCT-116 and breast MDA-MB-231 cancer cells. *Gen. Physiol. Biophys*. 36, 187–196. doi: 10.4149/gpb_2016036

Conflict of Interest: The authors declare that the research was conducted in the absence of any commercial or financial relationships that could be construed as a potential conflict of interest.

frontiers in Chemistry

REVIEW
published: 30 June 2020
doi: 10.3389/fchem.2020.00543

Recent Advances of Gold Compounds in Anticancer Immunity

Shuang Yue, Miao Luo, Huiguo Liu† and Shuang Wei*†*

Department of Respiratory and Critical Care Medicine, Tongji Hospital, Tongji Medical College Huazhong University of Science and Technology, Wuhan, China

In recent years, gold compounds have gained more and more attentions in the design of new metal anticancer drugs. Numerous researches have reported that gold compounds, in addition to their widely studied cytotoxic antitumor effects, also reverse tumor immune escape and directly facilitate the functions of immune cells, leading to enhanced anticancer effects. This review mainly summarizes our current understandings of antitumor effects of gold drugs and their relationships with various aspects of antitumor immunity, including innate immunity, adaptive immunity, immunogenic cell death, and immune checkpoints, as well as their roles in adverse effects. Some recent examples of anticancer gold compounds are highlighted. The property of gold compounds is expected to combine with anticancer immunotherapy, such as immune checkpoint inhibitors, to develop new anticancer therapeutic strategies.

Keywords: gold compounds, innate immunity, adaptive immunity, immunogenic cell death, immune checkpoints

OPEN ACCESS

Edited by:
Wukun Liu,
Nanjing University of Chinese Medicine, China

Reviewed by:
Yunlong Lu,
University of Illinois at Chicago, United States
Ding Ma,
Kennedy Krieger Institute, United States

****Correspondence:***
Huiguo Liu
huiguol@163.com
Shuang Wei
wsdavid2001@163.com

† These authors have contributed equally to this work

Specialty section:
This article was submitted to Medicinal and Pharmaceutical Chemistry, a section of the journal Frontiers in Chemistry

Received: *24 April 2020*
Accepted: *27 May 2020*
Published: *30 June 2020*

Citation:
Yue S, Luo M, Liu H and Wei S (2020) Recent Advances of Gold Compounds in Anticancer Immunity. Front. Chem. 8:543. doi: 10.3389/fchem.2020.00543

INTRODUCTION

From the accidental discovery of cisplatin's antitumor activity by Rosenberg and his coworkers, platinum-based complexes have been used as standard chemotherapeutic agents more than 40 years in clinical practice (Rosenberg et al., 1969). However, we found that platinum-based complexes are only effective against limited types of tumors and have a variety of serious side effects (such as gastrointestinal, nervous system toxicity and bone marrow suppression) (Hartmann and Lipp, 2003; Wang and Guo, 2013; Stojanovska et al., 2015, 2017; Oun et al., 2018). Additionally, intrinsic and acquired drug resistance attenuate the effectiveness of these agents (Martinez-Balibrea et al., 2015). For this reason, more efforts are urgently needed to explore novel anti-tumor metallodrugs to substitute the widely used platinum complexes. Many new metal complexes have been reported to have antitumor effects including gold, silver, copper, ruthenium and other active metals. Among them, coinage metals (especially Au and Ag) have shown greater application potential because they are less toxic to human body than other transition metals. Gold compounds deserve particular attention, from the view of chemical, because the unique position of gold in the periodic table, which ultimately leads to the highest electronegativity, electron affinity as well as redox potential compared to other metals. Gold compounds exert cytotoxic effects by inhibiting thiol-containing enzymes, especially TrxR (Liu and Gust, 2013; Ortego et al., 2014; Bian et al., 2019, 2020a,b; Fan et al., 2019), damaging mitochondrial (Rigobello et al., 2002; Rackham et al., 2007) and DNA function (Messori et al., 2005; Patel et al., 2013), all of which may contribute to their clinical anticancer activity. Recently, many groups have found that auranofin, a gold compound widely used in antirheumatic therapy (Sadler and Sue, 1994; Shaw, 1999), also has anticancer, antibacterial and other properties (Marzano et al., 2007; Fiskus et al., 2014; Harbut et al., 2015; Diez-Martinez et al., 2016; Thangamani et al., 2017; AbdelKhalek et al., 2019; Onodera et al., 2019; Raninga et al., 2020).

Therefore, there is growing interest in the investigation of gold compounds with new applications. Although no non-platinum metal compounds have been approved for cancer treatment, a number of gold drug candidates are being considered. Some novel gold compounds have shown promising results in preclinical researches (Ott and Gust, 2007).

Cancer immunotherapy is a promising research field and is gaining more and more attention from the scientific community. Recent immune checkpoint inhibitors are starting a golden age of tumor immunotherapy. In the early days, based on clinically observed chemotherapy-induced myelosuppression and lymphocytopenia (Grossman et al., 2015; Cao et al., 2016; Kamimura et al., 2016; Oun et al., 2018), it is taken for granted that the primarily effect of chemotherapy on the immune system is immunosuppression. Interestingly, Taro Shimizu and his coworkers (Shimizu et al., 2017) found that liposomal oxaliplatin could significantly suppress the growth of neoplasms implanted in immunocompetent murine, but not in immunodeficient murine. The phenomenon was also observed in other groups using different mice tumor models and mice strains with metal-based compounds (Tesniere et al., 2010; Jungwirth et al., 2012; Chang et al., 2013). Hence, we propose a hypothesis that in addition to the classical DNA damage pattern of platinum complexes, the immune system may increase the antitumor activity of these drugs in a synergistic manner. Furthermore, although gold is clinically used for immune suppression (in rheumatoid arthritis), it can also produce toxicities resulting from immune stimulation (Merchant, 1998). The use of gold drugs is often accompanied by adverse immune reactions including diverse forms of dermatitis, glomerulonephritis, cytopenias, hepatitis and pneumonitis (Havarinasab et al., 2007). A series of literatures have shown that gold compounds may stimulate an anticancer immune response. What are the complicated interactions between gold compounds and the immune system? However, The intricate interrelationships of gold compounds with the immune system and the underlying molecular biological mechanisms are unclear.

Given the revolutionary achievement of platinum-based complexes, it is not surprising that the field of inorganic medicinal chemistry has been predominated by researches on the antitumor activity of metal complexes. Particularly, the preparation of novel gold compounds for cancer therapy has been accelerating in recent decades, and a large number of research reports are published every year. In this review, we aim to summarize the complex relationship between various gold derivatives and immune system, and the role of immune system in their anticancer activity as well as adverse effects, in order to explore their novel applications in cancer combination immunotherapy.

IMMUNE SURVEILLANCE AND IMMUNE EVASION

Before introducing the anticancer immune activity of gold compounds, an overview on the general aspects of the body's immune response and the main players in the immune system are given in the following.

The body's immune system is equipped with elaborate innate and adaptive immune mechanisms devoted to effectively recognize and eliminate pathogens as well as preventing malignant transformation ("immune surveillance") (see **Figure 1**) (Chen and Mellman, 2013). Innate immunity is the body's first line of defense against foreign pathogens invasion, which is a rapid non-specific immune response to pathogens. Prominent among these are monocytes/macrophages, neutrophilic granulocytes (neutrophils), natural killing (NK) cells as well as dendritic cells (DC). During their patrols, innate immune cells may sense changes of molecular patterns in the malignant tissue, which is called as damage-associated molecular patterns (DAMP) or alarmins. Pattern recognition receptors (PRR) on the surface of immune cells mainly include the toll-like receptors (TLRs), which mediate the recognition, killing or phagocytosis of abnormal cells. At the same time, both are accompanied by immune-stimulating inflammation. In addition to PRR, the phagocytosis of cancer cells may be triggered by the opsonization of antibodies and complement on the cell surface. The T cell anticancer immune cycle is a process of self-proliferation and self-amplification, which connects innate immunity and adaptive immunity in a highly complex fashion, leading to antigen-specific T cell-mediated immune response. Professional antigen presenting cells (APC), especially DC, play a key role in activating specific anticancer immune responses. When they patrol the (pre)malignant tissue, they may sense a change of molecular patterns known as so-called DAMP. The activated DC migrates to the tumor draining lymph nodes and presents tumor-specific antigens to naive CD8 + or CD4 + T cells by MHC class I or MHC class II molecules, respectively ("first" signal). Additionally, under the action of costimulatory signals ("second" signal, including the coaction of B7-type CD80/86 receptor on DC with CD28 on T lymphocytes) and cytokines ("third" signal, such as IL-2 and IL-12), activated T lymphocytes travel to the (pre)neoplastic tissue through the bloodstream, and followed by specific destruction of (pre)neoplastic cells expressing the respective tumor-specific antigens.

However, cancer cells have evolved multiple immune-regulatory mechanisms to evade recognition and destruction of the innate and adaptive immune systems, leading to the development of clinical tumors ("immune escape") (see **Figure 1**). For example, cancer cells may elude recognition of innate immune cells (including macrophages, neutrophils) by upregulating "don't eat me" signals such as CD47 or CD73 (Chao et al., 2010). Malignant cancer cells can evade the recognition and destruction of cytotoxic T cells (CD8+T cells or CTL) by down-regulating the expression of MHC class I molecules (Bradley et al., 2015). More recently, the perspective of immune checkpoints has been proposed, including programmed-death/programmed-death ligand 1 (PD1/PD-L1) system, cytotoxic T-lymphocyte-associated protein 4 (CTLA-4). Blocking inhibitory receptors or ligands through immune checkpoint inhibitors is one of the most successful and promising anticancer immunotherapy strategies so far. The

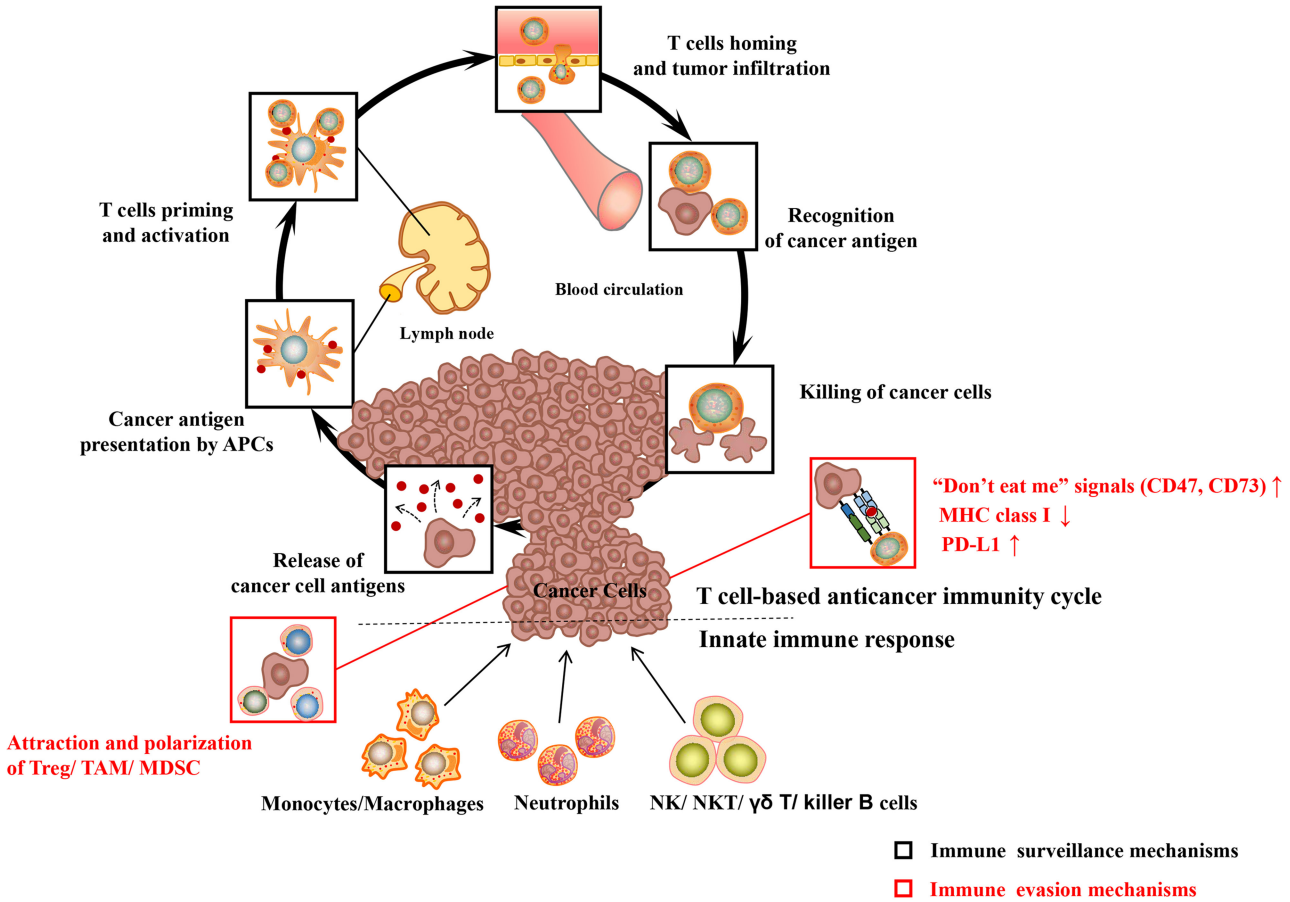

FIGURE 1 | Major cancer immune surveillance and immune evasion mechanisms. For detailed description see text. APCs, antigen presenting cells; MHC class I, major histocompatibility complex class I; PD-L1, programmed death-ligand 1; Treg, regulatory T cell; MDSC, myeloid-derived suppressor cell; TAM, tumor-associated macrophages; NK cell, natural killer cell; NKT cell, natural killer T cell. Adapted from Chen and Mellman (2013).

PD-L1 expressed on the surface of tumor cells is able to combine with the inactivating receptor PD1 on adaptive immune T cells, thus leading to their deactivation and CTL anergy. A large number of researches indicate that the high expression of PD-*L1* on cancer cells leads to the anergy and exhaustion of T cells, which restricts CTL from effectively targeting cancer cells (Zhang et al., 2018a). In the development of cancer, tumor cells can attract regulatory immune cells (including regulatory T cell, tumor-associated macrophages) to the tumor microenvironment (TME), which is dominated by immunosuppressive myeloid cell types, through the production of immunosuppressive chemokines (such as CCL2) (Muenst et al., 2016). In addition, cancer cells can induce the polarization of immune cells into immunosuppressive phenotypes, such as M2 macrophages (via CSF-1), TH 2 cells, and regulatory T cells (via TGF-β, IL-10) (Murray et al., 2014; Noy and Pollard, 2014). In conclusion, cancer cells have evolved multiple ways to escape the recognition and damage of innate and adaptive immune systems. Hence, more efforts have been focused on enhancing the body's anti-tumor immune response with regard to the current cancer immunotherapy.

A lot of evidence from experimental and clinical studies suggest that the antitumor mechanisms of gold compounds are extremely complex and diverse. Recently, it has been reported that gold compounds may have a potential relationship with anti-tumor immunity. Gold chemotherapy drugs, in addition to their widely studied cytotoxic antitumor effects, might reverse important aspects of tumor immune escape and directly affect several types of immune cells, leading to enhanced anticancer effects. In this article, we will summarize the relationship between gold compounds and various aspects of antitumor immunity, including innate immunity, adaptive immunity, immunogenic cell death, and immune checkpoints.

ANTITUMOR IMMUNE EFFECTS OF GOLD COMPOUNDS

Gold Compounds and Innate Immune System

The immune-regulatory effects of gold drugs have been comprehensively reviewed in the literatures concerning

rheumatoid arthritis as well as other immune-related diseases, such as HIV and malaria (Griem and Gleichmann, 1996; Madeira et al., 2012; Nardon et al., 2016). **Figure 2** shows the chemical structure of several common gold compounds. Several common metals (such as gold, nickel, copper, and mercury) have been found to have the ability to stimulate innate immunity (Suzuki et al., 2011; Rachmawati et al., 2015a). A series of *in vitro* and *in vivo* studies have shown that gold compounds can not only promote direct immune cell-mediated destruction, but also synergistic promote the T cell-based anticancer immunity cycle via DC (see **Figure 3**). The complex mechanisms of the effects of gold compounds on the innate immune system are summarized in **Table 1**. Gold compounds can induce cancer cells destruction through various forms of cytotoxic action, leading to the expression of proteins on the cell surface, secretion of cytokines, or rupture of the plasma membrane and release of intracellular substances. Released cytoplasmic molecules are danger signals, known as DAMPs, which enable the immune system more sensitive to the recognition of tumor antigens. Rachmawati et al. reported that the gold compound ($Na_3Au(S_2O_3)2{\cdot}_2H_2O$, **Figure 2D**) induced substantial release of the pro-inflammatory mediator IL-8 from DC, PBMC, and THP-1 cells and expression of CD40 on the surface of DC, indicating DC's maturation and adaptive immune stimulatory capacity. The ability of this gold compound to induce innate immune responses can be attributed to TLR3 dependent signaling (Rachmawati et al., 2015b). I. Stern et al. observed the effects of auranofin (**Figure 2A**), gold sodium thiomalate (**Figure 2C**), and HAuCl4 [Au (III)] (**Figure 2E**) on the ability of LPS-induced THP1 monocytes to secrete key inflammatory cytokines (IL6, IL8, IL10, and TNF α) *in vitro*. The results showed that sub-lethal concentrations of the three gold compounds could differentially modulate activation of monocytes. Among them, the effect of auranofin was slightly stronger (Stern et al., 2005). Another study suggested that the activation of monocytes may be related to the success of gold compounds in the treatment of rheumatoid arthritis (Hurst et al., 1986). Mast cells play key roles in allergic and inflammatory responses. There is considerable evidence that mast cells are important for adaptive and innate immunity (Galli et al., 2005), as well as the development of autoimmune diseases (Costela-Ruiz et al., 2018). In a previous review, gold, mercury, and silver all had effects on mast cell signaling, function, and survival, inducing aberrant immunological responses. All these compounds stimulated mast cells to degranulate and secrete arachidonic acid metabolites as well as cytokines such as interleukin-4 (Suzuki et al., 2011). HAuCl4 [Au (III)] at a non-toxic concentration ($\leq$50 μM) stimulated large amounts of degranulation and leukotriene C4 secretion in mast cells by a $Ca2^{+}$-dependent manner (Hayama et al., 2011). It has been reported that auranofin has a dose-dependent bidirectional effect on NK cell activity, enhancing NK cell activity at low dose and inhibiting NK cell activity at high dose *in vitro* (Russell et al., 1982; Pedersen and Abom, 1986). However, as for TLR signaling, Youn et al. found that auranofin suppressed LPS-induced homodimerization of TLR4 and TLR4-mediated activation of key transcription factors (such as NF-κB, IRF3, and COX-2) in mice pro-B as well as monocytic cell lines. In addition, auranofin also inhibited NF-κB activation induced by MyD88-dependent downstream signaling elements of TLR4, MyD88, IKKβ, and p65 (Youn et al., 2006). Auranofin suppressed multiple steps in TLR4 and downstream signaling, thereby inhibiting immune inflammation. The experimental results of Wang et al. showed that disodium aurothiomalate could inhibit the activity of CD45, a protein-tyrosine phosphatase expressed on all white blood cells, which could enhance the signaling of B and T cell antigen receptors (Wang et al., 1997).

Gold compounds have also been shown to affect some important signaling pathways and key transcription factors. The NF-κB and protein kinase C (PKC) signaling pathways play a key role in the process of activation, differentiation, and maturation of myeloid and lymphatic cells. NF-κB is a key transcription factor involved in the expression of many inflammatory genes and plays an important role in oncogenesis, which is associated with the proliferation of multiple types of tumors (Zeligs et al., 2016). There are growing interests in exploring novel regulators to inhibit NF-κB activation, because blocking different steps of NF-κB signaling pathway may slow tumor growth, progression, and chemotherapy resistance. Auranofin suppresses nuclear translocation of NF-κB by blocking IκB kinase (IKK) activation in macrophages. This inhibitory activity may be related to the suppression of TNF-α (Jeon et al., 2000). It also has been reported that auranofin inhibits NF-κB activation by modifying Cys-179 of IKKβ subunit in monkey kidney (COS-7) cells as well as LPS-stimulated macrophages (Jeon et al., 2003). Aurothioglucose (**Figure 2F**) has a strong inhibitory effect on the DNA binding activity of NF-κB, which is essential for its performance (Yang et al., 1995). The PKC activity was shown to be inhibited by auranofin as well as gold sodium thiomalate in human neutrophils (Parente et al., 1989).

However, gold (I) compounds have been clinically used to treat rheumatoid arthritis due to their anti-inflammatory properties, which appears contradictory to its immune stimulatory activity. This intrigues clinicians and toxicologists for many years. Anyway, the gold paradox is not unique, steroids are also known to have both immunostimulatory and immunosuppressive effects. Radka et al. reported a series of gold(I)-triphenylphosphine compounds (**Figure 2H**) with hypoxanthine-derived ligands. These complexes inhibited the secretion of pro-inflammatory cytokines, such as tumor necrosis factor-α (TNF-α) and interleukin-1β (IL-1β), in the lipopolysaccharide-activated macrophage-like THP-1 cell model (Krikavova et al., 2014). Gold sodium thiomalate (GST, **Figure 2B**) inhibited release of the key endogenous mediators of HMGB1 translocation, IFN-beta and NO, thus reducing the extracellular release of HMGB1 in murine RAW 264.7 and human THP-1 macrophages *in vitro* (Zetterstrom et al., 2008). The differential effects of gold compounds on the immune system may be related to drug dose, duration, cell lines, ligand composition, as well as the oxidation state of Au. The differences in the patterns of action of gold compounds between inflammation and cancer are not clear. The suppression of cancer-promoting inflammation has been presumed as one of the main mechanisms in the antitumor activity of gold compounds (Madeira et al., 2012). The anti-inflammatory

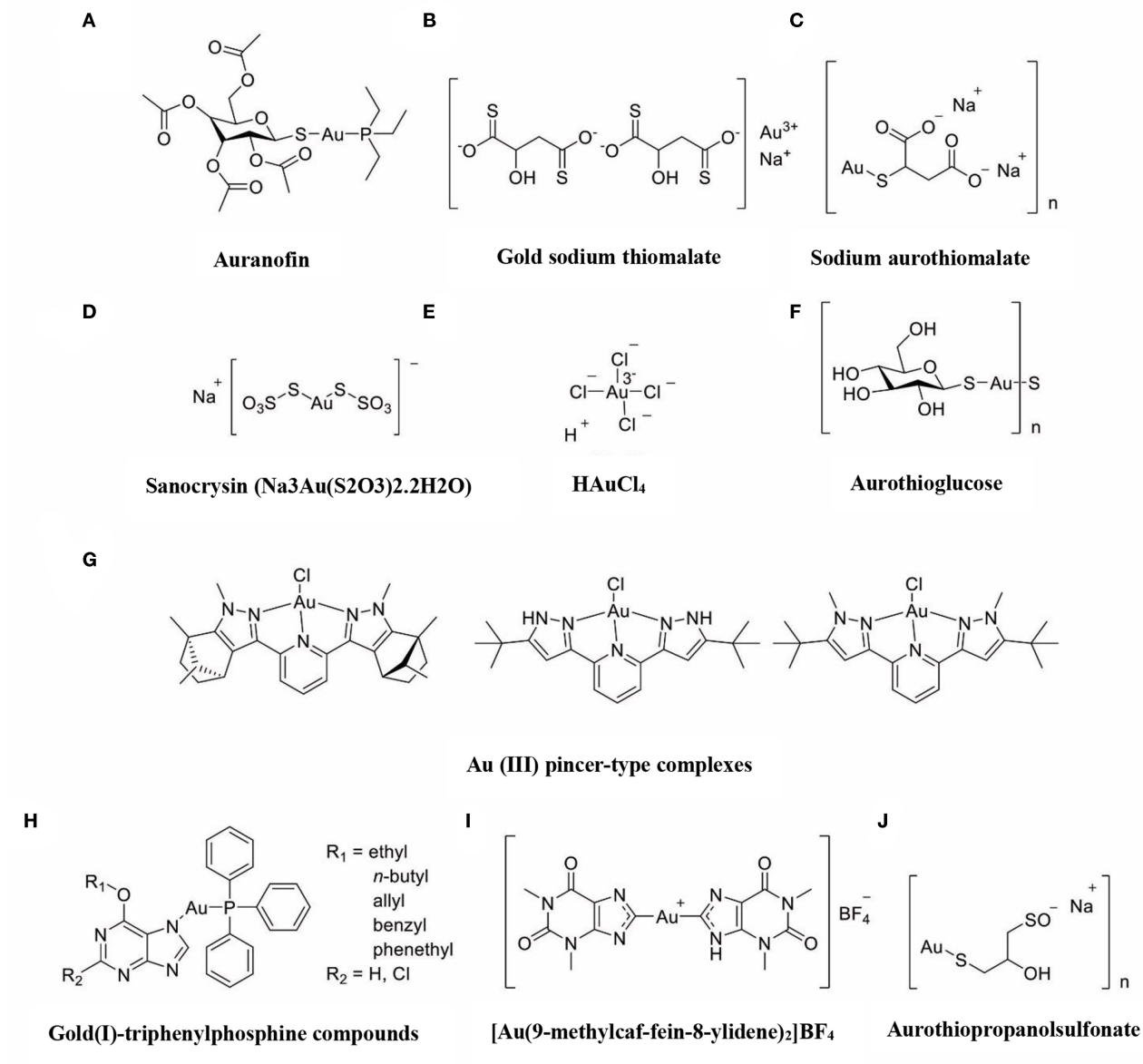

FIGURE 2 | The chemical structure of several common gold compounds. **(A)** Auranofin; **(B)** Gold sodium thiomalate; **(C)** Sodium aurothiomalate; **(D)** Sanocrysin $Na_3Au\ (S_2O_3)_2{\cdot}2H_2O$; **(E)** HAuCL4; **(F)** Aurothioglucose; **(G)** Au(III) pincer-type complexes; **(H)** Gold(I)-triphenylphosphine compounds; **(I)** [Au(9-methylcaf-fein-8-ylidene)2]BF4; **(J)** Aurothiopropanolsulfonate.

and anticancer activities of gold compounds may involve similar cytokines and molecular pathways but the degree of induction varies (Yamamoto and Gaynor, 2001). In addition to the inhibition of TLR signaling and NF-κB signaling pathway mentioned above, auranofin also reduces TNF-α synthesis and secretion, decreases STAT-3 transcription activity as well as inhibits angiogenesis (Kim et al., 2007; Han et al., 2008a), which are related to tumor growth and development. Pro-inflammatory cytokines like interleukins (IL) are wildly known to be related to malignant progression and metastasis in multiple types of tumors, by regulating the expression of matrix metalloproteinases (MMP) and angiogenic proteins growth factors including VEGF (Quail and Joyce, 2013). Auranofin and the heterobimetallic Ru-Au compound (RANCE-1) have a strong inhibition of several cytokines (IL-6, IL-5, IL17A, and IL-8) in Caki-1 renal cancer cells (Elie et al., 2018). Auranofin also decreased the production of nitric oxide (NO) as well as the pro-inflammatory cytokines (TNF-α, IL-1β and IL-6) in macrophages (Han et al., 2008a). The development and evolution of tumors are associated with a series of inflammatory pathways. The blocking of several inflammatory pathways associated with tumor development has a promising potential to promote its anticancer activity, although the direct effects of gold compounds on innate immune cells have been little studied. Given the promising anticancer activity of gold compounds in many types of tumors, the role of immuno-regulatory and

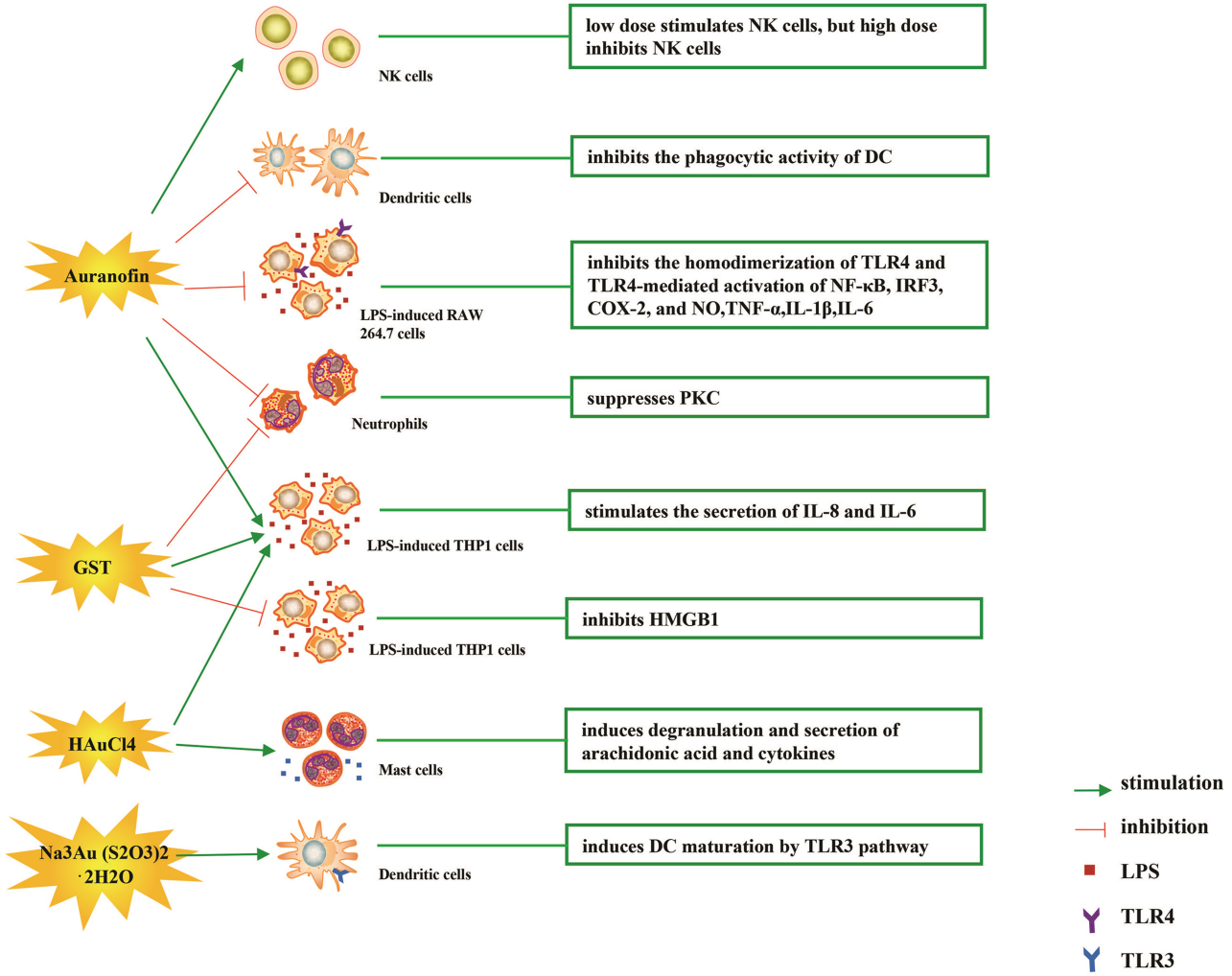

FIGURE 3 | Effects of several major gold complexes on innate immune system. gold compounds can not only promote direct immune cell-mediated destruction, but also synergistic promote the T cell-based anticancer immunity cycle via DC. Gold complexes can induce the activation and proliferation of NK, mast cells, monocytes/macrophages, neutrophils, and release of various inflammatory mediators. Furthermore, gold complexes induce DC maturation and enhance antigen presentation through TLR3 dependent signaling. For detailed description see text. NK cell, natural killer cell; DC, dendritic cell; LPS, lipopolysaccharide; TLR, toll-like receptor; TNF-α, tumor necrosis factor α; IL, interleukin; AuTM, sodium aurothiomalate; GST, gold sodium thiomalate; PKC, protein kinase C; HMGB1, high mobility group box chromosomal protein 1.

anti-inflammatory effects needs to be further investigated at the experimental level.

Gold Compounds and Adaptive Immune System

Figure 4 illustrates various aspects of the effect of gold compounds on the adaptive immune system. Gold compounds can enhance the antigenicity of cancer cells. The body's adaptive immune system is able to identify "non-self" antigens through MHC class I presentation of mutation derived immunogenic neoantigens or viral peptides (in virus-induced tumor) by the malignant cells. This is closely related to anticancer metal chemotherapy drugs which are believed to have mutagenesis in many cases. Indeed, the increased number of mutations as well as translocations would support adaptive immune system to identify "non-self" malignant neoantigens (Siniard and Harada, 2017). Although the interaction between gold-based drugs and DNA is weaker than that of platinum, they also induce some mutations. A panel of new Au (III) complexes with pincer type ligands (**Figure 2G**) had moderate binding affinity with calf thymus DNA (CT DNA), and molecular docking showed that they interacted with DNA by insertion (Radisavljevic et al., 2018). By a joint ESI MS and X ray diffraction (XRD) methods, the dicarbene gold(I) compound [Au(9-methylcaf-fein-8-ylidene)2] BF4 (**Figure 2I**) had a tight binding to Tel 23 DNA G-quadruplex (telomeric nucleic acid sequences with rich guanines) and formed stable adducts (Bazzicalupi et al., 2016). The complex interactions between gold compounds and DNA, including

TABLE 1 | Effects of gold compounds on innate immune system.

Gold compounds	Mechanism of action	Cell or animal models	Reference
Auranofin	Low dose stimulates NK cells, but high dose inhibits NK cells	NK cells	Russell et al., 1982; Pedersen and Abom, 1986
	Inhibits the homodimerization of TLR4 and TLR4-mediated activation of key transcription factors (NF-κB, IRF3, COX-2)	Murine pro-B, RAW264.7, 293T, COS-7cells	Jeon et al., 2003; Youn et al., 2006
	Suppresses PKC	Human neutrophils	Parente et al., 1989
	Activates monocytes to secrete key inflammatory cytokines (IL6, IL8)	THP1 cells	Stern et al., 2005
	Inhibits NO and pro-inflammatory cytokines (TNF-α, IL-1β and IL-6)	RAW 264.7	Han et al., 2008a
GST	Activates monocytes to secrete key inflammatory cytokines (IL6, IL8)	THP1 cells	Stern et al., 2005
	Inhibits PKC, HMGB1 translocation, IFN-beta, NO, and the release of HMGB1	RAW 264.7, THP-1 cells	Parente et al., 1989; Zetterstrom et al., 2008
AuTM	Activates monocytes and enhances release of superoxide	Human monocytes	Hurst et al., 1986
	Inhibits CD45		Wang et al., 1997
$Na_3Au\ (S_2O_3)_2{\cdot}2H_2O$	Induces release of IL-8, and expression of CD40 on the surface of DC	DC, PBMC, THP1 cells	Rachmawati et al., 2015b
HAuCl4 [Au(III)]	Stimulates monocytes to secrete IL6, IL8, and mast cells to degranulate and secrete arachidonic acid metabolites and cytokines (such as IL-4)	THP1, RBL-2H3, HMC-1 cells	Stern et al., 2005; Hayama et al., 2011; Suzuki et al., 2011
Aurothioglucose	Inhibits the DNA binding activity of NF-κB		Yang et al., 1995
Gold(I)-triphenylphosphine compounds	Inhibits pro-inflammatory cytokines (TNF-α IL-1β)	THP-1 cells	Krikavova et al., 2014

AuTM, sodium aurothiomalate; GST, gold sodium thiomalate; NK cell, natural killer cell; DC, dendritic cell; TLR, toll-like receptor; TNF-α, tumor necrosis factor α; HMGB1, high mobility group box chromosomal protein 1; IL, interleukin; PKC, protein kinase C; IFN, interferon.

insertion, covalent binding, and even unobserved ways of acting, generate a number of damaged DNA cells and even induce the DNA mutation when the self-repair mechanisms dysfunction, thus exposing more neoantigens. According to a research by Kazuo and his co-workers, pretreatment with Au(III) complex of a model protein antigen (bovine ribonuclease A) induced novel antigen peptide recognized by $CD4^+$ T cells (Takahashi et al., 1994) (**Table 2**).

Interestingly, gold compounds also stimulate the activation and proliferation of T as well as B cells (see **Table 2**). The mice treated with organic gold compounds showed immune stimulation, which was manifested as plaque-forming cells, rosette-forming cells, and serum antibody elevation (Measel, 1975). Some studies indicated that aurothiopropanolsulfonate (**Figure 2J**) could also enhance the antigen-specific IgE immune response in mice (Kermarrec et al., 1996). Gold, in the form of natrium aurothiomaleate (GSTM), had a strong B cell-stimulating effect, including T helper 1 (Th1)- and Th2- isotypes (Havarinasab et al., 2007). Moreover, Walz et al. found that the stimulatory effects of auranofin and GST on cell-mediated immunity as evidenced by oxazolone-induced contact sensitivity as well as delayed hypersensitivity to sheep red blood cells (DH-SRBC). Their results showed that gold in the form of auranofin was approximately 4 times more effective in stimulating cellular immunity than gold in the form of GST (Walz and Griswold, 1978). Gold salt (HAuCl4) stimulated $CD4^+$ T and $CD8^+$ T cell activation as well as promoted the secretion of IFN-γ in rats (Savignac et al., 2001). What's more, disodium aurothiomalate interfered with antigen presentation and $CD4^+$ T cell activation by binding peptides containing cysteine residues (Griem et al., 1995). GST preferentially inhibited B cells at much lower concentrations than required for T cells interference (Hirohata, 1996).

Furthermore, it is well-known that cancer cells tend to reduce MHC class I expression to prevent tumor-specific CTL clone cells from recognizing neoantigens or "tumor-associated antigens" (TAA) during immune evasion. Several researches have shown that metal-based treatment (like platinum) might increase the expression of MHC class I in cancer cells (Ohtsukasa et al., 2003; Gameiro et al., 2012). To our surprise, there is little research with regard to the specific effects of gold compounds on MHC expression. It's reported that GST stimulated the up-regulation of MHC class II expression at low concentration, but it was inhibited at high concentration (Sanders et al., 1987). Auranofin inhibited MHC class I and MHC class II-restricted antigen presentation in dendritic cells of mice (Han et al., 2008b). In addition, various papers have showed that metal nanoparticles (NPs) including gold, silver, nickel, and iron oxide are able to increase the immunogenicity of antigens (Niikura et al., 2013; Orlowski et al., 2018). A study by Piotr and his co-workers demonstrated that tannic acid-modified silver and gold nanoparticles (TA-Ag/AuNPs) stimulated DCs maturation, TLR9 expression and memory CD8+T cells activation, and helped to overcome virus-induced suppression of DCs activation by up-regulation of MHC II and CD 86 expression (Orlowski et al., 2018). We speculate that gold compounds can also enhance antigen presentation by up-regulating MHC expression, which requires more efforts to explore. All of this suggests that gold

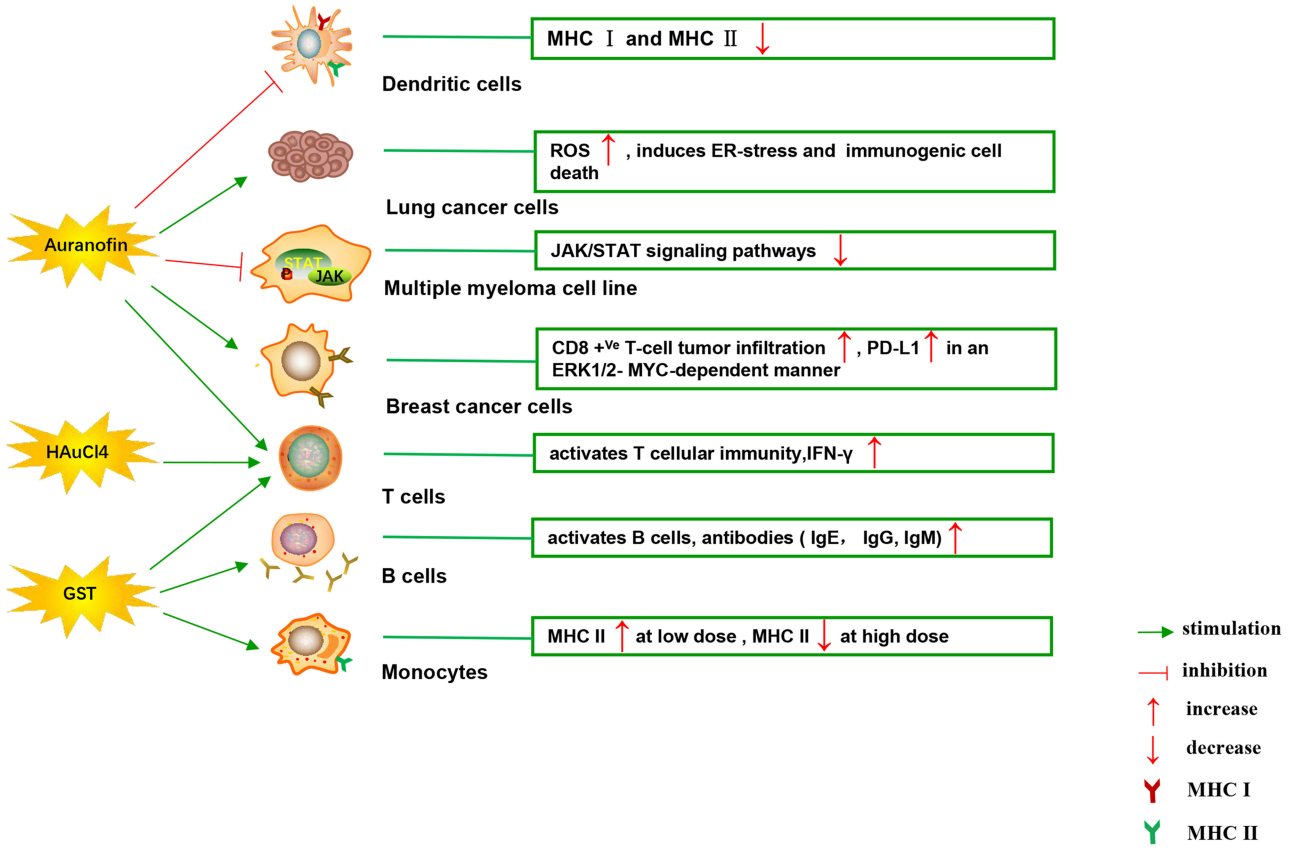

FIGURE 4 | Effects of several major gold complexes on adaptive immune system. Gold compounds stimulate the activation and proliferation of B cells and T cells. Antigen presenting cells (mainly dendritic cells) presents tumor antigens to T lymphocytes to initiate antigen-specific T cell immune responses. Gold derivatives can regulate the level of MHC class I and MHC class II molecules, and up-regulate the expression of PD-L1 on the surface of cancer cells. For detailed description see text. MHC, major histocompatibility complex; ROS, reactive oxygen species; ER-stress, endoplasmic reticulum stress; PD-L1, programmed death-ligand 1; GST, gold sodium thiomalate.

is a promising immune-regulator whose multiple effects on the adaptive immunity remain to be discovered (**Table 2**).

Gold Compounds Induce Immunogenic Cell Death

It is currently accepted that, in certain settings, chemotherapy drugs are able to activate the entire anticancer immune cycle and even cause a persistent immunological anticancer memory by inducing tumor cells death. This ideal form of tumor chemotherapy-induced cell death is known as immunogenic cell death (ICD) (Englinger et al., 2019). The conception of ICD was first proposed in 2005 in the context of antitumor chemotherapy, and based on the observation that mice colon tumor cells with anthracycline doxorubicin treatment *in vitro* were able to induce an effective anticancer vaccination reaction that inhibited the growth of inoculated cancers or caused the regression of the established tumor (Casares et al., 2005). Under normal physiological conditions, the process of apoptosis is immunologically "silent" and includes an efficient engulfment by phagocytes to prevent the release of intracellular components that activate inflammation and autoimmune responses. In contrast, ICD in cancer therapy induces immune-stimulatory rather than immunosuppressive reaction. ICD is able to reverse several crucial aspects of immune evasion, thus re-inducing the immune recognition of tumor cells. Generally, apoptotic cancer cells expose "find me" and "eat me" signals to attract innate immune cells (especially DCs), leading to the phagocytosis of apoptotic cells and antigen presentation. The initiation of ICD is based on several different molecular mechanisms in the dying tumor cells, mainly by endoplasmic reticulum (ER) stress- and autophagy-mediated release of DAMP molecules, including the protein chaperones calreticulin (CRT), the nucleotide ATP, DNA damage sensitizer HMGB1, CXCL10 as well as HSP70/90 (Terenzi et al., 2016).

The generation of ER stress mediated by ROS is the core of ICD induction, thus leading to the classification of ICD inducers into two categories. Type I ICD inducers exert multiple cytotoxic effects and trigger ER stress as a secondary mode of action, while type II inducers mediates ROS-related ER-stress as the main mechanism of action (Garg et al., 2015). By far most of the ICD inducers used in clinical anticancer chemotherapy belong to type I class, such as anthracyclines and mitoxantrone, the glycopeptide

TABLE 2 | Effects of gold compounds on adaptive immune system.

Gold compounds	Mechanism of action	Cell or animal models	Reference
Auranofin	Stimulates T effector and T suppressor lymphocytes	C57Bl mice	Walz and Griswold, 1978
	Inhibits MHC class I and MHC class II	DC2.4 cells, BM-derived DCs	Han et al., 2008a
Au (III) pincer-type complexes	Insert DNA and interfere with the cell cycle	A549, A375, and LS-174 cells	Radisavljevic et al., 2018
Dicarbene gold(I) complex	Forms stable adducts with Tel 23 DNA G-quadruplex		Bazzicalupi et al., 2016
GST	Activates B cell and antibody (IgE, IgG, IgM) production	BALBc, C_sH, C57Bl, AKR mice	Measel, 1975; Havarinasab et al., 2007
	Stimulates T effector and T suppressor lymphocytes	C57Bl mice	Walz and Griswold, 1978
	Low dose promotes MHC II, but high dose inhibits MHC II	human monocytes	Sanders et al., 1987
Aurothiopropanolsulfonate	Enhances the antigen-specific IgE immune response	Brown-Norway (BN) rats	Kermarrec et al., 1996
$HAuCl_4$	Activates CD4+T and CD8+T cell, and promotes release of IFN-γ	BN rats	Savignac et al., 2001
Gold nanoparticles	Promotes the immunogenicity of antigens, DC maturation, TLR9 expression, memory CD8+T cells activation, MHC II and CD 86 expression	BMDCs, and RAW264.7, GMK-AH1, JAWSII cells	Niikura et al., 2013; Orlowski et al., 2018

MHC, major histocompatibility complex; DC, dendritic cell; GST, gold sodium thiomalate; IFN-γ, interferon-γ; TLR, toll-like receptor.

bleomycin, the alkylating agent cyclophosphamide, bortezomib, as well as the metal-based agent oxaliplatin (Tesniere et al., 2010; Kroemer et al., 2013; Sun et al., 2019; Zhou et al., 2019). Although type II ICD inducers are rare, they have recently been identified in preclinical metal-containing compounds (Wong et al., 2015). Although some similarities between oxaliplatin and cisplatin, it is surprising that only the former has been reported as a true ICD inducer (type I) (Tesniere et al., 2010). The specific relationship between the ICD-inducing capacity of metal complexes and their structure and mode of action is unclear. Interestingly, multiple antitumor metal drugs, such as gold (Marmol et al., 2017; Huang et al., 2018), copper (Bortolozzi et al., 2014; Yang et al., 2017), iron (Liu and Connor, 2012; Kim et al., 2016), arsenic (Chiu et al., 2015), ruthenium (Flocke et al., 2016; Jayanthi et al., 2016), osmium (Suntharalingam et al., 2013), and iridium (Cao et al., 2013) complexes have been shown to activate a number of ICD markers involving ROS production, unfolded protein response (UPR) and ER stress. Considering the overexpression of the ROS, protein damage, UPR and ER stress also as mechanisms of action of gold compounds, it is reasonable to believe that there are more types I and II gold-based ICD inducers. Auronafin induced a concentration-dependent increase of cellular ROS in human lung cancer cell lines (A549) (Hou et al., 2018). Alkynyl gold(I) complex was able to disrupt mitochondrial normal function and induced the production of ROS, which triggered necroptosis in the colorectal adenocarcinoma (Caco-2) cell line (Marmol et al., 2017). Organometallic gold(III) complexes induced ER-stress-related apoptosis as well as pro-death autophagy in lung cancer (A549) cells, allowing lower toxicity and better antitumor activity in murine tumor model comparing with cisplatin (Huang et al., 2018). It has been reported that accumulated lethal DNA double strand breaks due to the increase of ROS render ovarian cancer cells more sensitive to auranofin in a BRCA1-deficient background. Furthermore, the antioxidant N-acetyl cysteine (NAC) protected BRCA1-deficient cells from auranofin-induced DNA damage and apoptosis (Oommen et al., 2016). Strikingly, the ICD induction ability of the experimental and clinically used gold compounds has not been systematically and fully identified so far.

Gold Compounds and Immune Checkpoints

Immune checkpoints can negatively regulate T-cell immunity. The discovery of immune checkpoint inhibitors has opened up new clinical possibilities for anticancer immunotherapy. Among them, programmed death receptor 1 (PD-1) and cytotoxic T lymphocyte antigen 4 (CTLA-4) are the most commonly studied. PD-1 is mainly expressed on the surface of activated T cells, B cells, as well as NK cells. The activation of PD-1 suppresses the phosphatidylinositol 3-kinase (PI3K)/Akt signaling pathway, leading to the inhibition of survival and proliferation of T cells (Pedoeem et al., 2014). PD-1 has two main ligands: PD-L1 and PD-L2, which are involved in inducing T-cell exhaustion. Targeting PD-L1 in some early clinical cancer studies has shown beneficial effects, which has been welcomed by researchers. PD-L1 is widely expressed and can be detected in both hematopoietic cells and non-hematopoietic healthy tissue cells. Numerous studies have confirmed that the expression of PD-L1 gene is controlled by inflammatory signaling. Many soluble factors secreted by immune cells have been described as inducers of PD-L1 in the past few years. INF can regulate the expression of PD-L1 in many types of tumors and immune cells, as well as healthy tissues (Brown et al., 2003). The binding of IFN-γ to its receptor activates the classical JAK/STAT signaling pathway, inducing an increase in the expression of a series of transcription factors, known as interferon-response factors (IRFs). Among these factors, IRF1 is prerequisite to the IFN-γ-mediated upregulation of PD-L1 (Lee et al., 2006). In addition, studies have reported that the up-regulation of PD-L1 depends on TLR4/STAT1 pathway, while the expression of PD-L2 depends on IL-4/STAT6 pathway. As discussed above, it makes sense for immunotherapy considering that STAT signaling is

key to activating immune checkpoint molecules such as PD-L1 (Loke and Allison, 2003). It was reported that auranofin inhibited IL-6-induced activation of JAK2/STAT3 signaling pathway and activation of NF-κB in human multiple myeloma cell line (U266, RPM8226, and IM9). The phosphorylation of STAT3 was inhibited by auranofin through IL-6, leading to down-regulation of the anti-apoptotic proteins Mcl-1 and apoptosis of myeloma cells (Nakaya et al., 2011). In some similar experiments, auranofin also blocked the IL-6-mediated JAK1/STAT3 signaling pathway in HepG2 human hepatoma cells and primary cells (i.e., human umbilical vein endothelial cells, fibroblast-like synoviocytes and rat astrocytes) (Kim et al., 2007). In human breast cancer cells (MDA-MB 231), STAT3 phosphorylation and telomerase activity were also decreased by auranofin, but N-acetyl-L-cysteine (a scavenger of ROS) pretreatment restored STAT3 and telomerase activity (Kim et al., 2013). What's more, in a recent study, Raninga et al. for the first time found that auranofin could increase CD8 $^{+Ve}$ T-cells tumor infiltration and upregulate the expression of PD-L1 by an ERK1/2-MYC-dependent manner in mice models of triple-negative breast cancer (TNBC). Their study provides a novel combination of cancer therapy using auranofin in combination with anti-PD-L1 targeting therapy, which has limited clinical efficacy in TNBC patients with monotherapy (Raninga et al., 2020). As far as we know, gold derivatives have no effect on other immune checkpoints. Although there is very little research on the direct effects of gold compounds on immune checkpoints, the evidence above suggests a close relationship between gold compounds and the regulation of immune checkpoints.

GOLD DRUGS COMBINED WITH ANTICANCER IMMUNOTHERAPY

Metal-based anticancer drugs are widely used in the clinical treatment of various types of tumors. This situation shows that the systemic anticancer treatment based on metal drugs has high activity and quality, and it is urgent to guide the development of anticancer metal drugs by multidisciplinary approaches. Based on the promising prospect of the anticancer activity of gold derivatives, a large number of articles have been published in recent years (Yeo et al., 2018; Zhang et al., 2018b; Englinger et al., 2019; Mora et al., 2019). By strengthening our understanding of the complex effects of gold compounds on the host immune system, we can develop them better. Immunotherapy is a great revolution in the history of tumor treatment. Tumor immunotherapy has made a series of progress in recent years, which has changed the treatment pattern of many cancers and plays a very important role in the current scientific research. Compared with traditional chemotherapy and targeted therapy, the essential difference is that immunotherapy targets the immune cells and strengthens the immune system, instead of impairing the immune system. As a result, it can treat various types of tumors and is less prone to drug resistance. As we described before, the apparent immunomodulatory effects of gold compounds *in vivo* and *in vitro* support the hypothesis that these antitumor drugs might be ideal combination partners for immunotherapeutic interventions. Among the various immunotherapeutic strategies, the treatment based on immune checkpoint inhibitors is a highly efficient anticancer therapy and has shown unparalleled efficacy in patients with advanced cancer. A central challenge in modern systemic cancer treatment research is to identify and develop personalized and multitargets combination therapy strategies to improve the efficacy of modern immunotherapies. In Raninga's research, auranofin combined with immune checkpoint PD-L1 inhibitor achieved excellent anti-tumor efficacy in breast cancer cell lines and in mice, demonstrating the promising prospect of combined immunotherapy based on gold derivatives (Raninga et al., 2020). Such experiments are difficult to carry out in humans, largely hindering the exploration of specific mechanisms of gold compounds and their complex interactions with immune system. More attempts should be made to explore the clinical efficacy and prognosis of gold derivatives in combination with other checkpoint inhibitors, CAR-T cell therapy, monoclonal antibodies and molecular-targeted agents.

THE ADVERSE EFFECTS OF GOLD DRUGS

The immune system plays an important role in the side effects of gold compounds. Interestingly, the effects of gold compounds on the immune system can be broadly divided into two categories. On the one hand, some adverse effects can be related to immune-stimulating reactions, such as various forms of dermatitis, glomerulonephritis, and enteritis. The most common toxicity of gold compounds includes allergic reactions of skin and mucous membranes, such as skin rash, pruritis, contact dermatitis, stomatitis, as well as conjunctivitis. Some patients developed proteinuria during treatment, and the most common renal histologic lesion was membranous glomerulonephritis (Tonroth and Skrifvars, 1974). There are no detailed cases of long-term severe or permanent renal damage caused by gold compounds. Pulmonary toxicity is rare and mainly in the form of diffuse interstitial lung disease when treated with injectable gold compounds. The presence of cholestatic jaundice and acute enterocolitis is also associated with injectable gold compounds. On the other hand, also immunosuppression reactions may occur, such as the impairment of macrophages, T and B cells, aplastic anemia (Hansen et al., 1985), and bone marrow suppression (Yan and Davis, 1990). Bone marrow aplastic anemia is the most severe, but relatively rare. Overall, the toxicity of early injectable gold compounds was greater than that of oral gold compounds. Furthermore, we can observe that gold compounds combine with different ligands to produce different toxic reactions, so we can design more optimized ligands to reduce side reactions of gold compounds. Among these, N-Heterocyclic carbine (NHC) ligands have shown very promising results in recent years because they fully meet the preconditions for efficient drug design and rapid optimization (Zhang et al., 2018b; Mora et al., 2019).

CONCLUSIONS

In this review article, we systematically summarize the unique modulatory effects of gold compounds on antitumor immunity, including the enhancement of antigenicity and immunogenicity of tumor cells, the effects on immune cells and immune checkpoints, as well as the induction of ICD. Elucidating these important issues will greatly improve the identification and development of anticancer gold derivatives. In the future, gold compounds may have great application prospects in the combination therapy, potentiating the efficacy of targeted therapies and immunotherapy, especially immune checkpoint inhibitors therapy. Further studies are required to understand the detailed mechanisms of the regulation of anticancer immune response by gold derivatives in order to promote their clinical application.

AUTHOR CONTRIBUTIONS

SW and HL: had full access to all of the data in the study and take responsibility for the integrity of the data and the accuracy of the data analysis, concept, design, and critical revision of the manuscript for important intellectual content. SY and ML: acquisition, analysis, or interpretation of data and administrative, technical, or material support. SY and SW: drafting of the manuscript. All authors contributed to the article and approved the submitted version.

FUNDING

This work was supported by funding from the National Natural Science Foundation of China (Nos. 81772477 and 81201848) awarded to SW.

REFERENCES

AbdelKhalek, A., Abutaleb, N. S., Mohammad, H., and Seleem, M. N. (2019). Antibacterial and antivirulence activities of auranofin against Clostridium difficile. *Int. J. Antimicrob. Agents* 53, 54–62. doi: 10.1016/j.ijantimicag.2018.09.018

Bazzicalupi, C., Ferraroni, M., Papi, F., Massai, L., Bertrand, B., Messori, L., et al. (2016). Determinants for tight and selective binding of a medicinal dicarbene gold(I) complex to a telomeric DNA G-quadruplex: a joint ESI MS and XRD investigation. *Angew. Chem. Int. Ed. Engl.* 55, 4256–4259. doi: 10.1002/anie.201511999

Bian, M., Fan, R., Zhao, S., and Liu, W. (2019). Targeting the thioredoxin system as a strategy for cancer therapy. *J. Med. Chem.* 62, 7309–7321. doi: 10.1021/acs.jmedchem.8b01595

Bian, M., Sun, Y., Liu, Y., Xu, Z., Fan, R., Liu, Z., et al. (2020b). A gold(I) complex containing an oleanolic acid derivative as a potential anti-ovarian-cancer agent by inhibiting TrxR and activating ROS-mediated ERS. *Chemistry.* 26, 7092–7108. doi: 10.1002/chem.202000045

Bian, M., Wang, X., Sun, Y., and Liu, W. (2020a). Synthesis and biological evaluation of gold(III) Schiff base complexes for the treatment of hepatocellular carcinoma through attenuating TrxR activity. *Eur. J. Med. Chem.* 193:112234. doi: 10.1016/j.ejmech.2020.112234

Bortolozzi, R., Viola, G., Porcu, E., Consolaro, F., Marzano, C., Pellei, M., et al. (2014). A novel copper(I) complex induces ER-stress-mediated apoptosis and sensitizes B-acute lymphoblastic leukemia cells to chemotherapeutic agents. *Oncotarget* 5, 5978–5991. doi: 10.18632/oncotarget.2027

Bradley, S. D., Chen, Z., Melendez, B., Talukder, A., Khalili, J. S., Rodriguez-Cruz, T., et al. (2015). BRAFV600E Co-opts a conserved MHC class I internalization pathway to diminish antigen presentation and CD8+ T-cell recognition of melanoma. *Cancer Immunol. Res.* 3, 602–609. doi: 10.1158/2326-6066.CIR-15-0030

Brown, J. A., Dorfman, D. M., Ma, F. R., Sullivan, E. L., Munoz, O., Wood, C. R., et al. (2003). Blockade of programmed death-1 ligands on dendritic cells enhances T cell activation and cytokine production. *J. Immunol.* 170, 1257–1266. doi: 10.4049/jimmunol.170.3.1257

Cao, R., Jia, J., Ma, X., Zhou, M., and Fei, H. (2013). Membrane localized iridium(III) complex induces endoplasmic reticulum stress and mitochondria-mediated apoptosis in human cancer cells. *J. Med. Chem.* 56, 3636–3644. doi: 10.1021/jm4001665

Cao, S., Wang, S., Ma, H., Tang, S., Sun, C., Dai, J., et al. (2016). Genome-wide association study of myelosuppression in non-small-cell lung cancer patients with platinum-based chemotherapy. *Pharmacogenom. J.* 16, 41–46. doi: 10.1038/tpj.2015.22

Casares, N., Pequignot, M. O., Tesniere, A., Ghiringhelli, F., Roux, S., Chaput, N., et al. (2005). Caspase-dependent immunogenicity of doxorubicin-induced tumor cell death. *J. Exp. Med.* 202, 1691–1701. doi: 10.1084/jem.20050915

Chang, C. L., Hsu, Y. T., Wu, C. C., Lai, Y. Z., Wang, C., Yang, Y. C., et al. (2013). Dose-dense chemotherapy improves mechanisms of antitumor immune response. *Cancer Res.* 73, 119–127. doi: 10.1158/0008-5472.CAN-12-2225

Chao, M. P., Jaiswal, S., Weissman-Tsukamoto, R., Alizadeh, A. A., Gentles, A. J., Volkmer, J., et al. (2010). Calreticulin is the dominant pro-phagocytic signal on multiple human cancers and is counterbalanced by CD47. *Sci. Transl. Med.* 2:63ra94. doi: 10.1126/scitranslmed.3001375

Chen, D. S., and Mellman, I. (2013). Oncology meets immunology: the cancer-immunity cycle. *Immunity* 39, 1–10. doi: 10.1016/j.immuni.2013.07.012

Chiu, H. W., Tseng, Y. C., Hsu, Y. H., Lin, Y. F., Foo, N. P., Guo, H. R., et al. (2015). Arsenic trioxide induces programmed cell death through stimulation of ER stress and inhibition of the ubiquitin-proteasome system in human sarcoma cells. *Cancer Lett.* 356, 762–772. doi: 10.1016/j.canlet.2014.10.025

Costela-Ruiz, V. J., Illescas-Montes, R., Pavon-Martinez, R., Ruiz, C., and Melguizo-Rodriguez, L. (2018). Role of mast cells in autoimmunity. *Life Sci.* 209, 52–56. doi: 10.1016/j.lfs.2018.07.051

Diez-Martinez, R., Garcia-Fernandez, E., Manzano, M., Martinez, A., Domenech, M., Vallet-Regi, M., et al. (2016). Auranofin-loaded nanoparticles as a new therapeutic tool to fight streptococcal infections. *Sci. Rep.* 6:19525. doi: 10.1038/srep19525

Elie, B. T., Pechenyy, Y., Uddin, F., and Contel, M. (2018). A heterometallic ruthenium-gold complex displays antiproliferative, antimigratory, and antiangiogenic properties and inhibits metastasis and angiogenesis-associated proteases in renal cancer. *J. Biol. Inorg. Chem.* 23, 399–411. doi: 10.1007/s00775-018-1546-8

Englinger, B., Pirker, C., Heffeter, P., Terenzi, A., Kowol, C. R., Keppler, B. K., et al. (2019). Metal drugs and the anticancer immune response. *Chem. Rev.* 119, 1519–1624. doi: 10.1021/acs.chemrev.8b00396

Fan, R., Bian, M., Hu, L., and Liu, W. (2019). A new rhodium(I) NHC complex inhibits TrxR: *in vitro* cytotoxicity and *in vivo* hepatocellular carcinoma suppression. *Eur. J. Med. Chem.* 183:111721. doi: 10.1016/j.ejmech.2019.111721

Fiskus, W., Saba, N., Shen, M., Ghias, M., Liu, J., Gupta, S. D., et al. (2014). Auranofin induces lethal oxidative and endoplasmic reticulum stress and exerts potent preclinical activity against chronic lymphocytic leukemia. *Cancer Res.* 74, 2520–2532. doi: 10.1158/0008-5472.CAN-13-2033

Flocke, L. S., Trondl, R., Jakupec, M. A., and Keppler, B. K. (2016). Molecular mode of action of NKP-1339 - a clinically investigated ruthenium-based drug - involves ER- and ROS-related effects in colon carcinoma cell lines. *Invest. New Drugs* 34, 261–268. doi: 10.1007/s10637-016-0337-8

Galli, S. J., Kalesnikoff, J., Grimbaldeston, M. A., Piliponsky, A. M., Williams, C. M., and Tsai, M. (2005). Mast cells as "tunable" effector and immunoregulatory cells: recent advances. *Annu. Rev. Immunol.* 23, 749–786. doi: 10.1146/annurev.immunol.21.120601.141025

Gameiro, S. R., Caballero, J. A., and Hodge, J. W. (2012). Defining the molecular signature of chemotherapy-mediated lung tumor phenotype modulation and

increased susceptibility to T-cell killing. *Cancer Biother. Radiopharm.* 27, 23–35. doi: 10.1089/cbr.2012.1203

Garg, A. D., Galluzzi, L., Apetoh, L., Baert, T., Birge, R. B., Bravo-San Pedro, J. M., et al. (2015). Molecular and translational classifications of DAMPs in immunogenic cell death. *Front. Immunol.* 6:588. doi: 10.3389/fimmu.2015.00588

Griem, P., and Gleichmann, E. (1996). [Gold antirheumatic drug: desired and adverse effects of Au(I) and Au(III) [corrected] on the immune system]. *Z Rheumatol.* 55, 348–358.

Griem, P., Takahashi, K., Kalbacher, H., and Gleichmann, E. (1995). The antirheumatic drug disodium aurothiomalate inhibits CD4+ T cell recognition of peptides containing two or more cysteine residues. *J. Immunol.* 155, 1575–1587.

Grossman, S. A., Ellsworth, S., Campian, J., Wild, A. T., Herman, J. M., Laheru, D., et al. (2015). Survival in patients with severe lymphopenia following treatment with radiation and chemotherapy for newly diagnosed solid tumors. *J. Natl. Compr. Cancer Netw.* 13, 1225–1231. doi: 10.6004/jnccn.2015.0151

Han, S., Kim, K., Kim, H., Kwon, J., Lee, Y. H., Lee, C. K., et al. (2008a). Auranofin inhibits overproduction of pro-inflammatory cytokines, cyclooxygenase expression and PGE2 production in macrophages. *Arch. Pharm. Res.* 31, 67–74. doi: 10.1007/s12272-008-1122-9

Han, S., Kim, K., Song, Y., Kim, H., Kwon, J., Lee, Y. H., et al. (2008b). Auranofin, an immunosuppressive drug, inhibits MHC class I and MHC class II pathways of antigen presentation in dendritic cells. *Arch. Pharm. Res.* 31, 370–376. doi: 10.1007/s12272-001-1166-9

Hansen, R. M., Csuka, M. E., McCarty, D. J., and Saryan, L. A. (1985). Gold induced aplastic anemia. Complete response to corticosteroids, plasmapheresis, and N-acetylcysteine infusion. *J. Rheumatol.* 12, 794–797.

Harbut, M. B., Vilcheze, C., Luo, X., Hensler, M. E., Guo, H., Yang, B., et al. (2015). Auranofin exerts broad-spectrum bactericidal activities by targeting thiol-redox homeostasis. *Proc. Natl. Acad. Sci. U.S.A.* 112, 4453–4458. doi: 10.1073/pnas.1504022112

Hartmann, J. T., and Lipp, H. P. (2003). Toxicity of platinum compounds. *Expert Opin. Pharmacother.* 4, 889–901. doi: 10.1517/14656566.4.6.889

Havarinasab, S., Johansson, U., Pollard, K. M., and Hultman, P. (2007). Gold causes genetically determined autoimmune and immunostimulatory responses in mice. *Clin. Exp. Immunol.* 150, 179–188. doi: 10.1111/j.1365-2249.2007.03469.x

Hayama, K., Suzuki, Y., Inoue, T., Ochiai, T., Terui, T., and Ra, C. (2011). Gold activates mast cells via calcium influx through multiple H2O2-sensitive pathways including L-type calcium channels. *Free Radical. Biol. Med.* 50, 1417–1428. doi: 10.1016/j.freeradbiomed.2011.02.025

Hirohata, S. (1996). Inhibition of human B cell activation by gold compounds. *Clin. Immunol. Immunopathol.* 81, 175–181. doi: 10.1006/clin.1996.0174

Hou, G. X., Liu, P. P., Zhang, S., Yang, M., Liao, J., Yang, J., et al. (2018). Elimination of stem-like cancer cell side-population by auranofin through modulation of ROS and glycolysis. *Cell Death Dis.* 9:89. doi: 10.1038/s41419-017-0159-4

Huang, K. B., Wang, F. Y., Tang, X. M., Feng, H. W., Chen, Z. F., Liu, Y. C., et al. (2018). Organometallic Gold(III) complexes similar to tetrahydroisoquinoline induce ER-stress-mediated apoptosis and pro-death autophagy in A549 cancer cells. *J Med. Chem.* 61, 3478–3490. doi: 10.1021/acs.jmedchem.7b01694

Hurst, N. P., Bell, A. L., and Nuki, G. (1986). Studies of the effect of D-penicillamine and sodium aurothiomalate therapy on superoxide anion production by monocytes from patients with rheumatoid arthritis: evidence for *in vivo* stimulation of monocytes. *Ann. Rheum. Dis.* 45, 37–43. doi: 10.1136/ard.45.1.37

Jayanthi, E., Kalaiselvi, S., Padma, V. V., Bhuvanesh, N. S., and Dharmaraj, N. (2016). Solvent assisted formation of ruthenium(III) and ruthenium(II) hydrazone complexes in one-pot with potential in vitro cytotoxicity and enhanced LDH, NO and ROS release. *Dalton Trans.* 45, 1693–1707. doi: 10.1039/C5DT03849A

Jeon, K. I., Byun, M. S., and Jue, D. M. (2003). Gold compound auranofin inhibits IkappaB kinase (IKK) by modifying Cys-179 of IKKbeta subunit. *Exp. Mol. Med.* 35, 61–66. doi: 10.1038/emm.2003.9

Jeon, K. I., Jeong, J. Y., and Jue, D. M. (2000). Thiol-reactive metal compounds inhibit NF-kappa B activation by blocking I kappa B kinase. *J. Immunol.* 164, 5981–5989. doi: 10.4049/jimmunol.164.11.5981

Jungwirth, U., Xanthos, D. N., Gojo, J., Bytzek, A. K., Korner, W., Heffeter, P., et al. (2012). Anticancer activity of methyl-substituted oxaliplatin analogs. *Mol. Pharmacol.* 81, 719–728. doi: 10.1124/mol.111.077321

Kamimura, K., Matsumoto, Y., Zhou, Q., Moriyama, M., and Saijo, Y. (2016). Myelosuppression by chemotherapy in obese patients with gynecological cancers. *Cancer Chemother. Pharmacol.* 78, 633–641. doi: 10.1007/s00280-016-3119-2

Kermarrec, N., Dubay, C., De Gouyon, B., Blanpied, C., Gauguier, D., Gillespie, K., et al. (1996). Serum IgE concentration and other immune manifestations of treatment with gold salts are linked to the MHC and IL4 regions in the rat. *Genomics* 31, 111–114. doi: 10.1006/geno.1996.0016

Kim, J. L., Lee, D. H., Na, Y. J., Kim, B. R., Jeong, Y. A., Lee, S. I., et al. (2016). Iron chelator-induced apoptosis via the ER stress pathway in gastric cancer cells. *Tumour Biol.* 37, 9709–9719. doi: 10.1007/s13277-016-4878-4

Kim, N. H., Lee, M. Y., Park, S. J., Choi, J. S., Oh, M. K., and Kim, I. S. (2007). Auranofin blocks interleukin-6 signalling by inhibiting phosphorylation of JAK1 and STAT3. *Immunology* 122, 607–614. doi: 10.1111/j.1365-2567.2007.02679.x

Kim, N. H., Park, H. J., Oh, M. K., and Kim, I. S. (2013). Antiproliferative effect of gold(I) compound auranofin through inhibition of STAT3 and telomerase activity in MDA-MB 231 human breast cancer cells. *BMB Rep.* 46, 59–64. doi: 10.5483/BMBRep.2013.46.1.123

Krikavova, R., Hosek, J., Vanco, J., Hutyra, J., Dvorak, Z., and Travnicek, Z. (2014). Gold(I)-triphenylphosphine complexes with hypoxanthine-derived ligands: in vitro evaluations of anticancer and anti-inflammatory activities. *PLoS ONE* 9:e107373. doi: 10.1371/journal.pone.0107373

Kroemer, G., Galluzzi, L., Kepp, O., and Zitvogel, L. (2013). Immunogenic cell death in cancer therapy. *Annu. Rev. Immunol.* 31, 51–72. doi: 10.1146/annurev-immunol-032712-100008

Lee, S. J., Jang, B. C., Lee, S. W., Yang, Y. I., Suh, S. I., Park, Y. M., et al. (2006). Interferon regulatory factor-1 is prerequisite to the constitutive expression and IFN-gamma-induced upregulation of B7-H1 (CD274). *FEBS Lett.* 580, 755–762. doi: 10.1016/j.febslet.2005.12.093

Liu, W., and Gust, R. (2013). Metal N-heterocyclic carbene complexes as potential antitumor metallodrugs. *Chem. Soc. Rev.* 42, 755–773. doi: 10.1039/C2CS35314H

Liu, Y., and Connor, J. R. (2012). Iron and ER stress in neurodegenerative disease. *BioMetals* 25, 837–845. doi: 10.1007/s10534-012-9544-8

Loke, P., and Allison, J. P. (2003). PD-L1 and PD-L2 are differentially regulated by Th1 and Th2 cells. *Proc. Natl. Acad. Sci. U.S.A.* 100, 5336–5341. doi: 10.1073/pnas.0931259100

Madeira, J. M., Gibson, D. L., Kean, W. F., and Klegeris, A. (2012). The biological activity of auranofin: implications for novel treatment of diseases. *Inflammopharmacology* 20, 297–306. doi: 10.1007/s10787-012-0149-1

Marmol, I., Virumbrales-Munoz, M., Quero, J., Sanchez-de-Diego, C., Fernandez, L., Ochoa, I., et al. (2017). Alkynyl gold(I) complex triggers necroptosis via ROS generation in colorectal carcinoma cells. *J. Inorg. Biochem.* 176, 123–133. doi: 10.1016/j.jinorgbio.2017.08.020

Martinez-Balibrea, E., Martinez-Cardus, A., Gines, A., Ruiz de Porras, V., Moutinho, C., Layos, L., et al. (2015). Tumor-related molecular mechanisms of oxaliplatin resistance. *Mol. Cancer Ther.* 14, 1767–1776. doi: 10.1158/1535-7163.MCT-14-0636

Marzano, C., Gandin, V., Folda, A., Scutari, G., Bindoli, A., and Rigobello, M. P. (2007). Inhibition of thioredoxin reductase by auranofin induces apoptosis in cisplatin-resistant human ovarian cancer cells. *Free Radical. Biol. Med.* 42, 872–881. doi: 10.1016/j.freeradbiomed.2006.12.021

Measel, J. W. Jr. (1975). Effect of gold on the immune response of mice. *Infect Immun.* 11, 350–354. doi: 10.1128/IAI.11.2.350-354.1975

Merchant, B. (1998). Gold, the noble metal and the paradoxes of its toxicology. *Biologicals* 26, 49–59. doi: 10.1006/biol.1997.0123

Messori, L., Marcon, G., Innocenti, A., Gallori, E., Franchi, M., and Orioli, P. (2005). Molecular recognition of metal complexes by DNA: a comparative study of the interactions of the parent complexes [PtCl(TERPY)]Cl and [AuCl(TERPY)]Cl2 with double stranded DNA. *Bioinorg. Chem. Appl.* 3, 239–253. doi: 10.1155/BCA.2005.239

Mora, M., Gimeno, M. C., and Visbal, R. (2019). Recent advances in gold-NHC complexes with biological properties. *Chem. Soc. Rev.* 48, 447–462. doi: 10.1039/C8CS00570B

Muenst, S., Laubli, H., Soysal, S. D., Zippelius, A., Tzankov, A., and Hoeller, S. (2016). The immune system and cancer evasion strategies: therapeutic concepts. *J. Intern. Med.* 279, 541–562. doi: 10.1111/joim.12470

Murray, P. J., Allen, J. E., Biswas, S. K., Fisher, E. A., Gilroy, D. W., Goerdt, S., et al. (2014). Macrophage activation and polarization: nomenclature and experimental guidelines. *Immunity* 41, 14–20. doi: 10.1016/j.immuni.2014.06.008

Nakaya, A., Sagawa, M., Muto, A., Uchida, H., Ikeda, Y., and Kizaki, M. (2011). The gold compound auranofin induces apoptosis of human multiple myeloma cells through both down-regulation of STAT3 and inhibition of NF-kappaB activity. *Leukemia Res.* 35, 243–249. doi: 10.1016/j.leukres.2010.05.011

Nardon, C., Pettenuzzo, N., and Fregona, D. (2016). Gold complexes for therapeutic purposes: an updated patent review (2010-2015). *Curr. Med. Chem.* 23, 3374–3403. doi: 10.2174/0929867323666160504103843

Niikura, K., Matsunaga, T., Suzuki, T., Kobayashi, S., Yamaguchi, H., Orba, Y., et al. (2013). Gold nanoparticles as a vaccine platform: influence of size and shape on immunological responses *in vitro* and *in vivo*. *ACS Nano* 7, 3926–3938. doi: 10.1021/nn3057005

Noy, R., and Pollard, J. W. (2014). Tumor-associated macrophages: from mechanisms to therapy. *Immunity* 41, 49–61. doi: 10.1016/j.immuni.2014.06.010

Ohtsukasa, S., Okabe, S., Yamashita, H., Iwai, T., and Sugihara, K. (2003). Increased expression of CEA and MHC class I in colorectal cancer cell lines exposed to chemotherapy drugs. *J. Cancer Res. Clin. Oncol.* 129, 719–726. doi: 10.1007/s00432-003-0492-0

Onodera, T., Momose, I., and Kawada, M. (2019). Potential anticancer activity of auranofin. *Chem. Pharm. Bull.* 67, 186–191. doi: 10.1248/cpb.c18-00767

Oommen, D., Yiannakis, D., and Jha, A. N. (2016). BRCA1 deficiency increases the sensitivity of ovarian cancer cells to auranofin. *Mutat. Res.* 784–785, 8–15. doi: 10.1016/j.mrfmmm.2015.11.002

Orlowski, P., Tomaszewska, E., Ranoszek-Soliwoda, K., Gniadek, M., Labedz, O., Malewski, T., et al. (2018). Tannic acid-modified silver and gold nanoparticles as novel stimulators of dendritic cells activation. *Front. Immunol.* 9:1115. doi: 10.3389/fimmu.2018.01115

Ortego, L., Cardoso, F., Martins, S., Fillat, M. F., Laguna, A., Meireles, M., et al. (2014). Strong inhibition of thioredoxin reductase by highly cytotoxic gold(I) complexes. DNA binding studies. *J. Inorg. Biochem.* 130, 32–37. doi: 10.1016/j.jinorgbio.2013.09.019

Ott, I., and Gust, R. (2007). Non platinum metal complexes as anti-cancer drugs. *Arch. Pharm.* 340, 117–126. doi: 10.1002/ardp.200600151

Oun, R., Moussa, Y. E., and Wheate, N. J. (2018). The side effects of platinum-based chemotherapy drugs: a review for chemists. *Dalton Trans.* 47, 6645–6653. doi: 10.1039/C8DT00838H

Parente, J. E., Walsh, M. P., Girard, P. R., Kuo, J. F., Ng, D. S., and Wong, K. (1989). Effects of gold coordination complexes on neutrophil function are mediated via inhibition of protein kinase C. *Mol. Pharmacol.* 35, 26–33.

Patel, M. N., Bhatt, B. S., and Dosi, P. A. (2013). Synthesis and evaluation of gold(III) complexes as efficient DNA binders and cytotoxic agents. *Spectrochim. Acta A Mol. Biomol. Spectrosc.* 110, 20–27. doi: 10.1016/j.saa.2013.03.037

Pedersen, B. K., and Abom, B. (1986). Characterization of the *in vitro* effect of triethylphosphine gold (auranofin) on human NK cell activity. *Clin. Exp. Rheumatol.* 4, 249–253.

Pedoeem, A., Azoulay-Alfaguter, I., Strazza, M., Silverman, G. J., and Mor, A. (2014). Programmed death-1 pathway in cancer and autoimmunity. *Clin. Immunol.* 153, 145–152. doi: 10.1016/j.clim.2014.04.010

Quail, D. F., and Joyce, J. A. (2013). Microenvironmental regulation of tumor progression and metastasis. *Nat. Med.* 19, 1423–1437. doi: 10.1038/nm.3394

Rachmawati, D., Alsalem, I. W., Bontkes, H. J., Verstege, M. I., Gibbs, S., von Blomberg, B. M., et al. (2015b). Innate stimulatory capacity of high molecular weight transition metals Au (gold) and Hg (mercury). *Toxicol. In Vitro* 29, 363–369. doi: 10.1016/j.tiv.2014.10.010

Rachmawati, D., Buskermolen, J. K., Scheper, R. J., Gibbs, S., von Blomberg, B. M., and van Hoogstraten, I. M. (2015a). Dental metal-induced innate reactivity in keratinocytes. *Toxicol In Vitro* 30, 325–330. doi: 10.1016/j.tiv.2015.10.003

Rackham, O., Nichols, S. J., Leedman, P. J., Berners-Price, S. J., and Filipovska, A. (2007). A gold(I) phosphine complex selectively induces apoptosis in breast cancer cells: implications for anticancer therapeutics targeted to mitochondria. *Biochem. Pharmacol.* 74, 992–1002. doi: 10.1016/j.bcp.2007.07.022

Radisavljevic, S., Bratsos, I., Scheurer, A., Korzekwa, J., Masnikosa, R., Tot, A., et al. (2018). New gold pincer-type complexes: synthesis, characterization, DNA binding studies and cytotoxicity. *Dalton Trans.* 47, 13696–13712. doi: 10.1039/C8DT02903B

Raninga, P. V., Lee, A. C., Sinha, D., Shih, Y. Y., Mittal, D., Makhale, A., et al. (2020). Therapeutic cooperation between auranofin, a thioredoxin reductase inhibitor and anti-PD-L1 antibody for treatment of triple-negative breast cancer. *Int. J. Cancer* 146, 123–136. doi: 10.1002/ijc.32410

Rigobello, M. P., Scutari, G., Boscolo, R., and Bindoli, A. (2002). Induction of mitochondrial permeability transition by auranofin, a gold(I)-phosphine derivative. *Br. J. Pharmacol.* 136, 1162–1168. doi: 10.1038/sj.bjp.0704823

Rosenberg, B., VanCamp, L., Trosko, J. E., and Mansour, V. H. (1969). Platinum compounds: a new class of potent antitumour agents. *Nature* 222, 385–386. doi: 10.1038/222385a0

Russell, A. S., Davis, P., and Miller, C. (1982). The effect of a new antirheumatic drug, triethylphosphine gold (auranofin), on *in vitro* lymphocyte and monocyte cytotoxicity. *J. Rheumatol.* 9, 30–35.

Sadler, P. J., and Sue, R. E. (1994). The chemistry of gold drugs. *Met. Based Drugs* 1, 107–144. doi: 10.1155/MBD.1994.107

Sanders, K. M., Carlson, P. L., and Littman, B. H. (1987). Effects of gold sodium thiomalate on interferon stimulation of C2 synthesis and HLA-DR expression by human monocytes. *Arthritis Rheum.* 30, 1032–1039. doi: 10.1002/art.1780300910

Savignac, M., Badou, A., Delmas, C., Subra, J. F., De Cramer, S., Paulet, P., et al. (2001). Gold is a T cell polyclonal activator in BN and LEW rats but favors IL-4 expression only in autoimmune prone BN rats. *Eur. J. Immunol.* 31, 2266–2276. doi: 10.1002/1521-4141(200108)31:8<2266::AID-IMMU2266>3.0.CO;2-6

Shaw, I. C. (1999). Gold-based therapeutic agents. *Chem. Rev.* 99, 2589–2600. doi: 10.1021/cr980431o

Shimizu, T., Abu Lila, A. S., Nishio, M., Doi, Y., Ando, H., Ukawa, M., et al. (2017). Modulation of antitumor immunity contributes to the enhanced therapeutic efficacy of liposomal oxaliplatin in mouse model. *Cancer Sci.* 108, 1864–1869. doi: 10.1111/cas.13305

Siniard, R. C., and Harada, S. (2017). Immunogenomics: using genomics to personalize cancer immunotherapy. *Virchows Archiv.* 471, 209–219. doi: 10.1007/s00428-017-2140-0

Stern, I., Wataha, J. C., Lewis, J. B., Messer, R. L., Lockwood, P. E., and Tseng, W. Y. (2005). Anti-rheumatic gold compounds as sublethal modulators of monocytic LPS-induced cytokine secretion. *Toxicol. In Vitro* 19, 365–371. doi: 10.1016/j.tiv.2004.11.001

Stojanovska, V., McQuade, R., Rybalka, E., and Nurgali, K. (2017). Neurotoxicity associated with platinum-based anti-cancer agents: what are the implications of copper transporters? *Curr. Med. Chem.* 24, 1520–1536. doi: 10.2174/0929867324666170112095428

Stojanovska, V., Sakkal, S., and Nurgali, K. (2015). Platinum-based chemotherapy: gastrointestinal immunomodulation and enteric nervous system toxicity. *Am. J. Physiol. Gastrointest. Liver Physiol.* 308, G223–G232. doi: 10.1152/ajpgi.00212.2014

Sun, F., Cui, L., Li, T., Chen, S., Song, J., and Li, D. (2019). Oxaliplatin induces immunogenic cells death and enhances therapeutic efficacy of checkpoint inhibitor in a model of murine lung carcinoma. *J. Recept. Signal Transduct. Res.* 39, 208–214. doi: 10.1080/10799893.2019.1655050

Suntharalingam, K., Johnstone, T. C., Bruno, P. M., Lin, W., Hemann, M. T., and Lippard, S. J. (2013). Bidentate ligands on osmium(VI) nitrido complexes control intracellular targeting and cell death pathways. *J. Am. Chem. Soc.* 135, 14060–14063. doi: 10.1021/ja4075375

Suzuki, Y., Inoue, T., and Ra, C. (2011). Autoimmunity-inducing metals (Hg, Au and Ag) modulate mast cell signaling, function and survival. *Curr. Pharm. Des.* 17, 3805–3814. doi: 10.2174/138161211798357917

Takahashi, K., Griem, P., Goebel, C., Gonzalez, J., and Gleichmann, E. (1994). The antirheumatic drug gold, a coin with two faces: AU(I) and AU(III). Desired and undesired effects on the immune system. *Met. Based Drugs* 1, 483–496. doi: 10.1155/MBD.1994.483

Terenzi, A., Pirker, C., Keppler, B. K., and Berger, W. (2016). Anticancer metal drugs and immunogenic cell death. *J. Inorg. Biochem.* 165, 71–79. doi: 10.1016/j.jinorgbio.2016.06.021

Tesniere, A., Schlemmer, F., Boige, V., Kepp, O., Martins, I., Ghiringhelli, F., et al. (2010). Immunogenic death of colon cancer cells treated

with oxaliplatin. *Oncogene* 29, 482–491. doi: 10.1038/onc.2009.356

Thangamani, S., Maland, M., Mohammad, H., Pascuzzi, P. E., Avramova, L., Koehler, C. M., et al. (2017). Repurposing approach identifies auranofin with broad spectrum antifungal activity that targets Mia40-Erv1 pathway. *Front. Cell Infect Microbiol.* 7:4. doi: 10.3389/fcimb.2017.00004

Tonroth, T., and Skrifvars, B. (1974). Gold nephropathy prototype of membranous glomerulonephritis. *Am. J. Pathol.* 75, 573–590.

Walz, D. T., and Griswold, D. E. (1978). Immunopharmacology of gold sodium thiomalate and auranofin (SK&F D-39162): effects on cell-mediated immunity. *Inflammation* 3, 117–128. doi: 10.1007/BF00910733

Wang, Q., Janzen, N., Ramachandran, C., and Jirik, F. (1997). Mechanism of inhibition of protein-tyrosine phosphatases by disodium aurothiomalate. *Biochem. Pharmacol.* 54, 703–711. doi: 10.1016/S0006-2952(97)00217-7

Wang, X., and Guo, Z. (2013). Targeting and delivery of platinum-based anticancer drugs. *Chem. Soc. Rev.* 42, 202–224. doi: 10.1039/C2CS35259A

Wong, D. Y., Ong, W. W., and Ang, W. H. (2015). Induction of immunogenic cell death by chemotherapeutic platinum complexes. *Angew Chem. Int. Ed. Engl.* 54, 6483–6487. doi: 10.1002/anie.201500934

Yamamoto, Y., and Gaynor, R. B. (2001). Therapeutic potential of inhibition of the NF-kappaB pathway in the treatment of inflammation and cancer. *J. Clin. Invest.* 107, 135–142. doi: 10.1172/JCI11914

Yan, A., and Davis, P. (1990). Gold induced marrow suppression: a review of 10 cases. *J. Rheumatol.* 17, 47–51.

Yang, J. P., Merin, J. P., Nakano, T., Kato, T., Kitade, Y., and Okamoto, T. (1995). Inhibition of the DNA-binding activity of NF-kappa B by gold compounds *in vitro*. *FEBS Lett.* 361, 89–96. doi: 10.1016/0014-5793(95)00157-5

Yang, Q., Wang, Y., Yang, Q., Gao, Y., Duan, X., Fu, Q., et al. (2017). Cuprous oxide nanoparticles trigger ER stress-induced apoptosis by regulating copper trafficking and overcoming resistance to sunitinib therapy in renal cancer. *Biomaterials* 146, 72–85. doi: 10.1016/j.biomaterials.2017.09.008

Yeo, C. I., Ooi, K. K., and Tiekink, E. R. T. (2018). Gold-based medicine: a paradigm shift in anti-cancer therapy? *Molecules* 23:1410. doi: 10.3390/molecules23061410

Youn, H. S., Lee, J. Y., Saitoh, S. I., Miyake, K., and Hwang, D. H. (2006). Auranofin, as an anti-rheumatic gold compound, suppresses LPS-induced homodimerization of TLR4. *Biochem. Biophys. Res. Commun.* 350, 866–871. doi: 10.1016/j.bbrc.2006.09.097

Zeligs, K. P., Neuman, M. K., and Annunziata, C. M. (2016). Molecular pathways: the balance between cancer and the immune system challenges the therapeutic specificity of targeting nuclear factor-kappaB signaling for cancer treatment. *Clin. Cancer Res.* 22, 4302–4308. doi: 10.1158/1078-0432.CCR-15-1374

Zetterstrom, C. K., Jiang, W., Wahamaa, H., Ostberg, T., Aveberger, A. C., Schierbeck, H., et al. (2008). Pivotal advance: inhibition of HMGB1 nuclear translocation as a mechanism for the anti-rheumatic effects of gold sodium thiomalate. *J. Leukocyte Biol.* 83, 31–38. doi: 10.1189/jlb.0507323

Zhang, C., Maddelein, M. L., Wai-Yin Sun, R., Gornitzka, H., Cuvillier, O., and Hemmert, C. (2018b). Pharmacomodulation on Gold-NHC complexes for anticancer applications - is lipophilicity the key point? *Eur. J. Med. Chem.* 157, 320–332. doi: 10.1016/j.ejmech.2018.07.070

Zhang, J., Dang, F., Ren, J., and Wei, W. (2018a). Biochemical aspects of PD-L1 regulation in cancer immunotherapy. *Trends Biochem. Sci.* 43, 1014–1032. doi: 10.1016/j.tibs.2018.09.004

Zhou, J., Wang, G., Chen, Y., Wang, H., Hua, Y., and Cai, Z. (2019). Immunogenic cell death in cancer therapy: present and emerging inducers. *J. Cell Mol. Med.* 23, 4854–4865. doi: 10.1111/jcmm.14356

Conflict of Interest: The authors declare that the research was conducted in the absence of any commercial or financial relationships that could be construed as a potential conflict of interest.

frontiers in Chemistry

ORIGINAL RESEARCH
published: 18 September 2020
doi: 10.3389/fchem.2020.00812

Mechanistic Insights Into the Anticancer Properties of the Auranofin Analog Au(PEt$_3$)I: A Theoretical and Experimental Study

Iogann Tolbatov[1†], Damiano Cirri[2†], Lorella Marchetti[2], Alessandro Marrone[1], Cecilia Coletti[1], Nazzareno Re[1], Diego La Mendola[3], Luigi Messori[4], Tiziano Marzo[3,5], Chiara Gabbiani[2†] and Alessandro Pratesi[2*†]*

[1] Department of Pharmacy, University "G. D'Annunzio" Chieti-Pescara, Chieti, Italy, [2] Department of Chemistry and Industrial Chemistry (DCCI), University of Pisa, Pisa, Italy, [3] Department of Pharmacy, University of Pisa, Pisa, Italy, [4] Laboratory of Metals in Medicine (MetMed), Department of Chemistry "U. Schiff", University of Florence, Florence, Italy, [5] CISUP-Centro per l'Integrazione della Strumentazione Scientifica dell'Università di Pisa, University of Pisa, Pisa, Italy

OPEN ACCESS

Edited by:
Tara Louise Pukala, University of Adelaide, Australia

Reviewed by:
Helio F. Dos Santos, Juiz de Fora Federal University, Brazil
Francesco Ortuso, University of Catanzaro, Italy

***Correspondence:**
Alessandro Pratesi
alessandro.pratesi@unipi.it
Tiziano Marzo
tiziano.marzo@unipi.it

[†] These authors have contributed equally to this work

Specialty section:
This article was submitted to Medicinal and Pharmaceutical Chemistry, a section of the journal Frontiers in Chemistry

Received: *30 June 2020*
Accepted: *03 August 2020*
Published: *18 September 2020*

Citation:
Tolbatov I, Cirri D, Marchetti L, Marrone A, Coletti C, Re N, La Mendola D, Messori L, Marzo T, Gabbiani C and Pratesi A (2020) Mechanistic Insights Into the Anticancer Properties of the Auranofin Analog Au(PEt$_3$)I: A Theoretical and Experimental Study. Front. Chem. 8:812. doi: 10.3389/fchem.2020.00812

Au(PEt$_3$)I (AF-I hereafter), the iodide analog of the FDA-approved drug auranofin (AF hereafter), is a promising anticancer agent that produces its pharmacological effects through interaction with non-genomic targets such as the thioredoxin reductase system. AF-I is endowed with a very favorable biochemical profile showing potent *in vitro* cytotoxic activity against several cancer types including ovarian and colorectal cancer. Remarkably, in a recent publication, some of us reported that AF-I induces an almost complete and rapid remission in an orthotopic *in vivo* mouse model of ovarian cancer. The cytotoxic potency does not bring about highly severe side effects, making AF-I very well-tolerated even for higher doses, even more so than the pharmacologically active ones. All these promising features led us to expand our studies on the mechanistic aspects underlying the antitumor activity of AF-I. We report here on an integrated experimental and theoretical study on the reactivity of AF-I, in comparison with auranofin, toward relevant aminoacidic residues or their molecular models. Results point out that the replacement of the thiosugar moiety with iodide significantly affects the overall reactivity toward the amino acid residues histidine, cysteine, methionine, and selenocysteine. Altogether, the obtained results contribute to shed light into the enhanced antitumoral activity of AF-I compared with AF.

Keywords: cancer, ESI-MS, DFT, auranofin, gold, metal-based anticancer drugs, protein metalation, ^{31}PNMR

INTRODUCTION

The approval of cisplatin by the FDA in the seventies triggered a huge challenge in the search for innovative metal complexes with improved efficacy and fewer side effects. Within these efforts, several transition metals, including Ag, Cu, Au, and Ru, have been exploited for the synthesis of experimental antitumor compounds (Garbutcheon-Singh et al., 2011; Tamasi et al., 2014; Massai et al., 2016; Pratesi et al., 2016; Ndagi et al., 2017). Among them, gold compounds have attracted growing attention. The leading compound of this family of metallodrugs is auranofin (2,3,4,6-tetra-o-acetyl-L-thio-β-D-glyco-pyranosato-S-(triethyl-phosphine)-gold(I), **Figure 1**). It

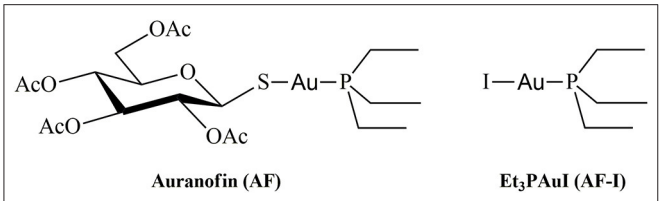

FIGURE 1 | Chemical structures of Auranofin (AF) and Iodo(triethylphosphine)gold(I) (AF-I).

is clinically approved for the treatment of rheumatoid arthritis; however, in the frame of the so called "drug repositioning" strategy, in recent years, an extensive reappraisal of its medicinal properties was started unveiling its potential application as antibacterial (Cassetta et al., 2014; Thangamani et al., 2016; Marzo et al., 2018), antiviral (AbdelKhalek et al., 2019; Marzo and Messori, 2020), antifungal, and antiparasitic agent (Bulman et al., 2015; Wiederhold et al., 2017). Moreover, the remarkable *in vitro* antiproliferative properties of this compound fueled the widespread studies of its antitumor activity. AF was found to be efficient in inducing cells apoptosis in various types of human cancers: ovarian (Marzano et al., 2007; Guidi et al., 2012), prostate (Shin et al., 2017), breast (Kim et al., 2013), lung (Liu et al., 2013; Fan et al., 2014; Li et al., 2016; Hu J. et al., 2018), bone (Topkas et al., 2016), and blood (Talbot et al., 2008; Nakaya et al., 2011; Habermann et al., 2017). It has also been included in a few clinical trials as an experimental antineoplastic agent (www.clicalTrials.gov). Unlike the platinum antitumor complexes, which target the nuclear DNA to exert their anticancer action, AF, as the majority of gold complexes, has a greater affinity for sulfur and selenium-containing proteins. For instance, AF binds extensively and quickly to albumin. Accordingly, beyond albumin (Roberts et al., 1996; Pratesi et al., 2018), several non-genomic targets able to coordinate gold metal fragments have been hypothesized to be involved in determining its anticancer activity. Among them are the proteasome system (Micale et al., 2014), the NF-κB protein complex (Nakaya et al., 2011; Hu M. et al., 2018), and thioredoxin reductase (TrxR) (Marzano et al., 2007; Pratesi et al., 2010, 2014; Harbut et al., 2015). The latter is believed to be the main target. Indeed, the inhibition of TrxR by AF through coordination of the gold fragment at the level of the redox-active site, may lead to oxidative stress in cells, eventually leading to apoptosis (Marzano et al., 2007; Harbut et al., 2015). Nevertheless, AF's mechanism of action is not yet fully understood at the molecular level despite multiple experimental and computational studies (Zou et al., 2000; Howell, 2009; Di Sarra et al., 2013; Marzo et al., 2017, 2019). There is a wide consensus that the true pharmacophore is the $[Au(PEt_3)]^+$ cation, whereas the thiosugar ligand is believed to act predominantly as a carrier ligand (Marzo et al., 2017, 2018). $[Au(PEt_3)]^+$ is generated after release of the thiosugar ligand and it is capable to bind the key cellular targets triggering the pharmacological effect (Zou et al., 2000; Marzo et al., 2017, 2019; Zoppi et al., 2020).

In recent years, some of us have started to explore the mechanistic implications determined by the replacement of the thiosugar moiety with different ligands, mainly halides or pseudohalides. The inclusion of halides in the place of the thiosugar ligand could modify the lipophilicity of this metallodrug and thus amplify its bioavailability. Nevertheless, the biologically active $[Au(PEt_3)]^+$ moiety is not affected by this modification. A systematic and comparative investigation concerning the effects on the anticancer properties of the structural modifications was also performed (Cirri et al., 2017, 2019; Marzo et al., 2017, 2019). Through this approach, the complex $Au(PEt_3)I$, i.e., the analog of AF where the thiosugar moiety is replaced by iodide, was eventually selected thanks to the very favorable biochemical profile accompanied by a remarkable anticancer activity (**Figure 1**). Indeed, this analog has a potent cytotoxic effect *in vitro* in colorectal and ovarian cancer, and, more importantly, it induces a rapid tumor mass reduction leading to an almost complete remission in an orthotopic mouse model of ovarian cancer combined with no side effects (Marzo et al., 2017, 2019).

These premises spurred us to further explore the mechanisms of interaction with relevant biological targets of AF-I in comparison with AF. We decided to use a multi-technique experimental approach (NMR, IR and ESI-MS) paired with theoretical calculations (DFT) to study the reactivity of these two gold compounds toward relevant amino acids (His, Met, Cys, and Sec) or their molecular models. This strategy is convenient because it allows us to formulate a quite comprehensive picture for the reactivity and for the mechanisms of activation of metallodrugs in the presence of biological targets or their simplified models avoiding the limits of using a single technique or approach. Also, the multi-technique strategy turned out to be very useful since the studied systems did not responded in the same manner to all the mentioned analytical techniques. In fact, in some cases not all of these were able to highlight the adducts formation, requiring a further interrogation grounded on another instrumental method. His, Met, Cys, and Sec aminoacidic residues were selected since they are generally recognized as the likely binding site for the coordination of gold complexes to proteins in reason to their nature of soft ligands (Abhishek et al., 2019; Pratesi et al., 2019). Results reveal differences in the reaction profiles between AF and AF-I in particular toward both cysteine and selenocysteine while -in our experimental conditions- no reactivity occurs toward His and Met. Furthermore, insights into the kinetic and thermodynamic features for the explored reactivities was gained. Altogether, the information achieved may turn crucial in shedding light into the relevant mechanisms of reaction for the enhanced antitumor activity of AF-I compared to AF.

RESULTS

NMR Spectroscopy

We first explored comparatively the reactivity of AF-I and AF through NMR experiments. Owing to solubility issues for both the investigated complexes, the NMR experiments were carried out in the presence of 50% of methanol-d_4 and 50% of 500 mM sodium bicarbonate buffer (pH=7.8). It is worth reminding that AF and AF-I possess a high stability in a wide

TABLE 1 | Results obtained by ^{31}PNMR experiments for the incubation at different time intervals ($t = 0$ and $t = 24$ h) of AF and AF-I with His, Met, Cys, or Sec.

	His		Met		Cys		Sec	
	t_{0h}	t_{24h}	t_{0h}	t_{24h}	t_{0h}	t_{24h}	t_{0h}	t_{24h}
AF	-	-	-	-	#	#	$Au(PEt_3)$-S-DTT *(39.1 ppm)** $Au(PEt_3)$-Se-CH_2-R *(62.6 ppm)***	$Au(PEt_3)$-Se-CH_2-R *(62.3 ppm)***
AF-I	-	-	-	-	$Au(PEt_3)$-S-CH_2-R *(38.7 ppm)****	$Au(PEt_3)$-S-CH_2-R *(38.7 ppm)****	$Au(PEt_3)$-S-DTT *(39.1 ppm)** $Au(PEt_3)$-Se-CH_2-R *(62.7 ppm)***	$Au(PEt_3)$-Se-CH_2-R *(62.9 ppm)***

- No adduct formation.

** Adduct with dithiothreitol (DTT); **Adduct with Se of selenocysteine; *** Adduct with S of cysteine (Cirri et al., 2019).*

 # ^{31}P signal of Auranofin overlaps that of $Au(PEt_3)$-S-CH_2-R, making impossible the study of the reactivity.

R= –CH(NH_2)COOH.

array of organic solvents including MeOH (Marzo et al., 2017, 2018), and no side reactions involving the solvent are thus expected. Following addition of AF or AF-I, ^{31}PNMR spectra were recorded immediately at sample preparation ($t = 0$), and after 24 h ($t = 24$ h). **Table 1** summarizes the results obtained for either AF or AF-I.

For the incubation in the presence of His or Met both complexes appear unreactive—or only a very small amounts of them reacts producing a quantity of the adducts that is not detectable through NMR analysis. Indeed, for AF, the ^{31}PNMR signal at 39 ppm, attributable to the phosphorus in the neutral complex (Marzo et al., 2017) remains stable even for incubation up to 24 h. Similarly, the ^{31}PNMR signal of the phosphorus of the iodide analog, falling at ∼41 ppm, remains unaltered. Only in the case of the incubation in the presence of Met, AF-I undergoes a partial scrambling reaction producing the signal at ∼47.5 ppm assignable to the cationic species $[Au(PEt_3)_2]^+$, according to the already reported mechanism (Marzo et al., 2017). Conversely, the comparative analysis unveils substantial differences in the reactivity profiles of the two drugs when incubated with Cys and Sec. In this case AF-I readily reacts with the thiol moiety of cysteine, producing the adduct where the iodide ligand is displaced, and the ^{31}PNMR signal of the adduct appears at ∼39 ppm. Moreover, the fast adduct formation in the case of AF-I, is further supported by the production of bubbles upon addition of the complex to the amino acid solution in the NMR tube. In fact, CO_2 bubbling takes place as neutralization of hydriodic acid by the bicarbonate buffer. On the other hand, it was not possible to elucidate the reactivity of AF against Cys by ^{31}PNMR because of the overlap of the signal of the hypothesized adduct $Au(PEt_3)$-S-CH_2-R (where R= –CH(NH_2)COOH) with that of AF. When AF and AF-I are incubated with Sec, a very similar reactivity occurs. At $t = 0$ h, in both cases two signals are detectable at ∼39 and 62.7 ppm. The former is attributable to the adduct of the metal cationic fragment $[Au(PEt_3)]^+$ with DTT necessary to reduce the Se-Se bridge of the selenocystine (Pratesi et al., 2010, 2014; Fabbrini et al., 2019). The latter signal is attributable to the adduct of the same cationic metal fragment with Sec (Ashraf and Isab, 2004). After 24 h of incubation, only the signal at 62.7 ppm appears in the ^{31}PNMR spectra in the case of AF as well as for AF-I, indicating that the transient species where DTT coordinates the gold-containing fragment, is quantitatively converted to the gold-selenium adduct (see SI for the NMR spectra). Even in the case of incubation of AF and its analog with Sec, the production of CO_2 -when the two reactants are mixed together- confirms a rapid interaction with consequent release of hydroiodic acid.

FT-IR Spectroscopy

To avoid the problems arising from ^{31}PNMR chemical shift overlap in the NMR experiments, the reactivity of Cys with AF and AF-I was further investigated through solid state ATR-FTIR spectroscopy. More precisely, Cys was incubated for 24 h in the presence of AF and AF-I in the same experimental conditions used for the ^{31}PNMR spectroscopy and then the two collected spectra were compared with the IR profile of untreated Cys. In both cases, the infrared spectra showed the disappearance of the absorption band located at 2,542 cm^{-1}, assigned to Cys -S-H stretching mode (Zhang et al., 2020). In **Figure 2** is reported the superimposition between the IR spectra of the unreacted Cys and of the Cys-AF adduct, and the disappearance of the diagnostic band is evident. These results are in agreement with those obtained with ^{31}PNMR in the case of AF-I and confirm a similar reaction pattern of AF toward the Cys -SH moiety.

ESI Mass Spectrometry

Beyond IR spectroscopy, additional evidence for the reactivity of AF with cysteine was obtained through ESI-MS experiments. To this aim, auranofin was incubated in the presence of cysteine. After 24 h of incubation a peak at 434.06 *m/z* assignable to the adduct where the cationic fragment $[AuPEt_3]^+$ is coordinated to the amino acid appeared (**Figure 3**). This evidence strengthens and supports the results already obtained with IR experiments. Similarly, also the reactivity of selenocysteine was assessed with both AF and AF-I (see **Supplementary Information**). Since this amino acid is commercially available as selenocystine, an initial reduction step with DTT is required to restore the reactive selenol group. Also in this case, the selenol group reacted with the

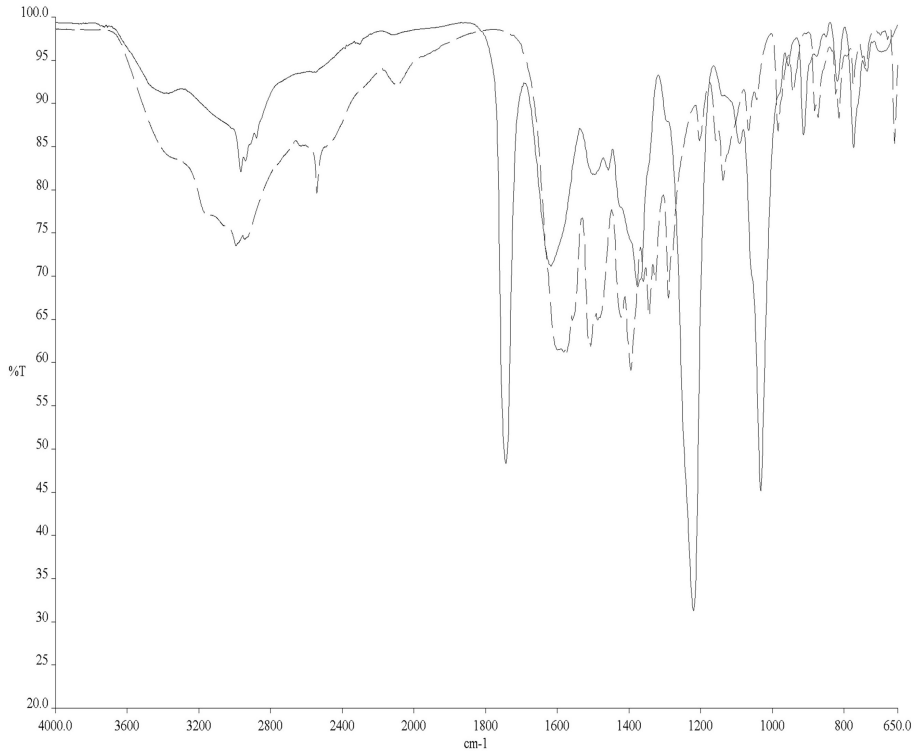

FIGURE 2 | ATR-FTIR spectra of Cys (dashed line) and Cys/AF adducts (solid line).

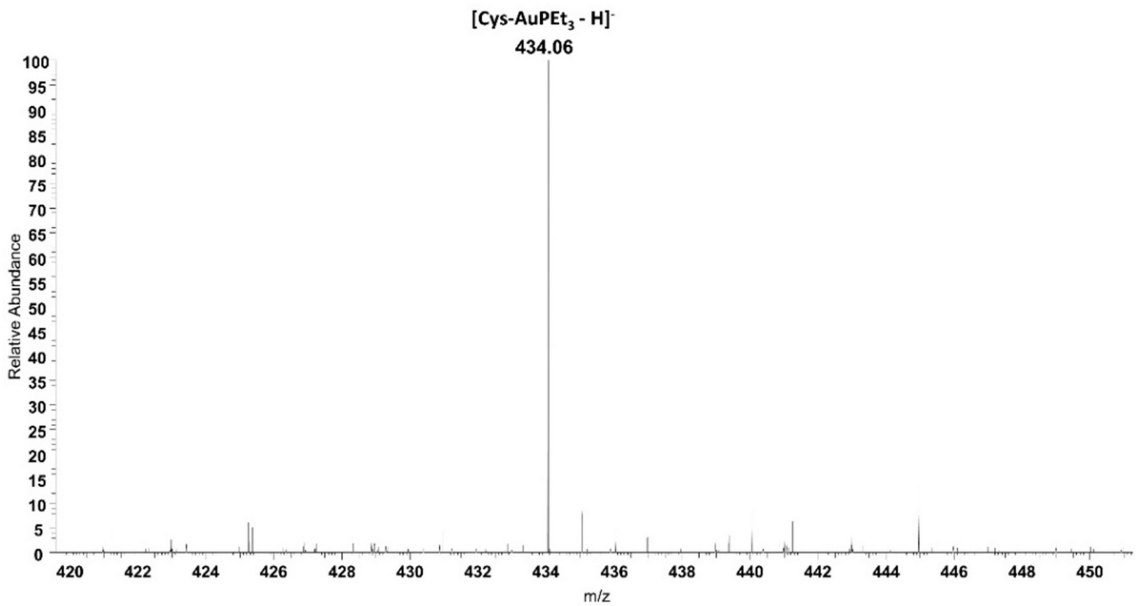

FIGURE 3 | ESI mass spectrum of auranofin (10^{-5} M) incubated for 24 h at 37 °C with cysteine (1:1 metal to amino acid ratio), in ammonium acetate buffer 500 mM pH=6.8 in presence of 50% MeOH.

$[AuPEt_3]^+$ cation from AF and from its iodido derivative. In both cases the signal at 530.02 *m/z* is diagnostic for the Sec reactivity and assignable to the adduct with the $[AuPEt_3]^+$ moiety plus one molecule of MeOH and one NH_4^+ deriving from the reaction buffer. Interestingly, those signals clusters show the characteristic selenium isotopic pattern.

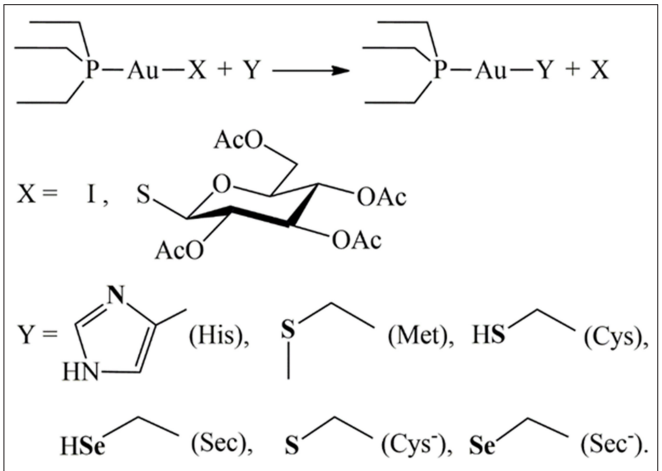

SCHEME 1 | Reaction scheme and considered nucleophiles. Attacking atoms in bold.

Next, we investigated more in depth the reactivity of both AF and AF-I with His and Met. In fact, the lack of adducts formation could be the consequence of a slower kinetics in the reaction of the two gold complexes with these amino acids compared with Cys and Sec. This may lead to a relatively scarce adducts formation in 24 h that might be non-detectable with NMR analysis. In this case, also the IR analysis failed due to the lack of characteristic bands that can be followed to determine His and Met reactivity. Thus, we performed ESI-MS experiments also for AF and AF-I incubated with the two latter amino acids. Results confirmed the lack of reactivity for these two target molecules with AF and AF-I, further supporting the findings already published by some of us regarding the reactivity of auranofin and its derivatives toward protein targets (Landini et al., 2017; Pratesi et al., 2018; Zoppi et al., 2020).

Both in case of His and Met, the spectra recorded with AF only show a main peak at 679.13 m/z corresponding to the unreacted auranofin. At variance, in the case of AF-I the peaks at 433.15, 442.96, and 459.99 *m/z* belong to $[Au(PEt_3)_2]^+$, AF-I, and $[AF\text{-}I+NH_4]^+$, respectively. The $[Au(PEt_3)_2]^+$ cation is a well-known species deriving from the ligand scrambling reaction of AF-I (Marzo et al., 2017). All these spectra are reported in the **Supplementary Material**.

DFT Calculations

Next, we have computed the reactivity of the neutral AF and AF-I complexes with water and with the side chains of histidine, methionine, cysteine, and selenocysteine residues. We have used simplified models of these residues (**Scheme 1**). Each side chain was represented by the nucleophilic group, while the rest of the chain was represented by the ethyl group.

In order to gain deeper insight into the binding mode of the AF and AF-I complexes with protein targets and their binding preference, we have taken advantage of a computational strategy aimed at evaluating the thermodynamic and kinetic basis of the proposed mechanistic hypotheses. A preliminary geometry optimization of the AF and AF-I complexes with various density functionals yield structures in good agreement with the crystallographic data (Hill and Sutton, 1980; Marzo et al., 2017). Indeed, the Au-P, Au-S, and Au-I bond distances fall within an error of 0.08 Å, and P-Au-S and P-Au-I angles are within 7°: in particular, the errors for all the calculated geometrical parameters indicate that the CAM-B3LYP functional provides the best description for these molecular structures (see **Table 2**, **Figure 4**) and will be employed in all subsequent calculations.

DFT calculations were therefore carried out on the thermodynamics and the kinetics of the ligand exchange reactions between the thiosugar of AF or the iodide in case of AF-I and the selected nucleophilic molecules. Moreover, simplified models of the amino acid residues side chains (**Scheme 1**) were conveniently used for the theoretical study as previously reported (Tolbatov et al., 2020b). The amino acid capped forms, although chemically resembling the protein residues, are connected to the side chain nucleophilic group through hydrocarbon chains of different lengths, thus leading to a large variation in the ligand's size reacting with metal complex. This latter aspect may bias the solvation free energies calculation, thus affecting the comparison of amino acid reactivity. All residues were assumed to be in their most stable protonation state at pH=7.8, as expected on the pKa of the side chain groups, i.e. neutral for histidine (pKa=5.9) and methionine and anionic for selenocysteine (pKa=5.2), for which we also considered the neutral form for sake of completeness). For cysteine (pKa=8.3) we considered both the neutral form, expected to be the most stable at pH 7.8, and the anionic form, which is still present in low concentrations (ca. 30%). Preliminary, we considered the hydrolysis reaction with substitution of the thiosugar or iodido ligand by a water molecule to probe the stability of AF and AF-I complexes in biological fluids. The calculated reaction free energy values for the aquation reaction of AF and AF-I are 18.3 and 23.0 kcal/mol, respectively. These values indicate that the reaction is negligible at physiological temperature, and that both complexes are likely to attack the biological targets in their administered form. This result is consistent with the experimental evidences showing as the solutions of both AF and AF-I complexes are stable at room temperature even for very long incubation times (days) (Marzo et al., 2017, 2018).

The ligand exchange reactions on AF and AF-I were investigated by assuming an associative interchange mechanism where both reagents and products form stable non-covalent adducts prior/after the reaction takes place. We have thus optimized the geometries of the reactant adducts (RA), transition states (TS), and product adduct (PA) intermediates and their energies with respect to the isolated species have been evaluated (see below). Calculations indicated a very low stability of RA and PA adducts, which cannot even be optimized for cysteine or selenocysteine side chains (*vide infra*). The activation enthalpies and free energies have been calculated as the difference between TS and the lowest between reactants and reactant adducts, while

TABLE 2 | Assessment of five density functionals for the geometry optimization via comparison of experimental and calculated values for structural parameters of AF and AF-I complexes (**Figure 1**).

Density functionals	AF				AF-I			Errors*
	Distances		Angles		Distances		Angles	
	Au-P	Au-S	P-Au-S	Au-S-C	Au-P	Au-I	P-Au-I	
wB97X	2.30	2.34	178.8	103.1	2.30	2.62	179.4	8.35
M06L	2.30	2.37	178.5	98.3	2.30	2.64	180.0	9.20
B3LYP	2.32	2.36	178.5	103.7	2.32	2.65	179.8	8.90
CAM-B3LYP	2.30	2.34	178.3	103.7	2.30	2.62	179.6	8.05
B3LYP-D3	2.30	2.37	177.8	99.1	2.31	2.65	179.9	8.10
Exp [39, 71]	2.26	2.29	173.6	105.6	2.27	2.59	178.9	-

All distances are in angstroms and all angles in degrees. No reactant-adducts for the reactions of AF/AF-I with deprotonated cysteine and selenocysteine could be optimized.

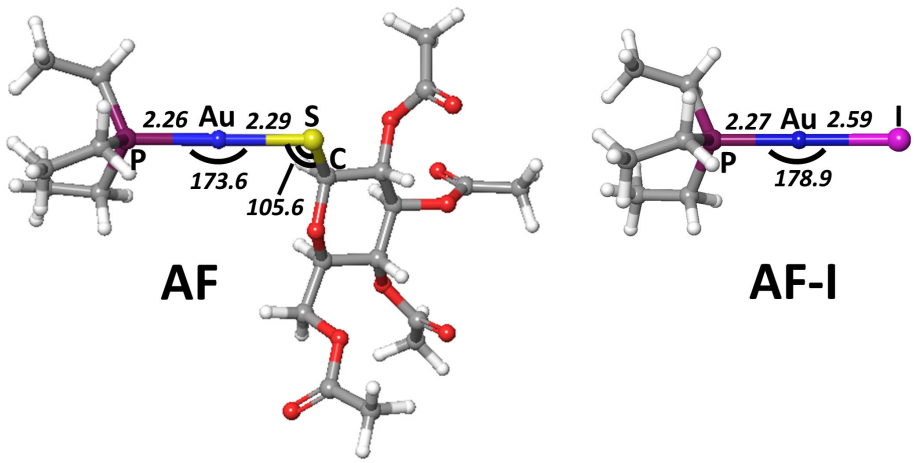

FIGURE 4 | Representation of the experimentally characterized structures of AF and AF-I complexes, the respective crystallographic cartesian coordinates are extrapolated from (Hill and Sutton, 1980; Marzo et al., 2017). All distances are in angstroms, all angles in degrees.

the reaction enthalpies and free energies have been calculated as the difference between reagents and products infinitely apart.

The calculated values of reaction enthalpy and free energy for the examined ligand exchange processes (**Table 3** and **Figure 5**) allow us to establish the thermodynamic preferences for the Au(I) binding toward the considered protein residues side chains. Indeed, we found that the substitution of iodide is always much more favored than the one of thiosugar, the latter being featured in higher reaction enthalpy and free energy values. Calculations also indicated that the reactions of both the Au(I) complexes with the considered neutral amino acid side chain are endothermic and endergonic, 9–10 kcal mol^{-1} for His and 16–17 kcal mol^{-1} for Met, Cys, and Sec, whereas the reactions with deprotonated cysteine and selenocysteine side chains are slightly exothermic and exergonic, by 3–4 kcal mol^{-1} for Cys^- and 2–3 kcal mol^{-1} for Sec^-. Based on the calculated thermodynamics, we can eventually state that the reaction trend for both AF and AF-I with the examined side chain models can be rationalized as Cys^- > Sec^- >> His > Met ≈ > Sec ≈ Cys, thus remarking the importance of the protonation state of the nucleophile. These results clearly show that the thiosugar or iodide substitution reaction is thermodynamically unfavorable for neutral amino acids, His, Met, Cys, and Sec and is therefore not expected to occur, while it is possible only for Cys and Sec in their anionic forms.

The reactivity of AF and AF-I toward molecular models for the side chain of His, Met, Cys, and Sec was then addressed by calculating the corresponding values of activation enthalpy and free energy.

The calculated transition state structures for the reaction of either AF or AF-I with the neutral amino acids, His, Met, Cys, and Sec, show a roughly planar trigonal coordination of the Au(I) center with entering group-metal-leaving group angles in the 82-96° range, whereas the transition states for the anionic Cys^- and Sec^- models species, show earlier transition state structures with almost T-shaped and with entering group-metal-leaving group angles of 104-105° (**Figure 5**).

The calculated activation free energies in **Table 3** show for neutral amino acids barriers much higher for AF than for AF-I, ca. 10–15 kcal mol^{-1}. Although the barriers for the iodide substitution in AF-I, 15–18 kcal mol^{-1}, are low (too low to foresee relatively fast substitution reactions), these are not

TABLE 3 | Enthalpies and Gibbs free energies for reaction of AF/AF-I with various biomolecular targets in solution.

Biomolecular target/ Side chain of protein residue	Metallodrug	R->P		R->TS		RA->TS	
		ΔH	ΔG	ΔH	ΔG	ΔH	ΔG
His	AF	9.4	9.6	11.3	25.6	10.0	14.4
	AF-I	5.7	9.8	5.1	16.3	3.3	7.4
Met	AF	14.8	16.4	18.7	32.4	18.8	23.6
	AF-I	11.2	16.6	5.9	17.8	5.2	10.1
Cys	AF	18.1	17.4	17.2	26.7	16.2	18.7
	AF-I	14.4	17.6	5.9	15.5	5.7	7.7
Sec	AF	15.5	16.8	17.9	27.2	16.6	19.2
	AF-I	11.9	17.0	5.9	16.3	6.0	9.0
Cys^-	AF	−2.4	−3.9	11.7	21.3	–*	–
	AF-I	−6.0	−3.7	2.8	12.0	–	–
Sec^-	AF	−0.9	−2.5	3.4	21.2	–	–
	AF-I	−4.4	−2.2	2.1	14.1	–	–

** No reactant-adducts for the reactions of AF/AF-I with deprotonated cysteine and selenocysteine could be optimized.*

expected to occur due to the unfavorable thermodynamics as discussed above. For thiosugar substitution by neutral amino acids, the activation barriers are relatively high, 25–32 kcal mol^{-1}, making these reactions not only thermodynamically but also kinetically unfavorable. On the other hand, significantly lower activation barriers were calculated for the reaction of either AF or AF-I with cysteine and selenocysteine in their anionic form. Namely, the calculated activation free energy values for substitution of iodide ligand by Cys^- and Sec^- were found to be particularly low 12.0 and 14.1 kcal mol^{-1}, respectively, while those for thiosugar substitution were found 21.2 and 21.3 kcal mol^{-1}, respectively, low enough to guarantee reaction half times of only a few minutes.

An overall picture of the thermodynamics and of the ligand exchange reactions for the anionic Cys^- and Sec^- amino acids, is provided in **Figure 6** and clearly shows as only for the anionic species thiosugar or iodide substitution is both thermodynamically and kinetically feasible, in agreement with experimental evidence.

DISCUSSION AND CONCLUSIONS

Starting from our previous findings on the reactivity of AF and its analogs toward protein targets (Pratesi et al., 2014, 2018; Marzo et al., 2017, 2019; Cirri et al., 2019; Zoppi et al., 2020), here we have extended the investigation—at the molecular level—on the mode of action of these medicinally relevant gold(I) compounds. Specifically, we have focused our attention on AF and its analog where the thiosugar moiety is replaced by the iodide ligand. All the previous data seem to converge toward an unambiguous predilection of these gold (I) complexes for the free and solvent accessible cysteine and selenocysteine amino acid residues of the studied proteins. Nonetheless, some other residues i.e., methionine and histidine may represent, at least theoretically, a possible binding site for these compounds.

Accordingly, in this work, we have further elucidated the reactivity of AF and its promising anticancer analog AF-I through a multi-techniques approach involving NMR, FTIR and ESI-MS.

Since the $[AuPEt_3]^+$ cation has been recognized as the reactive fragment, the ^{31}PNMR can be considered the election technique to characterize adducts formation with the selected amino acids. Hence, an extensive experimental work has been carried out demonstrating that AF and AF-I react quite completely with Sec after 24 h. Also, in case of Cys, the same reactivity has been highlighted with AF-I. Unfortunately, the reaction between Cys and AF did not produce any appreciable shift of the ^{31}P signal and makes difficult to assess adduct formation.

In this case, the reaction has been followed with the ATR-FTIR since Cys possesses a diagnostic band at 2,542 cm^{-1} due to the Cys -S-H stretching. The disappearance of this band is evidential for the amino acid reactivity because the formed -S-Au bond stretching falls below 200 cm^{-1}. Moreover, this band result disappeared entirely, leaving us to guess a near quantitative reaction after 24 h.

This behavior has been further assessed with ESI-MS; the obtained spectra show as the main peaks the signals corresponding to the AF and AF-I adducts with Sec and Cys.

Interestingly, the ^{31}PNMR spectra do not show any appreciable chemical shift also in the case of Met and His when reacted with AF and AF-I. In these cases, also the ATR-FTIR is not useful because, similarly to Cys, the two amino acids do not possess a diagnostic band. Thus, we eventually exploited ESI-MS analysis that confirmed the lack of reactivity for the gold complexes with Met and His. Indeed, the only signals present in the spectra are those belonging to AF and to a couple of well-known AF-I scrambling products in MeOH solution in the case of the iodide analog (Marzo et al., 2017).

As a completion of this study, the reactivities of AF and AF-I toward the selected amino acids have been evaluated

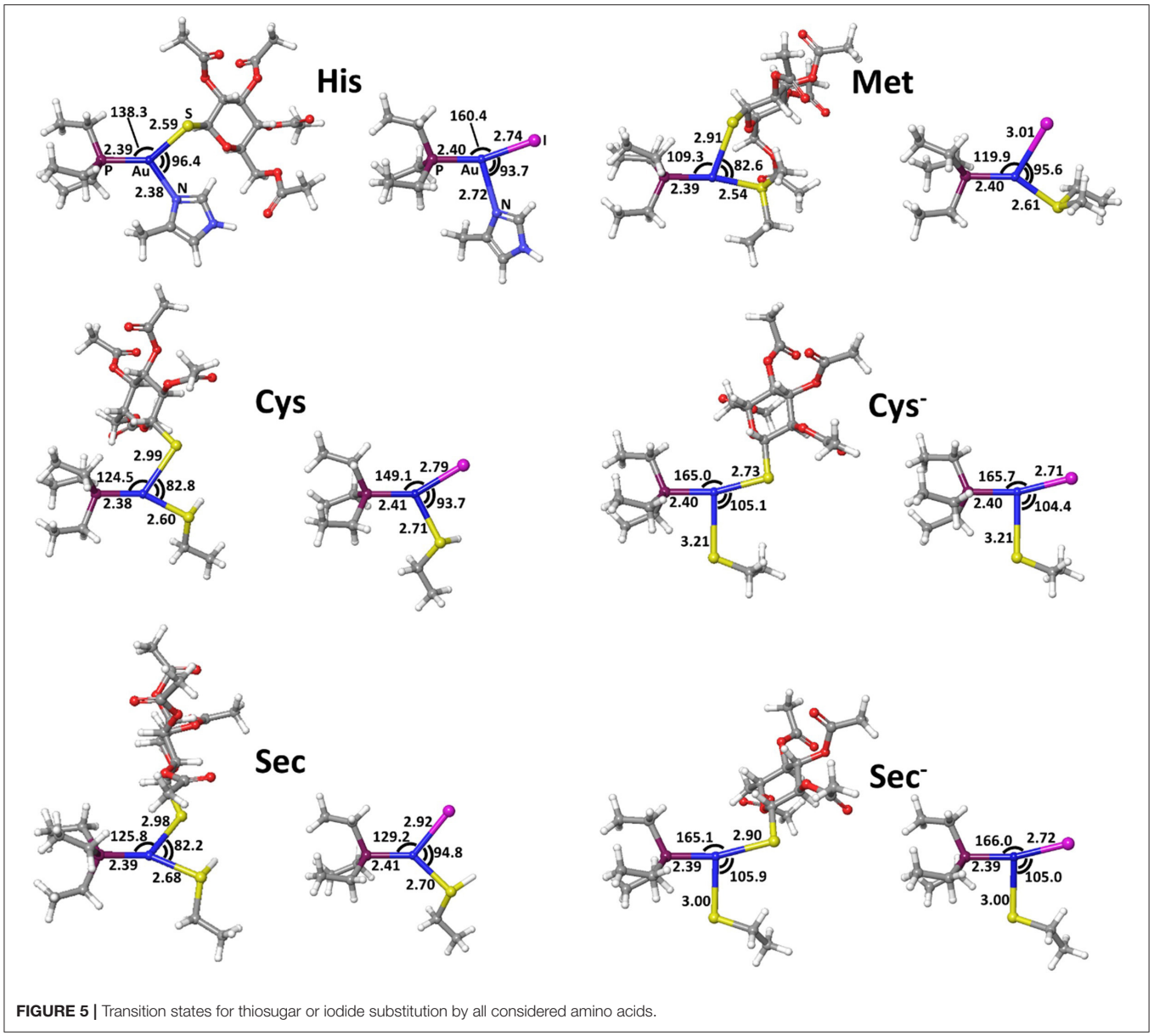

FIGURE 5 | Transition states for thiosugar or iodide substitution by all considered amino acids.

also with computational methods. We considered the free and unprotected amino acids and their reduced molecular models, i.e. imidazole, methylselenol, and methylthiol. This simplification can be done since the gold(I) complexes are unable to give bidentate coordination between the sidechain and the carboxyl or amine group of the amino acid.

Computational studies have often and successfully been applied to describe the reactivity of metals and metallodrugs with proteins (Graziani et al., 2016; Tolbatov et al., 2019b, 2020c). Understanding the binding preference of AF and AF-I would be very useful to fully understand their mechanisms of action *in vivo* and may be useful to conceive novel and more effective anticancer drugs.

On the other hand, computational studies about AF are very few. Density functional theory (DFT) calculations on a very simplified model of AF reacting with methylselenol displayed the preference of breakage of Au-S bond over the Au-phosphine bond that could be concluded from the difference in the gas phase free energy reaction barriers of 11.9 and 22.8 kcal mol^{-1} for the S-CH_3 and $(CH_3)_3P$ exchanges, respectively (Di Sarra et al., 2013). The computational study of the reactivity of AF against S-, Se-, and N-containing amino acids (Dos Santos, 2014) for the substrate and the nucleophiles has supported the conclusion that the replacement of the thiosugar by the protein residues is favored over the replacement of phosphine. This study found that the activation barriers of the amino acids with auranofin follow the trend Lys > His > Sec > Cys according to their activation enthalpy values. In recent studies, reactivity of AF with Cys and Sec was studied via DFT calculations (Howell, 2009; Shoeib et al., 2010) and the overall conclusions

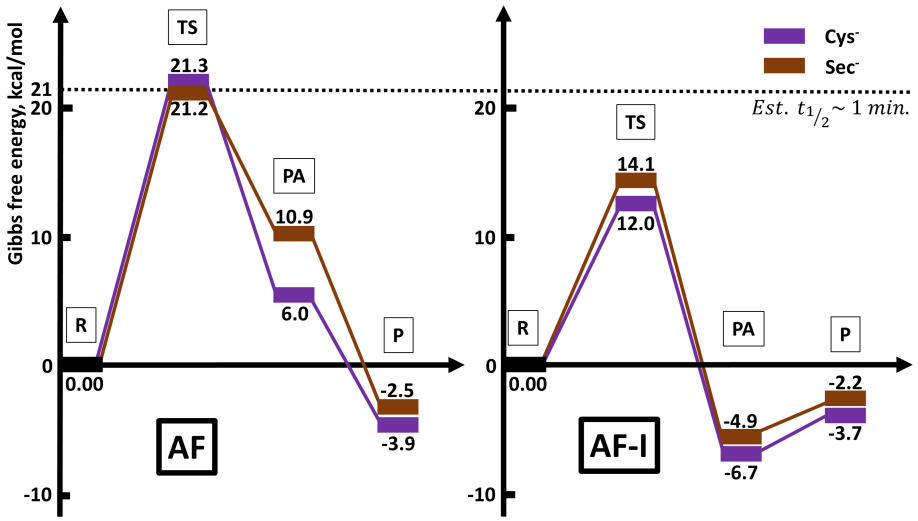

FIGURE 6 | Reaction profiles for AF and AF-I interacting with neutral His and Met and anionic Cys^- and Sec^- nucleophiles.

were that the Se moiety is the preferred coordination site over the cysteine.

Detailed mechanisms of reaction of AF and AF-I compounds with most amino acids and protein fragments remains largely undisclosed. In this study, we have computed the reactivity of both these complexes with various nucleophiles—side chains of neutral histidine, methionine, and cysteine, and selenocysteine in both neutral and anionic forms.

The high reaction free energy values calculated for the aquation of AF and AF-I indicate that this process is thermodynamically disfavored, and that both complexes are likely to attack their biological targets by the exchange of either thiosugar (AF) or iodide (AF-I).

The theoretical analysis of thermodynamics and kinetics for the ligand exchange processes of AF and AF-I with His, Met, Cys, and Sec side chain models unveiled that thiosugar or iodide substitution is both thermodynamically and kinetically favored only for Cys and Sec, but only in their anionic forms, with barriers for iodide substitution in AF-I significantly lower.

In conclusion, we have presented here a suitable multi-techniques approach allowing to gather mechanistic insights on the reactivity and the mode of action of two promising anticancer agents. The computational analysis is in good agreement with the experimental data, and the energy barrier calculated point out the enhanced reactivity of AF-I with respect to AF toward Cys and Sec. On the other hand, also the lower energetic barriers calculated for the reactivity with Sec and Cys, perfectly support the experimental data obtained, pinpointing a quite exclusive preference for these two aminoacidic residues instead of His and Met. This supports the view that proteins bearing cysteine and selenocysteine residues e.g., thioredoxin reductase, are the likely targets for the pharmacological activity of these gold complexes. In turn, the more pronounced reactivity of AF-I toward Cys and Sec compared to AF might be at the bases of its better anticancer properties *in vivo* (Marzo et al., 2019).

MATERIALS AND METHODS

Materials

Auranofin was purchased from Enzo Life Sciences (Famingdale, New York). AF-I was synthesized as described in (Marzo et al., 2017). Cysteine, histidine, methionine, and selenocysteine were purchased from Merck (Darmstadt, Germany) and used without further purification or manipulation. Water, methanol, and ammonium acetate were of LC-MS grade and were purchased from Merck. MeOD-d_4 was purchased from Merck with a deuteration grade of 99.9%.

NMR

AF and AF-I (6.25 mM) were incubated at 37 °C with amino acids or MM (complex to amino acid or MM ratio 1:1) in presence of 400 μL of MeOH and 400 μL of $NaHCO_3$ buffer (500 mM) at pH=7.8 and NMR experiments were recorded at increasing time intervals (0 h, 24 h) on a Bruker Ultrashield 400.13 MHz, Bruker Avance III equipped with Probe 5 mm PABBO BB-1H/D Z-GRD Z108618/0049. Calibration was made according to the residual peak of the solvent. Raw data were analyzed using TopSpin 2.1 software (Bruker). In the case of selenocysteine (Sec), this latter was generated *in situ* through the addition of 10 equivalents of DTT (dithiothreitol). Spectra are available in the **Supplementary Material**.

FT-IR

Experiments were carried out on Perkin-Elmer SPECTRUM 100 FT-IR Spectrometer equipped with the Perkin-Elmer Universal ATR Sampling Accessory. Samples were prepared as a 30 mM solution of interest compound dissolved in 1:1 MeOH and $NaHCO_3$ buffer (500 mM) at pH=7.8 (see **Supplementary Material** for further details). A drop of solution was deposed on the spectrometer ATR probe and let to completely evaporate in the air before scanning. The acquisition

was performed between 4,000 and 650 cm^{-1} with a resolution of 4 cm^{-1}.

ESI-MS

Sample Preparation

Stock solutions of AF and AF-I were freshly prepared in LC-MS grade water and methanol (50:50 v/v) to a final concentration of 10^{-2} M. Stock solutions of the amino acids and molecular models were prepared in 500 mM ammonium acetate solution with a pH 6.8 and methanol (50:50 v/v) at 10^{-2} M. As previously described, selenocysteine (Sec) was generated *in situ* through the addition of 10 equivalents of DTT to reduce the Se-Se bond of selenocystine.

For each gold compound/amino acid pair, appropriate aliquots of these stock solutions were mixed and diluted with 500 mM ammonium acetate solution (pH 6.8) to a final amino acid concentration of 10^{-4} M and an amino acid-to-metal molar ratio of 1:1. The solutions were incubated up to 24 h at 37 °C.

ESI-MS Analysis

Aliquots were sampled at after 24 h of incubation, diluted to a final concentration of 10^{-5} M with LC-MS grade water and ESI-MS spectra were recorded by direct injection at 5 (for positive polarity) and 7 (for negative polarity) μL min^{-1} flow rate in an Orbitrap high-resolution mass pectrometer (Thermo, San Jose, CA, USA), equipped with HESI source. The working conditions were as follows: positive polarity, spray voltage 3.5 kV, capillary temperature 300 °C, and S-lens RF level 55. The sheath and the auxiliary gases were set at 20 and 3 (arbitrary units), respectively. Negative polarity, spray voltage −3.4 kV, capillary temperature 300 °C, S-lens RF level 55. The sheath and the auxiliary gases were set at 35 and 8 (arbitrary units), respectively. For acquisition and analysis, Xcalibur 4.2 software (Thermo) was used. For spectra acquisition a nominal resolution (at *m/z* 200) of 140,000 was used.

Computational

All calculations were performed with the Gaussian 09 A.02 (Gaussian 09 | Gaussian.com[1]) quantum chemistry packages. Optimizations, electronic and solvation energy evaluations were carried out in solvated phase (C-PCM) (Barone and Cossi, 1998; Cossi et al., 2003) and by using the density functionals reported on **Table 1** (optimization) and **Table 2** (electronic and solvation energy) as described below.

All geometrical optimizations have been carried out with the LANL2DZ basis set (Dunning and Hay, 1977; Hay and Wadt, 1985; Roy et al., 2008), whereas single-point electronic and solvation energy calculations were calculated with the LANL08(f) effective core potential for gold (Hay and Wadt, 1985; Ehlers et al., 1993; Roy et al., 2008) and the basis set 6-311++G** for other elements (Krishnan et al., 1980; McLean and Chandler, 1980; Francl et al., 1982; Clark et al., 1983; Spitznagel et al., 1987). We used the DFT functionals in a preliminary geometry benchmarking study B3LYP (Becke, 1993; Stephens et al., 1994), M06L (Zhao and Truhlar, 2006), and range corrected wB97X (Chai-Da and Head-Gordon, 2008), B3LYP-D3 (Grimme et al., 2010), and CAM-B3LYP (Yanai et al., 2004). DFT functionals are known to give a good description of geometries and reaction profiles for transition-metal-containing compounds (Ciancetta et al., 2012; Paciotti et al., 2018, 2019; Todisco et al., 2020) including Au(I) (Tolbatov et al., 2019a, 2020a) based anticancer compounds. The preliminary benchmarking of performance of these density functionals has shown that CAM-B3LYP yields the geometrical structure slightly more accurate than the other functionals, and it was thus chosen as the best for our calculations.

Frequency calculations were performed to verify the correct nature of the stationary points and to estimate zero-point energy (ZPE) and thermal corrections to thermodynamic properties. Intrinsic reaction coordinate (IRC) calculations were employed to locate reagents and products minima connected with the transition states for each considered reaction step.

Single point electronic energy calculations were performed on the solvated-phase geometries. The C-PCM continuum solvent method was used to describe the solvation (Cossi et al., 2003). It has recently been shown to give considerably smaller errors than those for other continuum models for aqueous free energies of solvation for neutrals, cations and anions, and to be particularly effective for the computations of solution properties requiring a high accuracy of solution free energies (Chen et al., 2019). Solvation free energies, taken as the difference between the solution energies and the gas phase energies, were added to the gas phase enthalpies and free energies values to obtain the corresponding values in the aqueous solution.

DATA AVAILABILITY STATEMENT

All datasets presented in this study are included in the article/**Supplementary Material**.

AUTHOR CONTRIBUTIONS

AP and TM with the support of IT designed, coordinated, and supervised the whole study. IT and DC carried out theoretical calculations and NMR experiments. AM, CC, and NR revised the paper and suggested improvements and corrections for the theoretical section for which they were responsible with IT. AP carried out the MS experiments with the support of TM. CG and LMe revised the experimental part and suggested improvements and corrections together with DL and LMa. AP, IT, and TM wrote the manuscript. All the authors approved the final version of the manuscript.

FUNDING

AP, TM, DL, and CG gratefully acknowledge the Beneficentia Stiftung, Vaduz (BEN2020/34, BEN2019/48 and BEN2019/9, respectively), and the University of Pisa (Rating Ateneo 2019-2020) for the financial support. DC thanks AIRC-FIRC for his fellowship (project code 23852). NR, AM, CC, and IT gratefully acknowledge the University G. D'Annunzio (FAR 2019) for

[1]Gaussian 09 Citation | Gaussian.com Available online at: https://gaussian.com/g09citation/ (accessed June 18, 2020).

financial support. AP and LMe also acknowledge the Fondazione Italiana per la Ricerca sul Cancro (AIRC, Milan) and Fondazione Cassa Risparmio di Firenze (Multiuser Equipment Program 2016, ref. code 19650).

ACKNOWLEDGMENTS

The authors wish to thank Dr. Beatrice Muscatello (Department of Pharmacy and CISUP, University of Pisa) for the support with ESI-MS experiments. The CIRCMSB (Consorzio Interuniversitario di Ricerca in Chimica dei Metalli nei Sistemi Biologici, Italy) was also acknowledged.

SUPPLEMENTARY MATERIAL

The Supplementary Material for this article can be found online at: https://www.frontiersin.org/articles/10.3389/fchem.2020.00812/full#supplementary-material

REFERENCES

AbdelKhalek, A., Abutaleb, N. S., Mohammad, H., and Seleem, M. N. (2019). Antibacterial and antivirulence activities of auranofin against Clostridium difficile. *Int. J. Antimicrob. Agents* 53, 54–62. doi: 10.1016/j.ijantimicag.2018.09.018

Abhishek, S., Sivadas, S., Satish, M., Deeksha, W., and Rajakumara, E. (2019). Dynamic basis for auranofin drug recognition by thiol-reductases of human pathogens and intermediate coordinated adduct formation with catalytic cysteine residues. *ACS Omega* 4, 9593–9602. doi: 10.1021/acsomega.9b00529

Ashraf, W., and Isab, A. A. (2004). ^{31} P NMR studies of redox reactions of bis (Trialkylphosphine) gold(I) bromide (Alkyl = Methyl, Ethyl) with disulphide and diselenide ligands. *J. Coord. Chem.* 57, 337–346. doi: 10.1080/00958970410001671228

Barone, V., and Cossi, M. (1998). Quantum calculation of molecular energies and energy gradients in solution by a conductor solvent model. *J. Phys. Chem. A* 102, 1995–2001. doi: 10.1021/jp9716997

Becke, A. D. (1993). Density-functional thermochemistry. *III. The role of exact exchange. J. Chem. Phys.* 98, 5648–5652. doi: 10.1063/1.464913

Bulman, C. A., Bidlow, C. M., Lustigman, S., Cho-Ngwa, F., Williams, D., Rascón A. A. Jr., et al. (2015). Repurposing auranofin as a lead candidate for treatment of lymphatic filariasis and onchocerciasis. *PLoS Negl. Trop. Dis.* 9:e0003534. doi: 10.1371/journal.pntd.0003534

Cassetta, M. I., Marzo, T., Fallani, S., Novelli, A., and Messori, L. (2014). Drug repositioning: auranofin as a prospective antimicrobial agent for the treatment of severe staphylococcal infections. *BioMetals* 27, 787–791. doi: 10.1007/s10534-014-9743-6

Chai-Da, J., and Head-Gordon, M. (2008). Systematic optimization of long-range corrected hybrid density functionals. *J. Chem. Phys.* 128:084106. doi: 10.1063/1.2834918

Chen, J., Shao, Y., and Ho, J. (2019). Are explicit solvent models more accurate than implicit solvent models? *A case study on the menschutkin reaction. J. Phys. Chem. A* 123, 5580–5589. doi: 10.1021/acs.jpca.9b03995

Ciancetta, A., Coletti, C., Marrone, A., and Re, N. (2012). Activation of carboplatin by carbonate: a theoretical investigation. *Dalt. Trans.* 41, 12960–12969. doi: 10.1039/c2dt30556a

Cirri, D., Fabbrini, M. G., Massai, L., Pillozzi, S., Guerri, A., Menconi, A., et al. (2019). Structural and solution chemistry, antiproliferative effects, and serum albumin binding of three pseudohalide derivatives of auranofin. *BioMetals* 32, 939–948. doi: 10.1007/s10534-019-00224-1

Cirri, D., Pillozzi, S., Gabbiani, C., Tricomi, J., Bartoli, G., Stefanini, M., et al. (2017). PtI2(DACH), the iodido analogue of oxaliplatin as a candidate for colorectal cancer treatment: chemical and biological features. *Dalt. Trans.* 46, 3311–3317. doi: 10.1039/C6DT03867K

Clark, T., Chandrasekhar, J., Spitznagel, G. W., and Schleyer, P. V. R. (1983). Efficient diffuse function-augmented basis sets for anion calculations. III. The 3-21+G basis set for first-row elements, Li–F. *J. Comput. Chem.* 4, 294–301. doi: 10.1002/jcc.540040303

Cossi, M., Rega, N., Scalmani, G., and Barone, V. (2003). Energies, structures, and electronic properties of molecules in solution with the C-PCM solvation model. *J. Comput. Chem.* 24, 669–681. doi: 10.1002/jcc.10189

Di Sarra, F., Fresch, B., Bini, R., Saielli, G., and Bagno, A. (2013). Reactivity of auranofin with selenols and thiols - implications for the anticancer activity of gold(I) compounds. *Eur. J. Inorg. Chem.* 2013, 2718–2727. doi: 10.1002/ejic.201300058

Dos Santos, H. F. (2014). Reactivity of auranofin with S-, Se- and N-containing amino acids. *Comput. Theor. Chem.* 1048, 95–101. doi: 10.1016/j.comptc.2014.09.005

Dunning, T. H., and Hay, P. J. (1977). "Gaussian basis sets for molecular calculations," in *Methods of Electronic Structure Theory*, ed H. F. Schaefer III (Boston, MA: Springer), 1–27.

Ehlers, A. W., Böhme, M., Dapprich, S., Gobbi, A., Höllwarth, A., Jonas, V., et al. (1993). A set of f-polarization functions for pseudo-potential basis sets of the transition metals ScCu, YAg and LaAu. *Chem. Phys. Lett.* 208, 111–114. doi: 10.1016/0009-2614(93)80086-5

Fabbrini, M. G., Cirri, D., Pratesi, A., Ciofi, L., Marzo, T., Guerri, A., et al. (2019). A fluorescent silver(I) carbene complex with anticancer properties: synthesis, characterization, and biological studies. *ChemMedChem* 14, 182–188. doi: 10.1002/cmdc.201800672

Fan, C., Zheng, W., Fu, X., Li, X., Wong, Y. S., and Chen, T. (2014). Enhancement of auranofin-induced lung cancer cell apoptosis by selenocystine, a natural inhibitor of TrxR1 *in vitro* and *in vivo*. *Cell Death Dis.* 5, e1191–e1191. doi: 10.1038/cddis.2014.132

Francl, M. M., Pietro, W. J., Hehre, W. J., Binkley, J. S., Gordon, M. S., DeFrees, D. J., et al. (1982). Self-consistent molecular orbital methods. *XXIII. A polarization-type basis set for second-row elements. J. Chem. Phys.* 77, 3654–3665. doi: 10.1063/1.444267

Garbutcheon-Singh, K. B., Grant, M. P., Harper, B. W., Krause-Heuer, AM., Manohar, M., Orkey, N., et al. (2011). Transition metal based anticancer drugs. *Curr. Top. Med. Chem.* 11, 521–542. doi: 10.2174/156802611794785226

Graziani, V., Coletti, C., Marrone, A., and Re, N. (2016). Activation and reactivity of a bispidine analogue of cisplatin: a theoretical investigation. *J. Phys. Chem. A* 120, 5175–5186. doi: 10.1021/acs.jpca.6b00844

Grimme, S., Antony, J., Ehrlich, S., and Krieg, H. (2010). A consistent and accurate ab initio parametrization of density functional dispersion correction (DFT-D) for the 94 elements H-Pu. *J. Chem. Phys.* 132:154104. doi: 10.1063/1.3382344

Guidi, F., Landini, I., Puglia, M., Magherini, F., Gabbiani, C., Cinellu, M. A., et al. (2012). Proteomic analysis of ovarian cancer cell responses to cytotoxic gold compounds. *Metallomics* 4, 307–314. doi: 10.1039/c2mt00083k

Habermann, K. J., Grünewald, L., van Wijk, S., and Fulda, S. (2017). Targeting redox homeostasis in rhabdomyosarcoma cells: GSH-depleting agents enhance auranofin-induced cell death. *Cell Death Dis.* 8:e3067. doi: 10.1038/cddis.2017.412

Harbut, M. B., Vilchèze, C., Luo, X., Hensler, M. E., Guo, H., Yang, B., et al. (2015). Auranofin exerts broad-spectrum bactericidal activities by targeting thiol-redox homeostasis. *Proc. Natl. Acad. Sci. U.S.A.* 112, 4453–4458. doi: 10.1073/pnas.1504022112

Hay, P. J., and Wadt, W. R. (1985). Ab initio effective core potentials for molecular calculations. *Potentials for K to Au including the outermost core orbitale. J. Chem. Phys.* 82, 299–310. doi: 10.1063/1.448975

Hill, D. T., and Sutton, B. M. (1980). (2,3,4,6Tetra-O-acetyl-1-thio-b - D- glucopyranosato-S) (triethylphosphine) gold, C20H34AuO9PS. *Acta Crystallogr. Sect. C Cryst. Struct. Commun.* 9, 679–686.

Howell, J. A. S. (2009). DFT investigation of the interaction between gold(I) complexes and the active site of thioredoxin reductase. *J. Organomet. Chem.* 694, 868–873. doi: 10.1016/j.jorganchem.2008.10.029

Hu, J., Zhang, H., Cao, M., Wang, L., Wu, S., and Fang, B. (2018). Auranofin enhances ibrutinib's anticancer activity in EGFR-mutant lung adenocarcinoma. *Mol. Cancer Ther.* 17, 2156–2163. doi: 10.1158/1535-7163.MCT-17-1173

Hu, M., Zhang, Z., Liu, B., Zhang, S., Chai, R., Chen, X., et al. (2018). Deubiquitinase inhibitor auranofin attenuated cardiac hypertrophy by blocking NF-κB activation. *Cell. Physiol. Biochem.* 45, 2421–2430. doi: 10.1159/000488230

Kim, N. H., Park, H. J., Oh, M. K., and Kim, I. S. (2013). Antiproliferative effect of gold(I) compound auranofin through inhibition of STAT3 and telomerase activity in MDA-MB 231 human breast cancer cells. *BMB Rep.* 46, 59–64. doi: 10.5483/BMBRep.2013.46.1.123

Krishnan, R., Binkley, J. S., Seeger, R., and Pople, J. A. (1980). Self-consistent molecular orbital methods. *XX. A basis set for correlated wave functions. J. Chem. Phys.* 72, 650–654. doi: 10.1063/1.438955

Landini, I., Lapucci, A., Pratesi, A., Massai, L., Napoli, C., Perrone, G., et al. (2017). Selection and characterization of a human ovarian cancer cell line resistant to auranofin. *Oncotarget* 8, 96062–96078. doi: 10.18632/oncotarget.21708

Li, H., Hu, J., Wu, S., Wang, L., Cao, X., Zhang, X., et al. (2016). Auranofin-mediated inhibition of PI3K/AKT/mTOR axis and anticancer activity in non-small cell lung cancer cells. *Oncotarget* 7, 3548–3558. doi: 10.18632/oncotarget.6516

Liu, C., Liu, Z., Li, M., Li, X., Wong, Y.-S., Ngai, S.-M., et al. (2013). Enhancement of auranofin-induced apoptosis in MCF-7 human breast cells by selenocystine, a synergistic inhibitor of thioredoxin reductase. *PLoS ONE* 8:e53945. doi: 10.1371/journal.pone.0053945

Marzano, C., Gandin, V., Folda, A., Scutari, G., Bindoli, A., and Rigobello, M. P. (2007). Inhibition of thioredoxin reductase by auranofin induces apoptosis in cisplatin-resistant human ovarian cancer cells. *Free Radic. Biol. Med.* 42, 872–881. doi: 10.1016/j.freeradbiomed.2006.12.021

Marzo, T., Cirri, D., Gabbiani, C., Gamberi, T., Magherini, F., Pratesi, A., et al. (2017). Auranofin, Et3PAuCl, and Et3PAuI are highly cytotoxic on colorectal cancer cells: a chemical and biological study. *ACS Med. Chem. Lett.* 8, 997–1001. doi: 10.1021/acsmedchemlett.7b00162

Marzo, T., Cirri, D., Pollini, S., Prato, M., Fallani, S., Cassetta, M. I., et al. (2018). Auranofin and its analogues show potent antimicrobial activity against multidrug-resistant pathogens: structure-activity relationships. *ChemMedChem* 13, 2448–2454. doi: 10.1002/cmdc.201800498

Marzo, T., Massai, L., Pratesi, A., Stefanini, M., Cirri, D., Magherini, F., et al. (2019). Replacement of the thiosugar of auranofin with iodide enhances the anticancer potency in a mouse model of ovarian cancer. *ACS Med. Chem. Lett.* 10, 656–660. doi: 10.1021/acsmedchemlett.9b00007

Marzo, T., and Messori, L. (2020). A role for metal-based drugs in fighting COVID-19 infection? *The case of auranofin. ACS Med. Chem. Lett.* 11, 1067–1068. doi: 10.1021/acsmedchemlett.0c00190

Massai, L., Pratesi, A., Bogojeski, J., Banchini, M., Pillozzi, S., Messori, L., et al. (2016). Antiproliferative properties and biomolecular interactions of three Pd(II) and Pt(II) complexes. *J. Inorg. Biochem.* 165, 1–6. doi: 10.1016/j.jinorgbio.2016.09.016

McLean, A. D., and Chandler, G. S. (1980). Contracted Gaussian basis sets for molecular calculations. I. Second row atoms, Z=11-18. *J. Chem. Phys.* 72, 5639–5648. doi: 10.1063/1.438980

Micale, N., Schirmeister, T., Ettari, R., Cinellu, M. A., Maiore, L., Serratrice, M., et al. (2014). Selected cytotoxic gold compounds cause significant inhibition of 20S proteasome catalytic activities. *J. Inorg. Biochem.* 141, 79–82. doi: 10.1016/j.jinorgbio.2014.08.001

Nakaya, A., Sagawa, M., Muto, A., Uchida, H., Ikeda, Y., and Kizaki, M. (2011). The gold compound auranofin induces apoptosis of human multiple myeloma cells through both down-regulation of STAT3 and inhibition of NF-κB activity. *Leuk. Res.* 35, 243–249. doi: 10.1016/j.leukres.2010.05.011

Ndagi, U., Mhlongo, N., and Soliman, M. (2017). Metal complexes in cancer therapy – an update from drug design perspective. *Drug Des. Devel. Ther.* 11, 599–616. doi: 10.2147/DDDT.S119488

Paciotti, R., Tolbatov, I., Graziani, V., Marrone, A., Re, N., and Coletti, C. (2018). "Insights on the activity of platinum-based anticancer complexes through computational methods," in *AIP Conference Proceedings* (American Institute of Physics Inc.) (Thessaloniki), 020019. doi: 10.1063/1.5079061

Paciotti, R., Tolbatov, I., Marrone, A., Storchi, L., Re, N., and Coletti, C. (2019). "Computational investigations of bioinorganic complexes: the case of calcium, gold and platinum ions," *in AIP Conference Proceedings (American Institute of Physics Inc.)* (Rhodes), 030011. doi: 10.1063/1.5137922

Pratesi, A., Cirri, D., Ciofi, L., and Messori, L. (2018). Reactions of Auranofin and Its Pseudohalide Derivatives with Serum Albumin Investigated through ESI-Q-TOF MS. *Inorg. Chem.* 57, 10507–10510. doi: 10.1021/acs.inorgchem.8b02177

Pratesi, A., Cirri, D., Durović, M. D., Pillozzi, S., Petroni, G., and Bugarčić, Ž. D., et al. (2016). New gold carbene complexes as candidate anticancer agents. *BioMetals* 29, 905–911. doi: 10.1007/s10534-016-9962-0

Pratesi, A., Cirri, D., Fregona, D., Ferraro, G., Giorgio, A., Merlino, A., et al. (2019). Structural characterization of a gold/serum albumin complex. *Inorg. Chem.* 58, 10616–10619. doi: 10.1021/acs.inorgchem.9b01900

Pratesi, A., Gabbiani, C., Ginanneschi, M., and Messori, L. (2010). Reactions of medicinally relevant gold compounds with the C-terminal motif of thioredoxin reductase elucidated by MS analysis. *Chem. Commun.* 46, 7001–7003. doi: 10.1039/c0cc01465f

Pratesi, A., Gabbiani, C., Michelucci, E., Ginanneschi, M., Papini, A. M., Rubbiani, R., et al. (2014). Insights on the mechanism of thioredoxin reductase inhibition by Gold N-heterocyclic carbene compounds using the synthetic linear Selenocysteine containing C-terminal peptide hTrxR(488-499): an ESI-MS investigation. *J. Inorg. Biochem.* 136, 161–169. doi: 10.1016/j.jinorgbio.2014.01.009

Roberts, J. R., Xiao, J., Schliesman, B., Parsons, D. J., and Shaw, C. F. (1996). Kinetics and mechanism of the reaction between serum albumin and auranofin (and its isopropyl analogue) *in vitro*. *Inorg. Chem.* 35, 424–433. doi: 10.1021/ic9414280

Roy, L. E., Hay, P. J., and Martin, R. L. (2008). Revised basis sets for the LANL effective core potentials. *J. Chem. Theory Comput.* 4, 1029–1031. doi: 10.1021/ct8000409

Shin, D. W., Kwon, Y. J., Ye, D. J., Baek, H. S., Lee, J. E., and Chun, Y. J. (2017). Auranofin suppresses plasminogen activator inhibitor-2 expression through annexin A5 induction in human prostate cancer cells. *Biomol. Ther.* 25, 177–185. doi: 10.4062/biomolther.2016.223

Shoeib, T., Atkinson, D. W., and Sharp, B. L. (2010). Structural analysis of the anti-arthritic drug auranofin: its complexes with cysteine, selenocysteine and their fragmentation products. *Inorg. Chim. Acta* 363, 184–192. doi: 10.1016/j.ica.2009.08.034

Spitznagel, G. W., Clark, T., von Ragué Schleyer, P., and Hehre, W. J. (1987). An evaluation of the performance of diffuse function-augmented basis sets for second row elements, Na-Cl. *J. Comput. Chem.* 8, 1109–1116. doi: 10.1002/jcc.540080807

Stephens, P. J., Devlin, F. J., Chabalowski, C. F., and Frisch, M. J. (1994). Ab Initio calculation of vibrational absorption and circular dichroism spectra using density functional force fields. *J. Phys. Chem.* 98, 11623–11627. doi: 10.1021/j100096a001

Talbot, S., Nelson, R., and Self, W. T. (2008). Arsenic trioxide and auranofin inhibit selenoprotein synthesis: implications for chemotherapy for acute promyelocytic leukaemia. *Br. J. Pharmacol.* 154, 940–948. doi: 10.1038/bjp.2008.161

Tamasi, G., Carpini, A., Valensin, D., Messori, L., Pratesi, A., Scaletti, F., et al. (2014). {Ru(CO)x}-core complexes with selected azoles: synthesis, X-ray structure, spectroscopy, DFT analysis and evaluation of cytotoxic activity against human cancer cells. *Polyhedron* 81, 227–237. doi: 10.1016/j.poly.2014.05.067

Thangamani, S., Mohammad, H., Abushahba, M. F. N., Sobreira, T. J. P., and Seleem, M. N. (2016). Repurposing auranofin for the treatment of cutaneous staphylococcal infections. *Int. J. Antimicrob. Agents* 47, 195–201. doi: 10.1016/j.ijantimicag.2015.12.016

Todisco, S., Latronico, M., Gallo, V., Re, N., Marrone, A., Tolbatov, I., et al. (2020). Double addition of phenylacetylene onto the mixed bridge phosphinito-phosphanido Pt(i) complex [(PHCy2)Pt(μ-PCy2){κ2: P, O -μ-P(O)Cy2}Pt(PHCy2)](Pt-Pt). *Dalt. Trans.* 49, 6776–6789. doi: 10.1039/D0DT00923G

Tolbatov, I., Coletti, C., Marrone, A., and Re, N. (2019a). Reactivity of gold(I) monocarbene complexes with protein targets: a theoretical study. *Int. J. Mol. Sci.* 20:820. doi: 10.3390/ijms20040820

Tolbatov, I., Coletti, C., Marrone, A., and Re, N. (2020a). Insight into the substitution mechanism of antitumor Au(I) N-heterocyclic carbene

complexes by cysteine and selenocysteine. *Inorg. Chem.* 59, 3312–3320. doi: 10.1021/acs.inorgchem.0c00106

Tolbatov, I., Marzo, T., Cirri, D., Gabbiani, C., Coletti, C., Marrone, A., et al. (2020b). Reactions of cisplatin and cis-[PtI2(NH3)2] with molecular models of relevant protein sidechains: a comparative analysis. *J. Inorg. Biochem.* 209:111096. doi: 10.1016/j.jinorgbio.2020.111096

Tolbatov, I., Re, N., Coletti, C., and Marrone, A. (2019b). An insight on the gold(I) affinity of golB protein via multilevel computational approaches. *Inorg. Chem.* 58, 11091–11099. doi: 10.1021/acs.inorgchem.9b01604

Tolbatov, I., Re, N., Coletti, C., and Marrone, A. (2020c). Determinants of the lead(II) affinity in pbrR protein: a computational study. *Inorg. Chem.* 59, 790–800. doi: 10.1021/acs.inorgchem.9b03059

Topkas, E., Cai, N., Cumming, A., Hazar-Rethinam, M., Gannon, O. M., Burgess, M., et al. (2016). Auranofin is a potent suppressor of osteosarcoma metastasis. *Oncotarget* 7, 831–844. doi: 10.18632/oncotarget.5704

Wiederhold, N. P., Patterson, T. F., Srinivasan, A., Chaturvedi, A. K., Fothergill, A. W., Wormley, F. L., et al. (2017). Repurposing auranofin as an antifungal: *in vitro* activity against a variety of medically important fungi. *Virulence* 8, 138–142. doi: 10.1080/21505594.2016.1196301

Yanai, T., Tew, D. P., and Handy, N. C. (2004). A new hybrid exchange-correlation functional using the coulomb-attenuating method (CAM-B3LYP). *Chem. Phys. Lett.* 393, 51–57. doi: 10.1016/j.cplett.2004.06.011

Zhang, C., Gao, L., Yuan, Q., Zhao, L., Niu, W., Cai, P., et al. (2020). Is GSH chelated Pt molecule inactive in anti-cancer treatment? a case study of Pt_6GS_4. *Small* 16:2002044. doi: 10.1002/smll.202002044

Zhao, Y., and Truhlar, D. G. (2006). A new local density functional for main-group thermochemistry, transition metal bonding, thermochemical kinetics, and noncovalent interactions. *J. Chem. Phys.* 125:194101. doi: 10.1063/1.2370993

Zoppi, C., Messori, L., and Pratesi, A. (2020). ESI MS studies highlight the selective interaction of auranofin with protein free thiols. *Dalt. Trans.* 49, 5906–5913. doi: 10.1039/D0DT00283F

Zou, J., Taylor, P., Dornan, J., Robinson, S. P., Walkinshaw, M. D., and Sadler, P. J. (2000). First crystal structure of a medicinally relevant gold protein complex: unexpected binding of [Au(PEt3)]+ to histidine. *Angew. Chemie Int. Ed.* 39, 2931–2934. doi: 10.1002/1521-3773(20000818)39:16<2931::AID-ANIE2931>3.0.CO;2-W

Conflict of Interest: The authors declare that the research was conducted in the absence of any commercial or financial relationships that could be construed as a potential conflict of interest.

frontiers in Chemistry

ORIGINAL RESEARCH
published: 21 October 2020
doi: 10.3389/fchem.2020.581648

Reactions of Medicinal Gold(III) Compounds With Proteins and Peptides Explored by Electrospray Ionization Mass Spectrometry and Complementary Biophysical Methods

Lara Massai[1], *Carlotta Zoppi*[1], *Damiano Cirri*[2], *Alessandro Pratesi*[2*†] *and Luigi Messori*[1*†]

[1] *Department of Chemistry, University of Florence, Florence, Italy,* [2] *Department of Chemistry and Industrial Chemistry, University of Pisa, Pisa, Italy*

OPEN ACCESS

Edited by:
Tara Louise Pukala,
University of Adelaide, Australia

Reviewed by:
Fuyi Wang,
Institute of Chemistry (CAS), China
Andrei I. Khlebnikov,
Tomsk Polytechnic University, Russia

***Correspondence:**
Alessandro Pratesi
alessandro.pratesi@unipi.it
Luigi Messori
luigi.messori@unifi.it

†These authors have contributed equally to this work

Specialty section:
This article was submitted to Medicinal and Pharmaceutical Chemistry, a section of the journal Frontiers in Chemistry

Received: *09 July 2020*
Accepted: *16 September 2020*
Published: *21 October 2020*

Citation:
Massai L, Zoppi C, Cirri D, Pratesi A and Messori L (2020) Reactions of Medicinal Gold(III) Compounds With Proteins and Peptides Explored by Electrospray Ionization Mass Spectrometry and Complementary Biophysical Methods. Front. Chem. 8:581648. doi: 10.3389/fchem.2020.581648

Electrospray ionization mass spectrometry (ESI MS) is a powerful investigative tool to analyze the reactions of metallodrugs with proteins and peptides and characterize the resulting adducts. Here, we have applied this type of approach to four experimental anticancer gold(III) compounds for which extensive biological and mechanistic data had previously been gathered, namely, Auoxo6, Au_2phen, AuL12, and Aubipyc. These gold(III) compounds were reacted with two representative proteins, i.e., human serum albumin (HSA) and human carbonic anhydrase I (hCA I), and with the C-terminal dodecapeptide of thioredoxin reductase. ESI MS analysis allowed us to elucidate the nature of the resulting metal–protein adducts from which the main features of the occurring metallodrug–protein reactions can be inferred. In selected cases, MS data were integrated and supported by independent ^{1}HNMR and UV–Vis absorption measurements to gain an overall description of the occurring processes. From data analysis, it emerges that most of the investigated gold(III) complexes, endowed with an appreciable oxidizing character, undergo quite facile reduction to gold(I); the resulting gold(I) species tightly associate with the above proteins/peptides with a remarkable selectivity for free cysteine residues. In contrast, in the case of the less-oxidizing Aubipyc complex, the gold(III) oxidation state is conserved, and a gold(III) fragment still containing the original ligand is found to be associated with the target proteins. It is notable that the C-terminal dodecapeptide of thioredoxin reductase containing the characteristic –Gly–Cys–Sec–Gly metal-binding motif is able in all cases to trigger gold(III)-to-gold(I) reduction. Our investigation allowed us to identify in detail the nature of the gold fragments that ultimately bind the protein targets and determine the exact binding stoichiometry; some insight on the reaction kinetics was also gained. Notably, a few clear correlations could be established between the structure of the metal complexes and the nature of the resulting protein adducts. The mechanistic implications of these findings are analyzed and thoroughly discussed. Overall, the present results set the stage to better understand the real target biomolecules of these gold compounds and elucidate at the atomic level their interaction modes with proteins and peptides.

Keywords: anticancer metal complexes, gold, protein interaction, mass spectrometry, cytotoxic compounds

INTRODUCTION

During the last two decades, a number of studies highlighted the importance of gold compounds as a new family of cytotoxic agents with the potential of becoming new effective anticancer drug candidates endowed with original mechanisms of action and a peculiar spectrum of antitumor activities (Nobili et al., 2010; Zou et al., 2015). Indeed, a variety of gold(III) and gold(I) compounds, bearing different structural motifs, were reported to cause extensive cell death *in vitro* in numerous cancer cell lines, with a remarkable selectivity for cancer over normal cells (Casini et al., 2009). From the mechanistic studies conducted so far, the modes of action and the targets of antiproliferative gold compounds appear to be multifaceted and deeply distinct from those of clinically established platinum compounds (i.e., cisplatin); yet the "true" molecular mechanisms of medicinal gold compounds remain largely unexplored (Fiskus et al., 2014). A growing body of evidence suggests that a few selected protein targets such as the enzyme thioredoxin reductase (Scalcon et al., 2018) and some transcription factors with zinc finger motifs (Abbehausen, 2019) mediate primarily the biological effects of cytotoxic gold compounds. This prompted investigators to analyze in detail the reactions of medicinal gold compounds with proteins. A systematic investigation on the interactions of the reference gold(I) drug auranofin with a series of model proteins, i.e., human serum albumin, carbonic anhydrase, superoxide dismutase, and hemoglobin, was recently carried out in our laboratory through mass spectrometry, and the resulting adducts could be characterized in molecular detail (Pratesi et al., 2016, 2018, 2019; Magherini et al., 2018; Cirri et al., 2019; Zoppi et al., 2020). These studies revealed that auranofin targets quite selectively the free cysteine residues of proteins (Pratesi et al., 2018; Zoppi et al., 2020).

Here, we have extended this kind of investigation to four representative gold(III) compounds for which extensive biological and mechanistic data have been gathered in the last years, namely, Auoxo6, Au_2phen, AuL12, and Aubipyc (Marzano et al., 2011; Gabbiani et al., 2012a,b). More precisely, the remarkable antiproliferative effects of the structurally related Auoxo6 and Au_2phen complexes were highlighted since the late 2000s by our research group in connection with the group of Cinellu et al. (2010), Casini et al. (2006). The complex AuL12 was developed and characterized, in Padua, by the research group of Marzano et al. (2011); Aubipyc was prepared in Sassari by the research team of Marcon et al. (2002), and its biological profile was later analyzed in connection with our research group (Marzo et al., 2015; Massai et al., 2016a). Here, we have studied the reactions of the above-mentioned gold(III) compounds with two representative proteins, i.e., HSA and hCA I; in addition, we have decided to perform the same interaction studies against the C-terminal redox-active domain of thioredoxin reductase, an important enzyme involved in cellular redox homeostasis regulation that is the putative target for gold compounds. Our investigation mainly relies on MS determinations, but MS results are independently supported by other biophysical techniques such as ^{1}HNMR and UV–Vis. Notably, the results of this multi-technique approach turned out to be nicely consistent each other and allowed us to identify for each of the four selected gold complexes the precise nature of the metallic fragments that bind the investigated biomolecules. Characteristic trends in the analyzed metallodrug/biomolecule reaction could be identified and correlated to the structural and chemical features of the study compounds.

THE PANEL OF GOLD(III) COMPLEXES AND THE INVESTIGATIVE STRATEGY

The chemical formulas of the study compounds are synoptically shown in **Figure 1**.

Auoxo6 and its analogous Au_2phen, with two 2,9-dimethyl phenanthrolines in the place of two bipyridines, are binuclear Au(III) coordination compounds with a dioxo-bridge, which links the two gold(III) centers. Their main feature is the presence of an extended, roughly planar system containing the Au_2O_2 diamond core and the two aromatic moieties. Crystal structures for these compounds were previously determined (Gabbiani et al., 2008; Cinellu et al., 2010). These two gold(III) compounds are strictly related to each other from the structural point of view but greatly differ in their aqueous solubility, with Auoxo6 being far more soluble than Au_2Phen. Notably, both these gold(III) compounds manifest a frank oxidizing character and tend to undergo facile reduction to gold(I) or, alternatively, to elemental gold. Their reactions with biologically reducing agents such as glutathione and ascorbate were earlier investigated, and quick gold(III) reduction was indeed documented (Gabbiani et al., 2012b). However, in the absence of reducing agents, these gold(III) complexes are stable under physiological conditions for several hours or even days and are thus well suitable for pharmaceutical application (Gabbiani et al., 2012b).

AuL12 is a mononuclear gold(III) complex developed in the group of Prof. Dolores Fregona, in Padua, that revealed very promising anticancer properties both *in vitro* and *in vivo* (Ronconi et al., 2012; Nardon and Fregona, 2015). AuL12 consists of a square-planar gold(III) center with a bidentate dithiocarbamate ligand and two bromide ligands. Notably, AuL12 was shown to behave as a prodrug upon releasing its bromide ligands (Pratesi et al., 2019). Significant oxidizing properties were also documented for this gold(III) complex (Nardon et al., 2017).

Aubipyc is a gold(III) cyclometalated derivative of 6-(1,1-dimethylbenzyl)-2,2′-bipyridine, where the tetracoordinated square planar gold(III) center is surrounded by the N,N,C sequence of donor atoms from the terdentate bipyridine ligand plus an oxygen atom from the hydroxo ligand (Cinellu et al., 1996). At variance with the above gold(III) complexes, the direct carbon-to-metal bond greatly stabilizes the gold(III) center in Aubipyc; a notable consequence is that Aubipyc is not reduced by glutathione (Gamberi et al., 2014).

Some years ago, the *in vitro* anticancer properties of these four gold(III) complexes were evaluated comparatively in a standard 36-cancer cell line panel available in Oncotest (Freiburg, Germany) (Casini et al., 2009). The COMPARE algorithm

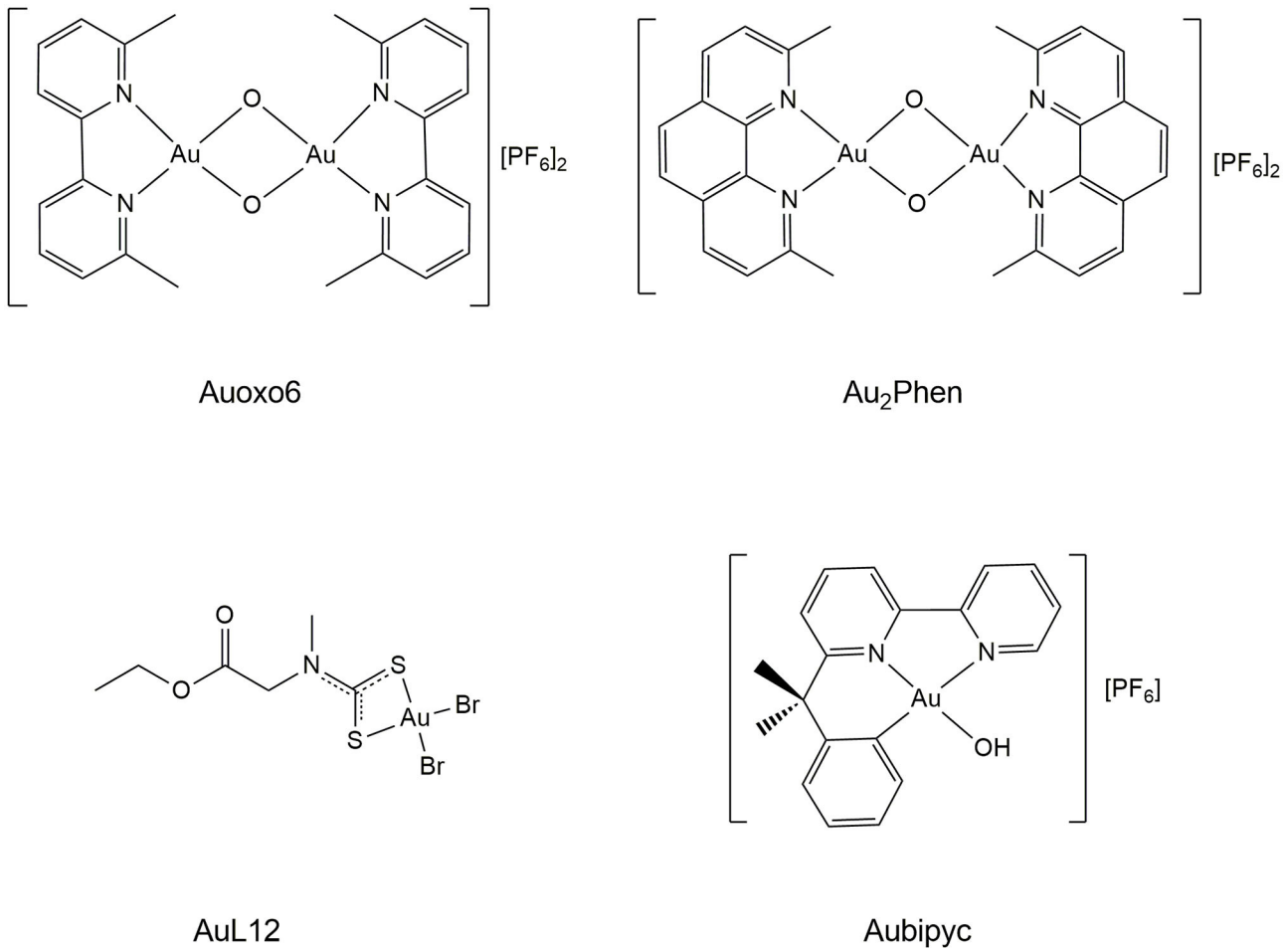

FIGURE 1 | The panel of the studied gold(III) compounds.

applied to the analysis of the obtained growth inhibition data revealed that the profiles of Au_2phen are very similar to those of Auoxo6, in agreement with their pronounced structural analogy (Cinellu et al., 2010). Tentatively, through bioinformatic analysis, the cytotoxicity patterns obtained for Au_2phen and Auoxo6 were mainly ascribed to inhibition of histone deacetylase. At variance, Aubipyc was found to be only moderately effective in the Oncotest panel (Casini et al., 2009). Also, AuL12 was confirmed to be highly cytotoxic in the Oncotest panel, with a mode of action resembling antiproteasomal agents (Casini et al., 2009; Zhang et al., 2010). Interestingly, the correlations in the antiproliferative profiles between these gold compounds and cisplatin were very poor, implying again the occurrence of profoundly different modes of action. On the whole, COMPARE analysis of these gold compounds suggested that a variety of proteins might be reliable biomolecular targets and thus account for the observed biological effects; this means that the biological actions of these gold compounds are best interpreted in terms of metalation and inactivation of a few crucial proteins that are effective cancer targets (Cinellu et al., 2010).

The biological studies were later supported by a number of proteomic studies highlighting the alterations in protein expression induced by the above gold(III) complexes (Magherini et al., 2010; Guidi et al., 2012; Gamberi et al., 2014).

During the last decade, the interactions of some of these gold(III) compounds with model proteins were also investigated from the crystallographic point of view, mostly in the research group of Prof. Antonello Merlino in Naples. Those crystallographic studies clearly supported the occurrence of gold(III)-to-gold(I) reduction in the cases of Auoxo6, Au_2phen, and AuL12 reacting with proteins (Russo Krauss et al., 2014; Merlino et al., 2017; Ferraro et al., 2019; Giorgio and Merlino, 2020).

In the last few years, ESI MS has emerged as a powerful tool to monitor the interactions of metallodrugs with proteins at the molecular level (Merlino et al., 2017). These recent developments are described in a couple of review articles (Merlino et al., 2017;

Messori and Merlino, 2017). Accordingly, we have exploited the ESI MS method to characterize in a systematic way and comparatively the interaction of the four study metallodrugs with two exemplary proteins and with the C-terminal dodecapeptide of thioredoxin reductase.

Briefly, the adopted experimental strategy was as follows. All four gold complexes were challenged with HSA, hCA I, and the TrxR dodecapeptide according to a well-established experimental protocol (Tamasi et al., 2014; Marzo et al., 2017, 2019; Michelucci et al., 2017; Pratesi et al., 2018; Ferraro et al., 2020; Zoppi et al., 2020). Different times and stoichiometries were explored to identify the best conditions to obtain adduct formation and to improve the quality of the ESI MS spectra. In addition, particular attention was paid to the kinetic aspects of these reactions.

Indeed, MS turned out to be a powerful tool to characterize the metallodrug/protein adduct that formed in the course of the above reaction. Systematic MS measurements were able to define the general patterns of reactivity between gold compounds and the model proteins; however, in selected cases, UV–Vis and NMR spectroscopies were valuable ancillary techniques to better understand specific features of the investigated systems and of the resulting adducts.

THE ELECTROSPRAY IONIZATION MASS SPECTROMETRY MEASUREMENTS

The ESI MS measurements were performed according to the procedure developed in our laboratory, which is described in detail in the Materials and Methods (Tamasi et al., 2014; Massai et al., 2016b; Pratesi et al., 2016, 2018; Zoppi et al., 2020). Briefly, each protein sample, dissolved in ammonium acetate solution 2 $\times$ 10^{-3} M at pH 6.8, was incubated with each selected gold(III) complex for 2 or 24 h in a well-defined molar ratio; then the samples were analyzed by high-resolution ESI MS through direct infusion in the mass spectrometer upon addition of a small aliquot of formic acid. The obtained MS results are shown below for each gold complex/biomolecule pair.

Remarkably, all the selected biomolecules contain a free exposed cysteine or selenocysteine (in the case of the TrxR dodecapeptide) residue, as gold–sulfur/selenium interactions are strongly preferred according to the Pearson concept (Dabrowiak, 2012).

The Reactions of Gold Compounds With Human Serum Albumin

HSA is characterized by the presence of 17 disulfide bonds and only one free cysteine residue (Cys34) (Rombouts et al., 2015). Interestingly, the only free cysteine (Cys34) of HSA is solvent accessible and is considered the primary binding site for gold compounds owing to the high affinity of gold to sulfur-containing ligands (Pratesi et al., 2018, 2019; Zoppi et al., 2020).

The deconvoluted high-resolution mass spectrum of HSA is shown in **Figure 2A**. The main peak at 66,437 Da corresponds to the native protein and the second intense peak at 66,556 Da is assigned to a common HSA posttranslational modification, i.e., the cysteinylated form of the native protein (Fasano et al., 2005; Talib et al., 2006; Fanali et al., 2012).

Upon reacting HSA with either Auxo6 or Au_2phen, an apparent decrease in the overall quality of the ESI MS spectra is noticed, which is accompanied by a strong baseline distortion, with both tested stoichiometries (1:3 or 1:0.9 protein/metal ratio). In our previous experience, this behavior is quite common when dealing with metal complexes where the metal center is present in its higher oxidation state; probably this arises from the occurrence of a direct redox reaction between the metal complex and the biomolecule, leading to a plethora of minor adducts that are present in small amounts and are difficult to assign (Massai et al., 2019; Pratesi et al., 2019).

In spite of that, the resulting spectra still allow the detection of a few metal–protein adducts with greater molecular masses that the native protein. The peaks corresponding to these adducts are annotated on the spectra shown in **Figure 2**. In the case of Auoxo6 and Au_2Phen (**Figures 2B,C**, respectively), the gold adducts are formed on the cysteinylated protein. These adducts are characterized by the probable presence of gold clusters, which in the case of the most reactive Auoxo6 (**Figure 2B**) complex consist of a maximum of 5 gold atoms, represented by the peak at 67,537 Da. Also in the case of Au_2Phen, the adducts are formed on the cysteinylated HSA, but due to the lower reactivity of Au_2Phen in comparison with Auoxo6, the gold clusters formed on the protein consist of a maximum of 2 gold atoms, with a total molecular mass of 66,951 Da (**Figure 2C**). A further confirmation of the presence of metallic gold clusters can be obtained from the inspection of the multicharged ESI spectra. In fact, the presence of a metal cluster, differently from the metal ions, does not bring any contribution to the overall charge of the adducts and does not affect the m/z ratio of the multicharged signals that is due in this case only to the protonation process inside the ESI source (Johnson et al., 2000; Johnson and Laskin, 2016; Chen et al., 2019).

Far better spectra are obtained upon reacting HSA with AuL12 (**Figure 2D**). Remarkably, the peak observed at 66,779 Da corresponds to a species where the Au(III) ethylsarcosine dithiocarbamate (ESDT) fragment is bound to the protein. Additional peaks at lower mass values are seen corresponding to the Au(I)/HSA adduct, implying that AuL12 may also undergo reduction to gold(I) with loss of the dithiocarbamate ligand, as already described in a previous work of ours concerning the reactivity of the bovine serum albumin (BSA) with AuL12 (Pratesi et al., 2019).

Contrariwise, the Aubipyc complex is far more stable from the redox point of view than the previously mentioned gold(III) compounds (Gabbiani et al., 2012b; Marzo et al., 2015; Kupiec et al., 2019). Usually, the reduction of the gold(III) center is not observed for this complex. It follows that upon reaction with Aubipyc, the spectrum of HSA is dominated by a peak at 66,906 Da corresponding to the native HSA bearing the Aubipyc moiety without the hydroxo group (**Figure 2E**). Another peak at 67,394 Da corresponds to the bis-adduct of HSA with the same molecular fragment. In contrast with the results described for the previous gold(III) compounds, in this case, the lack of adducts formed with cysteinylated HSA suggests that this modification

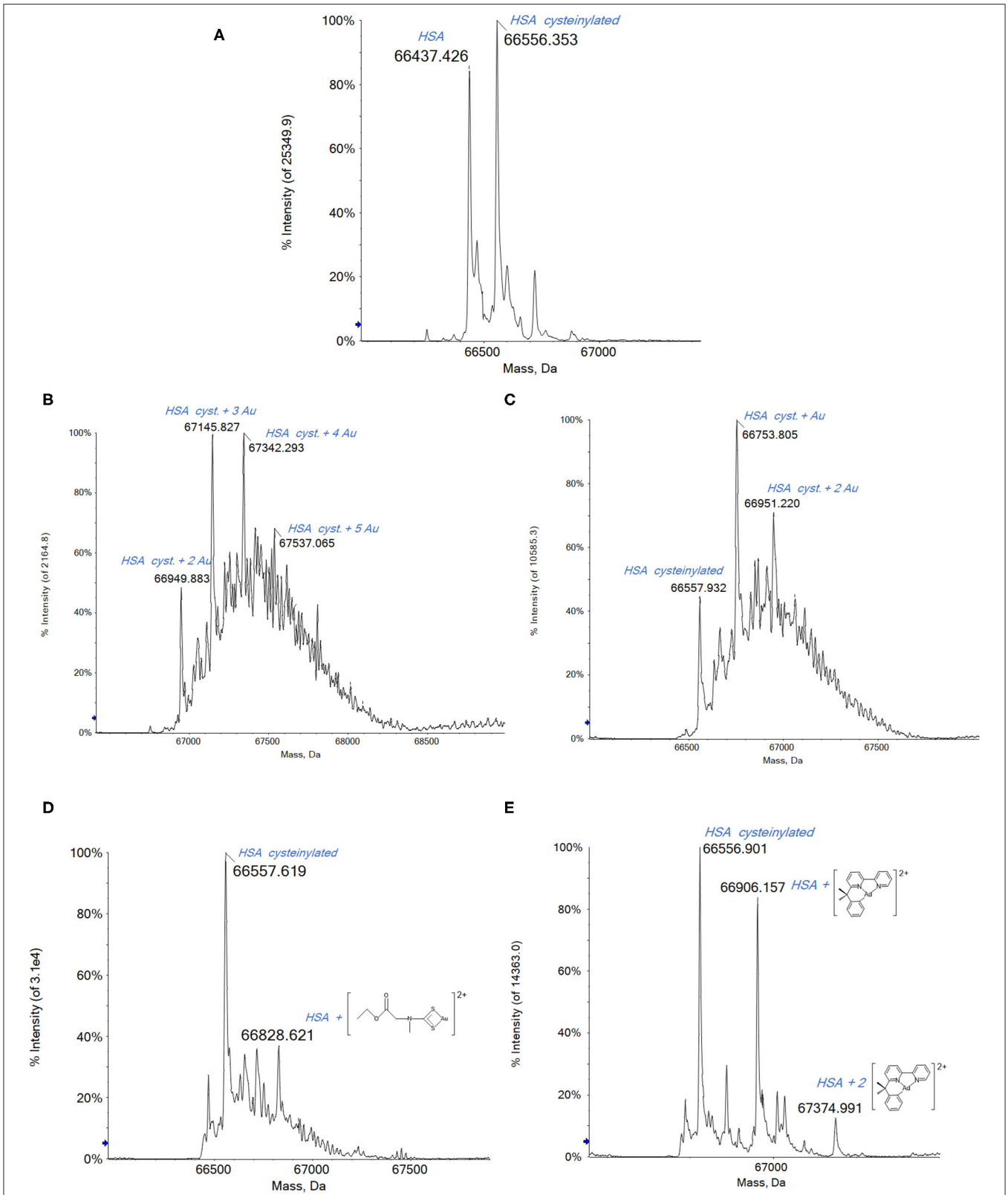

FIGURE 2 | (A) Deconvoluted electrospray ionization quadrupole time-of-flight (ESI-Q-TOF) spectra of human serum albumin (HSA) 5×10^{-7} M in 2 mM of ammonium acetate solution at pH 6.8 and incubated at 37 °C for 2 h with **(B)** Auoxo6, **(C)** Au_2phen, **(D)** AuL12, and **(E)** Aubipyc solution in dimethyl sulfoxide (DMSO) in a 1:0.9 protein-to-gold ratio; 0.1% v/v of formic acid was added just before infusion.

of the only free cysteine prevents the reaction with Aubipyc. This could be due to the greater stability of the –S–S– bond in the cysteinylated HSA with respect to the potential –S–Au(III) interaction with the Aubipyc reactive moiety. Thus, a clearly different behavior has been highlighted for the Aubipyc complex compared with Auoxo6 and Au_2phen.

The Reactions of Gold Compounds With Human Carbonic Anhydrase I

On the whole, the ESI MS spectra obtained for hCA I and its adducts with the study gold compounds turned out to be of greater quality than those of HSA, possibly in relation to the greater ionizability of this protein and its lower size.

Human carbonic anhydrase I (hCA I) consists of 261 amino acids and contains a Zn(II) ion essential for catalysis. The enzyme presents a free cysteine (Cys213) as a potential anchoring site for gold.

The analysis of the ESI MS spectra is quite straightforward. Indeed, when reacting hCA I with the three gold(III) complexes endowed with a more oxidizing character, i.e., Auoxo6, Au_2phen, and AuL12, adducts with an increasing number of Au atoms bound to apo-hCA I are again detected (**Figure 3**).

Regarding the complex AuL12, the recorded spectra show the formation of the mono- and bis-adduct with the Au atoms (**Figure 3D**).

Noteworthy, the ESI MS spectra of hCA I reacted with Auoxo6 or Au_2Phen show many signals that are attributed to the binding to hCA I of a number of Au atoms in different stoichiometries: from 3 to 7 in the case of Auoxo6 (**Figure 3B**) and from 2 to 4 for Au_2Phen (**Figure 3C**). Moreover, it is worth noting that in both spectra (**Figures 3B,C**), the signal of unreacted apo-hCA I (28,780 Da) is not observed any more, meaning that the reaction with the gold compounds is rapid and nearly quantitative.

Thus, in the cases of Auoxo6, Au_2Phen, and AuL12, a gold(III)-to-gold(0) reduction reaction occurs accompanied by the release of all the original gold(III) ligands. Also in this case, an inspection of the multicharged ESI spectra has been carried out to confirm the presence of gold clusters. Again, Aubipyc reveals a different behavior with no evident reduction of the gold(III) center and retention of the terdentate ligand. Only one Aubipyc moiety is found bonded to hCA I in the main adduct detected at 29,248 Da (**Figure 3E**).

The Reactions of Gold Compounds With the C-Terminal Dodecapeptide of TrxR1

Finally, the four gold(III) complexes were challenged with the C-terminal dodecapeptide of TrxR bearing the –Cys–Sec– motif. This peptide has been adopted since a few years by our research group as a model peptide mimicking the TrxR1 reactive site (Pratesi et al., 2010, 2014).

This peptide is characterized by the presence of an intramolecular –S–Se– bridge that requires reduction to give the reactive form of the peptide. This reaction is achieved by adding 10 eq. of dithiothreitol (DTT) before the incubation with the various gold complexes (Pratesi et al., 2014). The presence of the reductant greatly facilitates the reaction between selenocysteine and cysteine with the gold complexes.

A general reaction pattern is identified also in this case being perfectly superimposable to that of the other considered proteins. In particular, upon reacting Au_2phen, AuL12, and even Aubipyc with the dodecapeptide, the main adduct formed corresponds to the binding of a gold(I) ion to the peptide (**Figure 4**). In addition, other minor signals are also present, related to adducts with higher Au(I)/peptide ratios. Apparently, in the case of Auoxo6, no reaction is observed under the same experimental conditions.

Interestingly, in the case of this peptide, the gold compounds' reactivity is quite similar to that observed with the proteins. The main difference is that, in this latter case, the complete reduction from Au(III) to Au(0) does not occur. This behavior could be certainly ascribed to the marked difference in the chemical environment of the whole protein compared with a peptide fragment; however, this aspect will be further investigated.

Since Auoxo6 is the only compound that shows no reactivity with the peptide after a short time of incubation (2 h), other experiments were conducted. Different concentration ratios between the three reagents (the peptide, Auoxo6, and the DTT) were tested, in order to find the one that allows the adduct formation in short times. The best ratio was found to be the 1:1:10 (peptide to gold to DTT) in which a certain reactivity of the gold compound is observed even at short times of incubation. Indeed, after 2 h, the signal at 1,398 Da attributed to the adduct of the peptide with Au(I) (and a NH_4^+ ion from the solution) is clearly observed (see **Supplementary Figure 11**), even if the signals of the peptide alone are still quite intense. After 24 h of incubation, no adduct signal is detected anymore.

The Reactivity of Aubipyc in the Presence of a Reducing Agent

The above-described experiments highlighted a different behavior of Aubipyc depending on the substrate considered. Indeed, upon reaction with HSA and hCA I, Aubipyc binds these proteins through the $[Au(III)(bipydmb\text{-}H)]^{2+}$ fragment, with the gold center retaining the oxidation state +3; in contrast, upon reaction with the dodecapeptide, Aubipyc undergoes complete reduction and loss of the ligand so that an adduct containing a single Au(I) ion is formed.

When performing the experiments with the peptide, a reducing agent, i.e., DTT, is needed to break the bond between the cysteine and selenocysteine residue and promote the binding of the metal. In order to assess if the reduction of the gold center in Aubipyc is due to DTT or, instead, to the biological substrate, an additional experiment was conducted. A sample of HSA was prepared with Aubipyc and DTT in a ratio of 1:0.9:5 of protein to gold to reducing agent. After 2 and 24 h of incubation at 37 °C, the mass spectra (see **Supplementary Figure 1**) reveal the presence of the intense signal at 66,906 Da attributed to the native protein binding the $[Au(III)(bipydmb\text{-}H)]^{2+}$ moiety. Though less intense, the cysteinylated HSA signal is still present. So the spectra are identical to those registered in the absence of DTT (**Figure 4**). Therefore, despite the presence of an excess of a reducing agent like DTT, Aubipyc when reacting with HSA

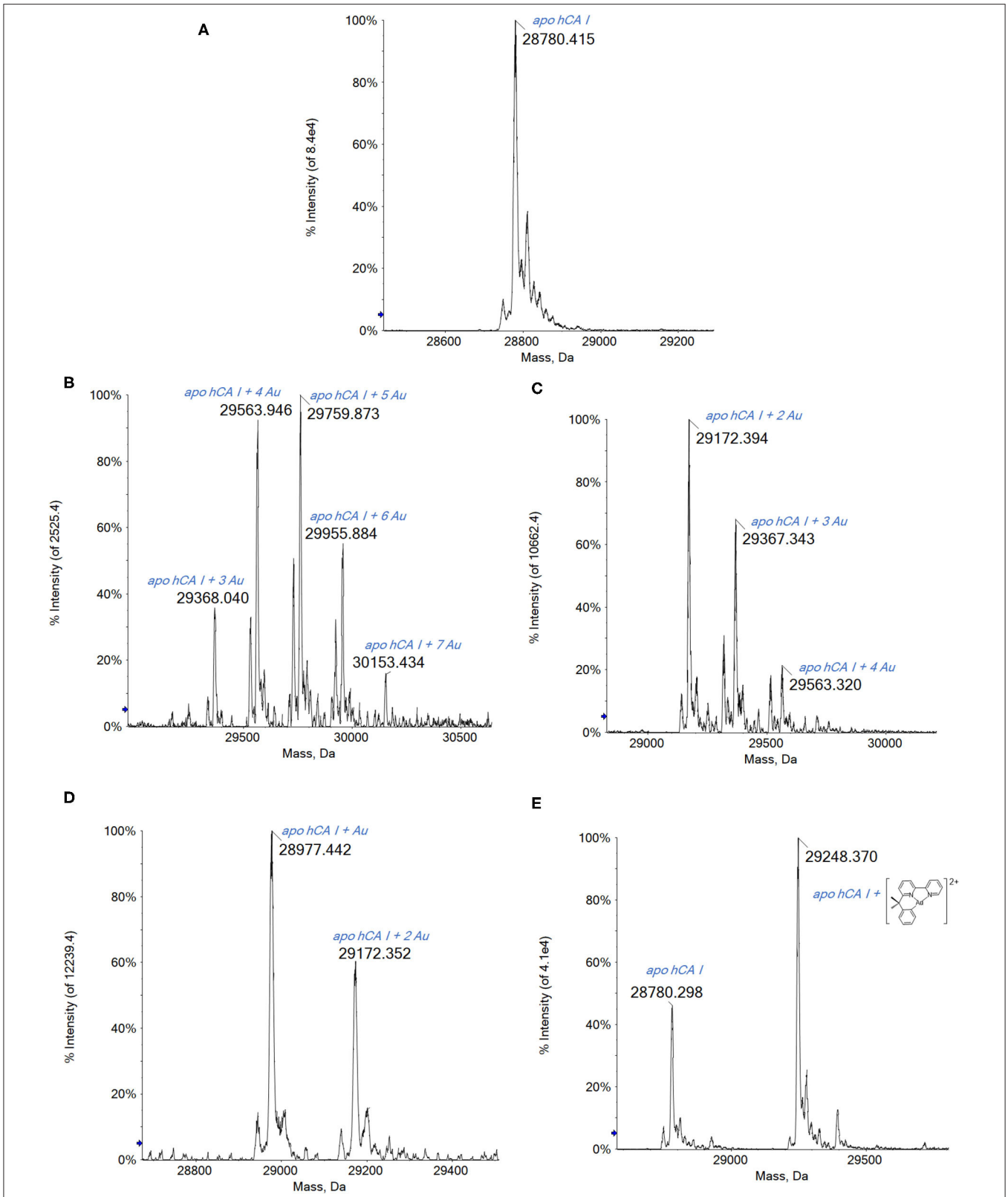

FIGURE 3 | (A) Deconvoluted electrospray ionization quadrupole time-of-flight (ESI-Q-TOF) spectra of human carbonic anhydrase I (hCA I) 7×10^{-7} M in 2 mM of ammonium acetate solution at pH 6.8 and incubated at 37 °C for 2 h with **(B)** Auoxo6, **(C)** Au_2phen, **(D)** AuL12, and **(E)** Aubipyc solution in dimethyl sulfoxide (DMSO) in a 1:0.9 protein-to-gold ratio; 0.1% v/v of formic acid was added just before infusion.

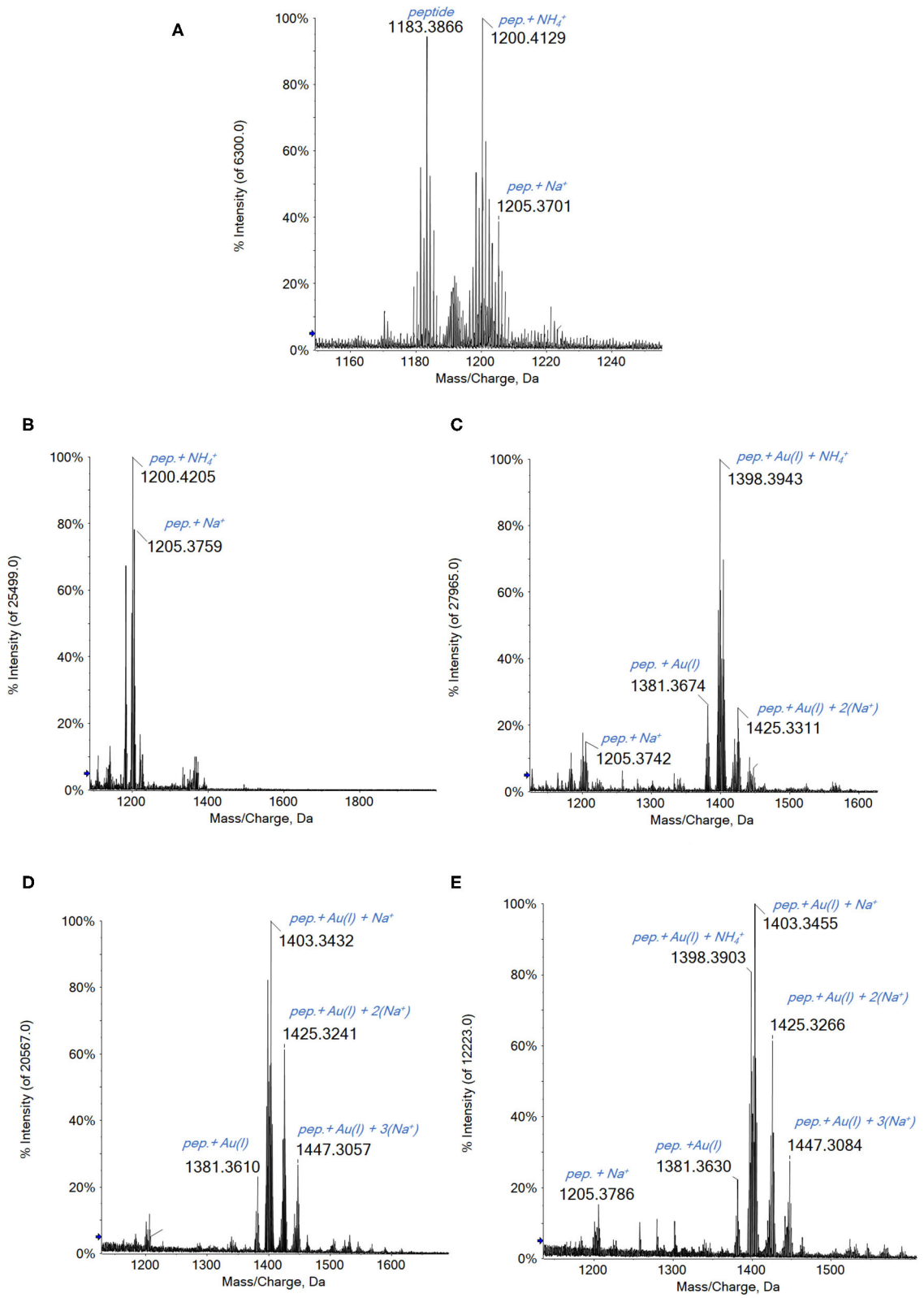

FIGURE 4 | (A) Multicharged electrospray ionization quadrupole time-of-flight (ESI-Q-TOF) spectra of the dodecapeptide 5×10^{-7} M in 2 mM of ammonium acetate solution at pH 6.8 and incubated at 37 °C for 2 h with **(B)** Auoxo6, **(C)** Au_2phen, **(D)** AuL12, and **(E)** Aubipyc solution in dimethyl sulfoxide (DMSO) in a 1:3:5 protein-to-gold-to-DTT ratio; 0.1% v/v of formic acid was added just before infusion.

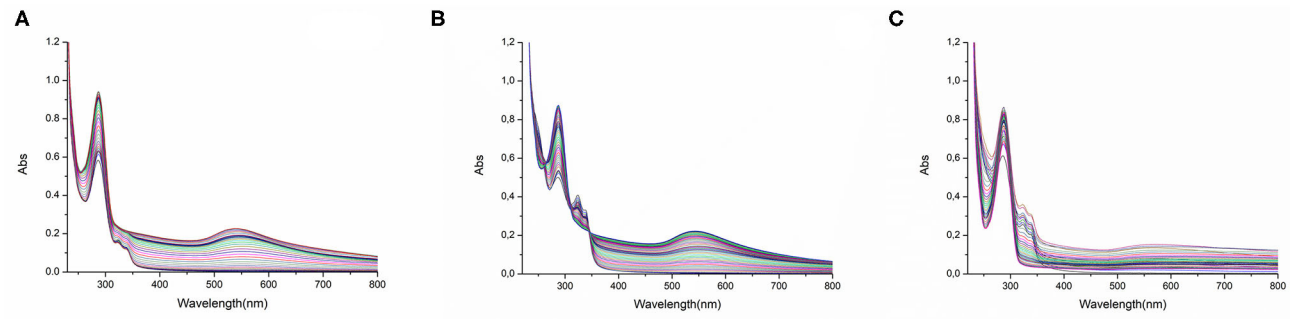

FIGURE 5 | UV–Vis spectra of Auoxo6 with **(A)** HSA, **(B)** hCA I and **(C)** the dodecapeptide 10^{-5} M in phosphate buffer 50 mM, pH 7.4 (1:3 biomolecule-to-gold ratio).

retains the ligand and the oxidation state of +3. So it can be inferred that the reduction of the gold center to gold(I) in the case of the C-terminal dodecapeptide of TrxR is due to the nature of the substrate and not to the presence of DTT.

COMPLEMENTARY BIOPHYSICAL MEASUREMENTS

To gain more information about the interaction of the selected gold(III) complexes with the three targets, other experiments were carried out. More precisely, spectrophotometric and ^{1}H NMR measurements were performed for achieving, if possible, independent confirmations of the results obtained through ESI MS measurements. In some cases, additional and valuable information was gained.

Spectrophotometric Measurements

In the case of Auoxo6, it was possible to elucidate a common redox-dependent binding process found for the interaction with all the three targets used in this investigation (**Figure 5**). More precisely, the time course spectra of samples offer a clear evidence of the occurrence of a gold(III) reduction mechanism, highlighted from the disappearance of the complex absorption bands located between 310 and 330 nm. Moreover, the reduction of Auoxo6 signals is accompanied by the growth of a new band located at 290 nm and assignable to the free 6,6′-dimethyl-2,2′-bipyridyl ligand. In the case of HSA and hCA I (**Figures 5A,B**), in addition, a new relevantly broad band appears in the visible region between 500 and 600 nm, usually diagnostic of the formation of elemental gold clusters (Dominguez-Medina et al., 2012; Tatini et al., 2014). Notably, all these results turned out to be in perfect agreement with those observed through the ESI MS experiments, in which HSA and hCA I show the binding with a polynuclear gold(0) cluster upon the interaction of Auoxo6, contrary to the case of thioredoxin reductase dodecapeptide model that was found to bind a naked gold(I) atom.

Also in the case of Au_2Phen, it was possible to gain a clear evidence of gold(0) formation at least in the case of the interaction with hCA I, confirming again the data collected through MS; on the other hand, Aubipyc, as already emerged from ESI MS measurements, does not seem to incur to any reduction process (see **Supplementary Material** for detailed spectra of these latter data: **Supplementary Figures 7–10**, **12**, **13**).

^{1}H Nuclear Magnetic Resonance Measurements

In order to confirm the reaction pattern observed in the ESI MS experiments, some NMR measurements were carried out. First of all, each investigated complex was incubated for 24 h with HSA. Subsequently, ^{1}HNMR spectra were acquired through a Carr–Purcell–Meiboom–Gill pulse sequence used as a T2 filter for removing the HSA signals. Indeed, this experimental procedure is used for achieving the suppression of all resonances with short T2, typically belonging to high-molecular-weight molecules such as HSA or HSA/metal–complex adducts, allowing to record spectra not affected from broad signals that might hide small trace of complexes' degradation products (Pratesi et al., 2019). The NMR experiments turned out to be nicely in agreement with the ESI MS study.

More precisely:

(i) Upon incubation with HSA, AuL12 shows the same fragmentation pattern seen upon interaction with BSA (Pratesi et al., 2019). Indeed, also in this case, it is possible to identify two small molecules originated from AuL12 degradation mechanisms, i.e., ethanol (δ 3.64, 1.17) and ethyl sarcosinate (δ 4.30, 3.96, 2.79, 1.29) (see **Supplementary Figure 5**). This occurrence is in agreement with ESI MS data, in which only a gold/HSA adduct is visible in the spectrum, with a complete loss of the ligand from the metal center.

(ii) Contrary to the previous case, no Aubipyc signals were detected after incubation with HSA. The fact that all its resonances were completely suppressed from the T2 filter upon HSA interaction can easily be explained by assuming a coordination process on the protein scaffold in which the organic moiety of the metal complex was retained on the gold center. This latter occurrence was again in agreement with ESI MS experiments.

(iii) In the case of Auoxo6, signals imputable to 6,6′-dimethyl-2,2′-bipyridyl ligand were detected in solution as a consequence of the degradation of the complex (δ 8.71, 7.48, 7.43, one proton each; δ 3.34, three protons from the methyl group); see **Figure 6**. This latter result was again

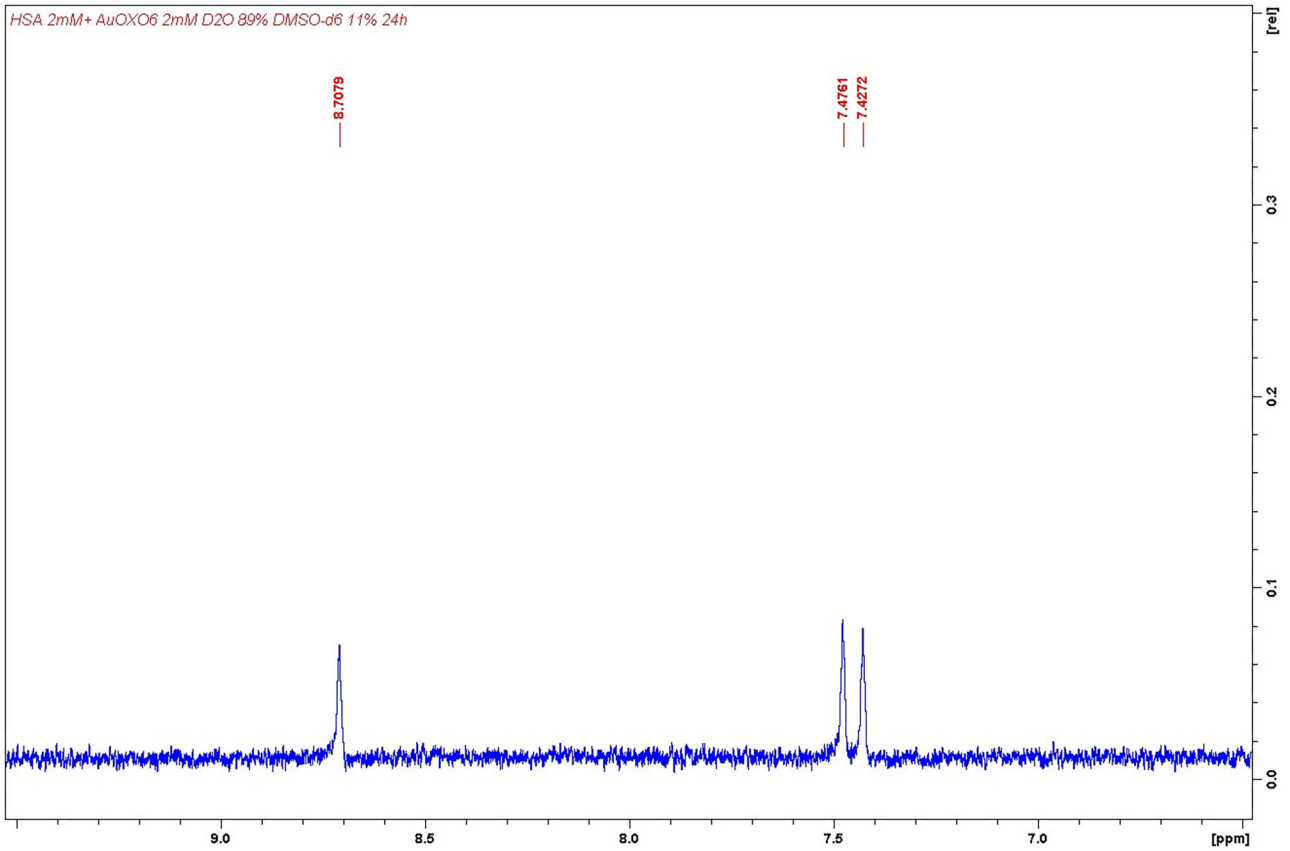

FIGURE 6 | Detail of 6,6′-dimethyl-2,2′-bipyridyl ^{1}HNMR aromatic signals. Detection performed after Auoxo6 interaction with human serum albumin (HSA).

in perfect agreement with that obtained through ESI MS measurements, in which only a gold/HSA adduct was found.

The case of the interaction of Au_2phen with HSA turned out to be slightly more complicated. More precisely, the spectrum of the sample showed no signals, suggesting a behavior of Au_2phen similar to that of Aubipyc. On the other hand, this occurrence seems to be in contrast with ESI MS results, in which only the presence of the same gold/HSA adduct was detected as in the case of interactions with AuL12 and Auoxo6. Anyway, this apparent contradiction can easily be explained, taking into account the precipitation of the ligand during the incubation process. Indeed, after the mixing of HSA and Au_2phen, the formation of a precipitate occurs, most probably an adduct between HSA and the aromatic ligand lost from Au_2phen. On the other hand, the formation of adducts between HSA and 1,10-phenanthroline systems was already reported in literature (Lin and Shen, 2017).

CONCLUSIONS—A GENERAL INTERPRETATION OF THE OBTAINED RESULTS

The above-reported results permit to identify some characteristic trends in the reactivity of the study gold(III) compounds with the tested protein targets. In particular, MS results provide a substantial body of comparative data on the various investigated systems. From the precise determination of the formed adducts, inferences may be drawn on the type of the occurring reactions in relation to the nature of the metal complex and of the interacting biomolecule.

From careful data analysis, some conclusions may be extracted, as follows:

The reactivity pattern first depends on the specific nature of the metal complex and its oxidizing character. Indeed, the more oxidizing gold(III) agents invariantly tend to undergo reduction to gold(I) or gold(0); the reduction process is generally associated with complete metal complex degradation, with the exception of AuL12, which retains the dithiocarbamate ligand. Typically, the less-oxidizing Aubipyc in its reaction with HSA and hCA I tends to conserve the gold center in the oxidation state +3 with complete retention of the terdentate ligand. Also, a not-negligible role is played by the nature of the protein. Indeed, the C-terminal dodecapeptide of thioredoxin reductase was found to be able to induce reduction even of the Aubipyc complex to gold(I) with the loss of the ligand.

In conclusion, from these results, the prodrug character of these metal complexes is further documented. All of them are able to be a source of gold(I) ions that are capable of metalating proteins mostly at cysteine and selenocysteine

residues. Production of gold(I) ions may be modulated through the oxidizing character of the complexes, especially for Auoxo6 and Au2phen, and the kinetics of the reduction reaction. Regarding Aubipyc, the different biomolecules promote the formation of different binding moieties; indeed, in the case of HSA and hCA I, the metal complex retains its oxidation state (+3), and the $[Au(III)(bipy^{dmb}\text{-}H)]^{2+}$ fragment binds the proteins, while in the presence of the dodecapeptide, a reduction of the gold center occurs, and the formation of Au(I)–peptide adduct is revealed.

Remarkably, in the presence of an excess of the gold complex, formation of small clusters containing 2–7 atoms of elemental gold is observed.

As indicated in several papers (Magherini et al., 2010; Cattaruzza et al., 2011; Huang et al., 2018; Altaf et al., 2019), the mechanisms of action of these gold(III) compounds seem to rely ultimately on protein metalation; moreover, the oxidizing character of the starting complex may play a role in the overall cytotoxic mechanism, further exacerbating the intracellular oxidative stress and reactive oxygen species (ROS) generation. The results of our work, highlighting the behavior of the gold(III) complexes in the presence of different biomolecules, seem to be an additional evidence to support the importance of redox mechanisms in the biological activity of these compounds.

MATERIALS AND METHODS

Materials

Lyophilized hCA I and HSA were purchased from Sigma-Aldrich and used without further purification or manipulation. Auoxo6, Au_2phen, Aubipyc, and AuL12, as well as the dodecapeptide of thioredoxin reductase (dTrxR), were synthetized in the MetMed Laboratories at the Department of Chemistry, University of Florence, following already established procedures (Pratesi et al., 2010, 2014).

DTT and dimethyl sulfoxide (DMSO) were purchased from Fluka. Liquid chromatography (LC)–MS materials (water, methanol, and ammonium acetate) were purchased from Sigma-Aldrich. Deuterated solvents (D_2O and DMSO-d_6) were purchased from Sigma-Aldrich.

Electrospray Ionization Mass Spectrometry Experimental Conditions

Sample Preparation

Stock solutions of hCA I 10^{-4} M, HSA 10^{-3} M, and dTrxR 10^{-3} M were prepared, dissolving the proteins and the peptide in H_2O of LC-MS grade. Stock solutions 10^{-2} M of the gold(III) compounds were prepared by dissolving the samples in DMSO. Stock solution 10^{-1} M of DTT was prepared in H_2O.

For the experiments with HSA, solutions of the protein 10^{-4} M and each gold compound at protein-to-metal ratios 1:0.9 or 1:3 were prepared by diluting with ammonium acetate solution 2×10^{-3} M, pH 6.8. The mixtures were then incubated at 37 °C up to 24 h.

For Aubipyc, another sample was prepared, as follows: a solution 10^{-4} M of the protein was prepared by diluting with ammonium acetate solution 2×10^{-3} M, pH 6.8. Then an aliquot of DTT stock solution was added in a protein/reducing agent 1:5 ratio; then the mixture was incubated at 37 °C up to 30 min. After that time, an aliquot of Aubipyc was added in a protein-to-metal compound ratio of 1:0.9. The mixture thus obtained was incubated at 37 °C up to 24 h.

For the experiments with hCA I, solutions of the protein 10^{-5} M and each gold compound at protein-to-metal ratio 1:3 were prepared by diluting with ammonium acetate solution 2×10^{-3} M, pH 6.8. The mixtures were then incubated at 37 °C up to 24 h.

For the experiments with TrxR peptide, solutions of the peptide 10^{-4} M were prepared by diluting with ammonium acetate solution 2×10^{-3} M, pH 6.8. Then aliquots of DTT stock solution were added in a peptide to reducing agent ratios (1:5, 1:10); then the mixtures were incubated at 37 °C up to 30 min. After that time, aliquots of the gold(III) compounds' solutions were added in peptide-to-metal compound ratios 1:1 or 1:3. The mixtures thus obtained were incubated at 37 °C up to 24 h.

Electrospray Ionization Mass Spectrometry Analysis: Final Dilutions

After the incubation time, all solutions were sampled and diluted to a final protein concentration of 7×10^{-7} M for hCA I, 5×10^{-7} M for HSA, and dTrxR using ammonium acetate solution 2×10^{-3} M, pH 6.8.

The HSA and hCA I final solutions were also added with 0.1% v/v of formic acid just before the infusion in the mass spectrometer.

Instrumental Parameters

The ESI mass study was performed using a TripleTOF® 5600^+ high-resolution mass spectrometer (Sciex, Framingham, MA, United States), equipped with a DuoSpray® interface operating with an ESI probe. Respective ESI MS spectra were acquired through direct infusion at 5 μl/min of flow rate.

The general ESI source parameters optimized for each protein and peptide analysis were as follows:

HSA: positive polarity, ion spray voltage floating 5,500 V, temperature 0, ion source Gas 1 (GS1) 45 L/min; ion source Gas 2 (GS2) 0; curtain gas (CUR) 12 L/min, collision energy (CE) 10 V; declustering potential (DP) 150 V, range 1,000–2,600 *m*/*z*.

hCA I: positive polarity, ion spray voltage floating 5,500 V, temperature 0, ion source Gas 1 (GS1) 40 L/min; ion source Gas 2 (GS2) 0; CUR 10 L/min, CE 10 V; DP 50 V, range 760–990 *m*/*z*.

dTrxR: positive polarity, ion spray voltage floating 5,500 V, temperature 100 °C, ion source Gas 1 (GS1) 25 L/min; ion source Gas 2 (GS2) 25 L/min; CUR 30 L/min, CE 10 V; DP 50 V, range 1,000–2,000 *m*/*z*.

For acquisition, Analyst TF software 1.7.1 (Sciex) was used, and deconvoluted spectra were obtained by using the Bio Tool Kit micro-application v.2.2 embedded in PeakView™ software v.2.2 (Sciex).

Nuclear Magnetic Resonance

Samples were prepared as an HSA solution in D_2O in which DMSO-d_6 stock solutions of the investigated compounds were added. The final concentrations were 2 mM of HSA with 1

equivalent of gold compound in D_2O/DMSO-d_6 9:1. Samples were then incubated for 24 h at 37 °C before acquisition.

Acquisitions were performed using cpmg1dpr Bruker pulse sequence (monodimensional Carr–Purcell–Meiboom–Gill sequence with solvent presaturation). Offset frequency was set up to 4.79 ppm for achieving residual H_2O suppression, while echo time was set up to 6 ms and the echo loop repeated for 126 times before free induction decay (FID) acquisition (1.512 s of total delay).

UV–Visible Spectrophotometric Studies

The electronic spectra were recorded by diluting small amounts of freshly prepared concentrated solutions of HSA, hCA I, or dodecapeptide, in the reference solution (2 mM of ammonium acetate, pH 6.8), at final protein/peptide concentration of 10^{-5} M. Each gold complex has been added, after the recording of the protein/peptide baseline, at a stoichiometric ratio of 3:1 (metal to protein). The resulting solutions were monitored by collecting the electronic spectra over 24 h at 37 °C.

DATA AVAILABILITY STATEMENT

All datasets generated for this study are included in the article/**Supplementary Material**.

AUTHOR CONTRIBUTIONS

AP, LMa, and LMe designed, coordinated, and supervised the whole study. DC carried out the NMR experiments. CZ and LMa acquired all the ESI MS and UV–Vis spectra. AP, DC, and LMe wrote the manuscript. All authors revised the experimental part and the discussion and approved the final version of the manuscript. All authors contributed to the article and approved the submitted version.

FUNDING

AP gratefully acknowledges the Beneficentia Stiftung, Vaduz (BEN2020/34) and University of Pisa (Rating Ateneo 2019–2020) for the financial support. DC gratefully acknowledges Associazione Italiana per la Ricerca sul Cancro for the financial support (AIRC 2-year Fellowship for Italy, Project Code: 23852). LMe, LMa, and AP acknowledge the Fondazione Italiana per la Ricerca sul Cancro (AIRC), Milan, and Fondazione Cassa Risparmio Firenze for funding the project Advanced mass spectrometry tools for cancer research: novel applications in proteomics, metabolomics, and nanomedicine (Multiuser Equipment Program 2016, ref. code 19650).

ACKNOWLEDGMENTS

All authors acknowledge the CIRCMSB (Consorzio Interuniveristario di Ricerca in Chimica dei Metalli nei Sistemi Biologici) for the fruitful and constructive scientific discussion.

SUPPLEMENTARY MATERIAL

The Supplementary Material for this article can be found online at: https://www.frontiersin.org/articles/10.3389/fchem.2020.581648/full#supplementary-material

REFERENCES

Abbehausen, C. (2019). Zinc finger domains as therapeutic targets for metal-based compounds-an update. *Metallomics* 11, 15–28. doi: 10.1039/C8MT00262B

Altaf, M., Casagrande, N., Mariotto, E., Baig, N., Kawde, A. N., Corona, G., et al. (2019). Potent *in vitro* and *in vivo* anticancer activity of new bipyridine and bipyrimidine gold (III) dithiocarbamate derivatives. *Cancers* 11:474. doi: 10.3390/cancers11040474

Casini, A., Cinellu, M. A., Minghetti, G., Gabbiani, C., Coronnello, M., Mini, E., et al. (2006). Structural and solution chemistry, antiproliferative effects, and DNA and protein binding properties of a series of dinuclear gold(III) compounds with bipyridyl ligands. *J. Med. Chem.* 49, 5524–5531. doi: 10.1021/jm060436a

Casini, A., Kelter, G., Gabbiani, C., Cinellu, M. A., Minghetti, G., Fregona, D., et al. (2009). Chemistry, antiproliferative properties, tumor selectivity, and molecular mechanisms of novel gold(III) compounds for cancer treatment: a systematic study. *J. Biol. Inorg. Chem.* 14, 1139–1149. doi: 10.1007/s00775-009-0558-9

Cattaruzza, L., Fregona, D., Mongiat, M., Ronconi, L., Fassina, A., Colombatti, A., et al. (2011). Antitumor activity of gold(III)-dithiocarbamato derivatives on prostate cancer cells and xenografts. *Int. J. Cancer* 128, 206–215. doi: 10.1002/ijc.25311

Chen, T., Yao, Q., Nasaruddin, R. R., and Xie, J. (2019). Electrospray ionization mass spectrometry: a powerful platform for noble metal nanocluster analysis. *Angew. Chem. Int. Ed.* 58, 11967–11977. doi: 10.1002/anie.201901970

Cinellu, M. A., Maiore, L., Manassero, M., Casini, A., Arca, M., Fiebig, H. H., et al. (2010). [Au2(phen2Me)2(μ-O)2] (PF6)2, a novel dinuclear gold(III) complex showing excellent antiproliferative properties. *ACS Med. Chem. Lett.* 1, 336–339. doi: 10.1021/ml100097f

Cinellu, M. A., Zucca, A., Stoccoro, S., Minghetti, G., Manassero, M., and Sansoni, M. (1996). Synthesis and characterization of gold(III) adducts and cyclometallated derivatives with 6-benzyl- and 6-alkyl-2,2′-bipyridines. *J. Chem. Soc. Dalton Trans.* 1996, 4217–4225. doi: 10.1039/DT9960004217

Cirri, D., Fabbrini, M. G., Massai, L., Pillozzi, S., Guerri, A., Menconi, A., et al. (2019). Structural and solution chemistry, antiproliferative effects, and serum albumin binding of three pseudohalide derivatives of auranofin. *BioMetals* 32, 939–948. doi: 10.1007/s10534-019-00224-1

Dabrowiak, J. C. (2012). Metals in medicine. *Inorg. Chim. Acta* 393, 1–2. doi: 10.1016/j.ica.2012.07.022

Dominguez-Medina, S., McDonough, S., Swanglap, P., F., Landes, C., and Link, S. (2012). *In situ* measurement of bovine serum albumin interaction with gold nanospheres. *Langmuir* 28, 9131–9139. doi: 10.1021/la3005213

Fanali, G., Di Masi, A., Trezza, V., Marino, M., Fasano, M., and Ascenzi, P. (2012). Human serum albumin: from bench to bedside. *Mol. Aspects Med.* 33, 209–290. doi: 10.1016/j.mam.2011.12.002

Fasano, M., Curry, S., Terreno, E., Galliano, M., Fanali, G., Narciso, P., et al. (2005). The extraordinary ligand binding properties of human serum albumin. *IUBMB Life* 57, 787–796. doi: 10.1080/15216540500404093

Ferraro, G., Giorgio, A., Mansour, A. M., and Merlino, A. (2019). Protein-mediated disproportionation of Au(I): insights from the structures of adducts of Au(III) compounds bearing: N, N -pyridylbenzimidazole derivatives with lysozyme. *Dalton Trans.* 48, 14027–14035. doi: 10.1039/C9DT02729G

Ferraro, G., Pratesi, A., Messori, L., and Merlino, A. (2020). Protein interactions of dirhodium tetraacetate: a structural study. *Dalton Trans.* 49, 2412–2416. doi: 10.1039/C9DT04819G

Fiskus, W., Saba, N., Shen, M., Ghias, M., Liu, J., Gupta, S., et al. (2014). Auranofin induces lethal oxidative and endoplasmic reticulum stress and exerts potent preclinical activity against chronic lymphocytic leukemia. *Cancer Res.* 74, 2520–2532. doi: 10.1158/0008-5472.CAN-13-2033

Gabbiani, C., Casini, A., Messori, L., Guerri, A., Cinellu, M. A., Minghetti, G., et al. (2008). Structural characterization, solution studies, and DFT calculations on a series of binuclear gold(III) oxo complexes: relationships to biological properties. *Inorg. Chem.* 47, 2368–2379. doi: 10.1021/ic701254s

Gabbiani, C., Cinellu, M. A., Maiore, L., Massai, L., Scaletti, F., and Messori, L. (2012a). Chemistry and biology of three representative gold(III) compounds as prospective anticancer agents. *Inorg. Chim. Acta* 393, 115–124. doi: 10.1016/j.ica.2012.07.016

Gabbiani, C., Massai, L., Scaletti, F., Michelucci, E., Maiore, L., Cinellu, M. A., et al. (2012b). Protein metalation by metal-based drugs: reactions of cytotoxic gold compounds with cytochrome c and lysozyme. *J. Biol. Inorg. Chem.* 17, 1293–1302. doi: 10.1007/s00775-012-0952-6

Gamberi, T., Massai, L., Magherini, F., Landini, I., Fiaschi, T., Scaletti, F., et al. (2014). Proteomic analysis of A2780/S ovarian cancer cell response to the cytotoxic organogold(III) compound aubipyc. *J. Proteomics* 103, 103–120. doi: 10.1016/j.jprot.2014.03.032

Giorgio, A., and Merlino, A. (2020). Gold metalation of proteins: structural studies. *Coord. Chem. Rev.* 407:213175. doi: 10.1016/j.ccr.2019.213175

Guidi, F., Puglia, M., Gabbiani, C., Landini, I., Gamberi, T., Fregona, D., et al. (2012). 2D-DIGE analysis of ovarian cancer cell responses to cytotoxic gold compounds. *Mol. BioSyst.* 8, 985–993. doi: 10.1039/C1MB05386H

Huang, K.-B., Wang, F.-Y., Tang, X.-M., Feng, H.-W., Chen, Z.-F., Liu, Y.-C., et al. (2018). Organometallic gold(III) complexes similar to tetrahydroisoquinoline induce ER-stress-mediated apoptosis and pro-death autophagy in A549 cancer cells. *J. Med. Chem.* 61, 3478–3490. doi: 10.1021/acs.jmedchem.7b01694

Johnson, G. E., and Laskin, J. (2016). Understanding ligand effects in gold clusters using mass spectrometry. *Analyst* 141, 3573–3589. doi: 10.1039/C6AN00263C

Johnson, K. A., Verhagen, M. F. J. M., Brereton, P. S., Adams, M. W. W., and Amster, I. J. (2000). Probing the stoichiometry and oxidation states of metal centers in iron- sulfur proteins using electrospray FTICR mass spectrometry. *Anal. Chem.* 72, 1410–1418. doi: 10.1021/ac991183e

Kupiec, M., Ziółkowski, R., Massai, L., Messori, L., and Pawlak, K. (2019). The electrochemical profiles of auranofin and aubipyc, two representative medicinal gold compounds: a comparative study. *J. Inorg. Biochem.* 198:110714. doi: 10.1016/j.jinorgbio.2019.110714

Lin, H. B., and Shen, Q. H. (2017). Luminescence studies of the ligand exchange between two phenanthroline complexes and bovine serum albumin. *J. Appl. Spectrosc.* 84, 170–176. doi: 10.1007/s10812-017-0446-y

Magherini, F., Fiaschi, T., Valocchia, E., Becatti, M., Pratesi, A., Marzo, T., et al. (2018). Antiproliferative effects of two gold(I)-N-heterocyclic carbene complexes in A2780 human ovarian cancer cells: a comparative proteomic study. *Oncotarget* 9, 28042–28068. doi: 10.18632/oncotarget.25556

Magherini, F., Modesti, A., Bini, L., Puglia, M., Landini, I., Nobili, S., et al. (2010). Exploring the biochemical mechanisms of cytotoxic gold compounds: a proteomic study. *J. Biol. Inorg. Chem.* 15, 573–582. doi: 10.1007/s00775-010-0624-3

Marcon, G., Carotti, S., Coronnello, M., Messori, L., Mini, E., Orioli, P., et al. (2002). Gold(III) complexes with bipyridyl ligands: solution chemistry, cytotoxicity, and DNA binding properties. *J. Med. Chem.* 45, 1672–1677. doi: 10.1021/jm010997w

Marzano, C., Ronconi, L., Chiara, F., Giron, M. C., Faustinelli, I., Cristofori, P., et al. (2011). Gold(III)-dithiocarbamato anticancer agents: activity, toxicology and histopathological studies in rodents. *Int. J. Cancer* 129, 487–496. doi: 10.1002/ijc.25684

Marzo, T., De Pascali, S. A., Gabbiani, C., Fanizzi, F. P., Messori, L., and Pratesi, A. (2017). ESI–MS studies of the reactions of novel platinum(II) complexes containing O,O′-chelated acetylacetonate and sulfur ligands with selected model proteins. *BioMetals* 30, 609–614. doi: 10.1007/s10534-017-0031-0

Marzo, T., Massai, L., Pratesi, A., Stefanini, M., Cirri, D., Magherini, F., et al. (2019). Replacement of the thiosugar of auranofin with iodide enhances the anticancer potency in a mouse model of ovarian cancer. *ACS Med. Chem. Lett.* 10, 656–660. doi: 10.1021/acsmedchemlett.9b00007

Marzo, T., Scaletti, F., Michelucci, E., Gabbiani, C., Pescitelli, G., Messori, L., et al. (2015). Interactions of the organogold(III) compound aubipyc with the copper chaperone Atox1: a joint mass spectrometry and circular dichroism investigation. *BioMetals* 28, 1079–1085. doi: 10.1007/s10534-015-9887-z

Massai, L., Cirri, D., Michelucci, E., Bartoli, G., Guerri, A., Cinellu, M. A., et al. (2016a). Organogold(III) compounds as experimental anticancer agents: chemical and biological profiles. *BioMetals* 29, 863–872. doi: 10.1007/s10534-016-9957-x

Massai, L., Pratesi, A., Bogojeski, J., Banchini, M., Pillozzi, S., Messori, L., et al. (2016b). Antiproliferative properties and biomolecular interactions of three Pd(II) and Pt(II) complexes. *J. Inorg. Biochem.* 165, 1–6. doi: 10.1016/j.jinorgbio.2016.09.016

Massai, L., Pratesi, A., Gailer, J., Marzo, T., and Messori, L. (2019). The cisplatin/serum albumin system: a reappraisal. *Inorg. Chim. Acta* 495:118983. doi: 10.1016/j.ica.2019.118983

Merlino, A., Marzo, T., and Messori, L. (2017). Protein metalation by anticancer metallodrugs: a joint ESI MS and XRD investigative strategy. *Chem. A Euro. J.* 23, 6942–6947 doi: 10.1002/chem.201605801

Messori, L., and Merlino, A. (2017). Protein metalation by metal-based drugs: x-ray crystallography and mass spectrometry studies. *Chem. Commun.* 53, 11622–11633 doi: 10.1039/C7CC06442J

Michelucci, E., Pieraccini, G., Moneti, G., Gabbiani, C., Pratesi, A., and Messori, L. (2017). Mass spectrometry and metallomics: a general protocol to assess stability of metallodrug-protein adducts in bottom-up MS experiments. *Talanta* 167, 30–38. doi: 10.1016/j.talanta.2017.01.074

Nardon, C., Boscutti, G., Gabbiani, C., Massai, L., Pettenuzzo, N., Fassina, A., et al. (2017). Cell and cell-free mechanistic studies on two gold(III) complexes with proven antitumor properties. *Eur. J. Inorg. Chem.* 2017, 1737–1744 doi: 10.1002/ejic.201601215

Nardon, C., and Fregona, D. (2015). Gold(III) complexes in the oncological preclinical arena: from aminoderivatives to peptidomimetics. *Curr. Topics Med. Chem.* 16, 360–380. doi: 10.2174/1568026615666150827094500

Nobili, S., Mini, E., Landini, I., Gabbiani, C., Casini, A., and Messori, L. (2010). Gold compounds as anticancer agents: chemistry, cellular pharmacology, and preclinical studies. *Med. Res. Rev.* 30, 550–580. doi: 10.1002/med.20168

Pratesi, A., Cirri, D., Đurović, M. D., Pillozzi, S., Petroni, G., Bugarčić, Ž. D., et al. (2016). New gold carbene complexes as candidate anticancer agents. *BioMetals* 29, 905–911. doi: 10.1007/s10534-016-9962-0

Pratesi, A., Cirri, D., Ciofi, L., and Messori, L. (2018). Reactions of auranofin and its pseudohalide derivatives with serum albumin investigated through ESI-Q-TOF MS. *Inorg. Chem.* 57, 10507–10510. doi: 10.1021/acs.inorgchem.8b02177

Pratesi, A., Cirri, D., Fregona, D., Ferraro, G., Giorgio, A., Merlino, A., et al. (2019). Structural characterization of a gold/serum albumin complex. *Inorg. Chem.* 58, 10616–10619. doi: 10.1021/acs.inorgchem.9b01900

Pratesi, A., Gabbiani, C., Ginanneschi, M., and Messori, L. (2010). Reactions of medicinally relevant gold compounds with the C-terminal motif of thioredoxin reductase elucidated by MS analysis. *Chem. Commun.* 46, 7001–7003. doi: 10.1039/c0cc01465f

Pratesi, A., Gabbiani, C., Michelucci, E., Ginanneschi, M., Papini, A. M., Rubbiani, R., et al. (2014). Insights on the mechanism of thioredoxin reductase inhibition by Gold N-heterocyclic carbene compounds using the synthetic linear selenocysteine containing C-terminal peptide hTrxR(488-499): an ESI-MS investigation. *J. Inorg. Biochem.* 136, 161–169. doi: 10.1016/j.jinorgbio.2014.01.009

Rombouts, I., Lagrain, B., Scherf, K. A., Koehler, P., and Delcour, J. A. (2015). Formation and reshuffling of disulfide bonds in bovine serum albumin demonstrated using tandem mass spectrometry with collision-induced and electron-transfer dissociation. *Sci. Rep.* 5:12210. doi: 10.1038/srep 15589

Ronconi, L., Aldinucci, D., Ping Dou, Q., and Fregona, D. (2012). Latest insights into the anticancer activity of gold(III)-dithiocarbamato complexes. *Anti Cancer Agents Med. Chem.* 10, 283–292. doi: 10.2174/187152010791 162298

Russo Krauss, I., Messori, L., Cinellu, M. A., Marasco, D., Sirignano, R., and Merlino, A. (2014). Interactions of gold-based drugs with proteins: the structure and stability of the adduct formed in the reaction between lysozyme and the cytotoxic gold(III) compound Auoxo3. *Dalton Trans.* 43, 17483–17488. doi: 10.1039/C4DT02332C

Scalcon, V., Bindoli, A., and Rigobello, M. P. (2018). Significance of the mitochondrial thioredoxin reductase in cancer cells: an update

on role, targets and inhibitors. *Free Rad. Biol. Med.* 127, 62–79. doi: 10.1016/j.freeradbiomed.2018.03.043

Talib, J., Beck, J. L., and Ralph, S. F. (2006). A mass spectrometric investigation of the binding of gold antiarthritic agents and the metabolite [Au(CN)2]- to human serum albumin. *J. Biol. Inorg. Chem.* 11, 559–570. doi: 10.1007/s00775-006-0103-z

Tamasi, G., Carpini, A., Valensin, D., Messori, L., Pratesi, A., Scaletti, F., et al. (2014). {Ru(CO)x}-core complexes with selected azoles: synthesis, X-ray structure, spectroscopy, DFT analysis and evaluation of cytotoxic activity against human cancer cells. *Polyhedron* 81, 227–237. doi: 10.1016/j.poly.2014.05.067

Tatini, F., Landini, I., Scaletti, F., Massai, L., Centi, S., Ratto, F., et al. (2014). Size dependent biological profiles of PEGylated gold nanorods. *J. Mater. Chem. B* 2, 6072–6080. doi: 10.1039/C4TB00991F

Zhang, X., Frezza, M., Milacic, V., Ronconi, L., Fan, Y., Bi, C., et al. (2010). Inhibition of tumor proteasome activity by gold-dithiocarbamato complexes via both redox-dependent and -independent processes. *J. Cell. Biochem.* 109, 162–172. doi: 10.1002/jcb.22394

Zoppi, C., Messori, L., and Pratesi, A. (2020). ESI MS studies highlight the selective interaction of auranofin with protein free thiols. *Dalton Trans.* 49, 5906–5913. doi: 10.1039/D0DT00283F

Zou, T., Lum, C. T., Lok, C. N., Zhang, J. J., and Che, C. M. (2015). Chemical biology of anticancer gold(III) and gold(I) complexes. *Chem. Soc. Rev.* 44, 8786–8801. doi: 10.1039/C5CS00132C

Conflict of Interest: The authors declare that the research was conducted in the absence of any commercial or financial relationships that could be construed as a potential conflict of interest.

frontiers in Chemistry

REVIEW
published: 06 November 2020
doi: 10.3389/fchem.2020.587207

Anticancer Gold(III) Compounds With Porphyrin or N-heterocyclic Carbene Ligands

Ka-Chung Tong[1,2], *Di Hu*[1,2], *Pui-Ki Wan*[1,2], *Chun-Nam Lok*[1,2] *and Chi-Ming Che*[1,2]*

[1] State Key Laboratory of Synthetic Chemistry, Department of Chemistry, The University of Hong Kong, Hong Kong, China, [2] Laboratory for Synthetic Chemistry and Chemical Biology, Health@InnoHK, Hong Kong, China

The use of gold in medicine has a long history. Recent clinical applications include anti-inflammatory agents for the treatment of rheumatoid arthritis (chrysotherapy), and is currently being developed as potential anticancer chemotherapeutics. Gold(III), being isoelectronic to platinum(II) as in cisplatin, is of great interest but it is inherently unstable and redox-reactive under physiological conditions. Coordination ligands containing C and/or N donor atom(s) such as porphyrin, pincer-type cyclometalated and/or N-heterocyclic carbene (NHC) can be employed to stabilize gold(III) ion for the preparation of anticancer active compounds. In this review, we described our recent work on the anticancer properties of gold(III) compounds and the identification of molecular targets involved in the mechanisms of action. We also summarized the chemical formulation strategies that have been adopted for the delivery of cytotoxic gold compounds, and for ameliorating the *in vivo* toxicity.

Keywords: gold(III), porphyrin, N-heterocyclic carbene, anticancer, biomolecular target, formulation, biosensing

OPEN ACCESS

Edited by:
Wukun Liu,
Nanjing University of Chinese Medicine, China

Reviewed by:
Zhe Liu,
Qufu Normal University, China
Justin Wilson,
Cornell University, United States
Jonathan Arambula,
OncoTEX, Inc, United States

***Correspondence:**
Chi-Ming Che
cmche@hku.hk

Specialty section:
This article was submitted to Medicinal and Pharmaceutical Chemistry, a section of the journal Frontiers in Chemistry

Received: *25 July 2020*
Accepted: *03 September 2020*
Published: *06 November 2020*

Citation:
Tong K-C, Hu D, Wan P-K, Lok C-N and Che C-M (2020) Anticancer Gold(III) Compounds With Porphyrin or N-heterocyclic Carbene Ligands. Front. Chem. 8:587207. doi: 10.3389/fchem.2020.587207

INTRODUCTION

The medicinal use of gold against disease has been recorded since ancient times. In the early twenty century, the discovery of the antiarthritic activity of gold(I) complex (sodium gold(I) thiopropanol-sulfonate; Allochrysine) led to the development of clinically useful gold(I)-thiolate drugs including sodium aurothiomalate (Myochrysine) and the acetylated glucose derivative of the gold(I)-phosphine complex (Auranofin) for the treatment of rheumatoid arthritis. Since the serendipitous discovery of the therapeutic value of cisplatin, cisplatin-based chemotherapy has been widely used in treatment against various types of cancers (Kelland, 2007; Hill and Sadler, 2016). Extensive studies on mechanisms of action have demonstrated that cisplatin covalently interacts with DNA, activates DNA damage response, inhibits DNA repair mechanisms, and consequently results in cellular apoptosis (Jung and Lippard, 2007). However, the issues of dose-limiting toxicity and chemoresistance to cisplatin remain challenging in clinical practice (Rabik and Dolan, 2007). Recently, there has been an upsurge of interest in the development of gold compounds for anticancer applications due to the cytotoxicity of the gold complex against cancer cells. Particularly, the isoelectronic nature (d^8) of gold(III) with platinum(II) suggests that gold(III) compounds may share similar properties with platinum(II)-based anticancer agents. Nonetheless, the instability and reactivity of the gold(III) ion, such as a facile reduction into gold(I) or gold(0) *via* intracellular redox reactions under physiological conditions, hamper the therapeutic application of these gold(III) compounds. Over the past few decades, we have made use of strong electron-donor ligands, such as porphyrin, pincer cyclometalated (C^N^C), and N-heterocyclic carbene, for the preparation

of cationic gold(III) compounds. All of them exhibit good stability in physiological environments and display a promising anticancer potency against a broad spectrum of cancer cells derived from human tumor tissues. More importantly, distinct from traditional platinum-based therapeutics targeting DNA *via* non-repairable interactions, the unique stable gold(III)–ligand coordination scaffold allows the complexes to bind to protein target(s) relevant to cancer cell survival and proliferation, and hence, leads to functional inhibition and associated anticancer activities.

ANTICANCER GOLD(III) PORPHYRIN COMPLEXES

In 2003, an anticancer gold(III) porphyrin system was established that was exemplified by a gold(III) *meso*-tetraphenylporphyrin complex [denoted **Au-1a** (**1**); **Figure 1**], demonstrating potential clinical applications (Che et al., 2003). The porphyrin ligand can stabilize the gold(III) ion against demetalation and reduction by the biological reductant glutathione (Sun et al., 2010). *In vitro* biological studies have proven the high anticancer potency of gold(III) porphyrin complexes against a wide range of cancer cell lines, such as neuroblastoma, melanoma, ovarian, breast, colorectal, lung, and nasopharyngeal cancers, with IC_{50} values at low micromolar or even nanomolar levels (Lammer et al., 2015; Toubia et al., 2019). Moreover, *in vivo* studies have demonstrated the promising tumor growth inhibitory ability of gold(III) porphyrins in different mouse models of cancer (**Figures 2A,B,D**) and the induction of apoptosis in tumor xenograft tissues (**Figure 2E**). Compared to the clinically used cisplatin, complex **1** displays higher cytotoxicity with IC_{50} values significantly lower than those of cisplatin and is equally active toward both cisplatin-sensitive and -resistant cancer cells (**Figure 2F**; Lum et al., 2014). Multiple mechanisms of chemoresistance to cisplatin involve a reduced intracellular accumulation, sequestration/detoxification by thiols (e.g., glutathione), increased DNA damage repair response, and efflux transports (Galluzzi et al., 2012). The

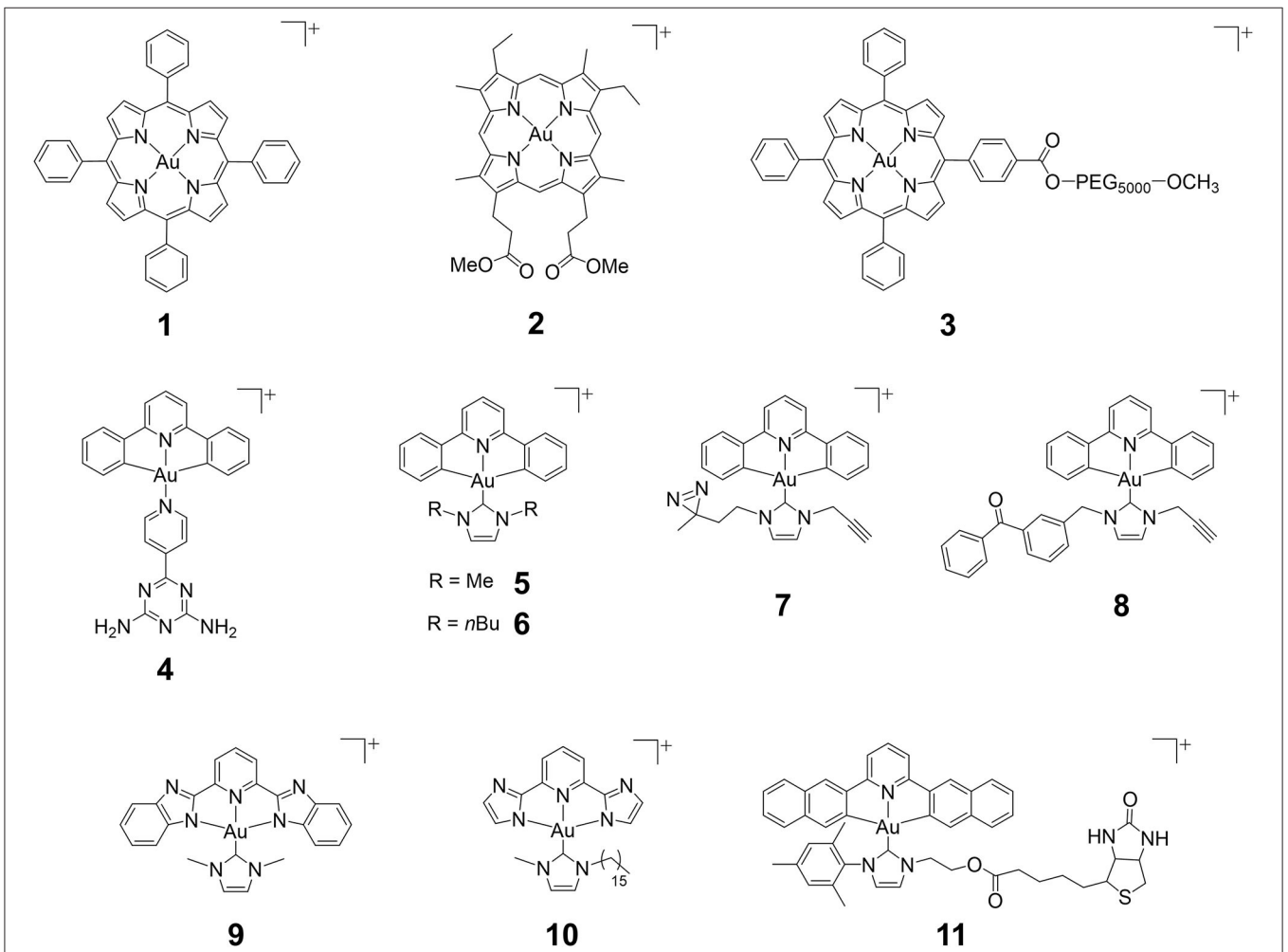

FIGURE 1 | Chemical structures of cationic gold(III) complexes with porphyrin, pincer cyclometalated and N-heterocyclic carbene (NHC) ligands.

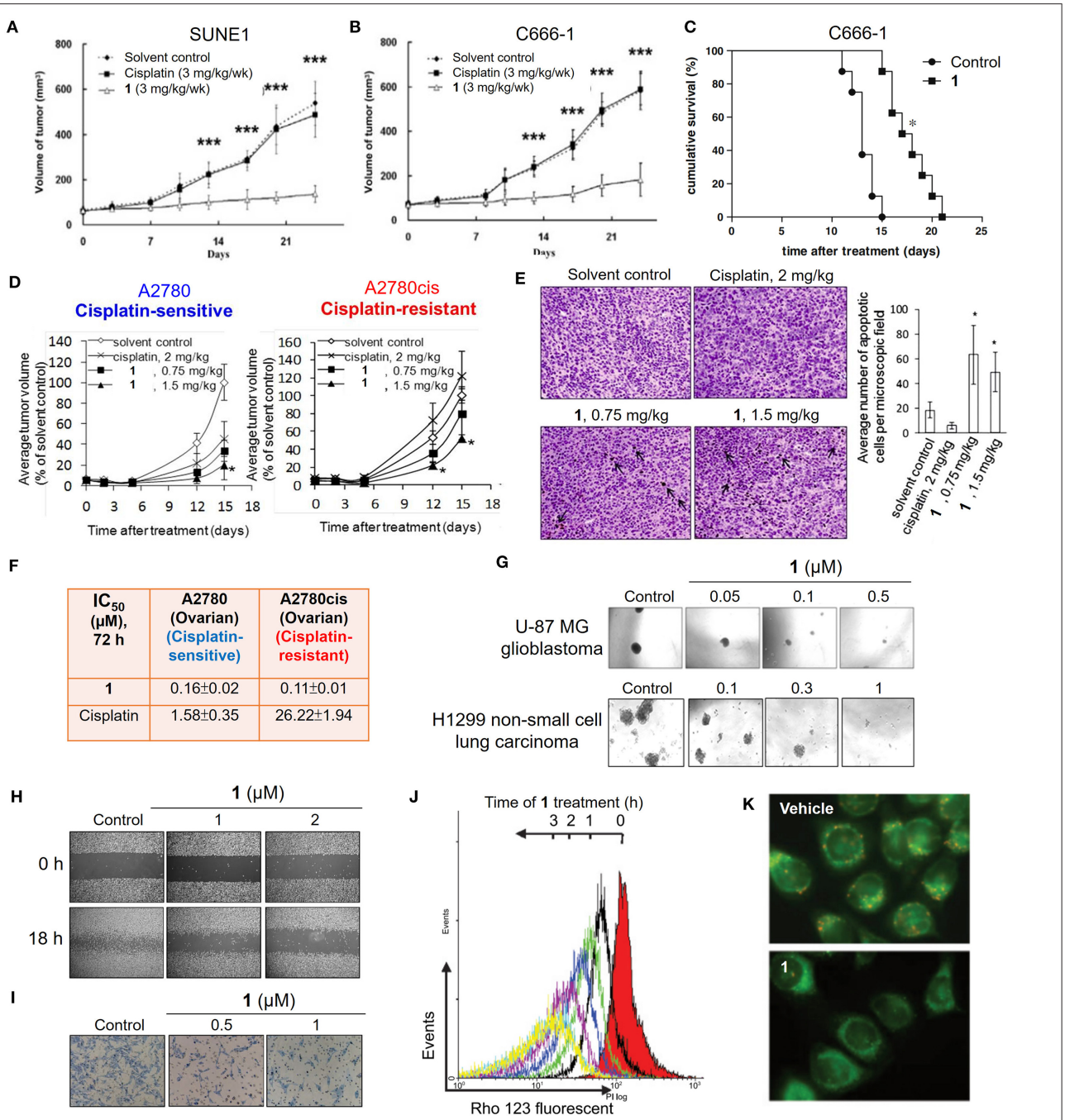

IC_{50} (μM), 72 h	A2780 (Ovarian) (Cisplatin-sensitive)	A2780cis (Ovarian) (Cisplatin-resistant)
1	0.16±0.02	0.11±0.01
Cisplatin	1.58±0.35	26.22±1.94

FIGURE 2 | Anticancer properties of the cationic gold(III) porphyrin complex. Tumor volumes of mice bearing **(A)** nasopharyngeal SUNE1, **(B)** C666-1 or **(D)** ovarian (cisplatin-sensitive A2780 and–resistant A2780cis) xenografts after treatment with **1** or vehicle control. **(C)** Survival curves of mice bearing NPC C666-1 metastatic tumors in control and **1**-treated groups. **(E)** TUNEL staining of A2780cis tumor tissues of mice in different groups (left; arrows indicate the apoptotic cells). Bar chart illustrates the average number of apoptotic cells per microscopic field in different groups (right). **(F)** *In vitro* cytotoxicity (IC_{50}, 72 h) of **1** and cisplatin on ovarian (cisplatin-sensitive and -resistant) cancer cell lines. **(G)** Representative images of the inhibitory activities of **1** in sphere formation by human glioblastoma U-87 MG and non-small cell lung cancer H1299 cells. **(H)** Antimigratory and **(I)** antimetastatic activities of **1** on the cell migration and invasion by NPC C666-1 cells. **(J)** Flow cytometric analysis of $\Delta\psi_m$ depolarization in **1**-treated HONE1 cells by fluorescent Rho-123 probe. **(K)** Fluorescence imaging of $\Delta\psi_m$ depolarization in **1**-treated cells by mitochondrial membrane potential JC-1 probe. **(A,B)** Reprinted with permission from To et al. (2009). Copyright 2010, Elsevier. **(C,H,I)** Reprinted with permission from Lum et al. (2010). Copyright 2010, Elsevier. **(D,E)** Reproduced from Lum et al. (2014) with permission from the Royal Society of Chemistry. **(G)** Reproduced from Lum et al. (2013) with permission from the Royal Society of Chemistry. **(J,K)** Adapted from Wang et al. (2005). Cancer Res, Vol. 65, Article ID CAN-05-2867, (2005). Data are presented as mean ± SEM (**A,B**; $n = 12$; Student's t test; $^{***}p < 0.005$, compared with vehicle control group), (**C**; $n = 8$; Student's t test; $^{*}p = 0.0001$, compared with vehicle control group), (**D**; **1**, $n = 3$; vehicle control, $n = 8$; Student's t test; $^{*}p \leq 0.05$, compared with vehicle control group) and (**E**; **1** (0.75 mg/kg), $n = 3$; **1** (1.5 mg/kg), $n = 6$; vehicle control, $n = 11$; Student's t test; $^{*}p < 0.05$, compared with vehicle control group).

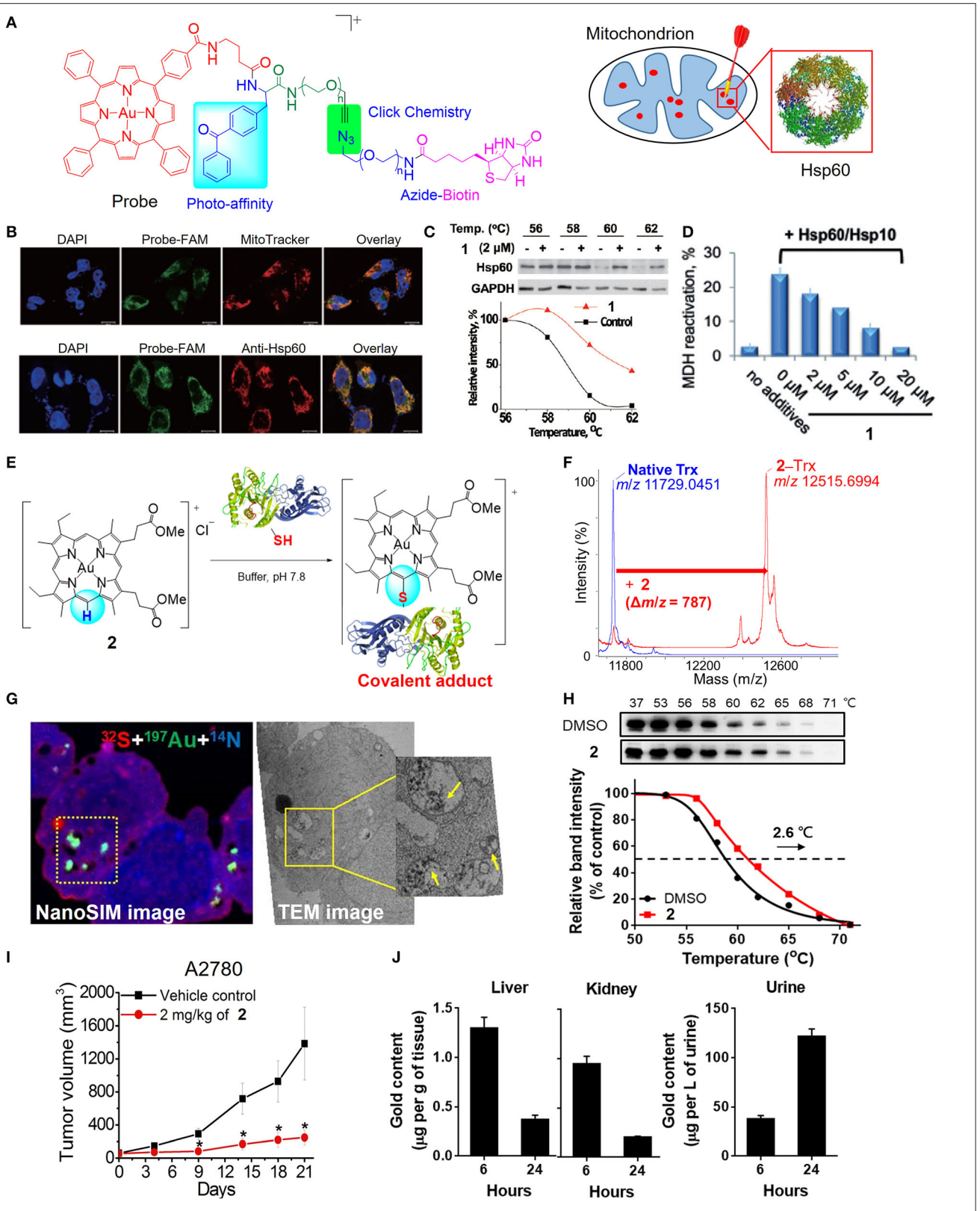

FIGURE 3 | Target engagement of anticancer gold(III) porphyrin complexes. **(A)** A clickable photoaffinity probe for the target identification of **1**. **(B)** Fluorescence imaging for colocalization of the probe with MitoTracker Orange and fluorescence-labeled Hsp60. **(C)** Thermal stabilization of Hsp60 after treatment of HeLa cells with

(Continued)

FIGURE 3 | 1 as determined by CETSA. **(D)** Inhibition of Hsp60 chaperone activity by **1**. **(E)** Proposed reaction scheme of **2** with protein cysteine thiol under physiological conditions. **(F)** MALDI-TOF-MS spectra of thioredoxin (Trx) before and after reaction with **2**. **(G)** NanoSIMS and EM imaging of the sulfur-rich, electron-dense aggregates in degraded mitochondria of **2**-treated cells. **(H)** Thermal stabilization of PRDX3 following treatment of A2780 ovarian cancer cells with **2** as determined by CETSA. **(I)** *In vivo* antitumor activity of **2** and **(J)** biodistribution of gold content in mice after treatment with **2**. **(A–D)** Reprinted with permission from Hu et al. (2016). Copyright 2015, John Wiley and Sons. **(E–J)** Reprinted with permission from Tong et al. (2020). Copyright 2020, National Academy of Sciences. Data are presented as mean ± SEM (**I**; $n = 5$; Student's t test; $^*p < 0.05$, compared with vehicle control group).

lack of cross-resistance to cisplatin suggests that the stable gold(III) porphyrin complex penetrates into the cancer cells and exerts anticancer activities *via* different mechanisms from cisplatin. Furthermore, **1** is capable of blocking the self-renewal of cancer stem-like cells (**Figure 2G**; Lum et al., 2013), suppressing angiogenesis *in vitro* and *in vivo* (Lum et al., 2011), inhibiting cancer cell migration (**Figure 2H**), invasion and metastasis (**Figure 2I**), and prolonging the survival lifetime of nasopharyngeal carcinoma metastasis-bearing mice (**Figure 2C**; Lum et al., 2010).

In previous studies, a number of approaches, including biochemical analyzes, transcriptomics, and proteomics, have been utilized to investigate the mechanisms of the anticancer action of gold(III) porphyrins. Several lines of evidence have revealed that complex **1** can target mitochondria. Treatment of cancer cells with **1** induces a rapid depletion of mitochondrial transmembrane potential (**Figures 2J,K**) and subsequently causes caspase-dependent and -independent apoptotic pathways (Wang et al., 2005). Cellular oxidative stress and shift of the balance between proapoptotic and antiapoptotic proteins were also observed in **1**-treated cancer cells. In addition, treatment of **1** can arrest the cell cycle progression in the G0/G1 phase, activate p38 mitogen-activated protein kinases (MAPK), and inhibit the redox regulation of thioredoxin reductase (TrxR) (Wang et al., 2007; Tu et al., 2009). To obtain deeper insights into the mechanisms of action of gold(III) porphyrins, efforts have been made to identify the direct molecular targets of **1** using a chemoproteomic approach with the aid of a clickable photoaffinity probe containing a benzophenone moiety (**Figure 3A**; Hu et al., 2016). In this regard, we identified a mitochondrial chaperone, heat shock protein 60 (Hsp60) as one of the molecular targets of **1** *in vitro* and *in cellulo*. The proposed non-covalent biomolecular interaction of **1** with Hsp60 was further supported by different binding studies including a cellular thermal shift assay, saturation-transfer difference NMR, and protein fluorescence quenching (**Figures 3B,C**). The dose-dependent inhibitory effect of **1** on the chaperone activity of Hsp60 in the reactivation of the denatured substrate of malate dehydrogenase (MDH) was also confirmed (**Figure 3D**). In addition, structure-activity relationship studies from the analogous gold(III) and platinum(II) complexes showed that gold(III) ion, porphyrin ligand, and the monocationic charge character governed by the central gold(III) ion play important roles for the inhibition of the chaperone activity of Hsp60. Our study provided a deeper understanding on the molecular targets of **1** in cancer cells, enabling the improvement of the anticancer activity of gold(III) porphyrins *via* structural modification.

By varying the *meso*-tetraphenylporphyrin ligand into quasiphysiological mesoporphyrin IX, we have uncovered a previously unknown biomolecular interaction of the gold(III) complex that can be exploited for anticancer applications (Tong et al., 2020). Gold complexes usually interact with cysteine thiols *via* M–S bond formation. Nonetheless, the gold(III) mesoporphyrin IX dimethyl ester (**2**) is unique in that the periphery (*meso*-carbon atom) of the porphyrin ligand is activated by the electrophilic gold(III) ion to undergo nucleophilic aromatic substitution with selectivity to the cysteine thiols of proteins, such as thioredoxin, relevant to cancer (**Figures 3E,F**). Notably, **2**-treated cancer cells resulted in the formation of gold-bound sulfur-rich protein aggregates in the cytosolic region and more specifically in mitochondria, as revealed by nanoscale secondary ion mass spectrometry (nanoSIMS) and electron microscopic imaging techniques (**Figure 3G**). Based on thermal proteome profiling mass spectrometry analysis and a cellular thermal shift assay (CETSA), potential protein targets including peroxiredoxin III (PRDX3) and deubiquitinase (UCHL3) were identified to engage with complex **2**, as supported by their increased thermal stability upon the treatment of **2** compared with vehicle control (**Figure 3H**). A series of biochemical experiments further validated the biological consequences of the treatment with **2** resulting in the inhibition of the protein activities, oxidative stress-mediated cytotoxicity, and the accumulation of ubiquitinated proteins. Importantly, **2** exhibited effective antitumor activities in two independent mouse models (**Figure 3I**) and demonstrated a favorable metabolism, biodistribution, and clearance conferred by the quasiphysiological mesoporphyrin IX ligand (**Figure 3J**). Taken together, these results demonstrated a new modality of cysteine targeting by the anticancer gold(III) complex.

FORMULATIONS OF GOLD(III) COMPLEXES FOR ANTITUMOR TREATMENT

Although gold(III) porphyrin complexes were demonstrated to exhibit promising anticancer activities in various human cancer cell lines, further applicability on cancer therapy remains challenging due to its high toxicity in normal cells and tissues. Formulation of the gold(III) porphyrin complexes by nanotechnology-based delivery systems is a potential strategy to mitigate the challenges of their short half-life in blood circulation and rapid distribution into major organs (**Figure 4**). By making use of biocompatible materials, the encapsulation of gold(III) porphyrin in gelatin-acacia microcapsules improved the aqueous solubility and stability, as well as the *in vivo* antitumor efficacy of the compound. With the use of RGD tripeptide acting as a targeting ligand, we have also described a cancer-targeted mesoporous silica nanoparticle (MSN) as a delivery carrier for complex **1** (**Figure 4A**; He et al., 2014). The **1**-encapsulated MSNs

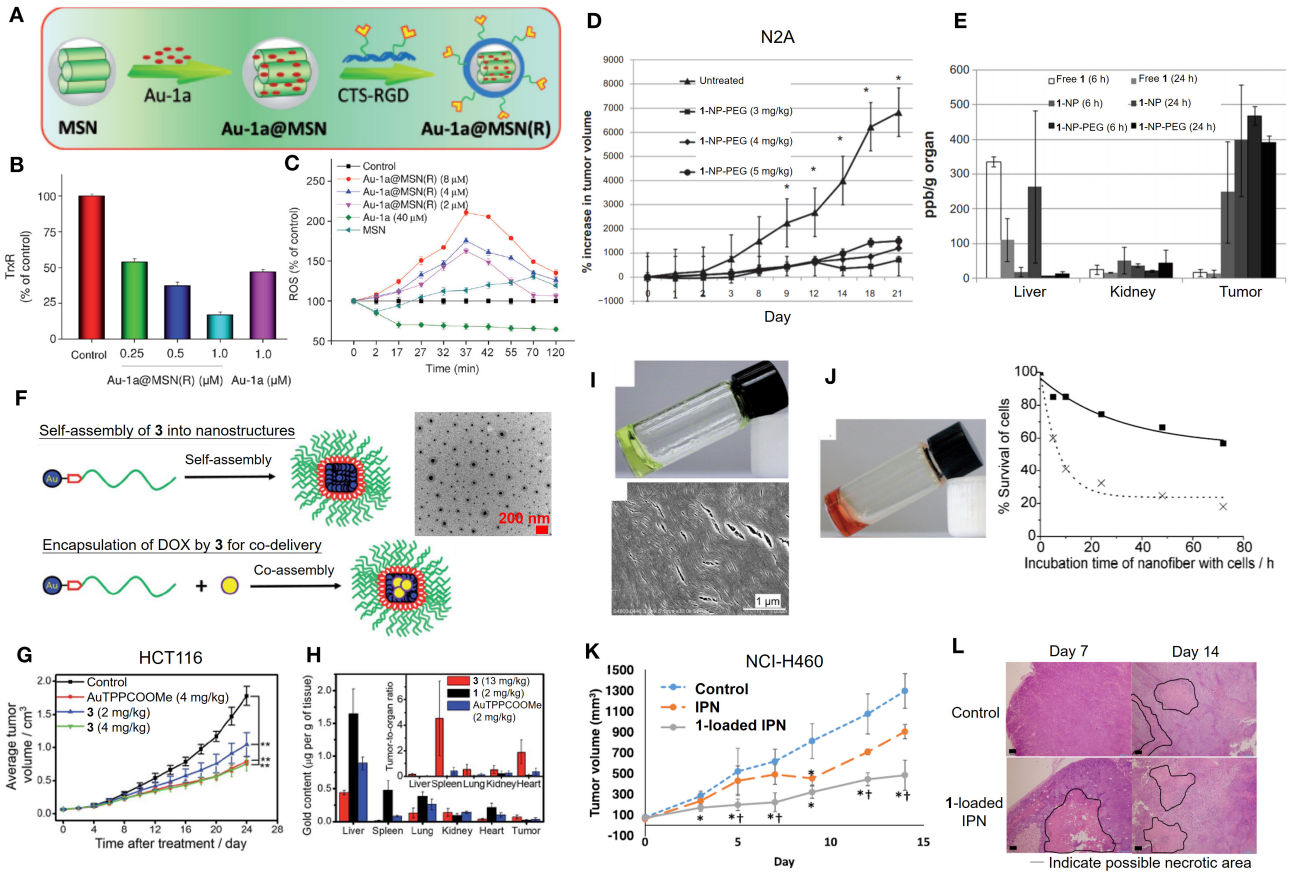

FIGURE 4 | Formulations of anticancer gold(III) porphyrin complexes. **(A)** Preparation of **1**-loaded RGD peptide-grafted mesoporous silica nanoparticles, **Au-1a**@MSN(R). Dose-dependent **(B)** inhibitory effect of **Au-1a**@MSN(R) on the *in vitro* TrxR activity and **(C)** induction of intracellular ROS level. **(D)** Antitumor activity of **1**-encapsulated PEG-modified lipid nanoparticles (**1**-NP-PEG) and **(E)** biodistribution of gold content on N2A tumor-bearing mice. **(F)** Schematic diagram of self-assembly of **3** into nanostructures and as a carrier with the co-assembly of doxorubicin (yellow circle). **(G)** Antitumor activity of conjugate **3** in mice bearing HCT116 xenografts. **(H)** Biodistribution and tumor-to-organ ratio of conjugate **3** in tumor-bearing mice. **(I)** Photograph (top) and SEM image (bottom) showing formation of supramolecular polymer (**4-SP**) after cooling the heated solution (323 K) to 298 K. **(J)** Photograph of **Au-1a**-encapsulated supramolecular polymer **(4-SP-Au-1a)** after cooling the heated solution to 298 K (left). *In vitro* cytotoxicity of **4-SP** (solid line) and **4-SP-Au-1a** (dotted line) against melanoma B16 cancer cells in a time-dependent manner (0-72 h) (right). **(K)** Antitumor activity of **1**-loaded IPN in NCI-H460 xenografted mice. **(L)** Hematoxylin and Eosin (H&E) stain of tumor tissues from mice at day 14 post-treatment. **(A–C)** Reprinted with permission from He et al. (2014). Copyright 2014, John Wiley and Sons. **(D,E)** Adapted from Lee et al. (2012). Int J Nanomedicine, Vol. 7, Article ID S28783, (2012); licensed under a Creative Commons Attribution (CC BY-NC-ND) license. **(F–H)** Reproduced from Chung et al. (2017) with permission from the Royal Society of Chemistry. **(I,J)** Reprinted with permission from Zhang et al. (2012). Copyright 2012, John Wiley and Sons. **(K,L)** Reprinted with permission from Lee et al. (2019). Copyright 2019, Springer Nature. Data are presented as mean ± SEM (**D**; $n = 5$–6; Student's t test; $^{*}p < 0.05$, compared with untreated group), (**G**; $n = 8$; Student's t test; $^{**}p < 0.01$, compared with solvent control group), and (**K**; $n = 6$; Student's t test; $^{*}p < 0.05$, compared with control group receiving UV exposure only; $^{\dagger}p < 0.05$, compared with IPN group).

coated with RGD-grafted polymeric chitosan [**Au-1a**@MSN(R)] displayed increased biocompatibility and colloidal stability in physiological media, and an enhanced cell-killing selectivity between cancer and normal cells. More importantly, **Au-1a**@MSN(R) exhibited an augmented inhibitory activity on TrxR (**Figure 4B**), elevated cellular oxidative stress (**Figure 4C**), and enhanced apoptosis-inducing efficacy. Poly(ethylene) glycol (PEG) is the most commonly employed hydrophilic and biocompatible polymer in the research of drug delivery systems (Knop et al., 2010). The use of PEG in a formulation can prolong the blood circulation half-life and provide a shield to the parental drug, avoiding rapid uptake by the organs (liver and spleen) of the reticuloendothelial system (RES) or clearance from the body (Harris and Chess, 2003). The advantages of which render PEG as an attractive material in the development of the formulation of improving the biodistribution and/or systemic toxicity of cytotoxic metal complexes. In this regard, we have reported the use of PEG surface-modified lipid nanoparticles made of the Brij 78 surfactant and cetyl alcohol for delivery of complex **1** into tumor xenografts of neuroblastoma (N2A) (**Figure 4D**; Lee et al., 2012). The PEGylated lipid nanoparticles (**1**-NP-PEG) enhanced the preferential tumor accumulation of complex **1** rather than in major organs (**Figure 4E**) and thereby, resulted in a higher tumor-killing efficacy when compared with free gold porphyrin treatment. Recently, we have also described a multifunctional PEGylated gold(III) porphyrin conjugate [Au(TPP-COO-PEG_{5000}-OCH_3)]Cl (**3**) that can self-assemble into nanostructures in aqueous media (**Figure 4F**; Chung et al., 2017). The cleavable ester linkage allows for the release of an active gold(III) porphyrin moiety

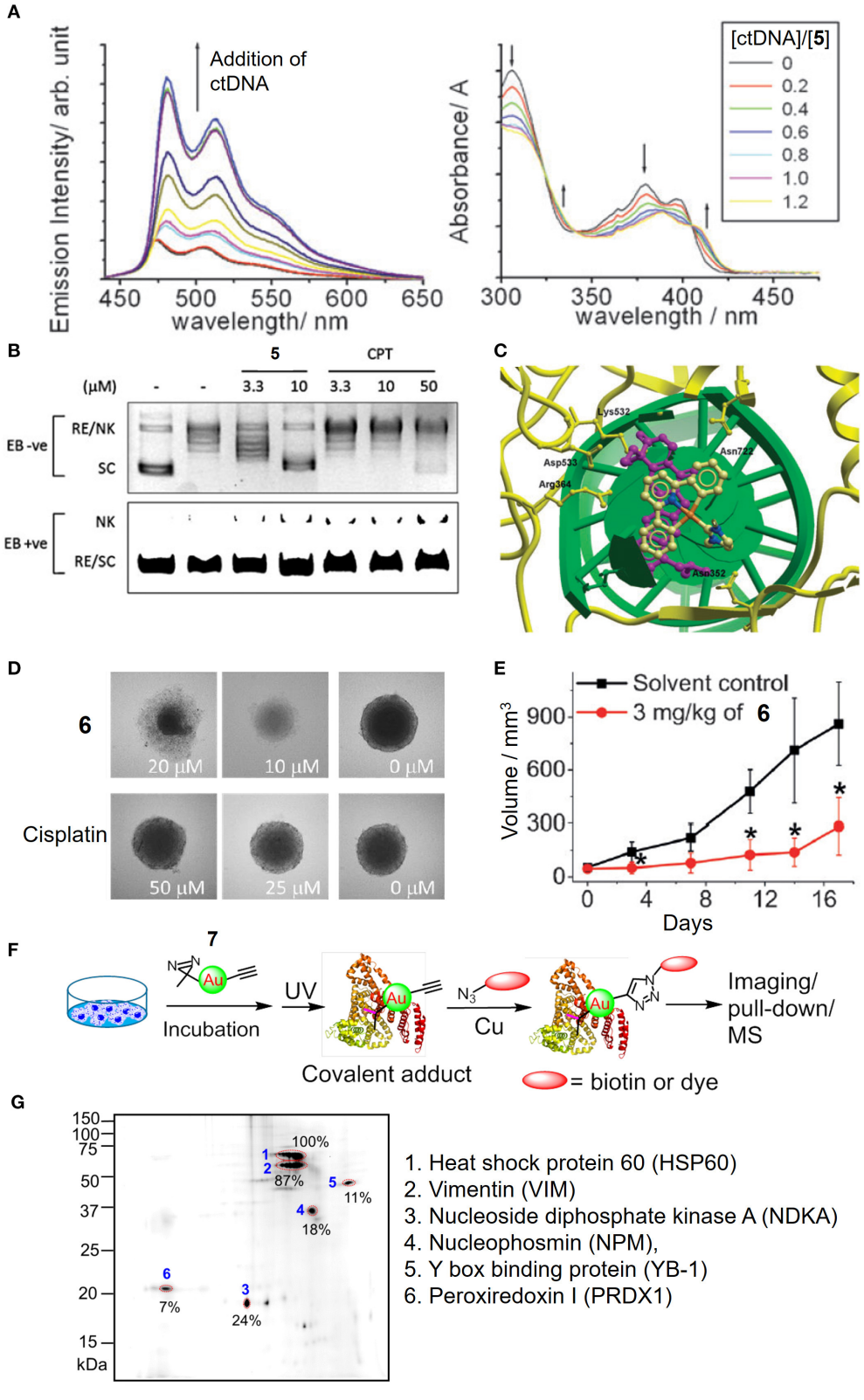

FIGURE 5 | Anticancer properties of cyclometalated gold(III)–NHC complexes. **(A)** Emission (left) and absorption (right) titrations of complex **5** to ctDNA. **(B)** Dose-dependent inhibitory effect of **5** and camptothecin (CPT) on the Topol-mediated DNA relaxation and induction of nicked DNA (EB, ethidium bromide;

(Continued)

FIGURE 5 | RE, relaxed; NK, nicked; SC, supercoiled). **(C)** Molecular modeling of **5** interacting with TopI-DNA (TopoI, yellow ribbon; DNA, green helix). Topotecan (purple) was also superimposed in the docking pose of **5**. **(D)** Images of HeLa cell spheroids after treatment of **6** or cisplatin at different concentrations for 72 h. **(E)** Tumor volume of HeLa xenograft-bearing mice after treatment of **6** for 17 days. **(F)** Schematic procedure of the identification of cellular protein targets of the gold(III)–NHC complex using diazirine-based probe **7**. **(G)** Fluorescence image of 2D gel electrophoresis of protein lysates from **7**-treated HeLa cells. The protein spots were visualized with an azide-Cy5 reporter through click reaction. **(A–C)** Reproduced from Yan et al. (2010) with permission from the Royal Society of Chemistry. **(D–G)** Reprinted with permission from Fung et al. (2017). Copyright 2017, John Wiley and Sons. Data are presented as mean ± SEM (**E**; **6**, $n = 3$; solvent control, $n = 4$; Student's t test; $^*p < 0.05$, compared with solvent control group).

from the conjugate *in cellulo*. This PEGylated conjugate displays a higher selectivity on different cancer cell lines over non-tumorigenic cells. Importantly, *in vivo* experiments have shown that conjugate **3** can significantly inhibit the growth of human colon cancer HCT116 xenografts (**Figure 4G**) or cisplatin-resistant ovarian cancer A2780cis xenografts in nude mouse models. The enhanced permeability and retention effect, which is a pathophysiological characteristic of some solid tumors, presumably promotes the accumulation of the conjugate **3** in tumors rather than in normal organs (**Figure 4H**), leading to low systemic toxicity. Additionally, the self-assembled PEGylated gold(III) porphyrin conjugate can act as a nanocarrier for the co-delivery of chemotherapeutics such as doxorubicin, to achieve a strong synergistic anticancer activity. By harnessing the non-covalent intermolecular interactions (hydrogen-bonding and π-π interactions), a pincer gold(III) complex containing a hydrogen-bonding motif $[Au^{III}(C\hat{}N\hat{}C)(4\text{-dpt})]^+$ (4-dpt = 2,4-diamino-6-(4-pyridyl)-1,3,5-triazine) (**4**) has been demonstrated self-assembling into a supramolecular polymer (**4-SP**) (**Figure 4I**), displaying sustained cytotoxicity with selectivity toward cancerous cells (Zhang et al., 2012). Intriguingly, such superstructures can also encapsulate cytotoxic agents such as complex **1** (**4-SP-Au-1a**) to achieve a sustained-release behavior for anticancer treatment (**Figure 4J**). Furthermore, recently, we have described a hydrogel formulation which forms an interpenetrating network system (IPN) *via* photoinitiated free radical polymerization for the delivery of gold(III) porphyrin **1** (Lee et al., 2019). Compared to free gold porphyrin, **1**-loaded IPN displayed a more effective cell-killing ability, inhibition of tumor growth, and suppression of angiogenesis in mice bearing lung cancer xenografts (**Figures 4K,L**), which are attributable to the controlled release property of the cross-linked hydrogel.

ANTICANCER CYCLOMETALATED GOLD(III) N-HETEROCYCLIC CARBENE COMPLEXES

In addition to the tetradentate porphyrin ligands, stabilization of the gold(III) ion can also be achieved by coordination with the tridentate (C^N^C, C^N^N or N^C^N) pincer ligand containing deprotonated C-donor atom(s) (C^-) and/or neutral σ-donating N-heterocyclic carbene (NHC) ligand(s), affording gold(III) complexes with high physiological stability and promising anticancer properties (Bertrand et al., 2017; Carboni et al., 2018; Bauer et al., 2019; Fares et al., 2020; Guarra et al., 2020). In this context, we have described the antitumor-active $[Au^{III}(C\hat{}N\hat{}C)(NHC)]^+$ ($H_2C\hat{}N\hat{}C$ = 2,6-diphenylpyridine) complexes (**5** and **6**). Complex **5** with a NHC ligand bearing two *N*-methyl substituents exhibits potent cytotoxicity with IC_{50} values at a low micromolar level on different human cancer cell lines and high selectivity by 167-fold lower in IC_{50} values to non-small cell lung carcinoma NCI-H460 relative to normal lung fibroblast CCD-19Lu cells (Yan et al., 2010). Mechanistic studies revealed that **5** interacts with DNA through intercalation (**Figure 5A**) and inhibits the topoisomerase I (TopoI) action on DNA relaxation (**Figures 5B,C**). Moreover, **5** treatment could effectively suppress the *in vivo* tumor growth of hepatocellular carcinoma xenograft model with no signs of toxicity such as body weight loss for a 28-day treatment. By varying the *N*-alkyl substituents on NHC into *N*-butyl groups, complex **6** is able to disintegrate the 3D cancer cells (HeLa) spheroids (**Figure 5D**) and significantly inhibit the tumor growth of cervical and lung carcinomas in two independent mouse models (**Figure 5E**; Fung et al., 2017). By employing a photoaffinity labeling-based chemoproteomics strategy, multiple protein targets have been identified to associate with the anticancer actions of pincer gold(III)–NHC complexes. For the clickable probes (**7** and **8**), the subtle modification of *N*-alkyl substituents on the NHC ligand with the photoaffinity diazirine or benzophenone group did not adversely affect the anticancer activity. Those molecular probes equipped with a photoaffinity group allow the engaged biomolecular targets to be covalently cross-linked with the gold(III)–NHC complex *via* UV light activation while the alkyne moiety functions as a ligation handle with an azido reporter for pull-down (biotin-streptavidin) or a photoluminescent labeling purpose *via* a copper(I)-catalyzed click reaction (**Figure 5F**). The diazirine-based probe **7** can label six (biotinylated) proteins from the two-dimensional protein blot of HeLa cervical cancer cell lysates as revealed by a fluorescent cyanine (azido-Cy5) reporter (**Figure 5G**). Based on tandem mass spectrometric analysis using MALDI-TOF mass spectrometry, the six labeled proteins were identified to be mitochondrial heat shock protein 60 (Hsp60), nucleophosmin (NPM), nucleoside diphosphate kinase A (NDKA), vimentin (VIM), peroxiredoxin I (PRDX1), and nuclease-sensitive element binding protein (Y box binding protein, YB-1), in which all of them are plausible anticancer targets. In contrast, four of which were labeled for probe **8** contained a benzophenone moiety. Based on a series of *in vitro* and cell-based experiments for target validation with unmodified complex **6**, the protein engagement was in line with the downstream biological responses. On the structural basis of molecular binding as revealed by molecular docking and hybrid quantum mechanics/molecular mechanics (QM/MM) studies, π-π interactions involving the pincer $[Au^{III}(C\hat{}N\hat{}C)]^+$ moiety of **6** and aromatic amino acid residues (i.e., Phe, Trp and Tyr) of the proteins were shown. It is worth noting that the analogous

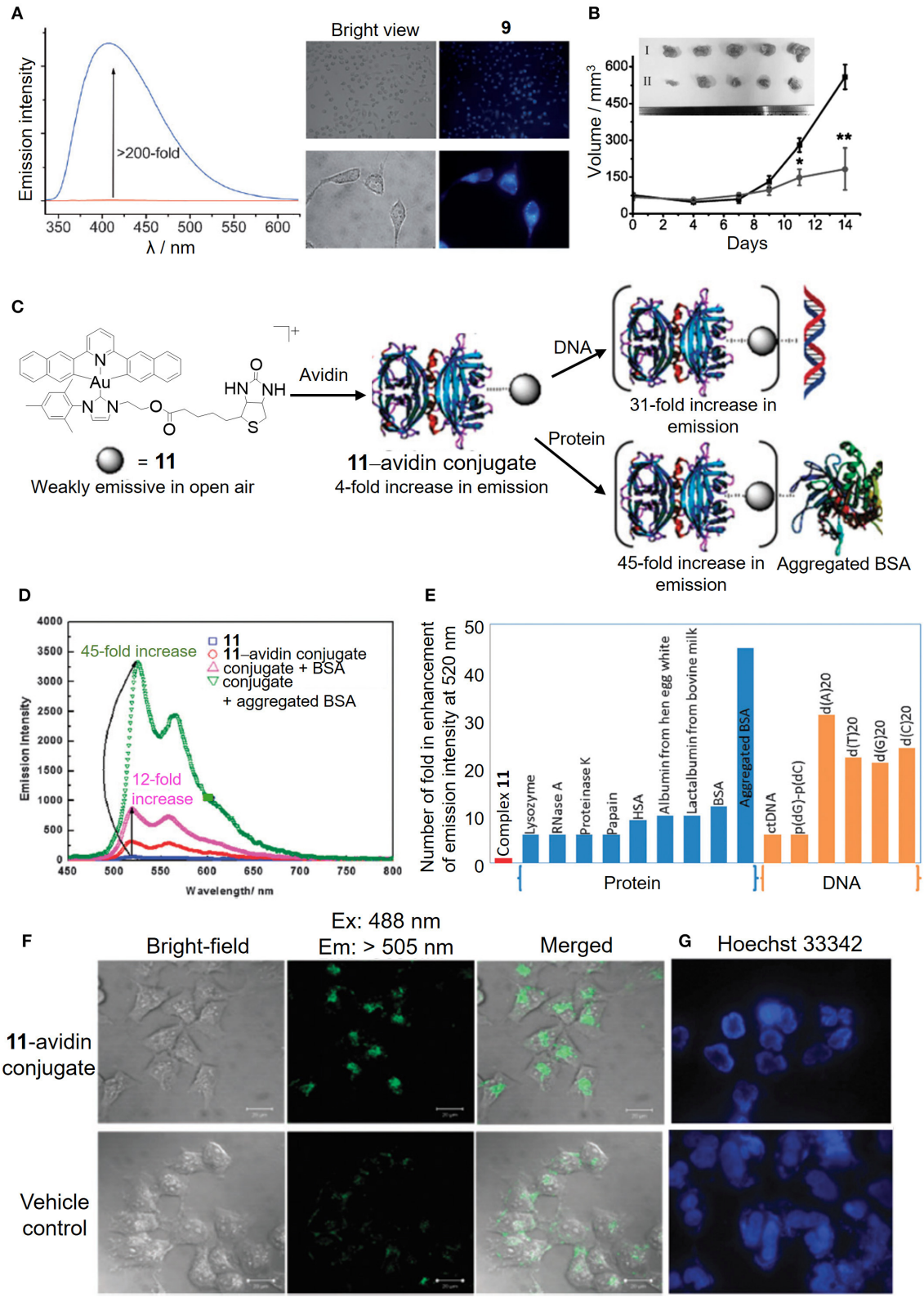

FIGURE 6 | Luminescent properties of cyclometalated gold(III)–NHC complexes for biosensing. **(A)** Fluorescence intensity before (red line) and after (blue line) the addition of GSH to complex **9** in PBS (left). Fluorescence imaging of HeLa cells treated with vehicle control or complex **9** for 10 min (right). **(B)** Tumor volume of HeLa xenograft-bearing mice treated with vehicle control or complex **10** via intratumoral injection for 14 days. [Inset: Photos of tumors for vehicle control (I) and

(Continued)

FIGURE 6 | 10 (3 mg/kg) (II)]. **(C)** Schematic illustration of the bioconjugation of complex **11** bearing a biotin moiety to the avidin forming **11**–avidin conjugate for the biosensing of proteins or DNA. **(D)** Emission enhancement of the **11**–avidin conjugate after the addition of BSA or aggregated BSA. **(E)** Selective molecular sensing of the **11**–avidin conjugate with the single stranded DNA or aggregated BSA. **(F)** Fluorescence imaging of HeLa cells treated with the **11**–avidin conjugate. **(G)** Hoechst 33342 nuclear staining of the apoptotic HeLa cells after treatment with the **11**–avidin conjugate. **(A,B)** Reprinted with permission from Zou et al. (2013). Copyright 2013, John Wiley and Sons. **(C–G)** Reproduced from Tsai et al. (2015) with permission from the Royal Society of Chemistry. Data are presented as mean ± SEM (**B**; $n = 5$; Student's t test; $^{*}p < 0.05$, $^{**}p < 0.01$ compared with vehicle control group).

complexes $[Pt^{II}(C^N^N)(NHC)]^+$, $[Pt^{II}(N^C^N)(NHC)]^+$, and $[Pd^{II}(C^N^N)(NHC)]^+$ possessing similar structural scaffolds compete with the gold(III)–NHC probe **7** for the protein bindings *in cellulo*, implying that the monocationic character and stable orthogonal structure of the pincer-type metal–NHC complexes are crucial parameters for anticancer activities.

LUMINESCENT PROBES FOR BIOSENSING

By judicious choice of the pincer ligands, as exemplified by the strongly fluorescent N^N^N (H_2N^N^N: 2,6-bis(imidazol-2-yl)pyridine [H_2IPI] and 2,6-bis(benzimidazol-2-yl)pyridine [H_2BPB]) pincer ligands, we have developed a number of gold(III)–NHC complexes (**9** and **10**) with a switchable fluorescent property for the detection of cellular thiols (Zou et al., 2013). Owing to the low energy $5d_{x^2-y^2}$ orbital of the gold(III) ion, the gold(III)–NHC complexes are non-emissive in solution. In the presence of physiological thiols, the gold(III) was found to be reduced to gold(I) and accompanied by the release of the fluorescent pincer ligand, and hence gave strong emission enhancement even in live cells as monitored by fluorescence microscopy (**Figure 6A**). The gold(I) species can be stabilized by the coordinated NHC ligand(s) without further reduction and/or demetalation, and delivered to the biomolecular protein target (e.g., thioredoxin reductase) leading to effective *in vivo* antitumor activity (**Figure 6B**).

In addition to the fluorescent property derived from the pincer ligand, we have also taken advantage of the π-extended C-deprotonated C^N^C pincer and strong σ-donating NHC ligands in combination with the biotin–avidin interaction as a bioconjugation strategy to design a luminescent gold(III) NHC–avidin bioconjugate (**Figure 6C**; Tsai et al., 2015). The gold(III)–NHC complex (**11**) is weakly emissive in phosphate buffer with the emission maximum at 520 nm (**Figure 6D**). Functionalization of the NHC ligand with the biotin moiety renders the complex with high affinity for the bioconjugation of avidin. Protected by the protein scaffold, the luminescence quenching of the gold(III)–NHC complex by oxygen is attenuated and even displays significant emission enhancement with selectivity to single-stranded DNA and aggregated bovine serum albumin (**Figure 6E**). Moreover, such bioconjugation allows the luminescent gold(III)–NHC complex to be delivered by the protein carrier into the cytosolic region of cancer cells for anticancer activity (**Figures 6F,G**).

CONCLUSIONS AND FUTURE PERSPECTIVES

Our works have demonstrated the use of porphyrin, pincer cyclometalated and/or N-heterocyclic carbene ligands for the stabilization of the electrophilic gold(III) ion and hence exhibit effective *in vitro* and *in vivo* antitumor activities. These unique lipophilic cations of gold(III) complexes with good stability under physiological conditions described herein display efficient cell penetration properties, a broad spectrum of anticancer activities in different human cancer cell lines, and effective *in vivo* antitumor responses in multiple mouse models. For target identification with the aid of the photoaffinity labeling-based chemoproteomics and cellular thermal shift proteomes, the anticancer gold(III) complexes consisting of the exposed gold(III) ion and a coordinated ligand scaffold are demonstrated to engage a number of anticancer molecular targets in association with expected downstream consequences of cancer suppression. Conceivably, these integrated approaches advance the understanding of the anticancer actions of gold(III) complexes, allowing for further structural optimization for targeted anticancer therapy. Taking advantage of the nanotechnology-based delivery system, the formulations of gold(III) complexes exhibit effective *in vivo* antitumor efficacies and improved biodistribution profiles, as well as ameliorate the systemic toxicity in mice caused by the free compounds. In addition, the resulting amphiphilic gold(III) complexes can self-assemble as drug carriers for the co-delivery of anticancer drugs to achieve synergistic therapy. It is envisaged that tumor targeting strategies through chemical modification can be adopted for the tumor-specific delivery of anticancer gold(III) complexes.

AUTHOR CONTRIBUTIONS

K-CT, DH, and P-KW wrote the article. C-NL and C-MC revised and edited the manuscript. All authors contributed to the article and approved the submitted version.

ACKNOWLEDGMENTS

The authors acknowledge the Innovation and Technology Fund (ITS/130/14FP and ITS/488/18) and funding support from Laboratory for Synthetic Chemistry and Chemical Biology under the Health@InnoHK Program launched by Innovation and Technology Commission of The Hong Kong SAR Government on the research in Anticancer Metal Medicines.

REFERENCES

Bauer, E. B., Bernd, M. A., Schutz, M., Oberkofler, J., Pothig, A., Reich, R. M., et al. (2019). Synthesis, characterization, and biological studies of multidentate gold(I) and gold(III) NHC complexes. *Dalton Trans.* 48, 16615–16625. doi: 10.1039/C9DT03183A

Bertrand, B., Fernandez-Cestau, J., Angulo, J., Cominetti, M. M. D., Waller, Z. A. E., Searcey, M., et al. (2017). Cytotoxicity of pyrazine-based cyclometalated (C^N(pz)^C)Au(III) carbene complexes: impact of the nature of the ancillary ligand on the biological properties. *Inorg. Chem.* 56, 5728–5740. doi: 10.1021/acs.inorgchem.7b00339

Carboni, S., Zucca, A., Stoccoro, S., Maiore, L., Arca, M., Ortu, F., et al. (2018). New variations on the theme of gold(III) C^N^N Cyclometalated complexes as anticancer agents: synthesis and biological characterization. *Inorg. Chem.* 57, 14852–14865. doi: 10.1021/acs.inorgchem.8b02604

Che, C.-M., Sun, R. W., Yu, W. Y., Ko, C.-B., Zhu, N. Y., and Sun, H. Z. (2003). Gold(III) porphyrins as a new class of anticancer drugs: cytotoxicity, DNA binding and induction of apoptosis in human cervix epitheloid cancer cells. *Chem. Commun.* 1718–1719. doi: 10.1039/b303294a

Chung, C. Y., Fung, S.-K., Tong, K.-C., Wan, P.-K., Lok, C.-N., Huang, Y., et al. (2017). A multi-functional PEGylated gold(III) compound: potent anti-cancer properties and self-assembly into nanostructures for drug co-delivery. *Chem. Sci.* 8, 1942–1953. doi: 10.1039/C6SC03210A

Fares, M., Wu, X., Ramesh, D., Lewis, W., Keller, P. A., Howe, E. N. W., et al. (2020). Stimuli-responsive cycloaurated "off-on" switchable anion transporters. *Angew. Chem. Int. Ed. Engl.* 59, 2–10. doi: 10.1002/anie.202006392

Fung, S.-K., Zou, T. T., Cao, B., Lee, P.-Y., Fung, Y. M. E., Hu, D., et al. (2017). Cyclometalated gold(III) complexes containing N-heterocyclic carbene ligands engage multiple anti-cancer molecular targets. *Angew. Chem. Int. Ed. Engl.* 56, 3892–3896. doi: 10.1002/anie.201612583

Galluzzi, L., Senovilla, L., Vitale, I., Michels, J., Martins, I., Kepp, O., et al. (2012). Molecular mechanisms of cisplatin resistance. *Oncogene* 31, 1869–1883. doi: 10.1038/onc.2011.384

Guarra, F., Terenzi, A., Pirker, C., Passannante, R., Baier, D., Zangrando, E., et al. (2020). (124) I radiolabeling of a Au(III) - NHC complex for *in vivo* biodistribution studies. *Angew. Chem. Int. Ed. Engl.* 59, 2–9. doi: 10.1002/anie.202008046

Harris, J. M., and Chess, R. B. (2003). Effect of pegylation on pharmaceuticals. *Nat. Rev. Drug Discov.* 2, 214–221. doi: 10.1038/nrd1033

He, L., Chen, T., You, Y., Hu, H., Zheng, W., Kwong, W. L., et al. (2014). A cancer-targeted nanosystem for delivery of gold(III) complexes: enhanced selectivity and apoptosis-inducing efficacy of a gold(III) porphyrin complex. *Angew. Chem. Int. Ed. Engl.* 53, 12532–12536. doi: 10.1002/anie.201407143

Hill, H. A., and Sadler, P. J. (2016). Bringing inorganic chemistry to life with inspiration from R. J. P. Williams. *J. Biol. Inorg. Chem.* 21, 5–12. doi: 10.1007/s00775-016-1333-3

Hu, D., Liu, Y., Lai, Y.-T., Tong, K.-C., Fung, Y. M., Lok, C.-N., et al. (2016). Anticancer gold(III) porphyrins target mitochondrial chaperone hsp60. *Angew. Chem. Int. Ed. Engl.* 55, 1387–1391. doi: 10.1002/anie.201509612

Jung, Y., and Lippard, S. J. (2007). Direct cellular responses to platinum-induced DNA damage. *Chem. Rev.* 107, 1387–1407. doi: 10.1021/cr068207j

Kelland, L. (2007). The resurgence of platinum-based cancer chemotherapy. *Nat. Rev. Cancer* 7, 573–584. doi: 10.1038/nrc2167

Knop, K., Hoogenboom, R., Fischer, D., and Schubert, U. S. (2010). Poly(ethylene glycol) in drug delivery: pros and cons as well as potential alternatives. *Angew. Chem. Int. Ed. Engl.* 49, 6288–6308. doi: 10.1002/anie.200902672

Lammer, A. D., Cook, M. E., and Sessler, J. L. (2015). Synthesis and anti-cancer activities of a water soluble gold(III) porphyrin. *J. Porphyr. Phthalocyanines* 19, 398–403. doi: 10.1142/S1088424615500236

Lee, P.-Y., Lok, C.-N., Che, C.-M., and Kao, W. J. (2019). A multifunctional hydrogel delivers gold compound and inhibits human lung cancer xenograft. *Pharm. Res.* 36, 61. doi: 10.1007/s11095-019-2581-z

Lee, P.-Y., Zhang, R., Li, V., Liu, X., Sun, R. W., Che, C.-M., et al. (2012). Enhancement of anticancer efficacy using modified lipophilic nanoparticle drug encapsulation. *Int. J. Nanomedicine* 7, 731–737. doi: 10.2147/IJN.S28783

Lum, C.-T., Huo, L., Sun, R. W., Li, M., Kung, H.-F., Che, C.-M., et al. (2011). Gold(III) porphyrin 1a prolongs the survival of melanoma-bearing mice and inhibits angiogenesis. *Acta Oncol.* 50, 719–726. doi: 10.3109/0284186X.2010.537693

Lum, C.-T., Liu, X., Sun, R. W., Li, X. P., Peng, Y., He, M. L., et al. (2010). Gold(III) porphyrin 1a inhibited nasopharyngeal carcinoma metastasis *in vivo* and inhibited cell migration and invasion *in vitro*. *Cancer Lett.* 294, 159–166. doi: 10.1016/j.canlet.2010.01.033

Lum, C.-T., Sun, R. W., Zou, T. T., and Che, C.-M. (2014). Gold(III) complexes inhibit growth of cisplatin-resistant ovarian cancer in association with upregulation of proapoptotic PMS2 gene. *Chem. Sci.* 5, 1579–1584. doi: 10.1039/c3sc53203h

Lum, C.-T., Wong, A. S., Lin, M. C., Che, C.-M., and Sun, R. W. (2013). A gold(III) porphyrin complex as an anti-cancer candidate to inhibit growth of cancer-stem cells. *Chem. Commun.* 49, 4364–4366. doi: 10.1039/C2CC37366A

Rabik, C. A., and Dolan, M. E. (2007). Molecular mechanisms of resistance and toxicity associated with platinating agents. *Cancer Treat. Rev.* 33, 9–23. doi: 10.1016/j.ctrv.2006.09.006

Sun, R. W., Li, C. K., Ma, D.-L., Yan, J. J., Lok, C.-N., Leung, C.-H., et al. (2010). Stable anticancer gold(III)-porphyrin complexes: effects of porphyrin structure. *Chem. Eur. J.* 16, 3097–3113. doi: 10.1002/chem.200902741

To, Y. F., Sun, R. W., Chen, Y., Chan, V. S., Yu, W. Y., Tam, P. K., et al. (2009). Gold(III) porphyrin complex is more potent than cisplatin in inhibiting growth of nasopharyngeal carcinoma *in vitro* and *in vivo*. *Int. J. Cancer* 124, 1971–1979. doi: 10.1002/ijc.24130

Tong, K.-C., Lok, C.-N., Wan, P.-K., Hu, D., Fung, Y. M. E., Chang, X.-Y., et al. (2020). An anticancer gold(III)-activated porphyrin scaffold that covalently modifies protein cysteine thiols. *Proc. Natl. Acad. Sci. U.S.A.* 117, 1321–1329. doi: 10.1073/pnas.1915202117

Toubia, I., Nguyen, C., Diring, S., Ali, L. M. A., Larue, L., Aoun, R., et al. (2019). Synthesis and anticancer activity of gold porphyrin linked to malonate diamine platinum complexes. *Inorg. Chem.* 58, 12395–12406. doi: 10.1021/acs.inorgchem.9b01981

Tsai, J. L., Chan, A. O., and Che, C.-M. (2015). A luminescent cyclometalated gold(iii)-avidin conjugate with a long-lived emissive excited state that binds to proteins and DNA and possesses anti-proliferation capacity. *Chem. Commun.* 51, 8547–8550. doi: 10.1039/C5CC00186B

Tu, S., Sun, R. W., Lin, M. C., Cui, J. T., Zou, B., Gu, Q., et al. (2009). Gold (III) porphyrin complexes induce apoptosis and cell cycle arrest and inhibit tumor growth in colon cancer. *Cancer* 115, 4459–4469. doi: 10.1002/cncr.24514

Wang, Y., He, Q. Y., Sun, R. W., Che, C.-M., and Chiu, J.-F. (2005). Gold(III) porphyrin 1a induced apoptosis by mitochondrial death pathways related to reactive oxygen species. *Cancer Res.* 65, 11553–11564. doi: 10.1158/0008-5472.CAN-05-2867

Wang, Y., He, Q. Y., Sun, R. W., Che, C.-M., and Chiu, J.-F. (2007). Cellular pharmacological properties of gold(III) porphyrin 1a, a potential anticancer drug lead. *Eur. J. Pharmacol.* 554, 113–122. doi: 10.1016/j.ejphar.2006.10.034

Yan, J. J., Chow, A. L., Leung, C.-H., Sun, R. W., Ma, D.-L., and Che, C.-M. (2010). Cyclometalated gold(III) complexes with N-heterocyclic carbene ligands as topoisomerase I poisons. *Chem. Commun.* 46, 3893–3895. doi: 10.1039/c001216e

Zhang, J. J., Lu, W., Sun, R. W., and Che, C.-M. (2012). Organogold(III) supramolecular polymers for anticancer treatment. *Angew. Chem. Int. Ed. Engl.* 51, 4882–4886. doi: 10.1002/anie.201108466

Zou, T. T., Lum, C.-T., Chui, S. S., and Che, C.-M. (2013). Gold(III) complexes containing N-heterocyclic carbene ligands: thiol "switch-on" fluorescent probes and anti-cancer agents. *Angew. Chem. Int. Ed. Engl.* 52, 2930–2933. doi: 10.1002/anie.201209787

Conflict of Interest: The authors declare that the research was conducted in the absence of any commercial or financial relationships that could be construed as a potential conflict of interest.

frontiers in Chemistry

ORIGINAL RESEARCH
published: 11 January 2021
doi: 10.3389/fchem.2020.602845

Multi-Targeted Anticancer Activity of Imidazolate Phosphane Gold(I) Compounds by Inhibition of DHFR and TrxR in Breast Cancer Cells

Rossana Galassi[1], Lorenzo Luciani[1], Valentina Gambini[2], Silvia Vincenzetti[2], Giulio Lupidi[3], Augusto Amici[2], Cristina Marchini[2], Junbiao Wang[2] and Stefania Pucciarelli[2]*

[1] School of Science and Technology, University of Camerino, Camerino, Italy, [2] School of Biosciences and Veterinary Medicine, University of Camerino, Camerino, Italy, [3] School of Drugs and Health Products Sciences, University of Camerino, Camerino, Italy

A class of phosphane gold(I) compounds, made of azoles and phosphane ligands, was evaluated for a screening on the regards of Breast Cancer cell panels (BC). The compounds possess N-Au-P or Cl-Au-P bonds around the central metal, and they differ for the presence of aprotic or protic polar groups in the azoles and/or the phosphane moieties to tune their hydrophilicity. Among the six candidates, only the compounds having the P-Au-N environment and not displaying neither the hydroxyl nor carboxyl groups in the ligands were found active. The compounds were screened by MTT tests in SKBR3, A17, and MDA-MB231 cancer cells, and two compounds (namely the 4,5-dicyano-imidazolate-1yl-gold(I)-(triphenylphosphane, 5, and 4,5-dichloro-imidazolate-1yl-gold(I)-triphenylphosphane, 6) were found very cytotoxic, with the most active with an IC_{50} value of 3.46 μM in MDA-MB231 cells. By performing enzymatic assays in the treated cells lysates, the residual enzymatic activity of dihydrofolate reductase (DHFR) has been measured after cell treatment for 4 or 12 h in comparison with control cells. Upon 12 h of treatment, the activity of DHFR was significantly reduced in both SKBR3 and A17 cells by compounds 5 and 6, but not in human MDA-MB231 cells; interestingly, it was found remarkably high after 4 h of treatment, revealing a time dependence for the DHFR enzymatic assays. The DHFR inhibition data have been compared to those for the thioredoxin reductase (TrxR), the most recognized molecular target for gold compounds. For this latter, similar residual activities (i.e., 37 and 49% for the match of SKBR3 cells and compound 5 or 6, respectively) were found. Binding studies on the regards of ct-DNA (calf-thymus-DNA) and of plasma transporters proteins, such as BSA (bovine serum albumin) and ATF (apo transferrin), were performed. As expected for gold compounds, the data support strong binding to proteins (K_{SV} values range: $1.51 \div 2.46 \times 10^4$ M^{-1}) and a weaker interaction with ct-DNA's minor groove (K_{SV} values range: $1.55 \div 6.12 \times 10^3$ M^{-1}).

Keywords: gold, enzyme inhibition, anticancer agents, metal based drug, gold phosphane compounds, DiHydroFolateReductase, thioredoxinReductase, breast cancer

OPEN ACCESS

Edited by:
Lara Massai,
University of Florence, Italy

Reviewed by:
Clemens Zwergel,
Sapienza University of Rome, Italy
Damiano Cirri,
University of Pisa, Italy

****Correspondence:***
Rossana Galassi
rossana.galassi@unicam.it

Specialty section:
This article was submitted to Medicinal and Pharmaceutical Chemistry, a section of the journal Frontiers in Chemistry

Received: *04 September 2020*
Accepted: *09 December 2020*
Published: *11 January 2021*

Citation:
Galassi R, Luciani L, Gambini V, Vincenzetti S, Lupidi G, Amici A, Marchini C, Wang J and Pucciarelli S (2021) Multi-Targeted Anticancer Activity of Imidazolate Phosphane Gold(I) Compounds by Inhibition of DHFR and TrxR in Breast Cancer Cells. Front. Chem. 8:602845. doi: 10.3389/fchem.2020.602845

INTRODUCTION

Breast Cancer (BC) is the second most frequent cancer worldwide and, by far, the most recurrent cancer among the female gender with the esteem of 2.1 million new cases detected in 2018 (25% of all cancers) (Bray et al., 2018). The term breast cancer expresses not a single disease but it includes four major molecular subtypes (Luminal A, Luminal B, HER2-positive and Basal Like Breast Cancer, BLBC), whose classification is based on the expression of hormone receptors (estrogen receptors (ER), and progesterone receptors (PR)) and Human Epidermal growth factor Receptor 2 (HER2) (Burstein, 2005). Optimal therapy for each patient depends on the tumor subtype. Luminal A (ER-positive (+) and PR+) and Luminal B (ER+, PR+ and HER2+) may benefit from endocrine therapy. HER2 overexpression is associated with poor prognosis, but HER2+ BC patients can be treated with HER2-targeted therapies, such as the monoclonal antibodies trastuzumab and pertuzumab, the antibody-drug conjugate trastuzumab emtansine (T-DM1), and the tyrosine kinase inhibitor lapatinib, alone or in combination with chemotherapy (see **Table 1**). These targeted treatments improve patient overall survival but drug resistance mechanisms often compromise their long-term effectiveness and most patients eventually relapse. Among BC subtypes, BLBC is the most aggressive. No targeted therapies are currently available for BLBC as it lacks the expression of both hormone receptors and HER2 (Yao et al., 2016; Waks and Winer, 2019). Thus, BLBC is treated with a combination of surgery, radiotherapy and chemotherapy (Schwentner et al., 2012; Nakai et al., 2016; Zheng et al., 2018), that is often not successful against metastatic BLBC. BC chemotherapy consists of a mixture of drugs (Fisher et al., 1990) that includes metal based compounds such as carboplatin or analogs (Silver et al., 2010), and alkaloids, such as taxanes (Waks and Winer, 2019). All these anticancer drugs are very effective but the intervention of serious side effects and/or the high incidence of drug resistance phenomena triggers the research of new medications (Correia et al., 2018).

As concern the metal based drugs, in alternative to platin(II) compounds a large variety of gold(I) (Nobili et al., 2010; Berners-Price and Filipovska, 2011; Bertrand and Casini, 2014) and gold(III) compounds (Nobili et al., 2010; Che and Sun, 2011; da Silva Maia et al., 2014; Zou et al., 2015) have been considered; the attention on phosphane gold(I) compounds takes its origin from a renewed interest in Auranofin, an old antirheumatic drug made of an apolar head of triethylphosphane and a tetraacetyl-thiosugar polar tail, discovered to be a potent anticancer agent mainly acting by the inhibition of ThioRedoxin Reductase enzyme (TrxR) (Cui et al., 2020; Raninga et al., 2020). In general, lipophilic phosphane gold(I) compounds are characterized by remarkable antiproliferative properties (Kim et al., 2019), optimal cellular uptake depending on the molecule hydro/lipophilic balance (McKeage et al., 2000; Liu et al., 2008; Scheffler et al., 2010) and protein binding (Messori et al., 2014; Kim et al., 2019), on the other hand, water soluble highly hydrophilic phosphane metal compounds showed appreciable cytotoxic activity on the regard of MCF-7 BC cells (Santini et al., 2011). Recently, our group has found that azolate/phosphane gold(I) compounds are active on the regards of many panels of cancer lines (Galassi et al., 2012) and they also inhibit TrxR, with Ki in the nanomolar range. The azolate/phosphane gold(I) compounds retain their activity

TABLE 1 | Current therapeutic approaches to BC subtypes (adapted from Waks and Winer, 2019).

Breast cancer receptor subtype	Therapeutic approach		Additional notes
	First line	Later lines of therapy	
Hormone receptor positive (HR+) and *ERBB2*-	Aromatase inhibitor plus CDK4/6 inhibitora ORR = 53–59%	Hormonal and/or targeted therapy If resistant to multiple lines of hormonal therapy, transition to single-agent chemotherapy.	Premenopausal patients with HR+ metastatic BC should undergo treatment to achieve hormonal and/or targeted therapy or surgical menopause.
ERBB2+	Taxane + trastuzumab + pertuzumab ORR° = 80% Selected patients with HR+/*ERBB2*+ disease can receive endocrine therapy plus *ERBB2*-targeted therapy	ERBB2-targeted agent plus chemotherapy or endocrine therapy if HR+ Trastuzumab + chemotherapy Trastuzumab + endocrine therapy Lapatinib + capecitabine	Very common brain metastases may be treated with both local and systemic therapies.
Triple-negative	Single-agent chemotherapy Taxane ORR = 36% Platinum ORR rate = 31% Anthracycline	Single-agent chemotherapy* Capecitabine Eribulin Vinorelbine Gemcitabine Olaparib or talazoparib (if germline *BRCA1/2* mutation)	There is no single recommended first-line chemotherapy regimen.

°*ORR, overall response rate.* **Other agents not administered in initial lines are also acceptable options.*

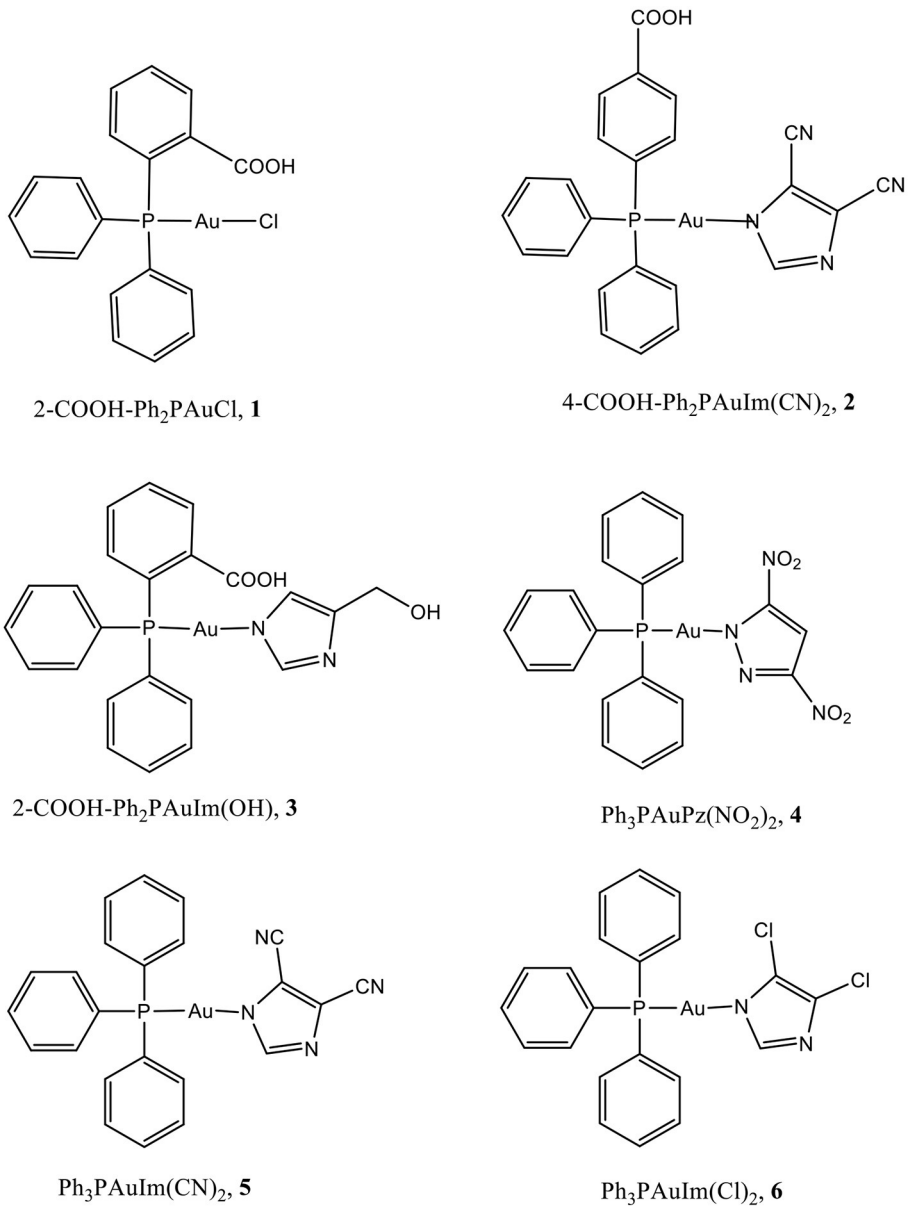

SCHEME 1 | Sketch of the molecular structures considered in this work.

also *in vivo*, and two compounds 4,5-dicyano-imidazolate-1yl-gold(I)-(triphenylphosphane) or 4,5-dichloro-imidazolate-1yl-gold(I)-(triphenylphosphane), were found to contrast BLBC tumors transplanted in syngeneic mice; these compounds were found much more active than cisplatin, one of the most used metal based chemotherapy applied in BC, displaying fewer side effects and being in general more tolerated by the mice (Gambini et al., 2018). By considering these promising findings and as prosecution of this work, some of the previously characterized gold(I) compounds and additional new compounds were used in the present study (**Scheme 1**). In particular, all the compounds contain the N-Au-P bonds, leaving apart compound **1** which contains P-Au-Cl bonds; in addition, compounds **2** and **3** contain hydrophilic groups such as OH or COOH in the azoles and/or phosphane groups to evaluate whether the presence of polar, protic groups in the molecular structure affects the cytotoxic activity in different BC cell lines (Santini et al., 2011); compound **4** contains a different 3,5-disubstituted polar azole, the 3,5-dinitropyrazolate, and compounds **5** and **6** are the ones already studied and resulted to be effective as anticancer drugs *in vivo* (Gambini et al., 2018).

All these compounds were first screened by MTT assay in human SKBR3 cells, representing an HER2-positive BC model. The most effective ones were then tested on both

human MDA-MB-231 cells and murine A17 cells, representing BLBC models (Galiè et al., 2005, 2008; Marchini et al., 2010; Bisaro et al., 2012). To shed light on molecular mechanisms underlying the anticancer effects of the selected azole/phosphane gold(I) complexes and to identify new targeted molecules, their inhibitory action on the key cell enzyme dihydrofolate reductase (DHFR) was evaluated using thioredoxin reductase (TrxR) as a reference target. DHFR and TrxR are two enzymes involved in unrelated metabolic pathways, both crucial for cancer cell's growth and survival. They are both overexpressed in tumor cells, and potential molecular target of chemotherapeutic drugs, such as antifolates for DHFR (e.g., methotrexate) (Raimondi et al., 2019), and alkylating agents selectively modifying the selenocysteine (Sec) residue for TrxR (Urig and Becker, 2006). Indeed, TrxR enzyme family has represented an optimal candidate for gold anticancer drugs, based on the strong affinity of the gold atom to thiols, making the nucleophilic selenolate of reduced TrxR the main target site of modification by this metal compounds. Thioredoxin reductase can thus be considered the reference target of gold-based anticancer drugs (Bindoli et al., 2009). Conversely, DHFR does not have selenocysteine residues, and the available thiol groups do belong to cysteines, which are not involved in the catalytic site. Nevertheless, in previous studies we have reported the inhibition of *E. coli* DHFR by gold(I) phosphane complexes with Ki values in the micromolar range (Galassi et al., 2015). Furthermore, supported by thermodynamic analysis, we have ascertained alternative non-covalent mechanisms, by which polyphosphane gold(I) complexes can modify the catalytic behavior of the molecular target without cysteines or selenocysteines modification as in the case of DHFR (Gambini et al., 2018). In this work, we found that phosphane gold(I) complexes can target dihydrofolate reductase by strongly inhibiting its enzymatic activity. In addition, to acquire additional information about the fate of the most active azole/phosphane gold(I) compounds once in contact with serum proteins, targeted spectrophotometric tests were led on BSA (bovine serum albumin) and ATF (apo transferrin): while BSA was already ascertained to bind gold moieties, the ATF, which is a plasmatic protein for iron ions transport, was never taken into account for gold compounds transport. Finally, DNA is not a preferential binding site for gold compounds, hence, to rule out any unusual interaction between some selected gold compounds and calf thymus DNA, spectroscopic studies have been addressed to this last issue. The experimental plan of this work, schematically represented in **Figure 1**, provides a set of results decisive for an overall assessment of multitarget mechanisms of action for the azolate/phophane gold compounds herein considered, contextually to the confirmation of their strong cytotoxic activity against aggressive BC subtypes.

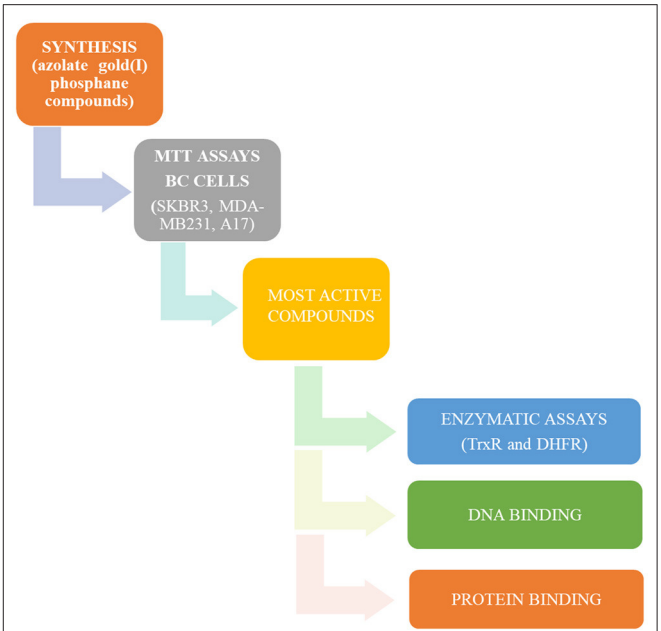

FIGURE 1 | Flow diagram of the experimental plan of this work.

MATERIALS AND METHODS

Syntheses and Characterization

Elemental analyses (C, H, N, S) were performed in-house with a Fisons Instruments 1,108 CHNS-O Elemental Analyser. Melting points were taken on an SMP3 Stuart Scientific Instrument. IR spectra were recorded from 4,000 to 600 cm^{-1} with a Perkin-Elmer SPECTRUM ONE System FT-IR instrument. IR annotations used: br = broad, m = medium, s = strong, sh = shoulder, vs = very strong, w = weak and vw = very weak. ^{1}H and ^{31}P NMR spectra were recorded on an Oxford-400 Varian spectrometer (400.4 MHz for ^{1}H and 162.1 MHz for ^{31}P). Chemical shifts, in ppm, for ^{1}H NMR spectra are relative to internal Me_4Si. ^{31}P NMR chemical shifts were referenced to a 85% H_3PO_4 standard. The ^{31}P NMR spectroscopic data were accumulated with ^{1}H decoupling. NMR annotations used: br = broad, d = doublet, dd = double doublet, t = triplet, m = multiplet, s = singlet. Chemicals were purchased from Merck and used without further purification. Electrospray mass spectra (ESI-MS) were obtained in positive- or negative-ion mode on a Series 1,100 MSD detector HP spectrometer, using an acetonitrile or methanol mobile phase. The compounds were added to reagent grade acetonitrile to give solutions of approximate concentration 0.1 mM. These solutions were injected (1 μl) into the spectrometer via a HPLC HP 1090 Series II fitted with an auto-sampler. The pump delivered the solutions to the mass spectrometer source at a flow rate of 300 μl min^{-1}, and nitrogen was employed both as a drying and nebulizing gas. Capillary voltages were typically 4,000 and 3,500 V for the positive- and negative-ion mode, respectively. Confirmation of all major species in this ESI-MS study was aided by comparison of the observed and predicted isotope distribution patterns, the latter calculated using the IsoPro 3.0 computer program. The used solvents were HPLC grade and they were used as purchased, unless water and oxygen sensitive reactions were led. Anhydrous and radical free THF was obtained by treating the solvent with

Na/acetophenone under N_2 atmosphere, while other solvents were used as purchased without any additional puification. The azoles, the triphenylphosphane, the 2-diphenylphosphine benzoic acid, and the 4-diphenylphosphine benzoic acid were purchased from Merck and dried under vacuum prior to the use. A foil of metal gold was purchased from Merck and used to synthesize tetrachloridegold(I) acid by dissolving the gold chop by boiling aqua regia and by the careful evaporation of water till almost to dryness. The compound Ph_3PAuCl was prepared by the reduction of tetrachloridegold(I) acid with a double molar amount of PPh_3 in ethyl alcohol (Bruce et al., 2007). Compound **1** and compound 4-diphenylphosphine benzoic acid gold(I) chloride were synthesized according to the procedure published in Galassi et al. (2015). The sodium 3,5-dinitropyrazolate was synthesized according to a procedure reported in Galassi et al. (2013). The crystalline samples were characterized according to elemental analysis, IR, melting points, ^1H and ^{31}P NMR spectroscopies, ESI mass spectrometry and the results were compared to previously reported data. The syntheses of compounds **3, 4, 5** and **6** are following reported.

Synthesis of compound **3**, [(4-hydroxy-methyl)imidazolyl-1H-gold(I)-(2-benzoic-diphenylphosphane acid)]

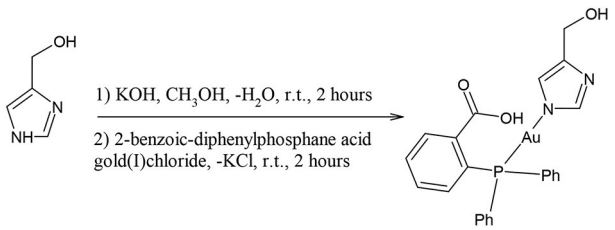

50 milligrams of solid 4-hydromethyl-imidazole (0.5 mmol) were dissolved in 5 mL of CH_3OH. To this solution 0.5 mL of a 1 M CH_3OH solution of KOH (0.5 mmol) were added. After an hour of magnetic stirring at room temperature, 12 mL of a methanol solution containing 275 mgs of compound 1 were added (0.5 mmol). The suspension was stirred for 2 h, concentrated to half volume, and then filtered off over a celite bed. The clear solution was concentrated to 10 mL and let to evaporate till a microcrystalline solid was obtained. Yield 63%. M. p. 195–197°C.

^1H-NMR (CD_3OD, δ): 8.11 (m, br 1H); 7.83 (s, 1H), 7.62–7.47 (m, 10H), 7.45 (m, 1H), 7.21 (s, 1H), 7.37 (s, 1H) 6.86 (m, 1H), 4.62 (br, 1H), 4.55 (s, 2H).

^{31}P-NMR (CD_3OD, δ): 31.57 (s).

MIR (cm^{-1}): 3,226 (m), 3,123 (m, br), 3,055 (m, br), 2,855 (m, br), 1,631 (m), 1,597 (s), 1,579 (s), 1,562 (sh), 1,557 (s), 1,480 (m), 1,435 (m), 1,371 (s), 1,280 (m), 1,257 (w), 1,241 (m), 1,206 (w), 1,158 (w), 1,101 (s), 1,063 (m), 1,019 (m), 982 (m), 937 (m), 879 (m), 830(m), 747 (s), 711 (s), 692 (vs) FIR (cm^{-1}): 654 (m), 619 (m), 549 (m), 512 (m, Au-N) 500 (m), 434 (m), 393 (m), 286 (w, Au-P), 227 (w).

ESI (–) (CH_3OH, m/z): 493 (100), 537 (50), 599 (20) [(2-COO-Ph_2P)Au + 4-CH_2OH-Im]$^-$. ESI (+) (CH_3OH, m/z): 809 (5) [(2-COOH-Ph_2P)$_2$Au]$^+$; 600 (100) [(2-COOH-Ph_2P)Au + 4-CH_2OH-Im + H]$^+$.

Elemental analysis for $C_{23}H_{20}AuN_2O_3P$, calcd %: C 46.01, H 3.36, N 4.67. Found C 46.36, H 3.71, N 4.99.

Synthesis of compound **4**, [(3,5-dintropyrazolyl-1H-gold(I)-(triphenylphosphane)]

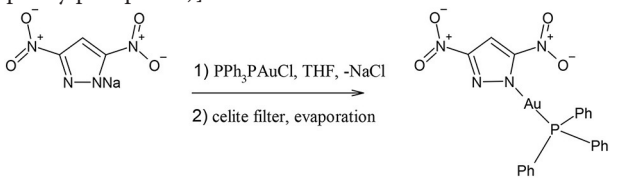

0.090 g of solid sodium 3,5-dinitropyrazolate (0.5 mmol) were added to 5 mL of THF. To this pale yellow suspension, solid PPh_3PAuCl was added (0.5 mmol). The suspension was stirred for 3 h, and then filtered off over a celite bed. The celite was washed with 2 mL of THF (3 times) and the clear solution was concentrated to 5 mL. By slow evaporation a microcrystalline solid was obtained. Yield 71%. M. p. 161–163°C.

^1H-NMR (CD_3OD, δ): 8.21 (m, br 1H); 7.72–7.41 (m, 15H).

^{31}P-NMR (CD_3OD, δ): 31.20 (s).

MIR (cm^{-1}): 3,168 w, 3,054 w, 3,030 w, 1,677 w, 1,585 w, 1,543 m, 1,480 vs, 1,451 s, 1,435 vs, 1,362 vs, 1,326 vs, 1,293 s, 1,181 s, 1,100 vs, 1,066 m, 1,046 m, 1,025 m, 995 m, 923 w, 832 s, 812 s, 740 vs, 711 s, 679 vs.

ESI (+) (CH_3OH) m/z %: 538.3 (31) [$AuPPh_3$]$^+$, 721.3 (100) [$Au(PPh_3)_2$]$^+$

Elemental analysis for $C_{23}H_{20}AuN_2O_3P$, calcd %: C 46.01, H 3.36, N 4.67. Found C 46.40, H 3.1, N 4.41.

Synthesis of compound **5**, [(3,5-dicyanoimdazolyl-1H-gold(I)-(triphenylphosphane)]

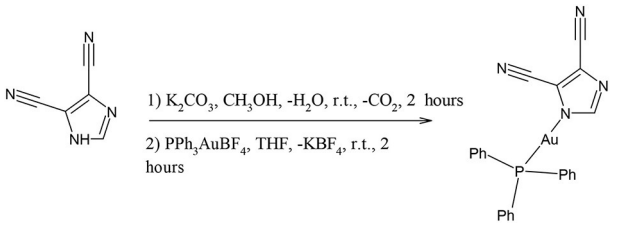

0.050 g of 4,5-dicyanoimidazole (0.423 mmol) was dissolved in 4 mL of methanol. To this solution, K_2CO_3 (0.059 g; 0.423 mmol) dissolved in few drops of water was added. The colorless solution was stirred overnight and added to a 4 mL of freshly prepared Ph_3PAuBF_4 in THF solution (0.423 mmol, the THF solution of Ph_3PAuBF_4 is prepared by adding a 1:1 mole ratio ammount of AgBF4 and by filtering through a celite bed). The cloudy solution was stirred for 3 h, filtered and the solution was evaporated to dryness. A white solid was obtained and crystallized by a mixture of CH_2Cl_2- diethyl ether. Yield 59%.

^1H NMR (CD_3OD, δ): 7.80 (s, 1H), 7.67÷7.59 (m, 15H).

^{31}P NMR (CD_3OD, δ): 30.63(s).

IR (cm^{-1}): 3214.4 (br, w), 3,047 (w), 2,228 (m), 1,572 (br, m), 1,499 (m), 1,471 (m), 1480.5 (m), 1,446 (sh, m), 1,435 (vs), 1331.5 (m), 1,303 (m), 1,249 (m),1,202 (m), 1,181 (m), 1159.3 (w), 115 (m), 1,103 (s), 1,072 (m), 1,027 (m), 998 (m), 920 (m), 878 (s), 849 (w), 754 (m), 745 (s), 712 (s), 692 (vs), 661 (vs).

ESI(–) (CH_3OH) m/z, %: 117 (71) [4,5-ImCN_2]$^-$, 431 (100) [(4,5-ImCN_2)$_2$ + Au]$^-$.

ESI(+) (CH_3OH) m/z %: 721 (100) [$(PPh_3)_2Au$]$^+$, 1,035 (16).

Elemental analysis for $C_{23}H_{16}N_4PAu$ calcd %: C 45.69, H 2.86, N 9.60. Found %: C 46.02; H 2.66, N 9.23.

Synthesis of compound **6**, [(3,5-dichloroimdazolyl-1H-gold(I)-(triphenylphosphane)]

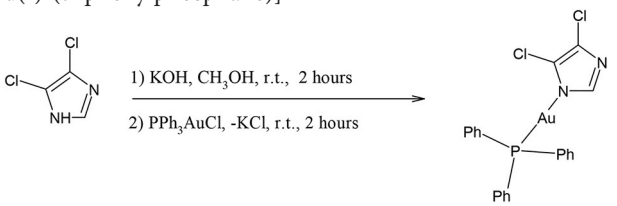

0.1 g of solid 4,5-dichloroimidazole (0.168 mmol) were dissolved in 2 mL of CH_3OH. To this solution 1.7 mL of a 0.1 M CH_3OH solution of KOH (0.168 mmol) were added. After 2 h of magnetic stirring at room temperature, 83 mgs of solid Ph_3PAuCl was added (0.168 mmol). The suspension was stirred for further 2 h, filtered off over a celite bed. The clear solution was concentrated to dryness, dissolved in CH_2Cl_2 and crystallized by layering hexane. Yield 59%. M.p. 154÷156.5°C.

^{1}H NMR (CD_3OD, δ): 7.74÷7.64 (m, 15H), 7.20 (s, 1H),

^{31}P NMR (CD_3OD, δ): 31.48 (s).

IR (cm^{-1}): 3,150 w (C_2-Him), 3,054 w, 3,032 w, 1,587 m, 1,499 m, 1,480 m, 1,434 s, 1,331 m, 1,309 m, 1,259 m, 1,222 s, 1,188 m, 1,101 s, 1,041 m, 1,011 s, 997 m, 963 m, 920 m, 812 m, 743 s, 711 s, 689 vs.

ESI(+) (CH_3OH), m/z (%): 1053.1 (100) $[Au(PPh_3)_2 + 4,5\text{-}Cl_2Im]^+$.

ESI(–) (CH_3OH), m/z (%): 134.9 (100) $[4,5\text{-}Cl_2Im]^-$, 468.9 (40) $[Au(4,5\text{-}Cl\text{-}Im)_2]^-$.

Elemental analysis for $C_{21}H_{16}AuCl_2N_2P$, calcd %: C, 42.38, H, 2.71, N, 4.71. Found %: C, 42.02, H, 2.84, N, 4.52.

Cancer Cells

Human MDA-MB-231 (ER–/PR–/HER2–) and SK-BR-3 (ER–/PR–/HER2+) cells were obtained from American Type Culture Collection (Rockville, MD) and cultured in Dulbecco's Modified Essential Medium (DMEM, Gibco, Life Technologies) supplemented with 10% fetal bovine serum (FBS, Gibco, Life Technologies) and 1% penicillin–streptomycin (Gibco, Life Technologies). A17 cells were established from a spontaneous lobular carcinoma that arose in an FVB/neuT mouse (Galiè et al., 2005), and maintained in DMEM plus 20% FBS and 1% penicillin-streptomycin. Cells were cultured at 37°C under humidified atmosphere with 5% CO_2.

MTT Assays

Stock solutions were prepared for each gold(I) compound (50 mM) using dimethyl sulfoxide (DMSO) (Sigma-Aldrich) as solvent. The effects of gold(I) compounds on SKBR3, A17 and MDA-MB231 cells viability were evaluated by seeding, respectively, 10, $*10^3$, 2.5 $*10^3$, 7, $*10^3$ cells/well in 96 wells plates in complete medium (DMEM supplemented with FBS) and compared to those of cisplatin. The day after, fresh medium containing vehicle alone (DMSO, 1 % v/v final concentration) or increasing concentrations of each compound ranging from 0.1 to 100 μM was added. Cell viability was determined using a MTT [3-(4,5-dimethylthiazol-2-yl)-2,5-diphenyl-2H-tetrazolium bromide Sigma Aldrich, St. Louis, MO] assay, which is based on the conversion of MTT to formazan crystals by mitochondrial enzymes, after 24, 48, and 72 h. The formazan deposits were dissolved in DMSO and the absorbance of each well was measured at 540 nm in Multiskan Ascent 96/384 Plate Reader. Each drug concentration was evaluated with 8 replicates and each experiment was repeated three times. At the end of the experiments a dose–response curve was plotted, and the IC50 concentrations were determined. Statistical analysis was performed using One-Way ANOVA analysis of variance followed by Dunnett's Multiple Comparison Test. Quantitative data are presented as means ± SEM. Differences were considered significant at $*P \leq 0.0332$; $**P \leq 0.0021$; $***P \leq 0.0002$; $****P \leq 0.0001$.

Enzymatic Assays on DHFR

SKBR3, MDA-MB-231 and A17 cells were plated onto 100 mm cell culture dishes (2×10^6 cells/ dish). The day after, cells were treated with vehicle alone (DMSO) as control or increasing concentrations of compound **5** and compound **6** in DMEM supplemented with 2% FBS (Invitrogen, Carlsbad, CA) for 4 h or 12 h. Representative pictures of cells treated with compound **5** or **6** at the indicated concentration for 4 or 12 h just before to take cell lysates for the enzymatic tests are reported as supplemental files. Cell lysates were collected using Cell Culture Lysis Reagent (Promega, Madison, WI) supplemented with BSA (1%) and protease inhibitors. DHFR activity was assessed by spectrophotometric assay as reported elsewhere (Wang et al., 2020) in which the reaction rate was followed by recording the decreasing absorbance at 340 nm due to oxidation of NADPH to $NADP^+$, using a Shimadzu UV-2450 spectrophotometer. When necessary, because of low protein content in the lysates, the DHFR enzymatic activity was measured by a discontinuous direct HPLC assay using an Agilent 1100 system. HPLC-DAD (Agilent 1100) was used to detect and quantify the presence of $NADP^+$, as one of the products of DHFR catalyzed reaction, in cell lysates. Fifty microliter of the cell lysate were incubated at 37°C in a reaction mixture containing 760 μl of buffer (0.05 M Hepes pH 7.3), 20 μl of NADPH 4 mM, and 20 μl of dihydrofolate (H_2F) 4 mM. The samples for HPLC analysis were prepared as follows: 50 μl aliquots of each mixture were stopped at different times (0, 5, 10, 20, 30, and 60 min) by adding 25 μl of $HClO_4$ 1.2 M; after 10 min on ice and centrifugation for 5 min at 12,000 g, 60 μl of each supernatant were neutralized by adding 17.5 μl of K_2CO_3 0.79 M, kept on ice and centrifuged again. Fifty microliter of the supernatant obtained were directly injected into the reversed phase column for separations of reagents and products of the enzyme catalyzed reaction. The column used is a Supelcosil LC RP 18 (4.6 × 250 mm) with pre-column SupelGuard. The HPLC settings are the same reported in Wang et al. (2020). The amounts of product ($NADP^+$) were determined from the peak areas of the HPLC-separated compounds with reference to appropriate standards. One enzyme unit is defined as the amount of enzyme which catalyzes the reduction of 1 μmol of dihydrofolate, per minute, at 37°C. Enzyme activities were normalized by the

protein content, determined by the Bradford assay (Bradford, 1976).

Enzymatic Assays on TrxR

The assay was performed as previously reported (Galassi et al., 2012) in 0.2 M Na, K-phosphate buffer (pH 7.4) containing 2 mM EDTA. The assay contained 0.12 mM NADPH and different amounts of cell lysate. The reaction was initiated by the addition of 3 mM 5,5′-dithiobis (2-nitrobenzoic acid) (DTNB) and the increase of absorbance was monitored at 412 nm over 5 min at 25°C.

DNA Interaction Studies

Stock solutions of calf thymus DNA (ct-DNA) (Sigma–Aldrich) were prepared by dissolving the DNA powder overnight in 10 mM Tris–HCl pH 7.4, 10 mM NaCl and incubated under stirrer at 4°C for 12h. The UV absorbance at 260 and 280 nm of the DNA solution gave a ratio A_{260}/A_{280} solution of ct-DNA of ca. 1.9, indicating that the DNA was sufficiently free from protein (Xu et al., 2014). The concentration of the ct-DNA solution was determined by UV absorbance at 260 nm. The molar absorption coefficient at 260 nm, was taken as 6,600 M^{-1} cm^{-1} (Marmur, 1961). Stock solutions of gold(I) complexes (compounds **5** and **6**) were prepared in DMSO. Absorption titration experiments performed with fixed concentrations of the different gold(I) complexes (25 μM, in 10 mM Tris–HCl pH 7.4, 10 mM NaCl), gradually increasing the concentration of DNA. After addition of DNA to the compounds, the resulting solution was allowed to where equilibrate at room temperature for 5 min. Then, the sample solution was scanned in the range 220–600 nm. For the different compounds the binding constant (Kb) was determined from the spectroscopic titration data using the following equation

$$[DNA]/(\varepsilon_a - \varepsilon_f) = [DNA]/(\varepsilon_b - \varepsilon_f) + 1/Kb(\varepsilon_b - \varepsilon_f), \text{Equation 1}$$

where [DNA] is the concentration of DNA in base pairs, the apparent absorption coefficient (ε_a) was obtained by calculating A_{obsd}/[compound]. The terms ε_f and ε_b correspond to the extinction coefficient of free (unbound) and the fully bound compound, respectively. A plot of [DNA]/(ε_a-ε_f) vs. [DNA] will give a slope 1/(ε_b-ε_f) and an intercept 1/Kb(ε_b-ε_f). Kb is given by the ratio of the slope to the intercept.

Fluorescence Spectral Study With EtBr

EtBr weakly emits fluorescence in aqueous solutions (Pasternack et al., 1983), however in presence of ct-DNA strongly emits at ∼600 nm due to strong intercalation between adjacent DNA base pairs. Ethidium bromide (EB) can be employed as a probe for the spectroscopic study of the interaction between DNA and intercalating species because of a 24-fold decrease in its fluorescence when displaced from an intercalation site by the addition of a competitive binding molecule probably due to decreasing in the number of binding sites accessible to EtBr (Tong et al., 2012). Competitive binding experiments were performed maintaining the ethidium bromide (EB) and ct-DNA concentration at 5 μM and 55.7 μM, respectively, while increasing concentrations of compounds **5** and **6** (5 mM in DMSO) were added to the buffer solution (10 mM Tris–HCl pH 7.4, 10 mM NaCl). Fluorescence quenching spectra were recorded using a Hitachi 4,500 spectrofluorometer with an excitation wavelength of 490 nm and emission spectrum 500–700 nm. The fluorescence spectra were recorded and the fluorescence value of the decrease in emission spectra was corrected according to the relationship:

$$F_c = F_m \times e(A_1 + A_2)/2 \quad (1)$$

where Fc and Fm are the corrected and measured fluorescence, respectively. A1 and A2 are the absorbance of tested compounds at the exciting and emission wavelengths. For fluorescence quenching experiments, Stern-Volmer's equation was used (Equation 3):

$$F_0/F_c = 1 + kq\tau 0[C] = 1 + K_{sv}[C] \quad (2)$$

where F_0 and F_c represent the fluorescence intensity in the absence and in the presence of the metal complex, [C] is the concentration of the metal complex and Ksv is the Stern-Volmer constant that can be obtained from fluorescence data plotted as F0/Fc vs. the metal complex concentration [C] (Lakowicz, 2006). All experiments involving ct-DNA were performed in buffer solution (10 mM tris-HCl buffer pH 7.4 10 mM NaCl) at room temperature.

Minor Groove Displacement Assay

The changes in the emission spectra of DAPI complex with the DNA in 10 mM tris-HCl buffer at pH 7.4, 10 mM NaCl, were monitored upon addition of increasing concentrations of gold-compounds **5** and **6** at room temperature. Fluorescence quenching data were evaluated after excitation of DAPI-ct-DNA complex at 338 nm and recording the spectra from 400 to 600 nm. Values of Ksv constants were evaluated using Equation 3 and the quenching fluorescence values obtained were corrected according to Equation 2.

Protein Binding

• BSA binding

The protein-binding studies were performed by tryptophan fluorescence quenching experiments using bovine serum albumin (BSA) from Sigma Aldrich prepared in 10 mM Tris-HCl buffer pH 7.4, 10 mM NaCl. The concentration was determined by measuring the absorbance at 280 nm. Assuming a molecular weight of 66,400 and a molar extinction coefficient at 280 nm of 43,824 M^{-1} cm^{-1}. Fluorescence measurements were recorded on a Hitachi 4,500 spectrofluorometer by keeping the concentration of BSA constant (15×10^{-6} M) while increasing compounds **5** or **6** concentrations (5 mM in DMSO) were added to protein solution at room temperatures. Protein fluorescence intensity was recorded after each successive addition of gold compound solution and equilibration (ca. 5 min). Fluorescence spectra were recorded from 300 to 450 nm at an excitation wavelength of 285 nm. The value of Stern Volmer constants of the different metal complexes to BSA was evaluated following Equation 3 and fluorescent values were corrected by Equation 2.

• Transferrin binding

Human apoTF (ATF) was purchased from Sigma Aldrich and its concentration was determined by measuring the absorbance at 278 nm ($\varepsilon = 92{,}300\ M^{-1}\ cm^{-1}$). To evaluate if compounds **5** and **6** were able to bind to ATF *in vitro*, fluorescence spectra were recorded from 300 nm to 450 nm upon tryptophan excitation at 285 nm. Fluorimetric titrations were performed by titrating a 2 mL sample (prepared in 10 mM Tris-HCl buffer pH 7.4, 10 mM NaCl) containing human ATF (12.5 μM) with incremental additions of different aliquots of gold-complexes (5 mM in DMSO). Protein fluorescence intensity was recorded after each successive addition of complex solution and equilibration (5 min). The value of Stern Volmer constants of the different metal complexes to ATF were evaluated following Equation 3 and fluorescent values were corrected by Equation 2. All titrations were performed at room temperature (25°C) and averages between two trials are reported.

RESULTS

Syntheses

The gold(I) compounds tested in this work are shown in **Scheme 1** and listed as compounds **1**-**6**. The nature of their molecular structure was ascertained by comparing the characterization results with the data previously reported in literature (*vide infra*). They were prepared as microcrystalline powders and used in the biochemical assays upon dissolution in DMSO. As concern compound **3**, the structure was mostly attributed from the elemental analysis, the ESI-MS and IR data. In detail, the IR spectrum displays a large band attributable to the OH group centered at 3226 cm^{-1} and a band at 1631 cm^{-1} which appears 52 cm^{-1} redshifted from the 1683 cm^{-1} carbonyl band of the starting 2-COOH-Ph_2PAuCl; moreover, the overall ^{1}H NMR patterns and the ESI(−) and ESI(+) MS peaks at 599 and 600 m/z, attributed to $[M]^-$ and $[M + H]^+$ ions, respectively, are diagnostic for the molecular structure of compound **3** reported in **Scheme 1**.

MTT Tests on Breast Cancer Cells

The effect on cancer cell viability of the gold(I) compounds reported in **Scheme 1** was first estimated by MTT assay on SKBR3 cells, representing the HER2-positive breast cancer subtype, after drug treatment for 72 h (**Figure 1S**). Considering the greater efficacy displayed by compounds **5** and **6** with respect to the others, we selected them for further studies. As shown in **Figure 2** and in **Table 2**, the viability of SKBR3 cells, exposed to compounds **5** and **6** for 48 h, significantly decreased in a dose-dependent manner, with IC_{50} values at low μM concentrations. The IC_{50} values were compared to those of cisplatin, a currently used chemotherapeutic drug (Serova et al., 2006; Gambini et al., 2018). The tests were performed also for the free azolate ligands, as controls, revealing absent or negligible cytotoxic activities (data not shown). Then, this study was extended to BLBC models. For this purpose, human MDA-MB231and murine A17 cells were treated with compounds **5** and **6** for 48 h and their viability was evaluated by MTT assay (**Figure 2S**). As reported in **Table 2**, IC_{50} values for compounds **5** and **6** indicate that 48 h of treatments with low μM concentrations are enough to significantly decrease A17 and MDA-MB231 cell viability (see also **Figure 2S**). These data confirm the previously obtained results in BLBC models, reported by Gambini et al. (2018).

Finally, the gold(I) compound having 3,5$(NO_2)_2$-pyrazolate (compound **4**), known to be cytotoxic (Galassi et al., 2012), was introduced in this analysis to evaluate the role of the azole in the anticancer activity. Thus, SKBR3, MDA-MB231 and A17 cells were treated with compound **4** for 24 h and their viability was assessed. The obtained data (**Table 2**) demonstrate that, besides compounds **5** and **6**, also the gold compound **4** is effective against both HER2-positive and basal like BC models.

Enzymatic Studies on DHFR

The effects of the most active compounds **5** and **6** on the DHFR enzymatic activity were investigated. The inhibition activity on the dihydrofolate reductase (DHFR) has been measured in BC cells treated with gold complexes **5** and **6** within either 4 or 12 h upon treatment and in not treated cells, at the same conditions, as control. Several concentrations of compound **5** and **6** were tested, based on the results of IC_{50} values obtained by MTT assays. In **Table 3** the DHFR specific enzymatic activity values, normalized with respect to the total protein content measured in each cell lysate, are shown. Both compounds **5** and **6** have produced a strong inhibition of DHFR enzymatic activity in all the tumor cell lines, reducing in some cases, the enzymatic activity to 35–40% of the control. In all the cancer cells, it was possible to observe a different effect depending on the time of treatment, as clearly evidenced in **Figure 3**. Taking into account the time necessary for the drugs to enter into the cells and interfere with the enzyme expression and functional activity, the A17 and SKBR3 cells are more efficiently inhibited at 12 h of treatment by both compounds **5** and **6**, while in the case of MDA-MB231 the stronger effect is observed at 4 h of treatment. Remarkably, the specific activity of DHFR in the untreated MDA-MB231 cells at 4 h is higher than the one measured at 12 h. This difference in the DHFR enzymatic levels between the two time points reflects the different inhibitory effects of compounds **5** and **6** on the DHFR activity.

Enzymatic Studies on TrxR

Complexes **5** and **6** were tested for their skill to inhibit the mostly recognized molecular target for gold compounds, the TrxR. With this aim, we evaluated the specific activity of TrxR on different tumor cells SKBR3, A17 and MDA-MB231 after incubation with the gold complexes **5** and **6**. The specific activity data in mU/mg are reported in **Table 4**. Residual activity data were reported in **Figures 3S, 4S** where we can observe that thioredoxin reductase activity decreases in a dose dependent manner upon treatment with the two gold(I) compounds with a major effect on MDA-MB231 with respect to those reported for A17.

Interactions With ct-DNA

UV-Vis Absorption Titration Analysis

Bindings between small molecules and DNA represent one of the primary mechanism of cytotoxic activity for metal based drugs. Experiments based on UV-visible spectrophotometric titrations were led to obtain dissociation constants (Kb) in order to

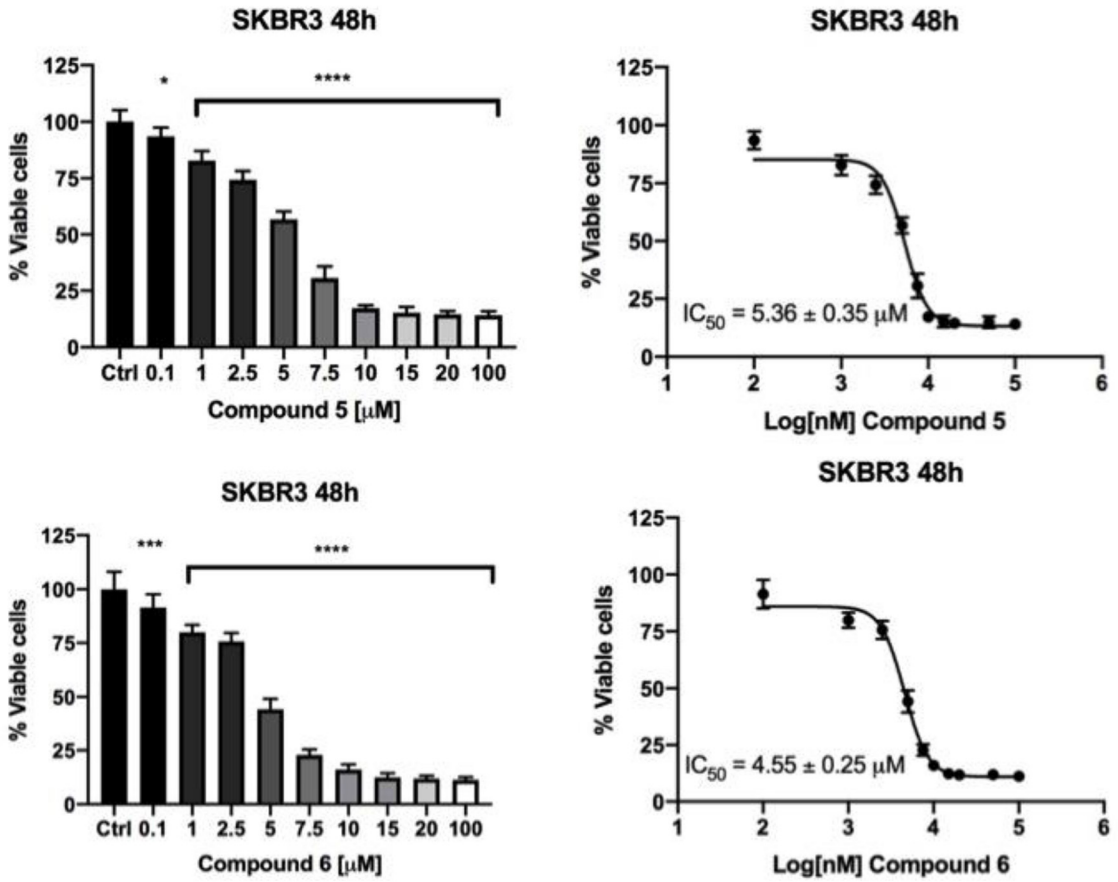

FIGURE 2 | Compounds **5** and **6** decreased SKBR3 cell viability. SKBR3 cells were incubated for 48 h in the presence of vehicle (DMSO) or increasing concentrations of Compound 5 (upper panel) and Compound 6 (lower panel) and cell viability was determined by MTT assay. The results are expressed as percentage of living cells with respect to control (vehicle alone). Columns, mean of three separate experiments wherein each treatment was repeated in 8 wells; bars, SE. $^{*}P \leq 0.0332$; $^{***}P \leq 0.0002$; $^{****}P \leq 0.0001$, One-way ANOVA followed by Dunnett's multiple comparisons test. IC_{50} values were calculated, by fitting the concentration-effect curves data obtained in the three experiments with the sigmoid-E_{max} model using non-linear regression, weighted by the reciprocal of the square of the predicted effect.

compare the binding properties of the selected cytotoxic gold(I) complexes with DNA. The absorption spectra of compound **5** and compound **6** were recorded in the absence and in the presence of calf thymus DNA (ct-DNA) (reported in **Figure 5S**) while the Kb values for gold compounds **5** and **6** are listed in **Table 5**. The titration was performed by using fixed amounts of complexes (25μ mM in DMSO) and titrating with an increasing amount of ct-DNA, resulting in an overall hyperchromism at the intraligand absorption bands in the 240–300 nm range which is attributed to π-π^* transitions. The "hyperchromic effect" has been observed for both tested compounds, in addition to a moderate red shift of the maxima of about 5 nm. The evaluation of the binding affinity of complexes with ct-DNA, was determined by the calculation of the intrinsic binding constants Kb by using the Equation 1, from the plot $[DNA]/[\varepsilon_a\text{-}\varepsilon_f]$ vs. [DNA] (**Figure 3S**) and values calculated for all complexes were reported in **Table 5**. The Kb analysis confirms that the two complexes interact with DNA with low affinity (compound **5** Kb $= 1.46 \pm 0.12\ 10^3\ M^{-1}$; compound **6** Kb $= 3.44 \pm 0.37\ 10^3\ M^{-1}$) reinforcing the concept of different mechanisms for their cellular toxicity. Among the two compounds, compound **6** shows a non-significant increase on interaction with DNA having 2-folds the value of Kb if compared to compound **5**.

Competitive Binding Fluorescence Studies With EtBr

The interaction of the gold(I) complexes with ct-DNA was determined by analyzing the competitive EtBr displacement according to fluorometric studies. **Figure 6S** reports the emission spectra of the EB-ct-DNA in buffer (10 mM Tris-HCl buffer pH 7.4, 10 mM NaCl) upon further addition of amounts of the tested gold(I) complexes. The addition of different concentrations of compounds **5** or **6** (5 mM in DMSO), to the EB-bound ct-DNA solution caused modest reduction in emission intensity, indicating that these compounds are able to substitute the EB in the ct-DNA-bound EB and to bind ct-DNA. The quenching behavior quantitatively related to the magnitude of the binding strength of gold(I) complexes, has been then analyzed by the Stern–Volmer equation (Equation 3, material and methods) and

TABLE 2 | IC_{50} values for compounds 4, 5, 6 and cisplatin against the BC cell lines SKBR3, MDAMB231, and A17.

Gold(I) compound	Cell line	Time (h)*	IC_{50} [μM ± S. D.]
Compound **4**	SKBR3	24	12.28 ± 1.1
	MDA-MB231	24	12.85 ± 0.7
	A17	24	11.00 ± 1.0
Compound **5**	SKBR3	48	5.36 ± 0.35
	MDA-MB231	48	7.03 ± 0.76
	A17	48	16.19 ± 0.59
Compound **6**	SKBR3	48	4.55 ± 0.25
	MDA-MB231	48	3.46 ± 0.29
	A17	48	14.43 ± 0.7
Cisplatin	SKBR3	24	43 ± 7.0^
	MDA-MB231	48	50.49 ± 2.0*
	A17	24	15.86 ± 1.17*

^*Serova et al., 2006*; **Gambini et al., 2018*.

TABLE 3 | Specific enzymatic activity of DHFR (mU/mg) measured in the untreated cells and upon treatment with the selected gold(I) compounds at the concentration causing the maximum inhibition: 6 μM for both A17 and SKBR3, 8 μM for MDA-MB231.

	Time (hours)	A17	MDA-MB231	SKBR3
Cells without treatment (control)	4	1.17 ± 0.06	5.38 ± 0.38	0.72 ± 0.05
	12	4.77 ± 0.78	0.64 ± 0.02	0.67 ± 0.10
Cells treated with compound **5**	4	1.07 ± 0.02	2.37 ±0.39	0.54 ± 0.04
	12	1.66 ± 0.07	0.42 ± 0.01	0.29 ± 0.05
Cells treated with compound **6**	4	1.03 ± 0.03	1.75 ± 0.34	0.64 ± 0.06
	12	2.01 ± 0.14	0.55 ± 0.002	0.34 ± 0.01

values of the quenching constants calculated, K_{sv}, were obtained as a slope from the plot of F_0/F vs. [C] (**Figure 4S**) and the K_{sv} values are reported in **Table 5**. Our findings confirmed that both compounds **5** and **6** bind to the EB-ctDNA with low affinity and only little differences were observed as shown from the titration experiments.

Competitive Binding Fluorescence Studies With DAPI

As shown in **Figure 4**, the addition of compound **5** or compound **6** to the DAPI-ct-DNA complex (in 10 mM Tris-HCl buffer pH 7.4 10 mM NaCl) reduces its fluorescence intensity (Zaitsev and Kowalczykowski, 1998), clearly suggesting that both gold compounds show binding affinity to adenine-thymine rich region of DNA and are able to display DAPI from the biopolymer. Data were analyzed by the Stern–Volmer equation (Equation 3, materials and methods) and values of the quenching constants calculated, K_{sv}, were evaluated for compounds **5** and **6** as previously described and reported in **Table 5**. Data revealed an increase in the value of the affinity of the tested compounds for DNA with respect to those reported with the two previous assays without differences between the two gold(I) complexes. The results are consistent with that of absorption spectroscopic studies and approximately indicate a major preference of these gold(I) complexes to bind on the minor groove of DNA.

Protein Binding Studies

Fluorescence Studies on BSA

The study of the interaction of gold-drugs with BSA affords information on the distribution, on the free concentration, on the metabolism and on the efficacy of the gold compound (Radisavljević et al., 2019). The BSA protein has large homology with Human Serum Albumin (HSA) and the quenching of the intrinsic tryptophan fluorescence represents a good tool to deeply investigate the possible interaction of our metallodrugs with BSA in an attempt to characterize the fate of the gold compounds once they are in physiological environments. Fluorescence quenching experiments have been carried out by monitoring the emission of tryptophan at 341 nm upon excitation at 285 nm and increasing concentrations of compounds **5** and **6** with BSA (Quinlan et al., 2005). The fluorescence emission spectra of BSA after the interaction with gold complexes to the protein are shown in the supplemental material, **Figure 7S**. The addition of the complexes to BSA results in a large reduction in the fluorescence intensity without any shift of the emission maximum and the Stern-Volmer binding constants K_{sv} to BSA for all evaluated complexes (**Table 5**) showing that all complexes bind BSA with good affinity and with a similar value of K_{sv}.

Fluorescence Quenching Studies of Transferrin

Transferrin has been looked to as a possible transport vehicle for metal-based drugs because of its abundance in the plasma and its ability to bind ferric ions (Worwood, 2002). Most trivalent metals, and a few divalent metals bind specifically to the iron-binding sites of the apoprotein (O'Hara and Koenig, 1986). Fluorimetric titration of human ATF with gold complexes **5** and **6** demonstrated a similar interaction to that with BSA. As an example, **Figure 5**, shows the titration spectra of ATF with increasing amounts of complexes. Tryptophan fluorescence emission was monitored at 330 nm for complexes The Stern-Volmer plots are shown in the inset images of **Figure 5**. The values of Ksv collected in **Table 5** were obtained from the initial linear section of the Stern-Volmer plots. As in the case of BSA, the Ksv values suggest good affinity of the two gold complexes with values similar to those reported for BSA and with no differences in binding properties between the two complexes.

DISCUSSION

Five gold(I) compounds containing the N-Au-P structural frames consisting of imidazole or pyrazole and triphenylphosphane moieties in addition to one compound with the structural frame P-Au-Cl, the 2-benzoic-diphenylphosphanegold chloride, were synthesized to test their cytotoxic activity on BC cell lines to verify an overall activity for these gold complexes for BC's subtypes and sketch a correlation between the structure and the anticancer activity. The compounds are featured by molecular backbones containing a polar azole and a lipophilic triphenylphosphane

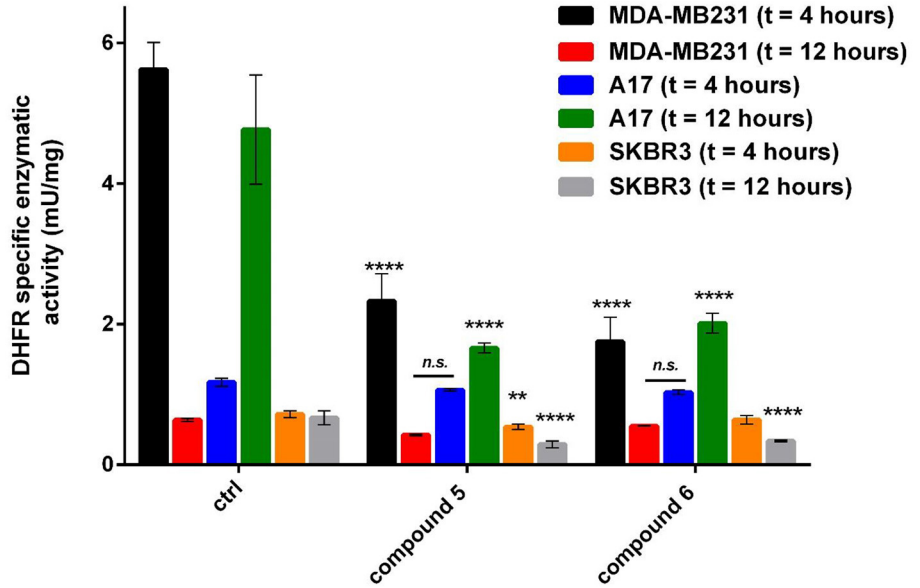

FIGURE 3 | Specific DHFR enzymatic activity measured in breast cancer cell lines after treatment with gold compounds **5**, 4,5-dicyano-imidazolate-1yl-gold(I)-(triphenylphosphane), and **6**, 4,5-dichloro-imidazolate-1yl-gold(I)-(triphenylphosphane), at two different times of treatment. The reported enzymatic activity are relative to the concentration of gold(I) compounds causing the maximum inhibition: 6 μM for A17 and SKBR3, 8 μM for MDA-MB231. The statistical significance relative to control for each cell line is reported: *****p* < *0.0001*, ****p* < *0.01*, *n.s. not significant*.

head, whose polarity and skill to bind was enhanced by the introduction of hydrophilic moieties such as COOH and/or OH groups (Santini et al., 2011). The BC SKBR3 cells display an epithelial morphology in tissue culture and are a useful preclinical model to screen for new therapeutic agents which could overcome the drawback of resistance to HER2-targeted therapies, therefore these cells were considered for MTT tests. The results, reported in **Figure 2** and **Figure 1S**, showed a trend of activity depending on the structure of the gold compounds; in fact, the most active compounds are the compounds **5** and **6**, while the compounds **1**, **2** and **3**, possessing the –COOH functional group on the PPh_3 moiety or the CH_2OH group on the imidazole, did not show relevant cytotoxic activity. Therefore, from the MTT assays screening on SKBR3 cells we can conclude that the presence of ligands with hydrogen bonding donor sites in the gold(I) compounds introduces in some way an impeding for the *in vitro* activity. After the screening on the HER2 overexpressing SKBR3 BC cells, the most active compounds **5** and **6** were chosen for other BC subtype cell models: the MDA-MB231 and the A17 (**Figure 2S**). In addition to compounds **5** and **6**, compound **4** was tested to verify the effect of a different azole, the 3,5-dinitropyrazole, resulting all strongly active with IC_{50} values depending on the cell phenotype. The analysis of the data (see **Table 3**) reveals an influence of the azolate ligands on the mechanism of action even though they result do not be cytotoxic if tested as free ligands. In particular, compound **4** is the fastest to reach the plateau of effect with all the cell lines, while as concerns compound **5** and **6**, the latter is the most effective supporting the attribution of a presumed role to the substituents on the imidazole. Remarkably, the treatment of human breast cancer MDA-MB231 cells, which is the panel corresponding to the worst diagnosis, show encouraging IC_{50} values, albeit they are in the micromolar range. Unfortunately, even though it was found to be cytotoxic and rapidly active, compound **4** was less stable in physiological condition, likely for the presence of reactive nitro groups. After these cytotoxic studies and their results, further studies were led only with compounds **5** and **6**.

TABLE 4 | Specific enzymatic activity of TrxR mU/mg measured in the untreated cells and upon treatment of 12 h with the selected gold(I) compounds at the concentration causing the maximum inhibition (in round brackets).

	A17	MDA-MB231	SKBR3
Cells without treatment (control)	4.95 ± 0.08	3.01 ± 0.01	4.07 ± 0.32
Cells treated with compound **5**	1.84 ± 0.06 (6 μM)	1.59 ± 0.03 (16 μM)	1.98 ± 0.06 (8 μM)
Cells treated with compound **6**	4.21 ± 0.09 (6 μM)	1.95 ± 0.06 (16 μM)	1.51 ± 0.04 (8 μM)

The cancer cells treated with the gold(I) compounds **5** and **6** were then used for enzymatic tests with the aim to determine the DHFR or the TrxR specific activities. The results are shown in **Tables 2** and **3**. While TrxR is fully recognized as the most likely target for gold(I) compounds, the former was serendipitously found to be inhibited *in vitro* by gold(I) phosphane compounds with IC_{50} in the micromolar range (Galassi et al., 2015). The DHFR specific activity for the three cancer cell lines are noticeably different, underlining that the inhibition was

TABLE 5 | Summarizing table showing K_{sv} obtained from fluorescence quenching experiments to evaluate compound 5 and compound 6 capacity to bind to proteins (BSA and ATF) and ct-DNA (Competitive binding fluorescence studies with DAPI and EB).

Compounds	BSA Ksv 10^4 M^{-1}	ATF Ksv 10^4 M^{-1}	Ct-DNA Kb 10^3 M^{-1}	EB-ct-DNA Ksv 10^3 M^{-1}	DAPI-ct-DNA Ksv 10^3 M^{-1}
5	2.46 ± 0.82	1.93 ± 0.44	1.46 ± 0.12	1.55 ± 0.34	6.12 ± 0.09
6	2.04 ± 0.71	1.51 ± 0.55	3.44 ± 0.37	4.22 ± 0.34	4.98 ± 0.08

K_b were obtained through UV-Vis absorption titration analysis.

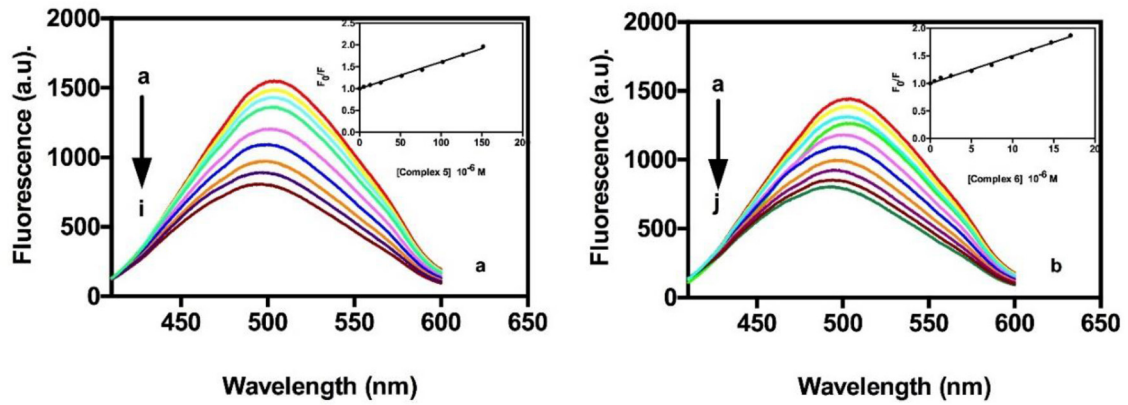

FIGURE 4 | Quenching behavior in fluorescence of the DAPI-ctDNA in the presence of different amounts of compound **5** (a) and compound **6** (b). The arrow indicates the changes of the bands upon addition of increasing concentrations of compounds **5** or **6**. Inset, Stern-Volmer plot of experimental data fitted by Equation 3.

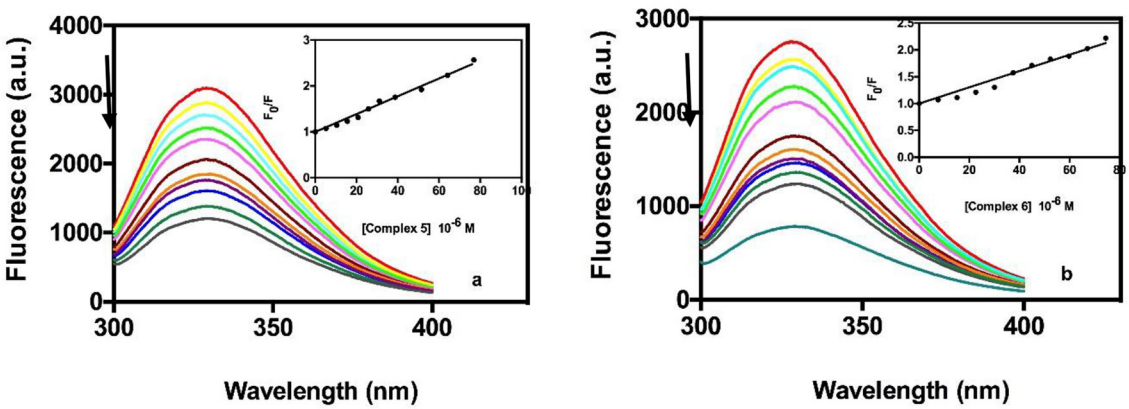

FIGURE 5 | Quenching behavior in fluorescence of the ATF in the presence of different amounts of compound 5 (a) and compound 6 (b). The arrows indicate the changes of the bands upon addition of increasing concentrations of compounds 5 or 6. Inset, Stern- Volmer plot of experimental data fitted by Equation 3.

remarkable for the SKBR3, the A17 and MDA-MB231 cells and featuring, in some way, the influence of the cell phenotype. Noteworthy, both gold(I) compounds exerted mild or not significant inhibitory action on the regard of DHFR of healthy NIH-3T3 cells (data not shown). Interestingly, comparing the DHFR's specific activity of the cells treated with gold compounds with those of the cells used as the control, as shown in **Figure 3**, it is evident that the DHFR's specific activity is differently affected by the gold based compound depending on the time of treatment. These results highlight the role of time in the inhibitory effect exerted by gold compounds toward this target enzyme. The diverse DHFR specific activities herein obtained may derive from the different levels of expression of the enzyme due to variances in cell cycle regulation. Being required for DNA synthesis, DHFR expression is transcriptionally regulated during the growth/cell cycle, with the highest expression levels occurring in the late G1 to early S phase following stimulation of quiescent (G0) cells (Jensen et al., 1997). The different specific activity of DHFR in non-treated MDA-MB231 and A17 cells at 4 h with respect to 12 h, could reflect a phenotypic response to the regulation of the G1 checkpoint and S-phase progression in these two cell lines.

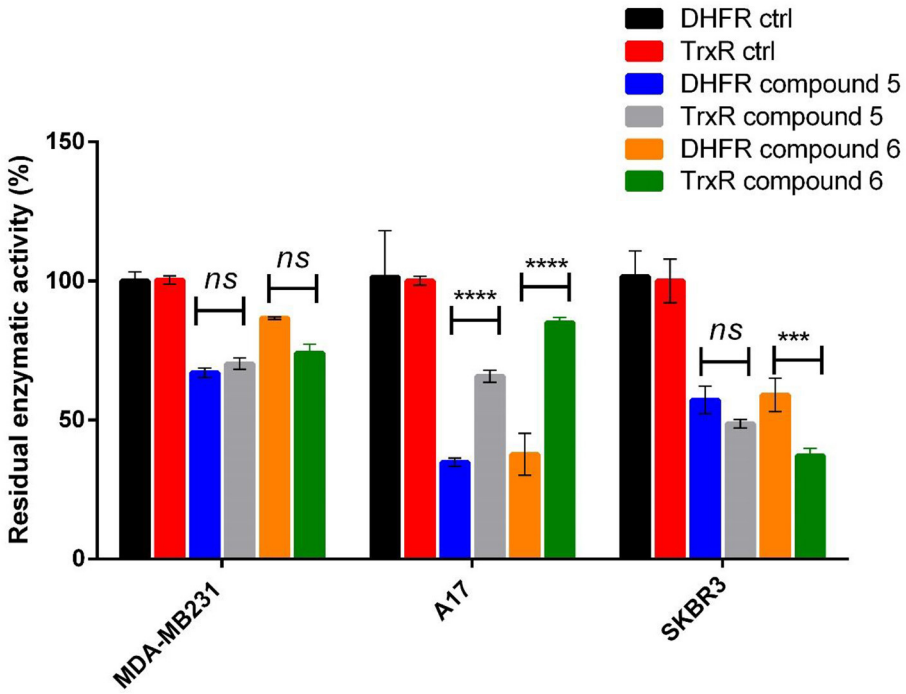

FIGURE 6 | Residual DHFR and TrxR enzymatic activity values measured in breast cancer cell lines after treatment with gold compounds **5**, 4,5-dicyano-imidazola te-1yl-gold(I)-(triphenylphosphane), and **6**, 4,5-dichloro-imidazolate-1yl-gold(I)-(triphenylphosphane), at 12 h of treatment. The reported percentage residual activities are relative to the concentration of gold(I) compounds nearest to the IC50 obtained by MTT assays: 8 μM of compound **5** and 4 μM of compound **6** for MDA-MB23, 12 μM of both compounds for A17, 6 μM of both compounds for SKBR3 cells. The statistical significance relative to the difference between residual DHFR and TrxR enzymatic activity in each cell line is reported: ****$p < 0.0001$, ***$p < 0.001$, *n.s. not significant*.

As concerns the enzyme TrxR, the system TrxR/Trx is responsible for the reduction of redox-sensitive proteins upon oxidative stress and the TrxR/Trx expression is augmented in a variety of human malignancies, including lung, colorectal, cervical, hepatic, and pancreatic cancer (Lincoln et al., 2003). Therefore, both DHFR and TrxR are enzymes involved in cell proliferation and cancer progression, and they represent suitable targets for multiple ligands approach in anticancer drug design (Hui-Li et al., 2016); moreover, the use of drugs with different biological targets can be a strategy in overcoming drug resistance. Compounds **5** and **6** exert this multi-targeted inhibitory activity with respect to both TrxR and DHFR. The presence of the soft metal gold(I) ion, confers selectivity toward the selenocysteine residue in the TrxR active site (Galassi et al., 2012), while the hydrophobic phosphane group and the amphipathic azolate moiety can easily fit in the DHFR's substrate binding pocket. In **Figure 6**, we report the comparison between the residual enzymatic activities of DHFR and TrxR in SKBR3, MDA-MB231 and A17 cell lines in presence of compounds **5** and **6** at the IC_{50} concentrations. While in the MDA-MB231 cells the two enzymes do not show significant differences in their response to both gold compounds, in the A17 cells DHFR activity undergoes a stronger decrease compared to TrxR; these effects were found for both compounds. As concern the SKBR3 cells, it is possible to observe a different behavior of the two gold(I) compounds, while compound **5** displays similar effects for both enzymes, compound **6** inhibits more strongly the TrxR. The different behavior of the gold(I) based complexes toward DHFR and TrxR enzymatic levels in the breast cancer cell lines MDA-MB231 and A17 can reflect either the different mechanism of action of the two compounds in interacting with DHFR and TrxR, and/or the differences in their impact on the two enzymes expression levels in cancer cells. While it is well-recognized that gold(I) complexes can modify the accessible selenocysteine residue in the active site of TrxR (Bindoli et al., 2009), the mechanism by which these drugs inhibit DHFR, seems to be independent by "auration" or oxidation of Cys residues, and rather to be based on reversible competition with the substrate in binding to the active site (Galassi et al., 2015).

It is mostly recognized that enzymes and proteins are preferred binding sites for Au(I) phosphane compounds once in a biological environment, whereas nucleic acids have been little investigated. In this regard, studies have been carried out on the effective interaction with the calf thymus DNA, ct-DNA. The data obtained show a poor aptitude for interaction with DNA, with binding constants of 1.46 mM^{-1} for compound **5** and 3.44 $mM^{-1}$for compound **6** (**Table 5**). These values are similar to those reported for other gold complexes (Nobili et al., 2010) but lower with respect to those observed for typical classical intercalators, as ethidium bromide, acridine orange and

methylene blue showing binding constants of $K_{EB} = 6.58 \times 10^4$ M^{-1}, $K_{AO} = 2.69 \times 10^4$ M^{-1} and $K_{MB} = 2.13 \times 10^4$ M^{-1}, respectively (Nafisi et al., 2007). The study carried out on the competitive displacement with classic DNA's intercalators such as ethidium bromide and DAPI gave an additional insight; as expected, the K_{sv} values calculated by the emission quenching experiments highlight that gold(I) compounds mildly compete with both intercalators with a major ability to displace the DAPI, showing that a left shifted equilibrium of interaction occurs in the minor groove of the DNA.

Lastly, the reactivity of gold(I) compounds with serum target proteins such as bovine serum albumin and apo transferrin has been investigated. The quenching of spontaneous emissions of these proteins upon addition of increasing concentration of gold(I) phosphane compounds have been detected in both cases; data were processed according to the Stern Volmer model of interaction having as results the values of the binding constants, which are resumed in **Table 5**. The data show high affinity for both proteins with similar K_{sv} values consisting of few unit $\times 10^4$ M^{-1}. BSA has been already identified as a likely transporter for gold moieties, while the transferrin has never been considered, even though it represents the preferred transporter for metal ions (Gkouvatsos et al., 2012). The biological activity of ATF is strictly linked to its interactions with transferrin receptors (TfR) that regulates cellular uptake; TfRs are upregulated in the surface of cancer cells and thus can be used as selective target in anticancer drug design (Wang et al., 2000; Daniels et al., 2012). Moreover, TfRs are efficient systems to internalize antitumor compounds through the carrier protein ATF directly into cancer cells, circumventing adverse effects against healthy cells receptors (Singh et al., 1998). Our results do encourage further studies to clarify the mechanism involved in ATF binding of compounds **5** and **6** and verify the ability to release these complexes in an active form.

CONCLUSIONS

A class of azolate/phosphane gold(I) compounds has been evaluated for a screening on the regards of BC cell panels. Among the six candidates, only the compounds having the P-Au-N environment and neither hydroxyl nor carboxyl groups in the ligands were found active. Hence, the presence of polar protic functional groups hampers in some way the cytotoxic activity. The most effective compounds are the 4,5-$(CN)_2$-imidazolate (compound **5**) and the 4,5-Cl_2-imidazolate (compound **6**) which were already found to be very active against BLBC *in vivo* (Gambini et al., 2018). Therefore, the present study provides further evidence of the efficacy of these two imidazolate phosphane gold(I) compounds *in vitro* as anticancer even against another BC's subtype, the HER2-positive breast cancer. The two compounds, even though they are very similar in their structure, show MTT and biochemical assays experimental results which are quite different, evidencing a sensitive relationship between the structure and the anticancer activity. For example, the determination of the residual activity of target enzymes in the treated cancer cells reveal the ability of these gold compounds **5** and **6** to strongly inhibit TrxR and DHFR. In fact, the enzymatic assays on the lysates of the treated cells of different BC subtypes showed the strong inhibition of TrxR seleno-enzyme and, surprisingly, of another selected enzyme such as DHFR in an extent not so much dissimilar, despite the fact that inhibition tests *in vitro* on the activity of these enzymes afforded to values of Ki different up to an order of 10^3 (Galassi et al., 2012, 2015). Remarkably, the enzymatic study on the cells' lysates underlined that the DHFR inhibition effects were observed to be dependent on treatment's time, likely as a consequence of the different cancer cells cycle regulation and the enzyme's expression levels (**Figure 6**). In this work, it was also highlighted that these compounds strongly bind plasma proteins as BSA and ATF, suggesting their possible role as transport vehicles for these metal-based drugs once administered *in vivo*. Conversely, as expected, they do not display any strong binding to ct-DNA, though they exhibit weak interactions with the minor groove of the biopolymer. On conclusion, two of the herein considered gold compounds confirm their strong anticancer activities *in vitro* on the regards of aggressive BC subtypes cells through multitarget mechanisms: it was assessed their action through the inhibition of both TrxR and DHFR enzymes and their binding to transporter proteins as BSA and ATF, that *in vivo* raised much attention for their possible involvement in the mechanism of action.

DATA AVAILABILITY STATEMENT

The original contributions presented in the study are included in the article/**Supplementary Materials**, further inquiries can be directed to the corresponding author/s.

AUTHOR CONTRIBUTIONS

VG and JW have performed the MTT tests. CM and AA have funded the cellular studies and elaborated the MTT data. GL has performed and made the interpretation on the protein binding studies and the Thioredoxin Reductase inhibition. SP has performed the study on the DHFR enzyme inhibition and made the interpretation of the data. SV has funded the DHFR studies and supervised the study on the DHFR. LL has prepared the gold compounds and followed some of the enzymatic studies. RG funded and supervised the synthesis of the compounds and wrote the manuscript. All the authors took part at the rielaboration of the data.

FUNDING

RG was grateful to University of Camerino for financial support. JW was supported by Fondazione Umberto Veronesi.

SUPPLEMENTARY MATERIAL

The Supplementary Material for this article can be found online at: https://www.frontiersin.org/articles/10.3389/fchem.2020.602845/full#supplementary-material

REFERENCES

Berners-Price, S. J., and Filipovska, A. (2011). Gold compounds as therapeutic agents for human diseases. *Metallomics* 3, 863–873. doi: 10.1039/c1mt00062d

Bertrand, B., and Casini, A. (2014). A golden future in medicinal inorganic chemistry: the promise of anticancer gold organometallic compounds. *Dalton Trans.* 43, 4209–4219. doi: 10.1039/C3DT52524D

Bindoli, A., Rigobello, M. P., Scutari, G., Gabbiani, C., Casini, A., and Messori, L. (2009). Thioredoxin reductase: a target for gold compounds acting as potential anticancer drugs. *Coord. Chem. Rev.* 253, 1692–1707. doi: 10.1016/j.ccr.2009.02.026

Bisaro, B., Montani, M., Konstantinidou, G., Marchini, C., Pietrella, L., Iezzi, M., et al. (2012). p130Cas/Cyclooxygenase-2 axis in the control of mesenchymal plasticity of breast cancer cells. *Breast Cancer Res.* 14:R137. doi: 10.1186/bcr3342

Bradford, M. M. (1976). A rapid and sensitive method for the quantitation of microgram quantities of protein utilizing the principle of protein-dye binding. *Anal. Biochem.* 72, 248–254. doi: 10.1016/0003-2697(76)90527-3

Bray, F., Ferlay, J., Soerjomataram, I., Siegel, R. L., Torre, L. A., and Jemal, A. (2018). Global cancer statistics 2018: GLOBOCAN estimates of incidence and mortality worldwide for 36 cancers in 185 countries. *CA Cancer J. Clin.* 68, 394–424. doi: 10.3322/caac.21492

Bruce, M. I., Nicholson, B. K., Shawkataly, O. B., Shapley, J. R., and Henly, T. (2007). "Synthesis of gold-containing mixed-metal cluster complexes," in *Inorganic Syntheses*, ed H. D. Kaesz (John Wiley & Sons Ltd), 324–328. doi: 10.1002/9780470132579.ch59

Burstein, H. J. (2005). The distinctive nature of HER2-positive breast cancers. *N. Engl. J. Med.* 353, 1652–1654. doi: 10.1056/NEJMp058197

Che, C. M., and Sun, R. W. Y. (2011). Therapeutic applications of gold complexes: lipophilic gold(III) cations and gold(I) complexes for anti-cancer treatment. *Chem. Commun.* 47, 9554–9560. doi: 10.1039/c1cc10860c

Correia, A., Silva, D., Correia, A., Vilanova, M., Gärtner, F., and Vale, N. (2018). Study of new therapeutic strategies to combat breast cancer using drug combinations. *Biomolecules* 8, 175–198. doi: 10.3390/biom8040175

Cui, X. Y., Park, S. H., and Park, W. H. (2020). Auranofin inhibits the proliferation of lung cancer cells via necrosis and caspase-dependent apoptosis. *Oncol. Rep.* 44, 2715–2724. doi: 10.3892/or.2020.7818

da Silva Maia, P. I., Deflon, V. M., and Abram, U. (2014). Gold(III) complexes in medicinal chemistry. *Future Med. Chem.* 6, 1515–1536. doi: 10.4155/fmc.14.87

Daniels, T. R., Bernabeu, E., Rodríguez, J. A., Patel, S., Kozman, M., Chiappetta, D. A., et al. (2012). Transferrin receptors and the targeted delivery of therapeutic agents against cancer. *Biochim. Biophys. Acta* 1820, 291–317. doi: 10.1016/j.bbagen.2011.07.016

Fisher, B., Brown, A. M., Dimitrov, N. V., Poisson, R., Redmond, C., Margolese, R. G., et al. (1990). Two months of doxorubicin-cyclophosphamide with and without interval reinduction therapy compared with 6 months of cyclophosphamide, methotrexate, and fluorouracil in positive-node breast cancer patients with tamoxifen-nonresponsive tumors: results from the national surgical adjuvant breast and bowel project B-15. *J. Clin. Oncol.* 8, 1483–1496. doi: 10.1200/JCO.1990.8.9.1483

Galassi, R., Burini, A., Ricci, S., Pellei, M., Rigobello, M. P., Citta, A., et al. (2012). Synthesis and characterization of azolate gold(I) phosphane complexes as thioredoxin reductase inhibiting antitumor agents. *Dalton Trans.* 41, 5307–5318. doi: 10.1039/c2dt11781a

Galassi, R., Oumarou, C. S., Burini, A., Dolmella, A., Micozzi, D., Vincenzetti, S., et al. (2015). A study on the inhibition of dihydrofolate reductase (DHFR) from *Escherichia coli* by gold(I) phosphane compounds. X-ray crystal structures of (4,5-dichloro-1H-imidazolate-1-yl)-triphenylphosphane-gold(I) and (4,5-dicyano-1H-imidazolate-1-yl)-triphenylphosphane-gold(I). *Dalton Trans.* 44, 3043–3056. doi: 10.1039/C4DT01542H

Galassi, R., Ricci, S., Burini, A., Macchioni, A., Rocchigiani, L., Marmottini, F., et al. (2013). Solventless supramolecular chemistry via vapor diffusion of volatile small molecules upon a new trinuclear silver(I)-nitrated pyrazolate macrometallocyclic solid: an experimental/theoretical investigation of the dipole/quadrupole chemisorption phenomena. *Inorg. Chem.* 52, 14124–14137. doi: 10.1021/ic401948p

Galiè, M., Konstantinidou, G., Peroni, D., Scambi, I., Marchini, C., Lisi, V., et al. (2008). Mesenchymal stem cells share molecular signature with mesenchymal tumor cells and favor early tumor growth in syngeneic mice. *Oncogene* 27, 2542–2551. doi: 10.1038/sj.onc.1210920

Galiè, M., Sorrentino, C., Montani, M., Micossi, L., Di Carlo, E., D'Antuono, T., et al. (2005). Mammary carcinoma provides highly tumourigenic and invasive reactive stromal cells. *Carcinogenesis* 26,1868–1878. doi: 10.1093/carcin/bgi158

Gambini, V., Tilio, M., Maina, E. W., Andreani, C., Bartolacci, C., Wang, J., et al. (2018). *In vitro* and *in vivo* studies of gold(I) azolate/phosphane complexes for the treatment of basal like breast cancer. *Eur. J. Med. Chem.* 155, 418–427. doi: 10.1016/j.ejmech.2018.06.002

Gkouvatsos, K., Papanikolaou, G., and Pantopoulos, K. (2012). Regulation of iron transport and the role of transferrin. *Biochim. Biophys. Acta* 1820, 188–202. doi: 10.1016/j.bbagen.2011.10.013

Hui-Li, N. G., Shangying, C., Eng-Hui, C., and Wai-Keung, C. (2016). Applying the designed multiple ligands approach to inhibit dihydrofolate reductase and thioredoxin reductase for anti-proliferative activity. *Eur. J. Med. Chem.* 115, 63–74. doi: 10.1016/j.ejmech.2016.03.002

Jensen, D. E., Black, A. R., Swick, A. G., and Azizkhan, J. C. (1997). Distinct roles for Sp1 and E2F sites in the growth/cell cycle regulation of the DHFR promoter. *J. Cell. Biochem.* 67, 24–31. doi: 10.1002/(SICI)1097-4644(19971001)67:1<24::AID-JCB3>3.0.CO;2-Y

Kim, J. H., Reeder, E., Parkin, S., and Awuah, S. G. (2019). Gold(I/III)-phosphine complexes as potent antiproliferative agents. *Sci. Rep.* 9:12335. doi: 10.1038/s41598-019-48584-5

Lakowicz, J. R. (2006). *Principles of Fluorescence Spectroscopy, 3rd Edn*. Springer US. doi: 10.1007/978-0-387-46312-4

Lincoln, D. T., Ali Emadi, E. M., Tonissen, K. F., and Clarke, F. M. (2003). The thioredoxin-thioredoxin reductase system: over-expression in human cancer. *Anticancer Res.* 23, 2425–2433.

Liu, J. J., Galettis, P., Farr, A., Maharaj, L., Samarasinha, H., McGechan, A. C., et al. (2008). *In vitro* antitumour and hepatotoxicity profiles of Au(I) and Ag(I) bidentate pyridyl phosphine complexes and relationships to cellular uptake. *J. Inorg. Biochem.* 102, 303–310. doi: 10.1016/j.jinorgbio.2007.09.003

Marchini, C., Montani, M., Konstantinidou, G., Orrù, R., Mannucci, S., Ramadori, G., et al. (2010). Mesenchymal/stromal gene expression signature relates to basal-like breast cancers, identifies bone metastasis and predicts resistance to therapies. *PLoS ONE* 5:e14131. doi: 10.1371/journal.pone.0014131

Marmur, J. (1961). A procedure for the isolation of deoxyribonucleic acid from micro-organisms. *J. Mol. Biol.* 3, 208–218. doi: 10.1016/S0022-2836(61)80047-8

McKeage, M. J., Berners-Price, S. J., Galettis, P., Bowen, R. J., Brouwer, W., Ding, L., et al. (2000). Role of lipophilicity in determining cellular uptake and antitumour activity of gold phosphine complexes. *Cancer Chemother. Pharmacol.* 46, 343–350. doi: 10.1007/s002800000166

Messori, L., Cinellu, M. A., and Merlino, A. (2014). Protein recognition of gold-based drugs: 3D structure of the complex formed when lysozyme reacts with aubipyc. *ACS Med. Chem. Lett.* 5, 1110–1113. doi: 10.1021/ml500231b

Nafisi, S., Saboury, A. A., Keramat, N., Neault, J. F., and Tajmir-Riahi, H. A. (2007). Stability and structural features of DNA intercalation with ethidium bromide, acridine orange and methylene blue. *J. Mol. Struct.* 827, 35–43. doi: 10.1016/j.molstruc.2006.05.004

Nakai, K., Hung, M. C., and Yamaguchi, H. (2016). A perspective on anti-EGFR therapies targeting triple-negative breast cancer. *Am. J. Cancer Res.* 6, 1609–1623.

Nobili, S., Mini, E., Landini, I., Gabbiani, C., Casini, A., and Messori, L. (2010). Gold compounds as anticancer agents: chemistry, cellular pharmacology, and preclinical studies. *Med. Res. Rev.* 30, 550–580. doi: 10.1002/med.20168

O'Hara, P. B., and Koenig, S. H. (1986). Electron spin resonance and magnetic relaxation studies of gadolinium(III) complexes with human transferrin. *Biochemistry* 25, 1445–1450. doi: 10.1021/bi00354a038

Pasternack, R. F., Gibbs, E. J., and Villafranca, J. J. (1983). Interactions of porphyrins with nucleic acids. *Biochemistry* 22, 2406–2414. doi: 10.1021/bi00279a016

Quinlan, G. J., Martin, G. S., and Evans, T. W. (2005). Albumin: biochemical properties and therapeutic potential. *Hepatology* 41, 1211–1219. doi: 10.1002/hep.20720

Radisavljević, S., Ćoćić, D., Jovanović S., Šmit, B., Petković, M., Milivojević, N., et al. (2019). Synthesis, characterization, DFT study, DNA/BSA-binding

affinity, and cytotoxicity of some dinuclear and trinuclear gold(III) complexes. *JBIC J. Biol. Inorg. Chem.* 24, 1057–1076. doi: 10.1007/s00775-019-01716-8

Raimondi, M. V., Randazzo, O., La Franca, M., Barone, G., Vignoni, E., Rossi, D., et al. (2019). DHFR inhibitors: reading the past for discovering novel anticancer agents. *Molecules* 24, 1140–1159. doi: 10.3390/molecules24061140

Raninga, P. V., Lee, A. C., Sinha, D., Shih, Y. Y., Mittal, D., Makhale, A., et al. (2020). Therapeutic cooperation between auranofin, a thioredoxin reductase inhibitor and anti-PD-L1 antibody for treatment of triple-negative breast cancer. *Int. J. Cancer* 146, 123–136. doi: 10.1002/ijc.32410

Santini, C., Pellei, M., Papini, G., Morresi, B., Galassi, R., Ricci, S., et al. (2011). *In vitro* antitumor activity of water soluble Cu(I), Ag(I) and Au(I) complexes supported by hydrophilic alkyl phosphine ligands. *J. Inorg. Biochem.* 105, 232–240. doi: 10.1016/j.jinorgbio.2010.10.016

Scheffler, H., You, Y., and Ott, I. (2010). Comparative studies on the cytotoxicity, cellular and nuclear uptake of a series of chloro gold(I) phosphine complexes. *Polyhedron* 29, 66–69. doi: 10.1016/j.poly.2009.06.007

Schwentner, L., Wolters, R., Koretz, K., Wischnewsky, M. B., Kreienberg, R., Rottscholl, R., et al. (2012). Triple-negative breast cancer: the impact of guideline-adherent adjuvant treatment on survival—a retrospective multi-centre cohort study. *Breast Cancer Res. Treat.* 132, 1073–1080. doi: 10.1007/s10549-011-1935-y

Serova, M., Calvo, F., Lokiec F., Koeppel, F., Poindessous, V., Larsen, A. K., et al. (2006). Characterizations of irofulven cytotoxicity in combination with cisplatinand oxaliplatin in human colon, breast, and ovarian cancer cells. *Cancer Chemother. Pharmacol.* 57, 491–499. doi: 10.1007/s00280-005-0063-y

Silver, D. P., Richardson, A. L., Eklund, A. C., Wang, Z. C., Szallasi, Z., Li, Q., et al. (2010). Efficacy of neoadjuvant cisplatin in triple-negative breast cancer. *J. Clin. Oncol.* 28, 1145–1153. doi: 10.1200/JCO.2009.22.4725

Singh, M., Atwal, H., and Micetich, R. (1998). Transferrin directed delivery of adriamycin to human cells. *Anticancer Res.* 18, 1423–1427.

Tong, J. Q., Tian, F. F., Li, Q., Li, L. L., Xiang, C., Liu, Y., et al. (2012). Probing the adverse temperature dependence in the static fluorescence quenching of BSA induced by a novel anticancer hydrazone. *Photochem. Photobiol. Sci.* 11, 1868–1879. doi: 10.1039/c2pp25162k

Urig, S., and Becker, K. (2006). On the potential of thioredoxin reductase inhibitors for cancer therapy. *Semin. Canc. Biol.* 16, 452–465. doi: 10.1016/j.semcancer.2006.09.004

Waks, A. G. and Winer, E. P. (2019). Breast cancer treatment: A review. *JAMA* 321:288–300. doi: 10.1001/jama.2018.19323

Wang, F., Jiang, X., Yang, D. C., Elliott, R. L., and Head, J. F. (2000). Doxorubicin-gallium-transferrin conjugate overcomes multidrug resistance: evidence for drug accumulation in the nucleus of drug resistant MCF-7/ADR cells. *Anticancer Res.* 20, 799–808.

Wang, J., Iannarelli, R., Pucciarelli, S., Laudadio, E., Galeazzi, R., Giangrossi, M., et al. (2020). Acetylshikonin isolated from lithospermum erythrorhizon roots inhibits dihydrofolate reductase and hampers autochthonous mammary carcinogenesis in Δ16HER2 transgenic mice. *Pharmacol. Res.* 161:105123. doi: 10.1016/j.phrs.2020.105123

Worwood, M. (2002). Serum transferrin receptor assays and their application. *Ann. Clin. Biochem.* 39, 221–230. doi: 10.1258/0004563021902152

Xu, L., Zhong, N. J., Xie, Y. Y., Huang, H. L., Jiang, G. B., and Liu, Y. J. (2014). Synthesis, characterization, *in vitro* cytotoxicity, and apoptosis-inducing properties of ruthenium(II) complexes. *PLoS ONE* 9:e96082. doi: 10.1371/journal.pone.0096082

Yao, H., He, G., Yan, S., Chen, C., Song, L., Rosol, T. J., et al. (2016). Triple-negative breast cancer: is there a treatment on the horizon? *Oncotarget* 8, 1913–1924. doi: 10.18632/oncotarget.12284

Zaitsev, E. N., and Kowalczykowski, S. C. (1998). Binding of double-stranded DNA by *Escherichia coli* RecA protein monitored by a fluorescent dye displacement assay. *Nucleic Acids Res.* 26, 650–654. doi: 10.1093/nar/26.2.650

Zheng, Z. Y., Li, J., Li, F., Zhu, Y., Cui, K., Wong, S. T., et al. (2018). Induction of N-Ras degradation by flunarizine-mediated autophagy. *Sci. Rep.* 8:16932. doi: 10.1038/s41598-018-35237-2

Zou, T., Lum, C. T., Lok, C. N., Zhang, J. J., and Che, C. M. (2015). Chemical biology of anticancer gold(III) and gold(I) complexes. *Chem. Soc. Rev.* 44, 8786–8801. doi: 10.1039/C5CS00132C

Conflict of Interest: The authors declare that the research was conducted in the absence of any commercial or financial relationships that could be construed as a potential conflict of interest.

Advantages of publishing in Frontiers

OPEN ACCESS
Articles are free to read for greatest visibility and readership

FAST PUBLICATION
Around 90 days from submission to decision

HIGH QUALITY PEER-REVIEW
Rigorous, collaborative, and constructive peer-review

TRANSPARENT PEER-REVIEW
Editors and reviewers acknowledged by name on published articles

Frontiers
Avenue du Tribunal-Fédéral 34
1005 Lausanne | Switzerland

Visit us: www.frontiersin.org
Contact us: frontiersin.org/about/contact

REPRODUCIBILITY OF RESEARCH
Support open data and methods to enhance research reproducibility

DIGITAL PUBLISHING
Articles designed for optimal readership across devices

FOLLOW US
@frontiersin

IMPACT METRICS
Advanced article metrics track visibility across digital media

EXTENSIVE PROMOTION
Marketing and promotion of impactful research

LOOP RESEARCH NETWORK
Our network increases your article's readership